Advances in Late-Metal Carbon-Nitrogen Bond Formation for the Synthesis of Substituted Heterocycles

by

Nicolas L. Rotta-Loria

A thesis submitted in conformity with the requirements
for the degree of Doctor of Philosophy

at

Dalhousie University
Halifax, Nova Scotia
July 2017

© Copyright by Nicolas L. Rotta-Loria, 2017

Table of Contents

List of Figures

List of Schemes

Abstract

Late-metal catalyzed cross-couplings have emerged as efficient and selective methodologies for the formation of C-C and C-N bonds. The ability to synthesize complex heterocycles from cheap and abundant starting materials is an invaluable asset to the pharmaceutical industry, given that many pharmaceuticals contain at least one heterocyclic component. This reactivity can be achieved by tuning the steric and electronic properties of ancillary ligands to support metal catalysts in the reaction steps leading to the target substrate.

The Stradiotto group has developed several state-of-the-art methodologies involving ligands for palladium catalysis, for both C-C and C-N bond-forming reactions. These methodologies can be amalgamated into a multicomponent reaction platform to synthesize more complex products from simple materials. Chapter 1 outlines this concept with the application of a Mor-DalPhos/Pd catalyst in the one-pot synthesis of indoles from acetone and simple amines involving C-C and C-N bond formation. The robust nature of this method can be extended to include benchtop reaction conditions in a one-step, one-pot synthesis of indoles, thus representing a useful synthetic protocol.

While palladium provides a powerful tool for C-C and C-N bond formation, the general trend in catalysis has shifted away from the precious metals toward first row metals as economic alternatives. Nickel complexes have recently emerged as excellent catalysts for a number of amination reactions. The ability to utilize ammonia also represents a sought after reaction, due to the widespread availability and synthetic utility of amino-functionalized products. In this regard, Chapter 2 will focus on the development and application of both commercially available and strategically designed ligand classes for the monoarylation of ammonia with substituted heterocycles.

Hydrazine represents an important synthon in synthetic chemistry. It is synthesized on multi-ton scale every year and represents an important building block in many industrial processes. Many synthetic challenges arise from using free hydrazine as reactant, which has led to lethargic growth of its application in the field of late-metal catalyzed C-N bond-formation. However, gold-catalyzed methodologies have been developed utilizing NHC ligands to allow for the hydrohydrazination of alkynes with parent hydrazine. Chapter 4 examines the development and application of a series of $(PR_3)AuCl$ complexes for use in such transformations, leading to the identification of the first effective phosphine-bound gold complex for use in the hydrohydrazination of alkynes at room temperature.

List of Abbreviations and Symbols Used

α position	first carbon adjacent to a carbonyl group in this thesis
β position	second carbon adjacent to a carbonyl group in this thesis
δ	chemical shift
η	hapticity - eta (contiguous donor atoms)
1-Ad	1-adamantyl
Ar	aryl
aq.	aqueous
BHA	Buchwald-Hartwig amination
BINAP	2,2-bis(diphenylphosphino)-1,1'-binaphthalene
CAAC	cyclic(alkyl)(amino)carbene
cat.	catalytic or catalyst
conc.	concentration
conv.	conversion
Cy	cyclohexyl
d	doublet
dba	dibenzylideneacetone
dppf	(1,1'-bisdiphenylphosphino)ferrocene
Dipp	2,6-diisopropylphenyl
d*i*ppf	1,1'-bis(di-isopropylphosphino)ferrocene
ESI	electrospray ionization
EWG	electron withdrawing group
GC	gas chromatography

GP	General Procedure
HRMS	high-resolution mass spectrometry
JXX’	coupling constant between atom X and atom X’
LDA	lithium diisopropylamide
m	multiplet
MCR	multicomponent reactions
MIC	mesoionic carbene
NHC	*N*-heterocyclic carbene
NMR	nuclear magnetic resonance
OMs	mesylate
OTf	triflate
OTs	tosylate
PTFE	poly(tetrafluoroethylene)
q	quartet
rt	room temperature
s	singlet
t	triplet
TBS	tert-butyl-dimethylsilyl
TIPS	triisopropylsilyl
TLC	thin layer chromatography
X	halide substituent or anionic ligand

Acknowledgements

First and foremost, I would like to extend my deepest and most sincere thanks to my supervisor and mentor Dr. Mark Stradiotto. His guidance, motivation and excellent vision made me realize a potential I never saw possible.

I would like to thank those Stradiotto group members that also made this body of work possible. I first thank Dr. Andrey Borenko (postdoctoral fellow) for his help in completing the scope in both the indole and JosiPhos ammonia projects. I would like to thank Preston MacQueen (PhD candidate) for his help applying ammonia gas to the monoarylation of heterocyclic aryl halides. I would also like to thank Chris Lavoie (PhD candidate) for his excellent work in the development of an air-stable nickel pre-catalyst and his further development of a new phosphine ligand, which I apply in my research work. I would like to especially thank my first mentor and friend Dr. Christopher Lavery for first introducing me to the core concepts and an understanding of graduate level chemistry.

I would also like to say thank you to every Stradiotto group member, past and present, for all thoughtful conversation, helpful analysis, and overall great fun. I have made excellent friends, have worked with some truly incredible people, and will cherish the memories of the last five years fondly.

I would like to thank my supervisory committee, including Dr. Alison Thompson, Dr. Alex Speed, Dr. Laura Turculet, and Dr. Jean Burnell for taking the time to review my thesis work and coaching me through this difficult process. Acknowledgement is also made to Dr. Mike Lumsden (NMR 3) for assistance with the NMR experiments, Mr. Xiao Feng (Dalhousie) for collecting mass-spectrometry data, and Drs. Robert McDonald and Michael Ferguson (Alberta) for providing all necessary X-ray crystallographic data.

Chapter 1: Introduction

1.1 Introduction to Catalysis

Catalysis in the context of modern synthetic chemistry has revolutionized the ability of chemists to access functionalized molecules through efficient and selective reaction pathways. The ongoing strategic development of superlative catalysts allows for the synthesis of new and complex molecules, often from inexpensive and abundant feedstock chemicals, thereby enabling processes that offer high levels of atom economy. In this regard, catalyst design remains an invaluable domain of modern synthetic chemistry.[1]

A successful catalyst lowers the activation energy of a reaction pathway, thereby allowing for more facile transformation of the target compound. The ability to utilize catalysts in sub-stoichiometric amounts offers a significant advantage versus more traditional synthetic methods. It allows for fewer by-products and reduced waste as well as accelerated kinetics to support rapid conversion of reagents. All of these advantages are attractive from an industrial perspective with regard to large-scale production.[2] Pharmaceuticals, agrochemicals, petrochemicals, and other industrially relevant materials must be synthesized on immense scales with a high degree of efficiency, requiring both active and stable catalysts. The most active and selective catalysts known are enzymes.[3] Enzymes catalyze every vital transformation in the human body and are the cornerstone for transformations that occur in nature every day. However, there is a significant drawback to using enzymes in many catalytic transformations. Enzymes are often so substrate selective that the application of a substrate variant, no matter how similar, may prove ineffective.[3] Significant work has been applied toward mimicking enzymatic activity within "man-made" catalysts of various types, in an effort to achieve more broad substrate scope

reactivity. Significant advancements have been made in this regard, with the development of catalytic protocols in which the turnover numbers (TONs) of substrates rival that of enzymatic processes. For example, a methodology established by Noyori[4] for the ruthenium-catalyzed asymmetric hydrogenation of ketones to afford chiral alcohols is capable of TONs in excess of one million. Although the focus of catalysis is the improvement of activity for a target reaction, the generality of use is also a consideration. A catalyst that is capable of performing a plethora of reactions under diverse reaction conditions allows for many transformations to occur in a single reaction vessel. This can allow for the formation of complex products from inexpensive and abundant starting materials without the need for unnecessary purification and intermediate steps.

There exist two main classes of catalysts: homogeneous and heterogeneous. Heterogeneous catalysts exist in a separate phase from the reactants, with most being solid catalysts that interact with reactants existing in the liquid or gas phase.[5] These are commonly applied in industry due to the ease of separation from the reactants, as well as their high thermal stability; however, these possess a poorly defined active site.[6] Homogeneous catalysts exist in the same phase as reactants and solvents. The active site of these catalysts can be well-defined and can be characterized by the use of traditional spectroscopic methods. This allows for homogeneous catalysts to be more easily identified and the reaction pathway to be determined more readily. Drawbacks to the use of homogeneous catalysts involve the difficulty of separation from the reaction mixture and the relatively low thermal stability. The focus of my doctoral thesis work is on the development of new or improved homogeneous catalysts for use in C-C and C-N bond-forming reactions employing simple and abundant substrate molecules.

1.2 Palladium-Catalyzed Cross-Coupling (C-C Bonds)

1.2.1 History of Palladium-Catalyzed C-C Bond Formation

Late-metal catalysts have emerged with unprecedented reactivity to accommodate the formation of novel C-C and C-heteroatom (N, O, P, S) bond-forming processes once thought unattainable through traditional synthetic protocols. The Nobel Prizes in 2001, 2005, and 2010 were each presented for advancements in organometallic catalysis. In 2001 the award was shared in part by Knowles and Noyori, for the development of selective asymmetric hydrogenation reactions.[7] In 2005 Chauvin, Grubbs, and Schrock received the prize for their development of the metathesis method.[8] These late-metal catalyzed processes both involve the conversion of relatively simple molecules (dihydrogen and simple olefins) into industrially relevant value-added products.

The background of this document, however, will begin with the Nobel Prize awarded in 2010 to Richard Heck, Ei-shi Negishi, and Akira Suzuki. This award was presented for the development of palladium-catalyzed cross-coupling as a novel C-C bond-forming process. These methodologies have revolutionized the way that C-C bonds are constructed and have further brought to light the utility of late-metal catalysis. These processes typically involve the reaction of an aryl or vinyl halide with an alkene, alkyne, zinc, magnesium or organoboron coupling partner (Scheme 1-1).[9] The Heck (or Mizoroki-Heck) reaction involves the cross-coupling of a (hetero)aryl halide with a range of alkenes to provide access to more complex alkenes. Negishi coupling proceeds via the reaction of an aryl, benzyl, acyl, or alkynyl halide with an aryl zinc-coupling partner to form a new substituted aryl compound. Suzuki reactions proceed in a similar fashion where substituted

aryl halides react with organoboronic acid coupling partners affording similar substituted aryl products.[10]

The development of these pioneering C-C bond-forming protocols led to the emergence of a plethora of different palladium-catalyzed C-C and C-X bond-forming reactions.[9] Reactions involving organo-magnesium coupling partners (Kumada coupling)[11] as well as tri-*n*-butyl tin coupling partners (Stille coupling)[12] have also been used to form functionalized biaryls. Sonogashira coupling involves the reaction of a (hetero)aryl halide with a terminal alkyne fragment to form substituted alkynyl products.[13] All of these C-C bond-forming methodologies have proven invaluable in both academic and industrial settings

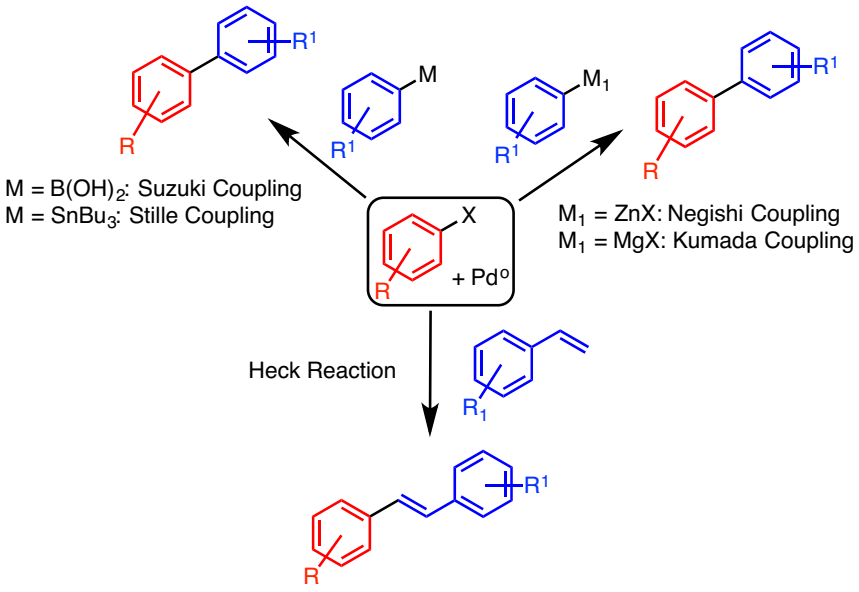

Scheme 1-1. Examples of palladium-catalyzed cross-coupling reactions

1.2.2 Reaction Mechanism and Related Ancillary Ligand Design Considerations

Each of the palladium-catalyzed reactions in Scheme 1-1 can be represented by a catalytic cycle in which palladium is involved in mediating several elementary steps (Scheme 1-2). The first step involves an oxidative addition of the aryl (pseudo)halide to the

palladium centre. This is followed by a transmetalation step, which abstracts the halide from the palladium metal and delivers the nucleophilic reactant to palladium. The final step is a reductive elimination to generate the product and regenerate the active ligated Pd^0 species. This process can be applied to a number of different palladium-mediated processes including both Suzuki and Negishi coupling. However, there are exceptions and variations to these catalytic steps. For example, the Heck reaction proceeds via an olefin insertion followed by a β-hydride elimination to release the final product.[14] This is more clearly demonstrated in Scheme 1-2.

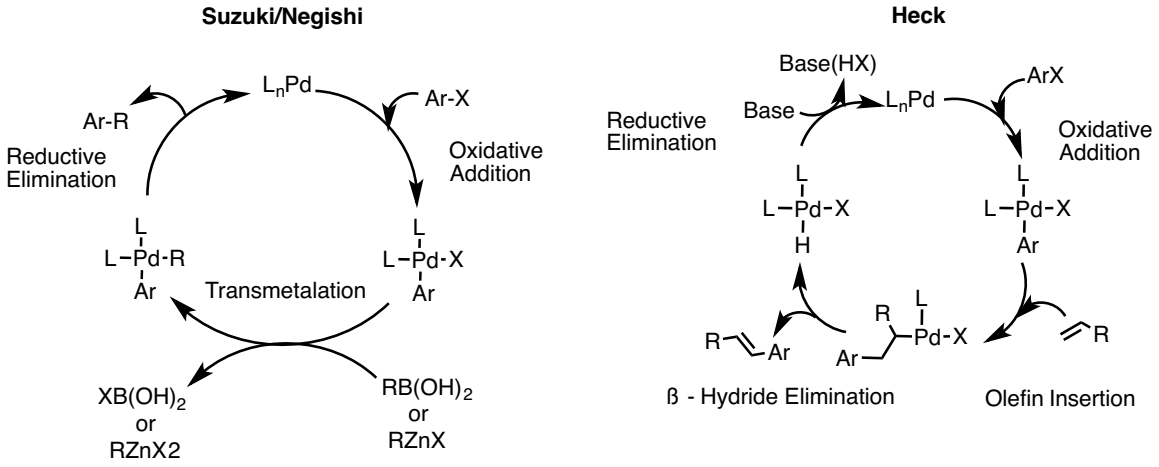

Scheme 1-2. Common Pd-catalyzed C-C catalytic cycles

Each step in the catalytic cycles shown in Scheme 1-2 is directly affected by the ancillary ligand(s) (L).[15] The electronic properties of the ligand have a particularly profound influence on the oxidative addition step in the catalytic cycle. This is due to the ability of ligand to donate electron density to the metal centre, allowing oxidative addition (i.e. net reduction of the Ar-X bond) to become more facile. The potential hemilability of a multidentate ligand affects the transmetalation step of the catalytic cycle. Certain ligands, which are strong donors, restrict the ability of substrates to engage the active site of the

metal, thus hindering transmetalation. The efficiency of reductive elimination is correlated with ligand steric bulk. More steric hindrance contributed by the ligand allows for an easier reductive elimination step. The reductive elimination step is also more facile when the ligand is less electron donating. The ligand can also restrict unwanted side reactions from occurring (β-hydride elimination, etc.). In the case of particularly challenging C-N coupling partners such as ammonia the ligand design becomes particularly important to discourage these unwanted reaction pathways (see Chapter Three). Notably, the electronic and steric demands of the ligand are sometimes orthogonal for these elementary reaction steps; as such, these properties must be balanced to allow for optimal catalytic activity.[15]

1.2.3 Alpha Arylation

Palladium-catalyzed C-C bond-forming methodologies can be extended to accommodate more challenging cross-coupling reactions. Direct arylation via C-H activation[16] and also the α-arylation of carbonyls[17] have emerged as useful synthetic protocols. The latter represents an important catalytic protocol to access substituted benzyl ketones, which include a number of important precursors in novel drug discovery. Shown in Scheme 1-3 is an early, and rare, example of a drug synthesized via the α-arylation method.[18] It should be noted that while this reaction is carried out with nickel as the reactive metal centre, most α-arylations conducted currently employ palladium as the metal of choice.

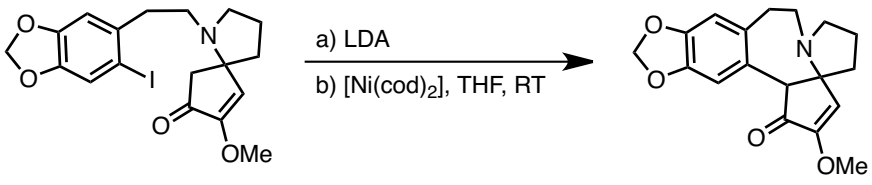

Scheme 1-3. Synthesis of cephalotaxinone

α-Arylation is a technique that involves the direct installation of an aryl group, derived from a (hetero)aryl (pseudo)halide, onto a carbonyl compound containing α-CH groups.[19] Previous pathways to access these types of molecules required the pre-formation of enol ethers (enolate) to allow the installation of the carbonyl. However, these previous methodologies lacked atom economy and required the use of stoichiometric toxic reagents.[20] Currently employed palladium-mediated methodologies allow for the facile cross-coupling of ketones, and related species, possessing accessible α-CH groups with (hetero)aryl (pseudo)halides.

The catalytic cycle for ketone α-arylation follows similar steps to that of other C-C bond-forming reactions (Scheme 1-4). The first step involves the oxidative addition of an aryl halide. The second step is an addition of the ketone enolate to the metal centre, followed by the reductive elimination of the final benzyl ketone product.[19]

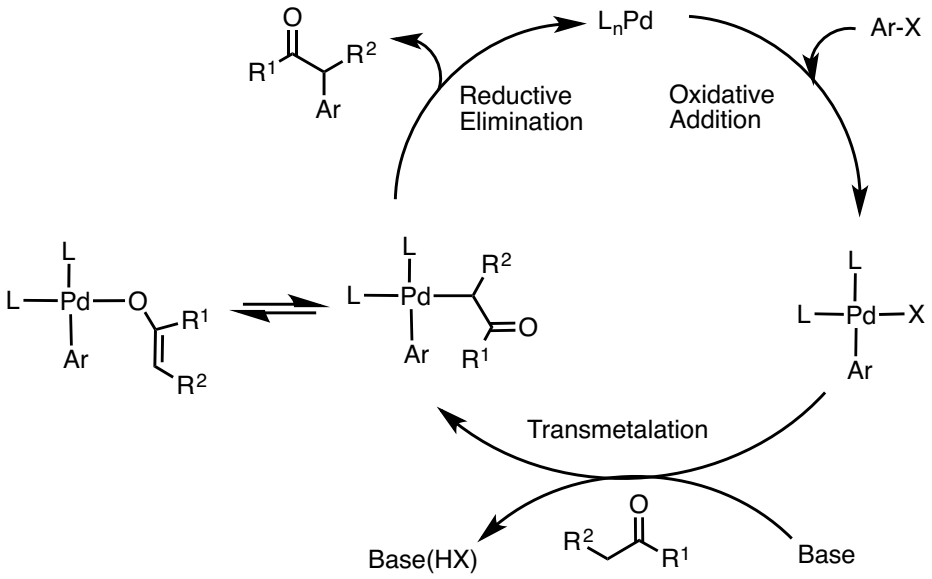

Scheme 1-4. α-Arylation catalytic cycle

The groups of Hartwig[21], Buchwald,[22] and Miura[23] independently reported the first alpha α-arylation reactions in 1997 without the pre-formation of enolates. Both

Buchwald and Hartwig showed the need for a bulky bisphosphine ligand to achieve high selectivity and reactivity (Scheme 1-5).

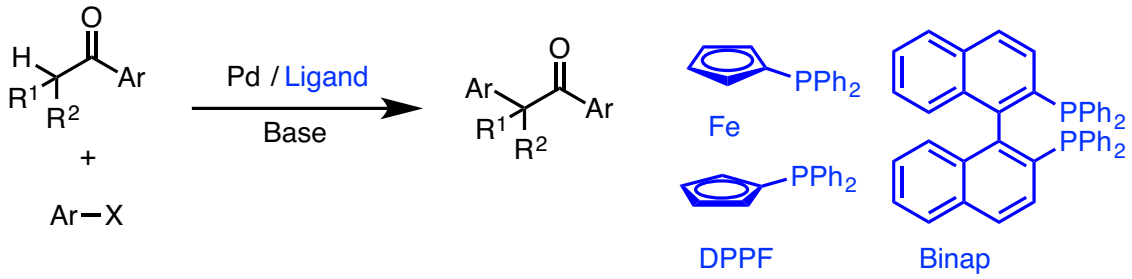

Scheme 1-5. First example of palladium-catalyzed α-arylation

The need for bulky bisphosphines is due to the steric interaction of the ligand in the second step of the catalytic cycle. The bulky nature of the ligand discourages β-hydride elimination (where R^2 is a C-H containing alkyl group) and allows the formation of a four-coordinate palladium species, which can then undergo a facile reductive elimination.[19] Although collectively these early reports were a major advancement, many limitations existed with these systems. The ability to accommodate aryl chlorides, as well as deactivated aryl bromides and iodides, was unexplored at the time. The ability to monoarylate ketones that possess multiple α-CH groups also remained a challenge. This is difficult due to the fact that the α-protons of the benzyl ketone product are more acidic than the ketone starting material. This can lead to the unwanted formation of di- and tri-substituted products.

Many α-arylation protocols arose from this method; however, the α-arylation of acetone remained unknown for another decade. In 2011 the Stradiotto group developed the first ever mono-α-arylation of acetone, applying a Mor-DalPhos/$[Pd(cinnamyl)Cl]_2$ catalyst system (Scheme 1-6).[24]

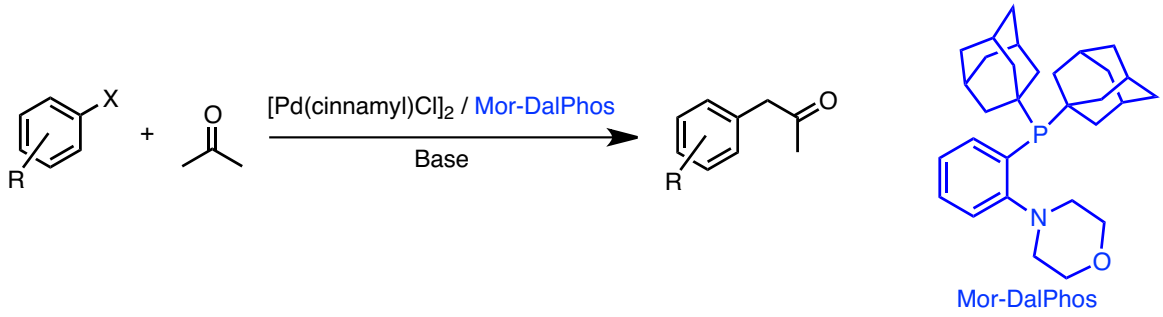

Scheme 1-6. Monoarylation of acetone with Mor-DalPhos/$[Pd(cinnamyl)Cl]_2$

This represents a potentially important methodology due to the abundance, availability, and widespread use of acetone in industrial applications. This Mor-DalPhos/$[Pd(cinnamyl)Cl]_2$ catalyst system was successful in the monoarylation of a range of structurally diverse aryl chlorides under reasonably mild conditions. The bulky nature of the $P(1\text{-}Ad)_2$ group coupled with the weaker electron donation of the morpholino moiety, compared with a highly electron donating bisphosphine, is presumed to contribute to the desirable catalytic performance. This is due to the potential hemilability of nitrogen donor fragment which can aid in the transmetalation step of the catalytic cycle and lead to optimal catalytic perfomance. This ligand has also shown to be a successful catalyst in several palladium-catalyzed C-N bond-forming reactions.[25] Inspired by this unique combined reactivity, a portion of my thesis research involved applying Mor-DalPhos/Pd catalysis toward the development of multicomponent reactions involving mono-α-arylation and C-N bond-forming reactions. My research results in this regard are presented in Chapter Two.

1.3 Palladium-Catalyzed C-N Bond-Forming Reactions

1.3.1 Early Development of Buchwald-Hartwig Amination

The ability of palladium to catalyze novel C-C bond-forming reactions led to the development of catalysts that could accommodate the formation of C-O, C-P, C-S, and C-

N bonds. The focus of this section will be the development of C-N bond-forming techniques and the application of Buchwald-Hartwig amination (BHA). Many traditional synthetic routes exist for the formation of C(sp^2)-N bonds. However, these methodologies often require extremely forcing reaction conditions, including the addition of strong acids and bases, as well as high temperatures to attain the target product. Some examples of these reactions include nucleophilic aromatic substitution (Scheme 1-7) and the Ullman amine synthesis (Scheme 1-8).[26]

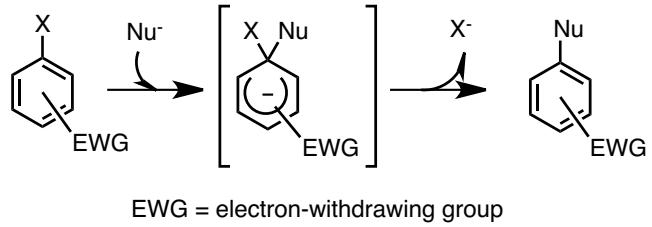

Scheme 1-7. Nucleophilic aromatic substitution

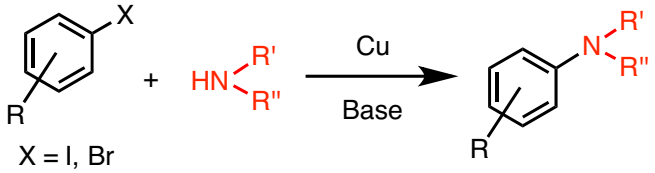

Scheme 1-8. Ullman coupling

These routes require the use of activated substrates, which involve the need for highly electron-withdrawing substituents appended to the target aryl halide. The need for these functionalities severely limits their substrate scope. Buchwald-Hartwig amination (Scheme 1-9) offers a one-step synthetic protocol to cross-couple a variety of NH substrates (amines, indoles, amides, etc.) with a plethora of aryl halides. These reactions can be completed efficiently and selectively by applying palladium and other late-metal catalysts, although the strict definition of BHA involves palladium catalysis.

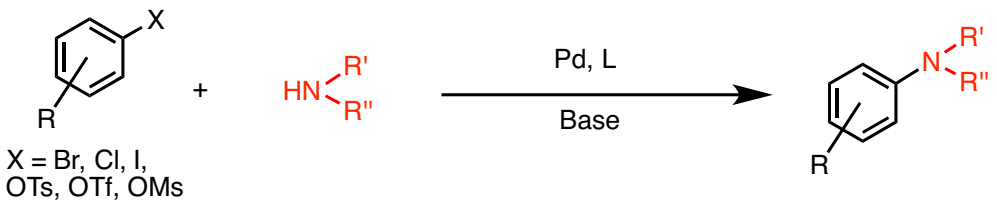

Scheme 1-9. General Buchwald-Hartwig amination reaction

The groups of Hartwig and Buchwald concurrently discovered the first direct aminations of aryl bromides in 1995.[27] These were the first examples of palladium-catalyzed aminations without the use of stoichiometric tin or boron reagents. These early catalytic systems were limited due to the fact that they could accommodate only simple aryl bromides and secondary amines. However, since this discovery, Buchwald, Hartwig, and many others have made incredible strides in advancing the efficiency and selectivity of BHA to accommodate an immense number of amines as well as (hetero)aryl (pseudo)halides. These methodologies have also been extended to include nickel, which will be discussed in more specific terms in Chapter Three of the document.

1.3.2 Buchwald-Hartwig Amination, Mechanism and Ligand Effects

The mechanism of BHA follows a similar pathway to that of many C-C bond-forming reactions. There are four major steps within the BHA catalytic cycle (Scheme 1-10). The initiation of the catalytic cycle begins with the formation of the catalytically active ligand-bound L_nPd^0 species. This involves either the reduction of a Pd^{II} species *in situ* or the formation of a pre-catalyst Pd^0 species. The first step of the catalytic cycle commences upon catalyst activation, whereby the aryl halide undergoes oxidative addition to the palladium centre. Subsequent amine binding and deprotonation by base forms the palladium-amido intermediate. These amine and amido intermediates can exist as either a 14-electron three-coordinate species, or a 16-electron four-coordinate species. This is

dependent on the binding mode of the nitrogen nucleophile and the properties of the ancillary ligand, which will be discussed shortly. The final step involves C-N bond reductive elimination to generate the final product and regenerate the catalytically active L_nPd^0 species.

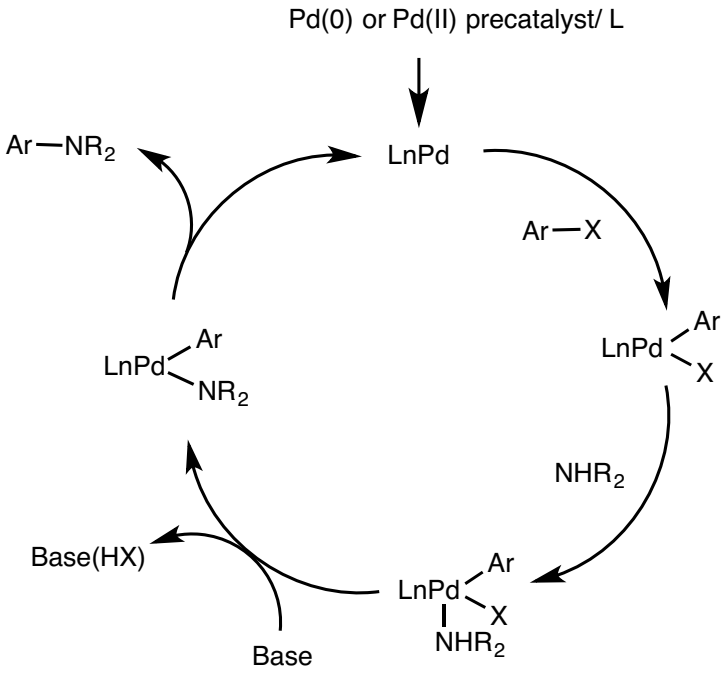

Scheme 1-10. Buchwald-Hartwig amination catalytic cycle

In many cases oxidative addition is the rate-limiting step in the BHA catalytic cycle.[28] However, reductive elimination can also be problematic. The steric influence of the ligand plays an essential role in this process. At the emergence of BHA, simple triaryl phosphines were sufficient ligands to accommodate the simple reactivity of secondary amines with aryl bromides.[27] As more complex amines and aryl halides were targeted in this chemistry the use of bis-phosphines such as XantPhos[29] and *rac*-BINAP[30] proved to be important in achieving the desired reactivity. Such ligands allow for greater reactivity and selectivity for these challenging substrates. Several common classes of ligands that have proven successful in BHA are presented in Figure 1-1. One of the largest families of

ligands, developed by the Buchwald group, employ a bulky biaryl dialkylmonophosphine structure.[31] These ligands have seen much success in this chemistry and are developed to suit particular C-N reactions on an "as needed" basis through alteration of the modular ancillary ligand structure. Other ligands have emerged from this motif including heterocyclic biaryl monophosphines such as BippyPhos,[32] which have shown to accommodate a number of amination reactions. N-Heterocyclic carbenes (NHCs) have also proven to be effective ligands in palladium-catalyzed C-N bond formation.[33] Hartwig has also applied previously developed bis-phosphines known as JosiPhos[34] employing a ferrocenyl backbone with a chiral dialkylphosphine structure toward BHA chemistry.[35]

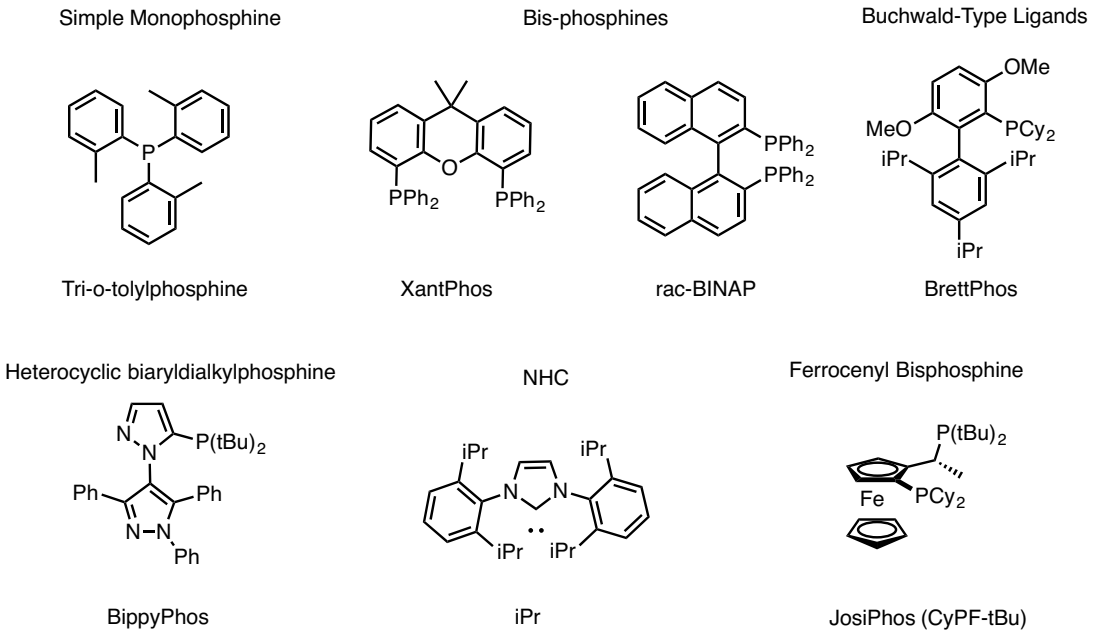

Figure 1-1. Common ligand classes applied in Buchwald-Hartwig aminations

1.3.3 Recent Advancements in Buchwald Hartwig Amination

The Stradiotto group has focused on developing ligands to facilitate difficult transformations in BHA. The monoarylation of small nucleophilic amines,[25b, 36] most notably ammonia,[25a] represents one of the most difficult reactions associated with BHA.

Ammonia is one of the most important inorganic feedstocks in the world. Almost 160 million tonnes of ammonia are produced every year.[37] It is employed mainly in the production of fertilizers as ammonium nitrates, but also can be applied in many industrial processes including the production of plastics and pharmaceuticals.[37] The ability to harness ammonia in metal-mediated cross-coupling reactions is a powerful tool to functionalize particularly challenging (hetero)aryl halides. These heterocyclic amines represent attractive intermediates in the formation of pharmaceuticals and biologically relevant materials.[38] Shen and Hartwig reported the first ever monoarylation of ammonia in 2006 using a JosiPhos-based catalyst system.[39] Since then the groups of Hartwig,[40] Beller,[41] Buchwald,[42] and Stradiotto[25a] have developed catalysts to support the monoarylation of ammonia. The Stradiotto group has gone on to report the monoarylation of ammonia at room temperature, utilizing a number of structurally varied (hetero)aryl halides. Their success in this regard was attributed to the development of the Mor-DalPhos/[Pd(cinnamyl)Cl]$_2$ catalyst system, which offers excellent reactivity and selectivity towards monoarylation.[25a] As mentioned previously, the second chapter of this document will showcase the unique reactivity of Mor-DalPhos/Pd to catalyze C-N bond-forming reactions and α-arylation in a multicomponent synthesis of indoles.

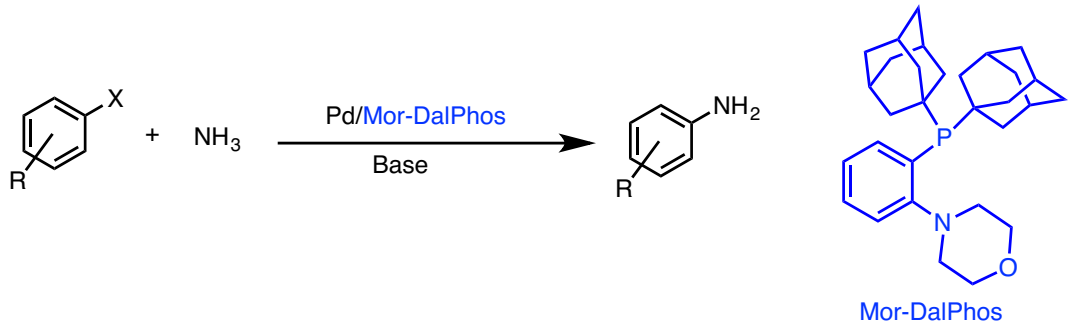

Scheme 1-11. Ammonia monoarylation applying Mor-DalPhos

1.3.4. The Movement to Nickel

Palladium-catalyzed bond-forming methodologies have been established as the most commonly applied tool to synthesize new C-C and C-(heteroatom) bonds. These methodologies have allowed for the formation of complex substrates from inexpensive, abundant starting materials. However, these reactions come at a cost. Palladium is a low-abundance metal and is therefore immensely expensive to produce. Due to the high cost of the platinum group metals (Pd, Pt, Rh, Ir, Ru, Os), many efforts have been made to shift away from these expensive and rare elements to more sustainable metal sources in catalysis. This general shift in catalysis has been towards the use of first row metals to accommodate this type of reactivity. Although copper has shown to be useful in several C-C and C-N bond-forming reactions, it is very limited in terms of substrate scope.[43]

This has led to the application of nickel as a successful, first row metal for a diverse array of metal-catalyzed bond-forming reactions. Nickel is almost 2,000 times cheaper than palladium and nearly 10,000 times cheaper than platinum on an elemental level.[44] Although the cost-efficient nature of nickel makes it an attractive alternative to its group 10 counterparts (Pd and Pt), nickel also possesses several characteristics that make it a particularly attractive metal for catalysis. The first is that it is an electron-rich metal in relation to Pd and Pt,[45] therefore it can undergo relatively facile oxidative addition with challenging electrophiles. This makes nickel particularly useful for the activation and coupling of challenging heteroaryl substrates, which represents the focus of Chapter Three. Nickel discourages unwanted beta-hydride eliminations, which represent a common decomposition pathway in palladium-catalyzed bond-forming protocols. Nickel also has access to varied oxidation states. This can lead to different reaction pathways and

mechanisms for potentially unexplored catalytic processes. The ability for nickel to conduct radical chemistry and single electron transfer involving Ni^{I} and Ni^{III} species allows for diverse reactivity profiles to be explored. This can also represent a disadvantage and has contributed to the relatively slow development of nickel chemistry compared to palladium. The well-established Pd^{0}/Pd^{II} catalytic pathway allows for the accurate and deliberate design of ligands and pre-catalysts to support this mechanism. The unpredictability of nickel in terms of redox behaviour and the propensity for radical chemistry represents an ongoing challenge in terms of designing ligands for nickel-catalyzed cross-couplings.

1.3.5 A Brief History of Nickel-Catalyzed Cross-Coupling

Although the first ever nickel-catalysis was discovered in the 1890s it was not until the 1970s that the potential for nickel-catalyzed cross-coupling was realized.[45] Kumada and Corriu were successfully able to couple aryl chlorides with Grignard-type reagents under forcing conditions.[11, 46] However, due to the unexplored mechanism and limited nickel sources, the use of nickel received scant attention relative to palladium in the coming decades. More recently, nickel has shown application in several C-C bond-forming reactions with heteroaryl coupling partners. Notably, Ge and Hartwig were able to utilize nickel to conduct the Suzuki-Miyaura cross-coupling of hetero-aromatic boronic esters with a range of heteroaryl halides under very mild conditions[47] (Scheme 1-12). This was further explored by Garg in 2013 to deliver a more diverse array of heteroaryl products[48] (Scheme 1-12). Hazari has explored the ability of nickel to access different oxidation states versus its palladium counterpart. This has allowed for the development of Ni^{I} catalysts that represent potentially active catalytic intermediates and alternative precursors in the Suzuki-Miyaura coupling of aryl sulfamates.[49] This has opened the door for many novel catalysts

designed in the vein of Ni^{I} catalysis.

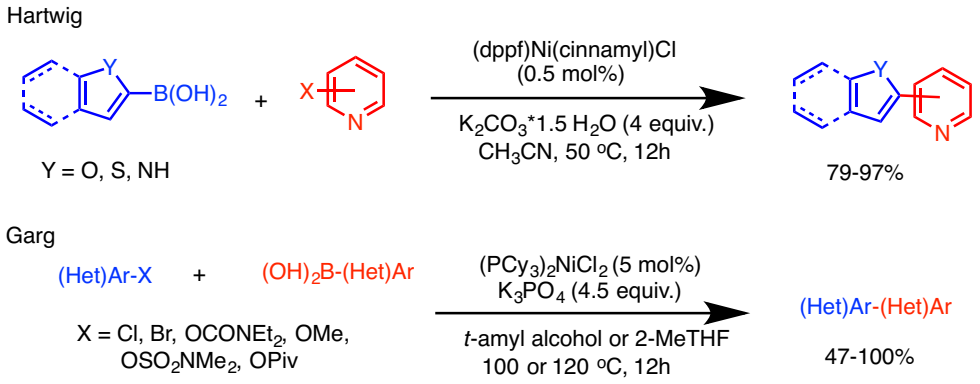

Scheme 1-12. Nickel-catalyzed Suzuki-Miyaura coupling of heteroaryl boronic acids

Nickel has also shown excellent reactivity in the cross-coupling of phenol derivatives, which represent diverse and attractive alternatives to aryl halides. The activation of the C-O bond represents a significant challenge in cross coupling; however, recent advances in nickel catalysis has led to the activation and cross-coupling of particularly challenging phenol derivatives including carbamates, mesylates and sulfamates.[50] Nickel is also capable of catalyzing the cross-coupling of challenging benzylic substrates,[51] sp^3-sp^3 coupling partners[52] along with other challenging C-C bond-forming reactions. Beyond demonstrating diverse reactivity in C-C bond formation, nickel has also emerged as an excellent catalyst for the formation of C-N bonds. The development of nickel-catalyzed amination, ligand design, and ultimately the discovery of the first nickel-catalyzed monoarylation of ammonia by the Stradiotto group will be discussed in Chapter Three of the thesis document.

1.4 Metal-Catalyzed Hydroamination of Alkynes

1.4.1 Introduction to Hydroamination

Hydroamination is a selective and atom economical methodology for the formation of new carbon-nitrogen bonds.[53] It involves the addition of an N-H bond across a C-C multiple bond. This allows for the formation of a variety of structurally diverse amine, enamine, and imine products, which represent important building blocks in many organic frameworks.[53d] These products can be further functionalized into value-added, industrially relevant materials.[53d] The perfect atom economy of these reactions is particularly attractive since products of hydroamination can be obtained without the formation of unwanted by-products.

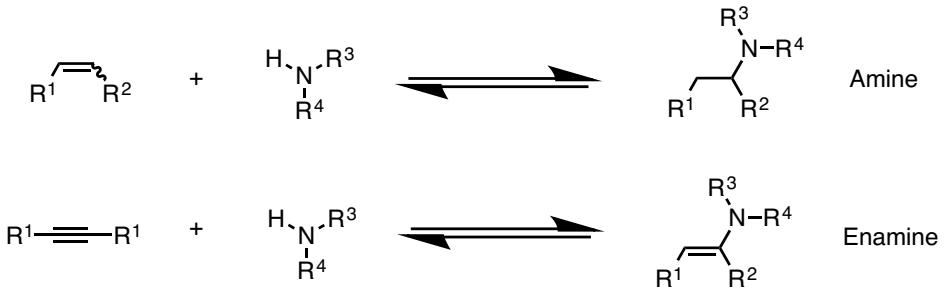

Scheme 1-13. General hydroamination of alkenes and alkynes

Direct addition of nitrogen nucleophiles across C-C multiple bonds in this manner represents an electronically unfavourable reaction, given repulsion of the nitrogen lone pair with the π-electrons of the alkyne or alkene lead to a negative entropy. Notwithstanding substrates (alkynes or alkenes) containing highly electron withdrawing groups, a catalyst is required to couple unactivated C-C multiple bonds with nitrogen nucleophiles. Although many catalyst systems have been developed to hydroaminate alkenes and allenes, research work featured in this document is focused on the hydroamination of alkynes.

1.4.2. Alkyne Hydroamination: Catalyst Development and Evolution

The first hydroamination of alkynes was realized nearly fourty years ago when Barluenga and coworkers were able to catalyze the hydroamination of terminal alkyl- and arylalkynes with secondary amines regioselectively using $HgCl_2$.[54] Subsequent work by Barluenga employed a $Tl(OAc)_3$ for the intermolecular hydroamination of phenylacetylene with aniline.[55] The use of toxic mercury and thallium in this work limited the substrate scope tolerance and further application. However, this work paved the way for future hydroamination development with alkynes. Since this pioneering work, a plethora of methodologies have emerged for the hydroamination of both internal and terminal alkynes. Early metal methodologies developed by Bergman applying Zr[56] and Ti[57] have allowed for the selective formation of both enamine and amine products. Although many hydroaminations have been conducted with early metal catalysts, the oxophilic nature of these metals requires the use of air and moisture-free environments. To complement this work late-metal catalysts including Ag,[58] Pd,[59] Pt,[60] Rh,[61] and Ru[62] have been developed that are able to furnish these types of products successfully. Although a great number of late-metals have been developed to address outstanding challenges within hydroamination chemistry, the focus of the document moving forward will be dedicated to the gold-catalyzed hydroamination of alkynes.

1.4.3 Gold-Catalyzed Hydroamination of Alkynes

Gold has emerged as a commonly utilized tool for alkyne hydroamination. It was realized in 1987 by Uchimoto,[63] however it received slight attention until around the year 2000. Since then, several gold-catalyzed hydroamination reactions have been developed incorporating a range of complex alkynes and a broad scope of nitrogen nucleophiles. Both

Au^{III} and cationic Au^{I} complexes have shown utility in the hydroamination of alkynes.[53a, 64] Many intramolecular methodologies applying gold catalysts have been described, however the intermolecular hydroamination remains a challenge. In 2003, Tanaka[65] was able to demonstrate the first example of intermolecular hydroamination applying a Au^{I} catalyst system to furnish a variety of imine products (Scheme 1-14). In 2006 Li also reported the Au^{III} hydroamination of terminal alkynes with anilines at room temperature (Scheme 1-14, **B**). These products could then be reduced with $NaBH_4$ to generate the target secondary amines.[66]

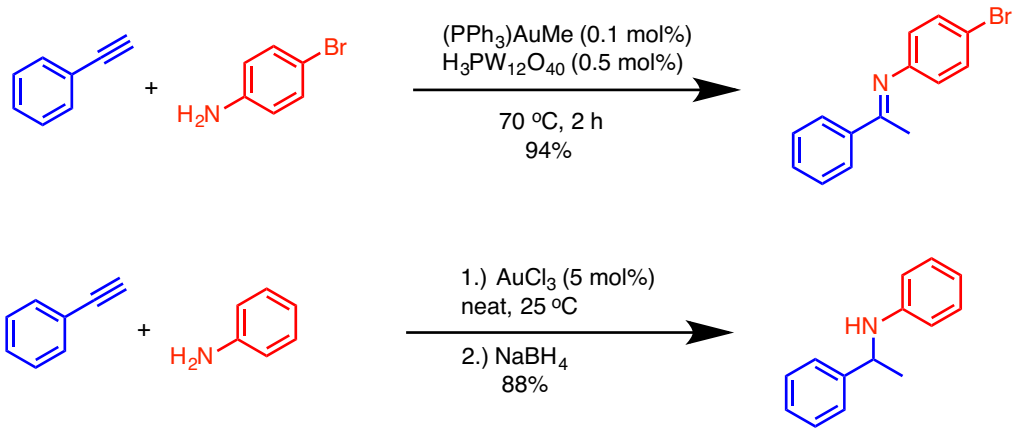

Scheme 1-14. First examples of intermolecular hydroamination with primary amines

Although this work represented a breakthrough in gold-catalyzed hydroamination many challenges remained. These first reports were conducted with terminal alkynes, which are directed toward an Markovnikov addition of the nitrogen nucleophile across the triple bond. The ability to control the regioselectivity of these reactions for unsymmetrical, internal alkynes remained unexplored. In 2010 the Stradiotto group was able to demonstrate the catalytic competency of a (Mor-DalPhos)AuCl pre-catalyst in the stereo- and regioselective hydroamination of internal alkynes with secondary dialkylamines.[67] Although this catalyst system demonstrated regioselectivity in gold-catalyzed

hydroamination, many questions still remained about the mechanism of action of Au-catalyzed hydroamination.

There are two generally accepted mechanisms for the gold-catalyzed hydroamination of alkynes: inner and outer-sphere (Scheme 1-15). The inner-sphere mechanism involves the complexation of an alkyne substrate to the carbophilic Au centre, followed by the formation of a gold-amido in the inner co-ordination sphere. Proton transfer would lead to the ultimate formation of the target imine product regenerating the catalytically active gold species. The second catalytic pathway involves an outer-sphere mechanism, whereby the alkyne substrate first complexes to the Au centre. The nitrogen nucleophile then attacks the now "activated" alkyne outer sphere generating a vinyl gold species which then eliminates via protonolysis, generating the target product.

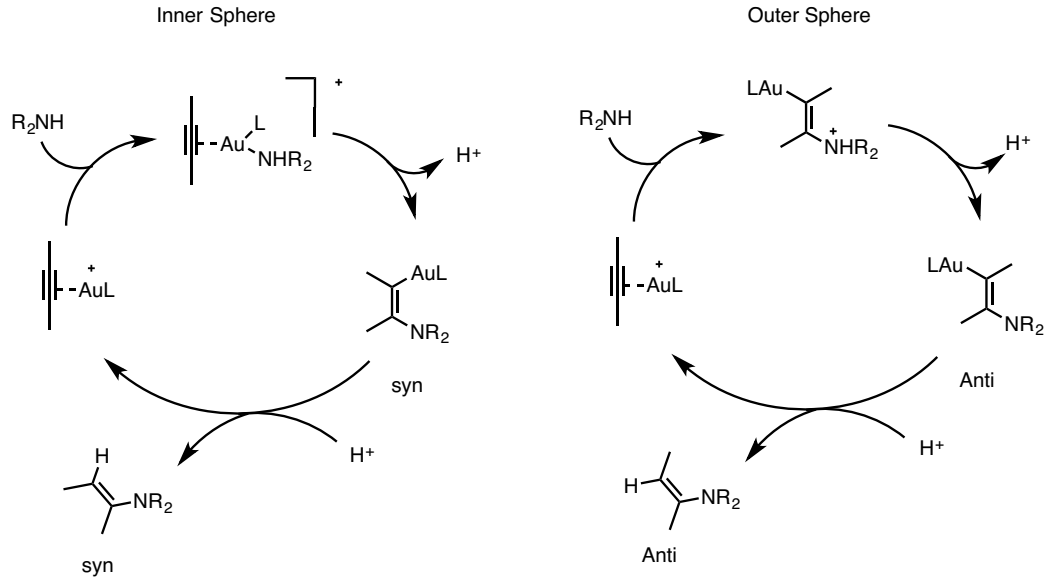

Scheme 1-15. Inner vs outer-sphere mechanism for gold-catalyzed hydroamination

A recent report by the Maier group has confirmed through strict mechanistic investigation that the outer sphere mechanism is the most likely pathway for gold-catalyzed hydroamination to generate the Markovnikov product.[68] Although a number of gold

pathways have been explored with numerous nitrogen reaction partners, the ability to understand the mechanism and specifically design ligands and Au complexes for this purpose can allow for more complex transformations with even more challenging reactants. Chapter Four of the thesis document will outline the hydrohydrazination of alkynes under mild conditions using bulky (PR_3)AuCl pre-catalyst complexes.

Chapter 2: Utilizing Mor-DalPhos/Palladium-Catalyzed Monoarylation in the Multicomponent One-Pot Synthesis of Indoles

2.1 Contributions

This chapter describes the palladium-catalyzed multicomponent synthesis of indoles via a one-pot protocol utilizing inexpensive and abundant dihaloarenes, amines, and ketones as starting materials to access more complex indole frameworks. This work was conducted in collaboration with a postdoctoral fellow, Andrey Borzenko, who contributed to the acetone substrate scope, as well as two former PhD students (Pamela Alsabeh and Chris Lavery) who conducted preliminary test experiments pertaining to the one-pot reactions reported herein.

2.2 Multicomponent Reactivity

2.2.1 An Introduction To Multicomponent Syntheses

Multicomponent reactions (MCRs) have emerged as efficient methodologies for the formation of structurally complex products.[69] The ability to access these highly decorated products has been a focal point of synthetic chemists for years. Many traditional synthetic routes require copious transformations in order to access the final product. Applying the knowledge of retrosynthesis and strategic catalyst design, these cumbersome protocols can be circumvented by the application of MCRs. An MCR typically involves the addition of three or more starting materials in a one-pot synthetic method to access a single product.[69] The isolation of unwanted intermediates is unnecessary in these processes, granting them advances from an atom economy perspective. With the emergence of late-metal catalyzed cross-coupling reactions, MCRs can be extended to incorporate a wide variety of starting materials and bond-forming processes.[70] These represent attractive synthetic routes to a

diversity of products, including pharmaceutically relevant, privileged heterocycles.[71] The synthesis of active pharmaceutical ingredients often requires many steps and complex transformations to access the final target compound.[72] If these elementary steps could be condensed into single reaction procedures this would represent a significant advancement for drug development. MCRs commonly involve several reaction conditions, varying substrates, temperatures, and solvents in a single reaction vessel. The need for strategically designed catalysts is essential for promoting these types of transformations. The catalyst must be robust enough to endure the reaction conditions, as well as selective enough as to not interfere with other reactants during the cascade pathway. In this context, a portion of my thesis research is focused on the development of a new, multicomponent one-pot synthesis of indoles.

2.2.2 The Indole Framework

The indole structure is one of the most ubiquitous heterocycles found in nature. It is also one of the most commonly observed heterocycles in novel drug discovery[73] and is an essential substructure of many biological processes due their ability to mimic natural products and bind to proteins.[74] Due to the number of substitution points and the biological activity, considerable work has been placed into synthesizing this privileged heterocycle. By far the most common synthetic protocol for constructing these compounds is the Fischer indole synthesis (Scheme 2-1).[75] This process begins with the reaction of an aryl hydrazine with a ketone or aldehyde under acidic conditions to form the enolizable aryl hydrazine. This enolizable species undergoes subsequent rearrangements and a nucleophilic attack of the enolized nitrogen. Upon subsequent loss of ammonia, the indole product is generated in good to excellent yield.[76]

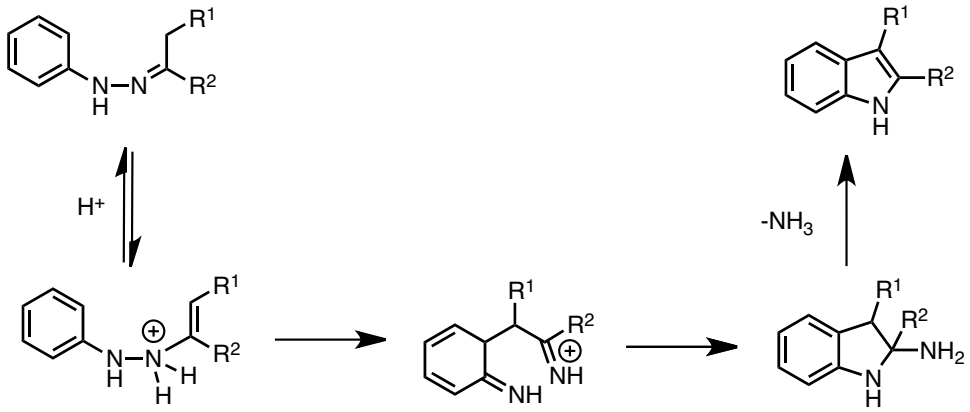

Scheme 2-1. The Fischer indole synthesis

This process has been the most commonly utilized synthetic protocol for indole synthesis for almost 100 years. However, there are several limitations associated with the Fischer indole synthesis. The ability to access aryl hydrazine synthons can be difficult and they are not commonly available starting materials. This leads to a lack of functional group tolerance within this protocol. Many metal-mediated routes have been developed as atom economical routes to access substituted indole structures (Scheme 2-2).[76] Palladium, in particular, has emerged as a successful metal for this type of chemistry.[77] The ability to harness palladium to form complex indoles from cheap feedstock chemicals make these attractive synthetic protocols.

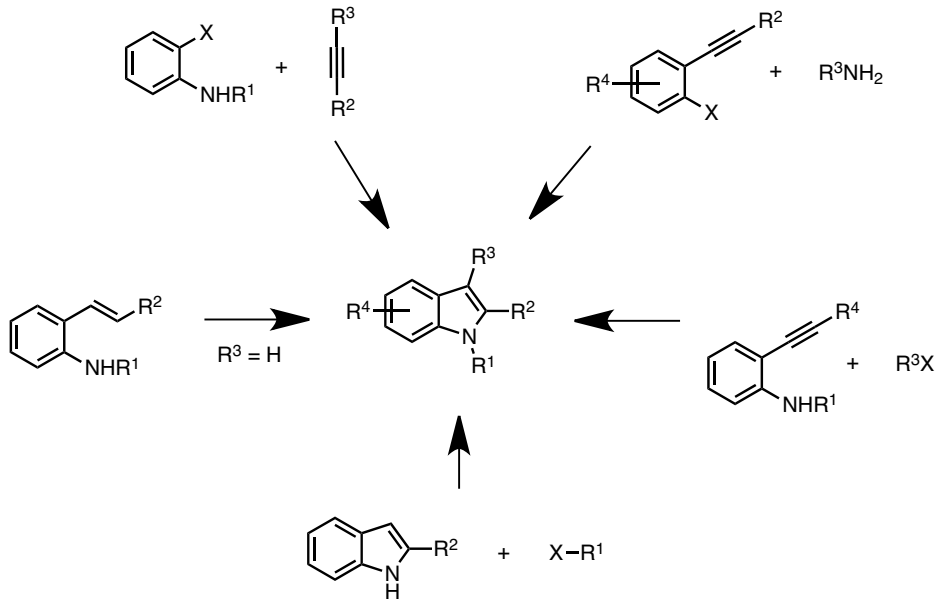

Scheme 2-2. Palladium-catalyzed indole syntheses

Many of these palladium-catalyzed protocols involve the formation of alkyne or alkene intermediates followed by a base-mediated cyclization (i.e. hydroamination) to access the target indole.[78] Commonly these intermediates must be isolated before the final cyclization step can take place. This can be a cumbersome process especially if the alkyne intermediate is volatile or particularly difficult to isolate. Buchwald has also developed 'decorative' processes to functionalize pre-formed indoles at the R^1 position.[79] In this context, the development of new multicomponent indole syntheses that exploit alternative disconnection strategies remains an important goal.

2.3 Motivation and Research Goals

As discussed in Chapter One of the thesis, Mor-DalPhos/Pd catalyst systems have been shown to promote the monoarylation of both amine and ketone substrates with a range of aryl electrophiles.[24, 25d, 80] This reactivity has been extended to incorporate particularly challenging nucleophiles including ammonia and hydrazine as well as challenging mono-

α-arylations utilizing acetone as the coupling partner. Encouraged by this unique reactivity, the Stradiotto group envisioned expanding and applying this methodology towards a new multicomponent indole synthesis that would utilize both methodologies (i.e. BHA and mono-α-arylation). This process would involve the use of commercially available *ortho*-dihaloarenes, alkyl ketones and primary amines (Scheme 2-3).

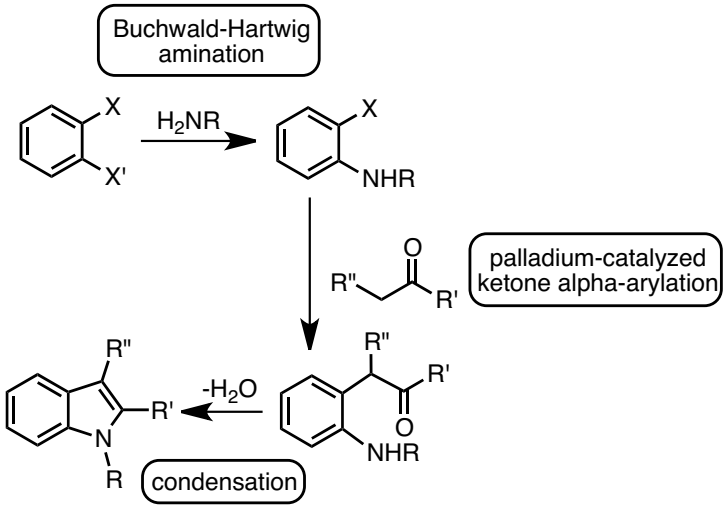

Scheme 2-3. Mechanism for proposed indole synthesis

This represents an attractive, streamlined synthesis of indoles due to the widespread availability of many alkyl ketone and primary amine coupling partners. During the course of our development of these syntheses, Kurth and co-workers[81] demonstrated the viability of such transformations employing dppf/$Pd_2(dba)_3$ catalyst mixtures. However, their described reaction system (10 examples, 52-69%) exhibits a number of important limitations, including: the absence of examples involving *ortho*-chlorohaloarenes, acyclic dialkyl ketones such as acetone, α-branched primary amines or anilines; the need for forcing conditions (130 °C, 48 h) and excess drying agent ($MgSO_4$) to promote the reaction; and the lack of demonstrated ability to conduct transformations in which all components are combined initially and without the strict exclusion of oxygen. As part of my thesis

research, my efforts were directed toward the development of a multicomponent indole synthesis of the type outlined in Scheme 2-3, which would address the issues associated with the synthesis reported by Kurth and co-workers.[81] The goal was to also extend this methodology to incorporate a one-step one-pot synthetic protocol whereby all of the reactants and catalysts could be added up-front to generate the target indole product.

2.4 Results and Discussion

2.4.1 Catalyst Optimization

For a preliminary exploration of the targeted indole synthesis 1-chloro-2-iodobenzene, octylamine, and acetone were chosen as reaction partners. The use of acetone was chosen specifically given the ubiquitous nature of this ketone and the potential applications of the derived 2-methylindoles.[82] Octylamine has proven to be an excellent test substrate for BHA reactions and was chosen as the primary amine coupling partner. Moreover, for the first time within an MCR sequence of this type, the unusual ability of Mor-DalPhos/Pd catalyst mixtures was exploited to promote the selective mono-α-arylation of acetone.[24] In a preliminary test reaction (Scheme 2-4), (Mor-DalPhos)Pd(η^1-cinnamyl)Cl (**2-C1**[25d])/Mor-DalPhos mixtures proved useful in catalyzing the chemoselective monoarylation of octylamine with 1-chloro-2-iodobenzene, affording *N*-(2-chlorophenyl)octylamine (**B**) in 96% isolated yield (4 mol% **2-C1**/2 mol% Mor-DalPhos, toluene, Cs_2CO_3, 90 ºC, 6 h unoptimized).

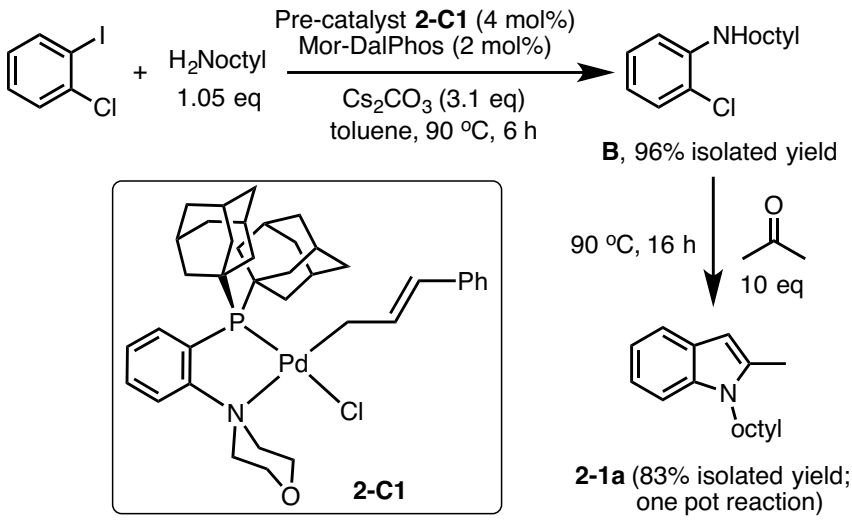

Scheme 2-4. Representative one-pot indole synthesis

Conversely, despite the established ability of Mor-DalPhos/Pd-based catalysts to promote the mono-α-arylation of acetone with various haloarene substrates under similar conditions when using acetone as the solvent,[24] the efforts to extend such reactivity to 1-chloro-2-iodobenzene using 10 equivalents of acetone proved inefficient. Nonetheless, it was observed that presumed mono-α-arylation of acetone occurs upon addition of 10 equivalents of acetone to the reaction flask upon formation of **B** as described above, followed by heating for an additional 16 h (unoptimized) at 90 °C, thus affording the desired 1-octyl-2-methyl-1*H*-indole (**2-1a**) in 83% isolated yield (Scheme 2-4).

2.4.2 Substrate Scope with Acetone

Having demonstrated for the first time the viability of utilizing acetone in the targeted one-pot, multicomponent assembly of indoles, the scope of reactivity was explored initially by varying the amine coupling partner, leading to the successful formation of **2-1b** to **2-1i** (35-90% isolated yield, Scheme 2-5). Gratifyingly, both α-branched primary amines (**2-1b** and **2-1c**) and substituted primary anilines (**2-1e** to **2-1i**) were successfully accommodated for the first time. The feasibility of employing 1-bromo-2-chlorobenzene

as the *ortho*-dihaloarene was demonstrated initially in the case of **2-1c**; additional examples are described in Section 2.4.4. Notably, the incorporation of either sterically demanding *ortho*-substituents or an electron-withdrawing group on the aniline afforded comparatively lower isolated yields of the desired indole (**2-1h** and **2-1i**, respectively). While definitive mechanistic data are lacking (*vide infra*), the established ability of Mor-DalPhos/Pd catalysts to promote BHAs involving various substituted primary anilines,[24, 80] in combination with the rather sterically unencumbered nature of the acetone reaction partner, suggests that reactivity problems arising when using such anilines may be attributable to the putative nucleophilic attack/condensation segment of the proposed reaction cascade (Scheme 2-3).

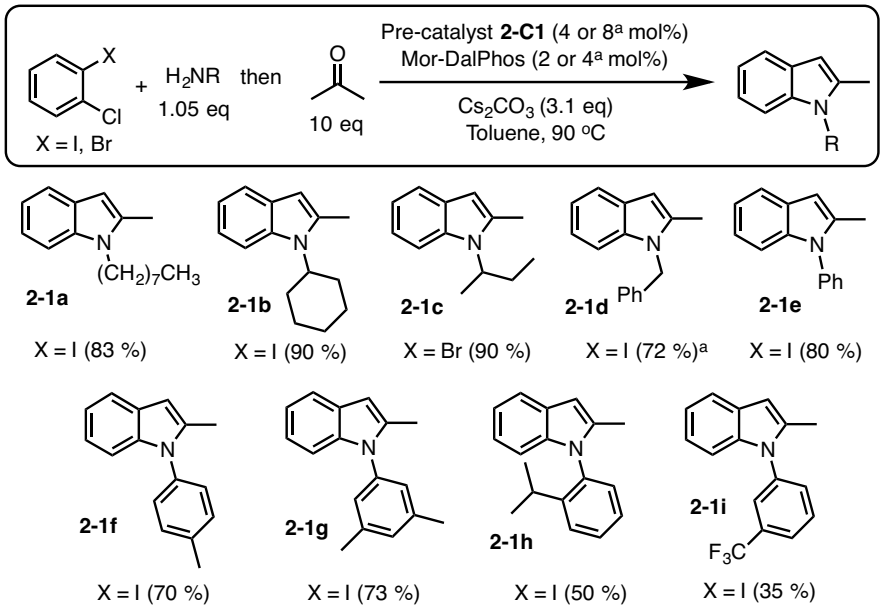

Scheme 2-5. Scope of reactivity applying acetone

2.4.3 Substrate Scope Varying the Ketone Coupling Partner

The focus was then shifted to varying the ketone coupling partner in combination with octylamine (Scheme 2-6). In replacing acetone as the coupling partner, the number of added ketone equivalents was reduced to two; in several test cases one equivalent of ketone

also afforded the desired indole in lower, yet acceptable, isolated yield. A broad spectrum of methyl ketones and related cyclic ketones were accommodated, leading to various 2-substituted *N*-octylindoles. Acetophenone performed well in this chemistry (affording **2-2a**, 63-82% isolated yield), as did related derivatives featuring *ortho*-, *meta*-, or *para*-substituted methyl, methoxy, or fluoro substituents (**2-2b** to **2-2g**, 70-81% isolated yield). Building on the new transformations involving acetone (Scheme 2-5), more complex acyclic alkyl methyl ketones could be employed with success in this chemistry for the first time (**2-2h**, 71%; **2-2i**, 78%), albeit requiring higher catalyst loadings. Each of these latter transformations confirms that the methyl ketone group is the preferred site of reactivity; indeed, efforts to incorporate alternative acyclic dialkylketones (e.g., 4-heptanone) were unsuccessful. Cyclic ketones and acetophenone derivatives featuring ester and ether functional groups performed well (**2-2k** to **2-2n**, 70-83% isolated yield), as did heteroaryl methyl ketones featuring pyridine, thiophene, and furan moieties (**2-2o** to **2-2r**, 65-73% isolated yield).

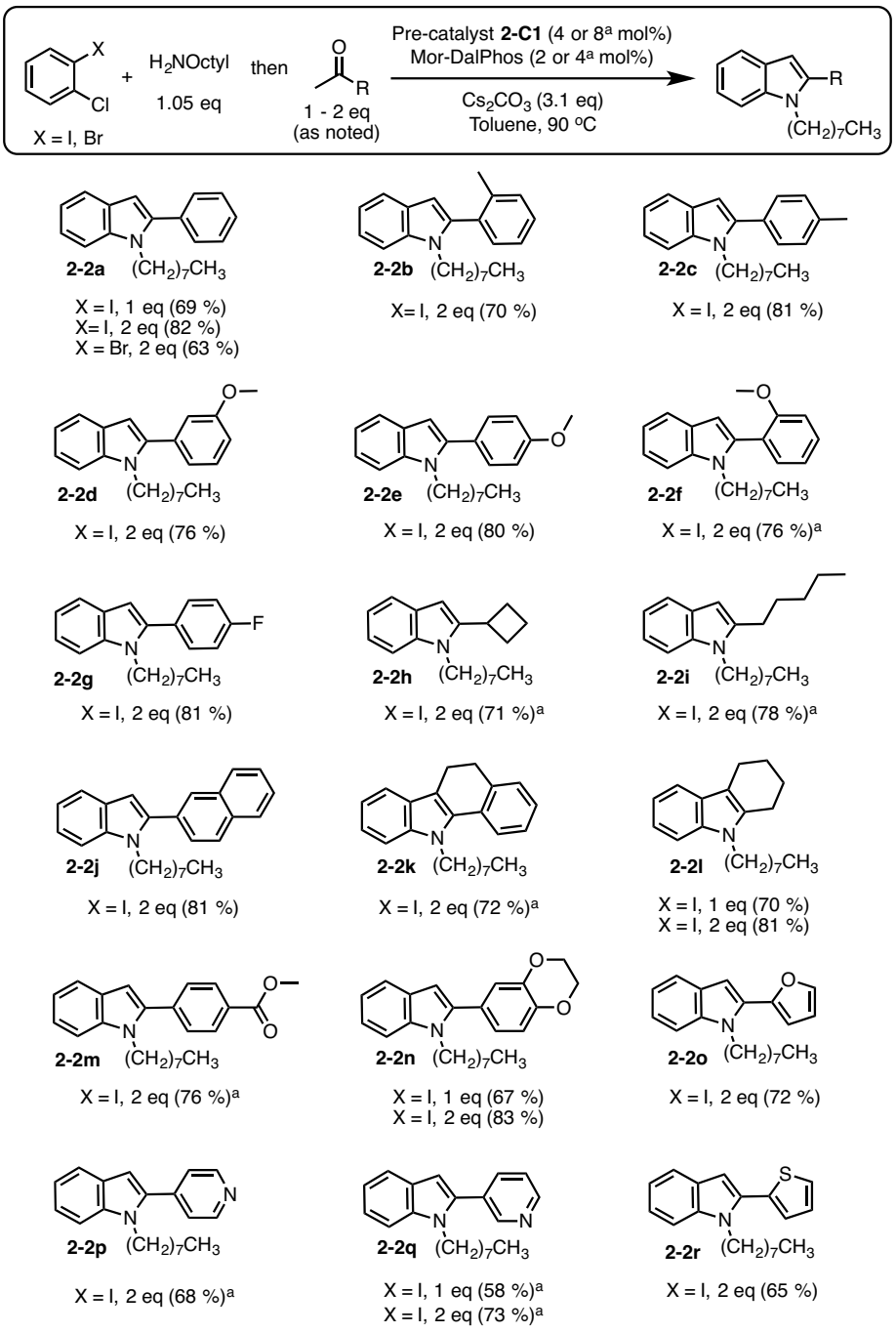

Scheme 2-6. Scope of reactivity applying different methyl ketones

2.4.4 One-Pot Reactions Under Non-Inert Conditions

The successful multicomponent indole syntheses described above (Schemes 2-5 and 2-6), as well as those described previously by Kurth and co-workers[81] were conducted with

strict exclusion of air in a two-step process whereby the ketone was added in a secondary step. In an effort to further probe the practical utility of the protocols described herein, a series of analogous test experiments were conducted in which all three reactants (i.e. *ortho*-chlorohaloarene, methyl ketone, and primary amine) were added at the start of the reaction, and whereby the reaction was conducted under an atmosphere of air, rather than purified dinitrogen (Scheme 2-7). For all substrate groupings examined, the reactions afforded the desired indole product. However, where direct comparisons were made, the isolated yields were found to be lower than those achieved when using one-pot, two-step multicomponent reaction protocols under inert-atmosphere conditions (Schemes 2-5 and 2-6). Nonetheless, transformations involving 1-chloro-2-iodobenzene or 1-bromo-2-chlorobenzene in combination with acetone or acetophenones and alkyl or aryl primary amines all proved viable. While not examined in detail, the ability to accommodate a functionalized 1-chloro-2-iodobenzene was confirmed in the three-component assembly of **2-3b** under non-inert atmosphere conditions.

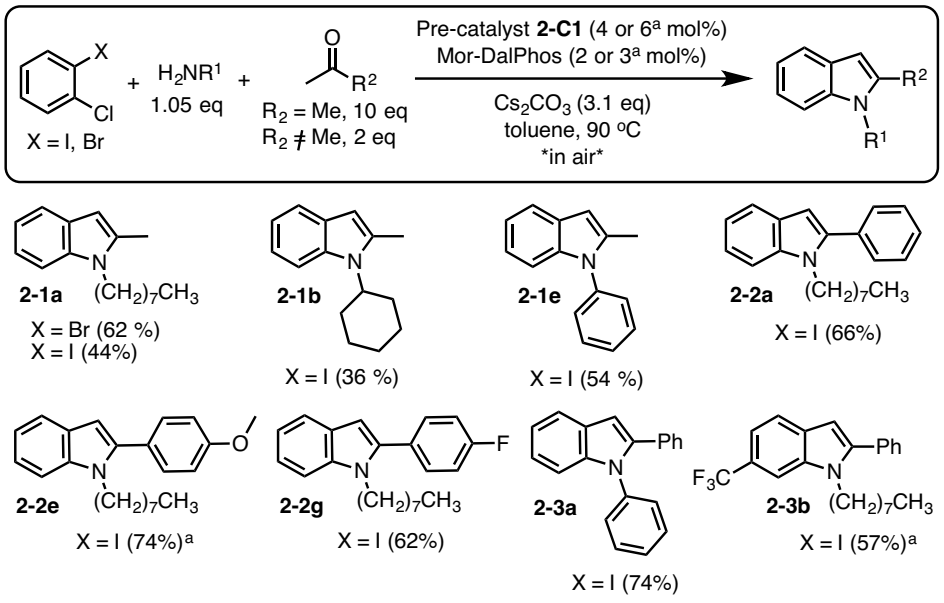

Scheme 2-7. Scope of reactivity applying a "true" one-pot synthesis

2.4.5 Examining the Reaction Pathway

The one-pot, two-step multicomponent indole synthesis proceeds via initial Buchwald-Hartwig amination of the *ortho*-chlorohaloarene; the efficiency and chemoselectivity of this step when using 1-chloro-2-iodobenzene and octylamine was demonstrated via the clean formation of **B** (Scheme 2-4). The corresponding indole can then be viewed as arising from the palladium-catalyzed mono-α-arylation of the subsequently added ketone, followed by the elimination of water (Scheme 2-3). This became of interest in evaluating if such a reaction sequence might be operational under the one-pot, one-step multicomponent reaction conditions featured in Scheme 2-7, in which the 1-chloro-2-iodobenzene, acetone (10 equiv.) or acetophenone (2 equiv.), and octylamine were each present at the start of the reaction.

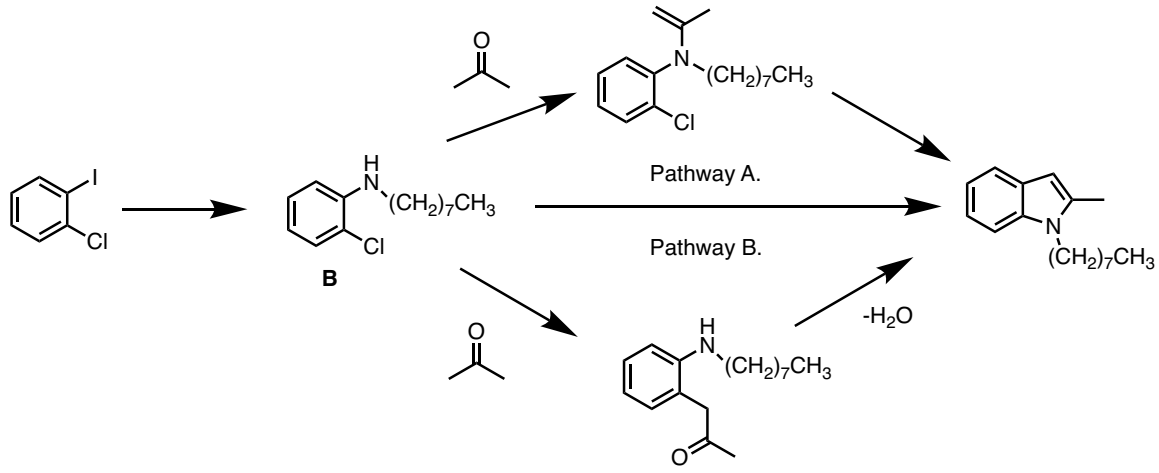

Scheme 2-8. Mechanistic investigation of indole formation

In monitoring the progress of catalytic reactions of this type by use of ^{1}H NMR spectroscopic and GC methods, the clean formation of **B** was observed early in all cases, with the product indoles **2-1a** (for acetone) and **2-2b** (for acetophenone) growing in with time in the absence of significant quantities of other observable intermediates. In combining

rationally prepared **B** and either of the mentioned ketones in toluene at 90 ºC in the absence of catalyst, no reaction was observed by use of ^{1}H NMR spectroscopic and GC methods (Pathway A). While this would appear to preclude facile, thermally promoted intermolecular imine formation (i.e. condensation) under the catalytic conditions employed herein, thereby providing indirect support for the intermediacy of a palladium-catalyzed ketone mono-α-arylation step involving **B** as suggested in Scheme 2-3, imine formation cannot be unequivocally ruled out as a key mechanistic step in the presence of Mor-DalPhos/Pd catalyst mixtures. The inability to observe the product of this putative ketone mono-α-arylation reaction involving **B** may be attributable to rapid intramolecular condensation that gives rise to indole formation (Pathway B). Collectively, the preliminary mechanistic observations suggest the possibility of a reaction mechanism (Scheme 2-3) that differs from that proposed by Kurth and co-workers[81] for the dppf/$Pd_2(dba)_3$ catalyst system using excess $MgSO_4$, in which the key involvement of enolate chemistry was discounted.

2.4.6 Attempts at Ammonia Coupling and Heteroindole Formation

Although a diverse range of substrates were accommodated in both the one and two-step indole protocols outlined in this chapter there were several limitations associated with this catalyst system that could not be overcome. The first and most notable was the inability to utilize ammonia as the amine coupling partner. Although palladium-catalyzed ammonia monoarylation is well-established, the target N-H indole was unattainable by either the one or two-step protocols employing a plethora of reaction conditions. This is likely due to complications arising from ammonia-promoted catalyst decomposition during the transmetalation step of the catalytic pathway (see Chapter Three for more details). This

represents a significant limitation due to the fact that a variety of commercially available indole-containing drug structures incorporate an N-H indole as the core motif.[83] The second limitation was the inability to accommodate dihaloheteroarenes as coupling partners. A number of dihalopyridines, thiophenes, and furans were attempted to access value-added heterocylic indole products, to no avail. In the case of thiophenes and furans poor conversion of the starting material was observed in the first-step BHA reaction. In the case of pyridine, significant formation of azine product was observed during the BHA step. This is due to the self-reaction of a dihalopyridine in the presence of catalyst to form an unwanted byproduct. Notwithstanding these limitations, a number of structurally diverse indole products were obtained utilizing this catalytic protocol.

2.5 Conclusions

In summary, a Mor-DalPhos/Pd catalyst system has proven effective in promoting the multicomponent assembly of substituted indoles (29 unique examples, 35-90%) from *ortho*-chlorohaloarenes (3 examples), alkyl ketones (19 examples), and primary amines (9 examples). Beyond enabling the use of lower reaction temperatures and shorter reaction times without the need for an additional drying agent, the described protocols represent an advance relative to the only other report of this type[81] with regard to substrate scope, including but not restricted to the use of *ortho*-chlorohaloarenes, α-branched primary amines and anilines, as well as acyclic dialkyl ketones such as acetone in apparent mono-α-arylation reactions. Furthermore, for the first time, MCRs in the synthesis of substituted indoles can be conducted successfully in a protocol whereby all reactants are combined at the outset of the reaction without the need for inert-atmosphere reaction conditions. Notably, the average isolated yield across all one-pot, multicomponent indole syntheses

reported herein was 70%, corresponding to an average yield of 89% across each of the three putative reaction steps (i.e. Buchwald-Hartwig amination, ketone mono-α-arylation, condensation).

2.6 Experimental: General Procedures and Characterization Data

2.6.1 General Considerations

Unless otherwise stated, all reactions were set up inside a nitrogen-filled inert atmosphere glovebox and worked-up in air using bench-top procedures. Toluene was deoxygenated by sparging with nitrogen gas followed by passage through an mBraun double column solvent purification system packed with alumina and copper-Q5 reactant and storage over activated 4 Å molecular sieves. Mor-DalPhos[13] and (Mor-DalPhos)Pd(η^1-cinnamyl)Cl **2-C1**[20] were prepared according to literature procedures; all other reagents, solvents and materials were used as received from commercial sources. Column chromatography was carried out using neutral alumina (150 mesh; Brockmann-III; activated). Preparatory thin layer chromatography was carried out using Silicycle (TLG-R1001B-341) glass backed TLC plates (extra hard layer, 60 Å, 1 mm thickness, indicator F-254). All ^{1}H NMR (500.1 MHz) and ^{13}C NMR (125.8 MHz) spectra were recorded at 300 K in $CDCl_3$. Chemical shifts are expressed in parts per million (ppm) using the solvent signal as an internal reference. Splitting patterns are indicated as follows: br, broad; s, singlet; d, doublet; t, triplet; q, quartet; m, multiplet. All coupling constants (*J*) are reported in Hertz (Hz). Mass spectra were obtained using ion trap (ESI) instruments operating in positive mode, and GC data were obtained on an instrument equipped with a SGE BP-5 column (30 m, 0.25 mm i.d.).

2.6.2 Synthetic Protocols

General Catalytic Procedure for the Formation of Indoles Using a "One-Pot, Two-Step" Protocol (GP2-1). Unless specified otherwise, pre-catalyst complex (Mor-DalPhos)Pd(η^1-cinnamyl)Cl **2-C1** (17.7 mg, 0.024 mmol), Mor-DalPhos (5.6 mg, 0.012 mmol), Cs_2CO_3 (606 mg, 1.8 mmol), amine (0.63 mmol), dihaloarene (0.6 mmol), and toluene (0.6 mL) were added to a screw-capped vial containing a small magnetic stir-bar. The vial was sealed with a cap containing a PTFE septum, removed from the glovebox, placed in a temperature-controlled aluminum heating block set at 90 °C, and vigorous magnetic stirring was initiated. The reaction progress was monitored qualitatively by use of GC methods. For example, in the case of reactions involving *n*-octylamine, upon formation of the independently prepared and characterized intermediate *N*-(2-chlorophenyl)octylamine **B** (6 h) the vial was removed from the heat, cooled to room temperature and returned to the glovebox. The cap was removed and the corresponding ketone (0.6-1.2 mmol as specified, except 10 equivalents in the case of acetone) was added to the reaction mixture. The PTFE septum cap was then re-affixed to the vial, the vial was removed from the glovebox and placed back on the aluminum heating block set at 90 °C for 16 h. Subsequently, the vial was removed from the heating block and left to cool to ambient temperature. The crude reaction mixture was dissolved in ethyl acetate (10 mL) and poured onto brine (10 mL). The layers were separated and the organic layer was extracted with ethyl acetate (2 x 10 mL). The organic fractions were combined, dried over Na_2SO_4 and concentrated under reduced pressure. The crude residue was purified by use of column chromatography over alumina or preparative thin layer chromatography using a

Silicycle (TLG-R1001B-341) glass-backed silica plate. Note that for reactions employing acetone, a resealable glass reaction vessel equipped with a PTFE stopper was employed.

General Catalytic Procedure for the Formation of Indoles Using a "One-Pot, One-Step" Protocol Under Non-Inert Atmosphere Conditions (GP2-2). Unless specified otherwise, pre-catalyst complex (Mor-DalPhos)Pd(η^1-cinnamyl)Cl **2-C1** (17.7 mg, 0.024 mmol), Mor-DalPhos (5.6 mg, 0.012 mmol), Cs_2CO_3 (606 mg, 1.8 mmol), octylamine (0.63 mmol), 1-chloro-2-iodobenzene (73.3 μL, 0.6 mmol), ketone (1.2 mmol), and toluene (0.6 mL) were all added to a screw-capped vial containing a small magnetic stir-bar within the glovebox. Please note that the use of the glovebox in this manner was necessitated by the location of the high-precision analytical balance within the laboratory. The vial was sealed with a cap containing a PTFE septum, removed from the glovebox, opened to an atmosphere of air for a minimum of three minutes and subsequently sealed under air. The vial was then placed in a temperature-controlled aluminum heating block set at 90 °C for 16 h. The vial was removed from the heating block and left to cool to ambient temperature. The crude reaction mixture was dissolved in ethyl acetate (10 mL) and poured onto brine (10 mL). The layers were separated and the organic layer was extracted with ethyl acetate (2 x 10 mL). The organic fractions were combined, dried over Na_2SO_4 and concentrated under reduced pressure. The crude residue was purified by use of column chromatography over alumina (see general considerations) or preparative thin layer chromatography using a glass-backed silica plate (see general considerations). Note that for reactions employing acetone, a resealable glass reaction vessel equipped with a PTFE stopper was employed.

Synthetic Procedure for the Synthesis of *N*-(2-chlorophenyl)octylamine, B. Pre-catalyst complex (Mor-DalPhos)Pd(η^1-cinnamyl)Cl **2-C1** (17.7 mg, 0.024 mmol), Mor-DalPhos (5.6 mg, 0.012 mmol), Cs_2CO_3 (606 mg, 1.8 mmol), octylamine (104.1 uL, 0.63 mmol), 1-chloro-2-iodobenzene (73.3 uL, 0.6 mmol), and toluene (0.6 mL) were added to a screw-capped vial containing a small magnetic stir-bar. The vial was sealed with a cap containing a PTFE septum, removed from the glovebox, placed in a temperature-controlled aluminum heating block set at 90 °C, and vigorous magnetic stirring was initiated. After 6 h the vial was removed from the heating block and left to cool to ambient temperature. The crude reaction mixture was dissolved in ethyl acetate (10 mL) and poured onto brine (10 mL). The layers were separated and the organic layer was extracted with ethyl acetate (2 x 10 mL). The organic fractions were combined, dried over Na_2SO_4 and concentrated under reduced pressure. The crude residue was purified by column chromatography. The title product was isolated as a brown oil (96%) over alumina using 100% hexanes as the eluent system. ^{1}H NMR (500 MHz, $CDCl_3$): δ 7.30 (d, *J* = 7.5 Hz, 1H), 7.19 (t, *J* = 7.8 Hz, 1H), 6.72-6.65 (m, 2H), 4.32 (s, 1H), 3.23-3.19 (m, 2H), 1.75-1.70 (m, 2H), 1.50-1.36 (m, 10H), 0.96 (t, *J* = 7.2 Hz, 3H); ^{13}C{^{1}H} NMR (125.8 MHz, $CDCl_3$): δ 144.6, 129.4, 128.1, 119.3, 117.1, 111.4, 44.0, 32.2, 29.7 (two signals), 29.6, 27.5, 23.0, 14.4. HRMS *m/z* ESI$^+$ found 240.1514 [M+H]$^+$ calculated for $C_{14}H_{23}ClN$ 240.1519.

2.6.3 Characterization Data

1-octyl-2-methyl-1*H*-indole (2-1a)

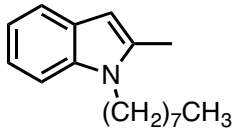

Following **GP2-1** (6 mmol acetone, 0.60 mmol 1-chloro-2-iodobenzene, 0.63 mmol octylamine) the title product was isolated as a yellow oil (83%). An ethyl acetate: hexanes (1:10) eluent system was used for preparatory thin layer chromatography. ^{1}H NMR (500 MHz, $CDCl_3$): δ 7.52 (d, *J* = 7.8 Hz, 1H), 7.29-7.25 (m, 1H), 7.13 (apparent t, *J* = 7.6 Hz, 1H), 7.05 (apparent t, *J* = 7.4 Hz, 1H), 6.24 (s, 1H), 4.05 (t, *J* = 7.5 Hz, 2H), 2.43 (s, 3H), 1,74 (m, 2H), 1.41-1.21 (m, 10H), 0.88 (t, *J* = 6.8 Hz, 3H); $^{13}C\{^{1}H\}$ NMR (125.8 MHz, $CDCl_3$): δ 136.7, 136.5, 128.2, 120.4, 119.8, 119.2, 109.1, 99.9, 43.4, 31.9, 30.4, 29.5, 29.4, 27.2, 22.8, 14.2, 13.0; HRMS *m/z* ESI$^+$ found 244.2050 $[M+H]^+$ calculated for $C_{17}H_{26}N$ 244.2065. Following **GP2-2** the title product was isolated as a yellow oil (44% from 1-chloro-2-iodobenzene; 62% from 1-bromo-2-iodobenzene). In all cases the spectral data were in agreement with the title compound.

1-cyclohexyl-2-methyl-1*H*-indole (2-1b)

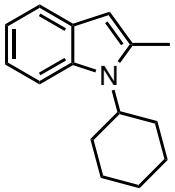

Following **GP2-1** (6 mmol acetone, 0.60 mmol 1-chloro-2-iodobenzene, 0.63 mmol cyclohexylamine) the title product was isolated as a yellow oil (90%). An ethyl acetate: hexanes (1:10) eluent system was used for preparatory thin layer chromatography. ^{1}H NMR (500 MHz, $CDCl_3$): δ 7.52 (d, *J* = 8.5 Hz, 2H), 7.10 (m, 1H), 7.04 (apparent t, *J* = 7.6 Hz, 1H), 6.23 (s, 1H), 4.17 (tt, *J* = 3.5, 12.4 Hz, 1H), 2.46 (s, 3H), 2.36-2.19 (m, 2H), 2.02-1.88 (m, 4H), 1.85-1.77 (m, 1H), 1.53-1.42 (m, 2H), 1.39-1.32 (m, 1H); $^{13}C\{^{1}H\}$ NMR (125.8 MHz, $CDCl_3$): δ 136.4, 135.8, 128.8, 120.0, 119.9, 118.9, 111.4, 100.7, 56.0, 31.7, 26.7, 25.7, 14.4; HRMS *m/z* ESI$^+$ found 214.1590 $[M+H]^+$ calculated for $C_{15}H_{20}N$ 214.1596.

Following **GP2-2** the title product was isolated as a yellow oil (36%, from 1-chloro-2-iodobenzene). In all cases the spectral data were in agreement with the title compound.

1-*sec*-butyl-2-methyl-1*H*-indole (2-1c)

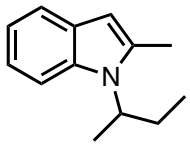

Following **GP2-1** (6 mmol acetone, 0.60 mmol 1-bromo-2-iodobenzene, 0.63 mmol isobutylamine) the title product was isolated as a yellow oil (90%). An ethyl acetate: hexanes (1:10) eluent system was used for preparatory thin layer chromatography. ^{1}H NMR (500 MHz, $CDCl_3$): δ 7.56-7.51 (m, 1H), 7.48-7.42 (m, 1H), 7.13-7.02 (m, 2H), 6.58-5.92 (s br, 1H), 4.42-4.28 (m, 1H), 2.45 (s, 3H), 2.32-2.13 (m, 1H), 1.99-1.83 (m, 1H), 1.62 (d, J = 11.7, 3H), 0.79 (t, J = 12.3 Hz, 3H); ^{13}C{^{1}H} NMR (125.8 MHz, $CDCl_3$): δ 136.9, 128.9, 120.0, 119.9, 118.9, 111.1, 100.5, 53.3, 28.7, 20.1, 14.3, 11.6; HRMS m/z ESI$^+$ found 188.1442 $[M+H]^+$ calculated for $C_{13}H_{18}N_1$ 188.1439.

benzyl-2-methyl-1*H*-indole (2-1d)

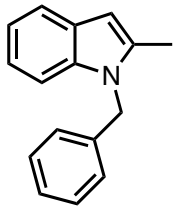

Following **GP2-1** (6 mmol acetone, 0.60 mmol 1-chloro-2-iodobenzene, 0.63 mmol benzylamine) the title product was isolated as a yellow oil (72%). An ethyl acetate: hexanes (1:10) eluent system was used for preparatory thin layer chromatography. ^{1}H NMR (500 MHz, $CDCl_3$): δ 7.60 (d, J = 7.6 Hz, 1H), 7.33-7.22 (m, 4H), 7.13 (m, 2H), 7.02 (d, J = 7.4 Hz, 2H), 6.37 (s, 1H), 5.35 (s, 2H), 2.41 (s, 3H); ^{13}C{^{1}H} NMR (125.8 MHz, $CDCl_3$):

δ138.1, 136.9, 129.0, 127.5, 126.2, 121.0, 119.9, 119.7, 109.4, 100.7, 46.7, 13.0; HRMS *m/z* ESI$^+$ found 222.1272 $[M+H]^+$ calculated for $C_{16}H_{16}N$ 222.1283.

1-phenyl-2-methyl-1*H*-indole (2-1e)

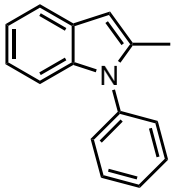

Following **GP2-1** (6 mmol acetone, 0.60 mmol 1-chloro-2-iodobenzene, 0.63 mmol aniline) the title product was isolated as a yellow oil (80%). An ethyl acetate: hexanes (1:10) eluent system was used for preparatory thin layer chromatography. ^{1}H NMR (500 MHz, $CDCl_3$): δ 7.59-7.56 (m, 1H), 7.55-7.51 (m, 2H), 7.45 (apparent t, *J* = 7.3 Hz, 1H), 7.36 (d, *J* = 7.8 Hz, 2H), 7.14-7.06 (m, 3H), 6.41 (s, 1H), 2.31 (s, 3H); ^{13}C{^{1}H} NMR (125.8 MHz, $CDCl_3$): δ 138.3, 138.1, 137.2, 129.6, 128.3, 128.1, 127.8, 121.2, 120.1, 119.7, 110.1, 101.4, 13.5; HRMS *m/z* ESI$^+$ found 208.1131 $[M+H]^+$ calculated for $C_{15}H_{14}N$ 208.1126. Following **GP2-2** the title product was isolated as a yellow oil (54%, from 1-chloro-2-iodobenzene). In all cases the spectral data were in agreement with the title compound.

2-Methyl-1-*p*-tolyl-1*H*-indole (2-1f)

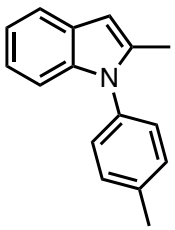

Following **GP2-1** (6 mmol acetone, 0.60 mmol 1-chloro-2-iodobenzene, 0.63 mmol *p*-toluidine) the title product was isolated as a yellow oil (70%). An ethyl acetate: hexanes (1:10) eluent system was used for preparatory thin layer chromatography. ^{1}H NMR (500 MHz, $CDCl_3$): δ 7.60 (d, *J* = 6.7 Hz, 1H), 7.37 (d, *J* = 8.0 Hz, 2H), 7.27 (d, *J* = 8.2 Hz, 2H),

7.16-7.08 (m, 3H), 6.43 (s, 1H), 2.50 (s, 3H), 2.33 (s, 3H); $^{13}C\{^{1}H\}$ NMR (125.8 MHz, $CDCl_3$): δ 138.5, 137.8, 137.4, 135.5, 130.2, 128.4, 128.0, 121.1, 120.1, 119.7, 110.3, 101.2, 21.4, 13.5; HRMS *m/z* ESI^+ found 222.1277 $[M+H]^+$ calculated for $C_{16}H_{16}N$ 222.1283.

1-(3,5-dimethylphenyl)-2-methyl-1H-indole (2-1g)

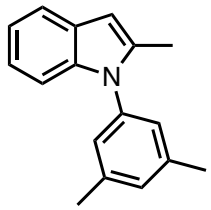

Following **GP1** (6 mmol acetone, 0.60 mmol 1-chloro-2-iodobenzene, 0.63 mmol 3,5-dimethylaniline) the title product was isolated as a yellow oil (73%). An ethyl acetate: hexanes (1:10) eluent system was used for preparatory thin layer chromatography. ^{1}H NMR (500 MHz, $CDCl_3$): δ 7.65-7.59 (m, 1H), 7.20-7.11 (m, 4H), 7.03 (s, 2H), 6.45 (s, 1H), 2.46 (s, 6H), 2.37 (s, 3H); $^{13}C\{^{1}H\}$ NMR (125.8 MHz, $CDCl_3$): δ 139.3, 138.5, 138.0, 137.3, 129.6, 128.4, 125.9, 121.0, 120.3, 119.7, 110.5, 101.3, 21.6, 13.6; HRMS *m/z* ESI^+ found 236.1434 $[M+H]^+$ calculated for $C_{17}H_{18}N$ 236.1439.

1-(2-isopropylphenyl)-2-methyl-1H-indole (2-1h)

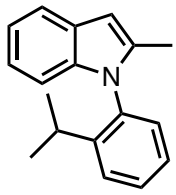

Following **GP2-1**, (6 mmol acetone, 0.60 mmol 1-chloro-2-iodobenzene, 0.63 mmol 2-diisopropylaniline) the title product was isolated as a yellow oil (50%). An ethyl acetate: hexanes (1:10) eluent system was used for preparatory thin layer chromatography. ^{1}H NMR (500 MHz, $CDCl_3$): δ 7.62 (d, J = 7.6 Hz, 1H), 7.57-7.50 (m, 2H), 7.36 (td, J = 2.1, 7.3 Hz,

1H), 7.20 (d, *J* = 7.7 Hz, 1H), 7.13 (t, *J* = 7.2 Hz, 1H), 7.09 (t, *J* = 7.2, 1H), 6.85 (d, *J* = 8.0, 1H), 6.45 (s, 1H), 2.50 (apparent septet, *J* = 1.9 Hz, 1H), 2.22 (s, 3H), 1.15 (d, *J* = 6.8 Hz, 3H), 1.08 (d, *J* = 6.8 Hz, 3H); $^{13}C\{^{1}H\}$ NMR (125.8 MHz, $CDCl_3$): δ 148.4, 139.0, 137.7, 135.5, 129.8, 129.4, 128.3, 127.1, 126.9, 121.1, 119.9, 119.7, 110.3, 110.6, 27.9, 24.4, 23.8, 13.2; HRMS *m/z* ESI^+ found 250.1592 $[M+H]^+$ calculated for $C_{18}H_{20}N$ 250.1596.

2-methyl-1-(3-(trifluoromethyl)phenyl)-1*H*-indole (2-1i)

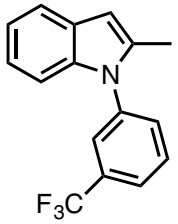

Following **GP2-1** (6 mmol acetone, 0.60 mmol 1-chloro-2-iodobenzene, 0.63 mmol 3-(trifluoromethyl)aniline) the title product was isolated as a yellow oil (35%). An ethyl acetate: hexanes (1:10) eluent system was used for preparatory thin layer chromatography. ^{1}H NMR (500 MHz, $CDCl_3$): δ 7.76 (d, *J* = 8.1 Hz, 1H), 7.74-7.67 (m, 2H), 7.63-7.58 (m, 2H), 7.20-7.09 (m, 3H), 6.47 (s, 1H), 3.11 (s, 3H); $^{13}C\{^{1}H\}$ NMR (125.8 MHz, $CDCl_3$): δ 138.9, 138.2, 136.8, 131.5, 130.4, 128.6, 125.1, 124.7, 121.8, 120.8, 120.1, 109.9, 102.5, 13.6; HRMS *m/z* ESI^+ found 276.1007 $[M+H]^+$ calculated for $C_{16}H_{13}F_3N$ 276.1000.

1-octyl-2-phenyl-1*H*-indole (2-2a)

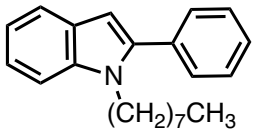

Following **GP2-1** (1.2 mmol ketone, 0.63 mmol octylamine), the title product was isolated as a dark brown oil (82 % from 1-chloro-2-iodobenzene; 63% from 1-bromo-2-iodobenzene). An ethyl acetate: hexanes (1:100) eluent system was used for column

chromatography. ^{1}H NMR (500 MHz, $CDCl_3$): δ 7.69 (d, *J* = 7.7 Hz, 1H), 7.56-7.50 (m, 4H), 7.48-7.44 (m, 2H), 7.29 (apparent t, *J* = 8.0 Hz, 1H), 7.19 (apparent t, *J* = 7.4 Hz, 1H), 6.58 (s, 1H), 4.20 (apparent t, *J* = 7.6 Hz, 2H), 1.78-1.72 (m, 2H), 1.33-1.23 (m, 10H), 0.92 (t, *J* = 7.1 Hz, 3H); ^{13}C{^{1}H} NMR (125.8 MHz, $CDCl_3$): δ 141.7, 137.7, 133.7, 129.8, 128.8, 128.6, 128.2, 121.8, 120.9, 120.0, 110.4, 102.4, 44.3, 32.1, 30.3, 29.4, 29.4, 27.1, 22.9, 14.4; HRMS *m/z* ESI^{+} found 328.2036 [M+Na]$^{+}$ calculated for $C_{22}H_{27}NNa$ 328.2041. Following **GP2-1** (0.6 mmol ketone, 0.63 mmol octylamine, using 1-chloro-2-iodobenzene) the title product was isolated as a dark brown oil (69%). Following **GP2-2** the title product was isolated as a dark brown oil (66% from 1-chloro-2-iodobenzene). In all cases the spectral data were in agreement with the title compound.

1-octyl-2-(*o*-tolyl)-1*H*-indole (2-2b)

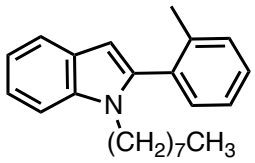

Following **GP2-1** (1.2 mmol ketone, 0.63 mmol octylamine, using 1-chloro-2-iodobenzene), the title product was isolated as a yellow oil (70 %). A 100 % hexanes eluent system was used for column chromatography. ^{1}H NMR (500 MHz, $CDCl_3$): δ 7.69 (d, *J* = 8 Hz, 1H), 7.44-7.36 (m, 4H), 7.33-7.26 (m, 2H), 7.19 (t, *J* = 7.5 Hz, 1H), 6.46 (s, 1H), 3.96 (apparent t, *J* = 7.2 Hz, 2H), 2.25 (s, 3H), 1.66-1.60 (m, 2H), 1.32-1.26 (m, 2H), 1.19-1.15 (m, 8H), 0.90 (t, *J* = 7.5 Hz, 3H); ^{13}C{^{1}H} NMR (125.8 MHz, $CDCl_3$): δ 140.3, 138.3, 136.8, 133.2, 131.5, 128.9, 129.61, 125.8, 121.4, 121.4, 129.8, 119.8, 110.2, 102.1, 44.0, 32.1, 30.1, 29.4, 29.3, 27.1, 22.9, 20.4, 14.4; HRMS *m/z* ESI^{+} found 342.2192 [M+Na]$^{+}$ calculated for $C_{23}H_{29}NNa$ 342.2198.

1-octyl-2-(*p*-tolyl)-1*H*-indole (2-2c)

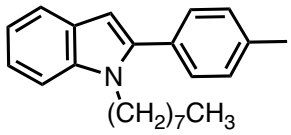

Following **GP2-1** (1.2 mmol ketone, 0.63 mmol octylamine, using 1-chloro-2-iodobenzene), the title product was isolated as a red-brown oil (81 %). An ethyl acetate: hexanes (1:100) eluent system was used for column chromatography. ^{1}H NMR (500 MHz, $CDCl_3$): δ 7.68 (d, *J* = 7.9 Hz, 1H), 7.44-7.42 (m, 3H), 7.32 (d, *J* = 7.9 Hz, 2H), 7.27 (apparent t, *J* = 8.1 Hz, 1H), 7.17 (t, *J* = 7.6 Hz, 1H), 6.54 (s, 1H), 4.18 (apparent t, *J* = 7.6 Hz, 2H), 2.48 (s, 3H), 1.78-1.72 (m, 2H), 1.32-1.23 (m, 2H), 1.22 (s, 8H), 0.92 (t, *J* = 7.1 Hz, 3H); ^{13}C{^{1}H} NMR (125.8 MHz, $CDCl_3$): δ 141.8, 138.1, 137.6, 130.8, 129.7, 129.5, 128.6, 121.7, 120.8, 120.0, 110.3, 102.1, 44.3, 32.1, 30.3, 29.4 (two signals), 27.1, 23.0, 21.6, 14.4; HRMS *m/z* ESI^{+} found 342.2192 [M+Na]$^{+}$ calculated for $C_{23}H_{29}NNa$ 342.2198.

2-(4-methoxyphenyl)-1-octyl-1*H*-indole (2-2d)

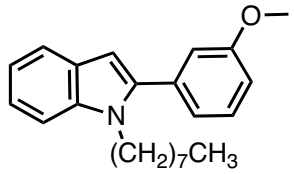

Following **GP2-1** (1.2 mmol ketone, 0.63 mmol octylamine, using 1-chloro-2-iodobenzene), the title product was isolated as a yellow oil (76 %). An ethyl acetate: hexanes (1:100) eluent system was used for column chromatography. ^{1}H NMR (500 MHz, $CDCl_3$): δ 7.68 (d, *J* = 7.8 Hz, 1H), 7.43 (apparent t, *J* = 8.1 Hz, 2H), 7.28 (apparent t, *J* = 8.1 Hz, 1H), 7.18 (apparent t, *J* = 7.4 Hz, 1H), 7.13 (d, *J* = 7.6 Hz, 1H), 7.09 (s, 1H), 7.01 (apparent d of d, *J* = 8.3 Hz, 1H), 6.58 (s, 1H), 4.21 (t, *J* = 7.6 Hz, 2H), 3.91 (s, 3H), 1.77-1.74 (m, 2H), 1.32-1.23 (m, 10H), 0.91 (t, *J* = 7.2 Hz, 3H); ^{13}C{^{1}H} NMR (125.8 MHz,

$CDCl_3$): δ 159.9, 141.5, 137.7, 135.0, 129.8, 128.5, 122.2, 121.8, 120.9, 120.0, 115.4, 113.9, 110.4, 102.4, 55.6, 44.4, 32.1, 30.3, 29.4 (two signals), 27.1, 22.9, 14.4; HRMS *m/z* ESI$^+$ found 358.2141 $[M+Na]^+$ calculated for $C_{23}H_{29}NNaO$ 358.2147.

2-(4-methoxyphenyl)-1-octyl-1*H*-indole (2-2e)

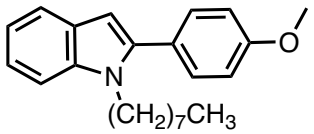

Following **GP2-1** (1.2 mmol ketone, 0.63 mmol octylamine, using 1-chloro-2-iodobenzene), the title product was isolated as a brown oil (80 %). An ethyl acetate: hexanes (1:100) eluent system was used for column chromatography. ^{1}H NMR (500 MHz, $CDCl_3$): δ 7.63 (d, *J* = 7.8 Hz, 1H), 7.42 (d, *J* = 8.7 Hz, 2H), 7.38 (d, *J* = 8.2 Hz, 1H), 7.22 (apparent t, *J* = 7.2 Hz, 1H), 7.13 (apparent t, J = 7.2 Hz, 1H), 7.01 (d, J = 8.7 Hz, 2H) 6.47 (s, 1H), 4.12 (apparent t, *J* = 7.7 Hz, 2H), 3.89 (s, 3H), 1.70 (apparent t, *J* = 7.4 Hz, 2H), 1.27-1.19 (m, 10H), 0.87 (t, *J* = 7.1 Hz, 3H); ^{13}C{^{1}H} NMR (125.8 MHz, $CDCl_3$): δ 159.8, 141.5, 137.5, 131.0, 128.6, 126.1, 121.5, 120.7, 120.0, 114.3, 110.3, 101.9, 55.7, 44.2, 32.1, 30.3, 29.4, 29.4, 27.1, 23.0, 14.4; HRMS *m/z* ESI$^+$ found 358.2141 $[M+Na]^+$ calculated for $C_{23}H_{29}NNaO$ 358.2147. Following **GP2-2**, the title compound was isolated as a brown oil (74%, from 1-chloro-2-iodobenzene). In all cases the spectral data were in agreement with the title compound.

2-(2-methoxyphenyl)-1-octyl-1*H*-indole (2-2f)

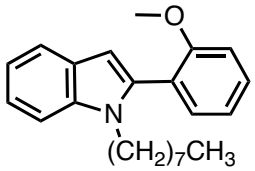

Following **GP2-1** (1.2 mmol ketone, 0.63 mmol octylamine, using 1-chloro-2-iodobenzene), the title product was isolated as a dark brown oil (76 %). An ethyl acetate: hexanes (1:50) eluent system was used for column chromatography. ^{1}H NMR (500 MHz, $CDCl_3$): δ 7.65 (d, *J* = 7.9 Hz, 1H), 7.44 (apparent t, *J* = 7.7 Hz, 1H), 7.39-7.34 (m, 2H), 7.22 (apparent t, *J* = 7.3 Hz, 1H), 7.12 (apparent t, *J* = 7.5 Hz, 1H), 7.06 (apparent t, *J* = 7.4 Hz, 1H), 7.01 (d, *J* = 8.4 Hz, 1H), 6.47 (s, 1H), 3.99 (apparent t, *J* = 7.5 Hz, 2H), 3.80 (s, 3H), 1.66-1.61 (m, 2H), 1.27-1.22 (m, 2H), 1.15-1.11 (m, 8H), 0.87 (t, *J* = 7.1 Hz, 3H); ^{13}C{^{1}H} NMR (125.8 MHz, $CDCl_3$): δ 157.8, 138.4, 137.1, 133.1, 130.3, 128.6, 122.8, 121.4, 120.9, 120.9, 119.5, 111.2, 110.2, 102.3, 55.8, 44.5, 32.1, 30.0, 29.4 (two signals), 27.2, 22.9, 14.4; HRMS *m/z* ESI^{+} found 358.2141 $[M+Na]^{+}$ calculated for $C_{23}H_{29}NNaO$ 358.2147.

2-(4-fluorophenyl)-1-octyl-1*H*-indole (2-2g)

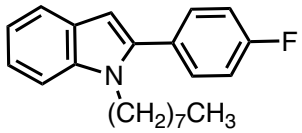

Following **GP2-1** (1.2 mmol ketone, 0.63 mmol octylamine, using 1-chloro-2-iodobenzene), the title product was isolated as a dark brown oil (81 %). A 100 % hexanes eluent system was used for column chromatography. ^{1}H NMR (500 MHz, $CDCl_3$): δ 7.69 (d, *J* = 7.9 Hz, 1H), 7.50 (d of d, *J* = 8.6 Hz, 2H), 7.43 (d, *J* = 8.4 Hz, 1 H), 7.29 (apparent t, *J* = 7.7 Hz, 1H), 7.23-7.18 (m, 3H), 6.54 (s, 1H), 4.15 (t, *J* = 7.7 Hz, 2H), 1.75-1.70 (m,

2H), 1.33-1.23 (m, 10H), 0.92 (t, J = 7.3 Hz, 3H); $^{13}C\{^{1}H\}$ NMR (125.8 MHz, $CDCl_3$): δ 164.0, 162.0, 140.5 137.6, 131.5 (d, J_{CF} = 32.3 Hz), 129.8 (J_{CF} = 12.2 Hz), 128.5, 121.9, 120.9, 120.2, 115.9, 115.8, 110.4, 102.5, 44.3, 32.1, 30.3, 29.4, 27.1, 22.9, 14.4. Following **GP2-2**, the title product was isolated as a dark brown oil (62%, from 1-chloro-2-iodobenzene). In all cases the spectral data were in agreement with the title compound.

2-cyclobutyl-1-octyl-1*H*-indole (2-2h)

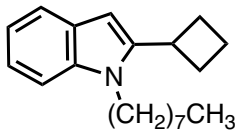

Following **GP2-1** (1.2 mmol ketone, 0.63 mmol octylamine, using 1-chloro-2-iodobenzene), the title product was isolated as a brown oil (71 %). An ethyl acetate: hexanes (1:100) eluent system was used for column chromatography. ^{1}H NMR (500 MHz, $CDCl_3$): δ 7.61 (d, J = 7.8 Hz, 1H), 7.31 (d, J = 7.8 Hz, 1H), 7.19 (apparent t, J = 7.2 Hz, 1H), 7.11 (apparent t, J = 7.3 Hz, 1H), 6.37 (s, 1H), 4.02 (apparent t, J = 7.7 Hz, 2H), 3.70 (quint, J = 8.4 Hz, 1H), 2.51-2.45 (m, 2H), 2.36-2.28 (m, 2H), 2.20-2.10 (m, 1H), 2.05-1.98 (m, 1H), 1.80-1.74 (m, 2H), 1.43-1.33 (m, 10H), 0.95 (t, 6.7 Hz, 3H); $^{13}C\{^{1}H\}$ NMR (125.8 MHz, $CDCl_3$): δ 145.3, 137.1, 128.3, 120.8, 120.3, 119.4, 109.4, 97.6, 43.8, 33.0, 32.2, 30.7, 30.6, 29.7, 29.6 (two signals), 27.6, 23.0, 19.1, 14.4; HRMS m/z ESI^+ found 306.2192 $[M+Na]^+$ calculated for $C_{20}H_{29}NNa$ 306.2198.

2-hexyl-1-octyl-1*H*-indole (2-2i)

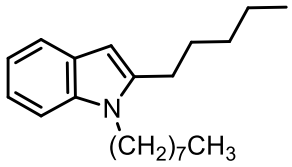

Following **GP2-1** (1.2 mmol ketone, 0.63 mmol octylamine, using 1-chloro-2-iodobenzene), the title product was isolated as a dark brown oil (78 %). An ethyl acetate: hexanes (1:100) eluent system was used for column chromatography. ^{1}H NMR (500 MHz, $CDCl_3$): δ 7.58 (d, *J* = 7.8 Hz, 1H), 7.32-7.30 (m, 1H), 7.17 (apparent t, *J* = 7.2 Hz, 1H), 7.10 (apparent t, *J* = 7.2 Hz, 1H), 6.29 (s, 1H), 4.09 (apparent t, *J* = 7.7 Hz, 2H), 2.76 (t, *J* = 7.7 Hz, 2H), 1.83-1.78 (m, 4H), 1.49-1.32 (m, 16H), 0.99 (t, *J* = 7.2 Hz, 3H), 0.93 (t, *J* = 6.7 Hz, 3H); ^{13}C{^{1}H} NMR (125.8 MHz, $CDCl_3$): δ 141.4, 136.9, 128.4, 120.6, 120.1, 119.4, 109.4, 98.9, 43.5, 32.1 (two signals), 30.6, 29.7, 29.5, 28.6, 27.5, 27.0, 23.0, 22.9, 14.4 (two signals). HRMS *m/z* ESI^{+} found 300.2686 [M+H]$^{+}$ calculated for $C_{21}H_{34}N$ 300.2691.

2-(naphthalene-2-yl)-1-octyl-1*H*-indole (2-2j)

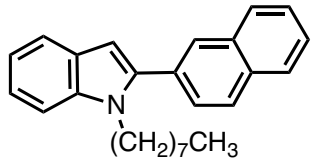

Following **GP2-1** (1.2 mmol ketone, 0.63 mmol octylamine, using 1-chloro-2-iodobenzene), the title product was isolated as a brown oil (81 %). An ethyl acetate: hexanes (1:50) eluent system was used for column chromatography. ^{1}H NMR (500 MHz, $CDCl_3$): δ 8.02-7.94 (m, 4H), 7.72 (d, *J* = 7.8 Hz, 1H), 7.67 (d, *J* = 8.4 Hz, 1H), 7.61-7.57 (m, 2H), 7.47 (d, *J* = 8.2 Hz, 1H), 7.32-7.29 (m, 1H), 7.21 (apparent t, *J* = 7.4 Hz, 1H), 6.68 (m, 1H), 4.27 (t, *J* = 7.6 Hz, 2H), 1.79-1.75 (m, 2H), 1.26-1.14 (m, 10H), 0.87 (t, *J* = 7.1 Hz, 3H);

$^{13}C\{^{1}H\}$ NMR (125.8 MHz, $CDCl_3$): δ 141.7, 137.9, 133.6, 133.1 (two signals), 128.7 (two signals), 128.5, 128.4, 128.1, 127.6, 126.8, 126.7, 121.9, 121.0, 120.1, 110.5, 102.9, 44.5, 32.0, 30.3, 29.4 (two signals), 27.1, 22.9, 14.4; HRMS *m/z* ESI^+ found 378.2192 $[M+Na]^+$ calculated for $C_{26}H_{29}NNa$ 378.2918.

11-octyl-6,11-dihydro-5*H*-benzo[*a*]carbazole (2-2k)

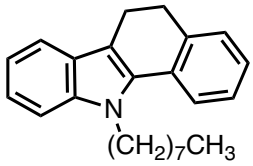

Following **GP2-1** (1.2 mmol ketone, 0.63 mmol octylamine, using 1-chloro-2-iodobenzene), the title product was isolated as a dark purple oil (72 %). An ethyl acetate: hexanes (1:10) eluent system was used for column chromatography. ^{1}H NMR (500 MHz, $CDCl_3$): δ 7.63-7.59 (m, 2H), 7.42-7.34 (m, 3H), 7.30-7.21 (m, 2H), 7.18 (apparent t, *J* = 7.5 Hz, 1H), 4.43 (t, *J* = 8.0 Hz, 2H), 3.04-3.01 (m, 2H), 2.98-2.95 (m, 2H), 2.01-1.96 (m, 2H), 1.49-1.33 (m, 10H; overlapping with water), 0.94 (m, 3H); $^{13}C\{^{1}H\}$ NMR (125.8 MHz, $CDCl_3$): δ 139.1, 138.6, 130.1, 129.1, 127.0, 126.5 (two signals), 122.3 (two signals), 119.7, 119.1, 114.5, 110.0, 45.6, 32.1, 31.2, 30.8, 29.6 (two signals), 27.3, 23.0, 20.5, 14.4; HRMS *m/z* ESI^+ found 332.2373 $[M+H]^+$ calculated for $C_{24}H_{30}N$ 332.2378.

9-octyl-2,3,4,9-tetrahydro-1*H*-carbazole (2-2l)

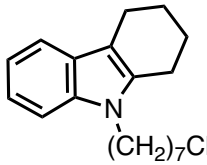

Following **GP2-1** (1.2 mmol ketone, 0.63 mmol octylamine, using 1-chloro-2-iodobenzene), the title product was isolated as a light brown oil (81 %). An ethyl acetate: hexanes (1:100) eluent system was used for column chromatography. ^{1}H NMR (500 MHz,

$CDCl_3$): δ 7.52 (d, *J* = 8.0 Hz, 1H), 7.31 (d, *J* = 8.0 Hz, 1H), 7.19 (t, *J* = 7.2 Hz, 1H), 7.11 (t, *J* = 7.6 Hz, 1H), 4.04 (t, *J* = 7.4 Hz, 2H), 2.78 (m, 4H), 2.00 (m, 2H), 1.92 (m, 2H), 1.78 (apparent q, *J* = 7.6 Hz, 2H), 1.34 (m, 10H), 0.95 (t, *J* = 6.6 Hz, 3H); $^{13}C\{^1H\}$ NMR (125.8 MHz, $CDCl_3$): δ 136.4, 135.6, 127.6, 120.7, 118.8, 118.1, 109.5, 109.1, 43.3, 32.2, 30.8, 29.7, 29.6, 27.5, 23.7, 23.6, 23.0, 22.7, 21.5, 14.4; HRMS *m/z* ESI^+ found 306.2178 $[M+Na]^+$ calculated for $C_{20}H_{29}NNa$ 306.2198. Following **GP2-2** (0.6 mmol ketone, 0.63 mmol octylamine, using 1-chloro-2-iodobenzene), the title product was isolated as a light brown oil (70 %). In all cases the spectral data were in agreement with the title compound.

methyl 4-(1-octyl-1*H*-indol-2-yl)benzoate (2-2m)

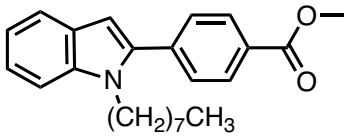

Following **GP2-1** (1.2 mmol ketone, 0.63 mmol octylamine, using 1-chloro-2-iodobenzene), the title product was isolated as a dark brown oil (76 %). An ethyl acetate: hexanes (1:50) eluent system was used for column chromatography. ^1H NMR (500 MHz, $CDCl_3$): δ 8.18 (d, *J* = 8.3 Hz, 2H) 7.69 (d, *J* = 7.9 Hz, 1H), 7.62 (d, *J* = 8.4 Hz, 2H), 7.44 (d, *J* = 8.3 Hz, 1H), 7.30 (apparent t, *J* = 6.1 Hz, 1H), 7.19 (apparent t, *J* = 7.2 Hz, 1H), 6.64 (s, 1H), 4.20 (apparent t, *J* = 7.6 Hz, 2H), 4.01 (s, 3H), 1.75-1.69 (m, 2H), 1.33-1.20 (m, 10H), 0.89 (t, *J* = 7.0 Hz, 3H); $^{13}C\{^1H\}$ NMR (125.8 MHz, $CDCl_3$): δ 167.2, 140.5, 138.2, 130.1, 129.7, 129.5, 128.5, 122.4, 121.2, 120.3, 110.5, 103.5, 52.5, 44.5, 32.1, 30.3, 29.4, 29.3, 27.1, 22.9 14.4; HRMS *m/z* ESI^+ found 386.2091 $[M+Na]^+$ calculated for $C_{24}H_{29}NNaO_2$ 386.2096.

2-(2,3-dihydrobenzo[*b*][1,4]dioxin-6-yl)-1-octyl-1*H*-indole (2-2n)

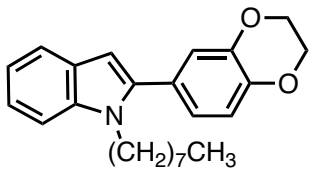

Following **GP2-1** (1.2 mmol ketone, 0.63 mmol octylamine, using 1-chloro-2-iodobenzene), the title product was isolated as a brown oil (83 %). An ethyl acetate: hexanes (1:100) eluent system was used for column chromatography. ^{1}H NMR (500 MHz, $CDCl_3$): δ 7.62 (d, *J* = 7.9 Hz, 1H), 7.37 (d, *J* = 8.2 Hz, 1H), 7.22 (apparent t, *J* = 7.3 Hz, 1H), 7.12 (apparent t, *J* = 7.1 Hz, 1H), 7.01 (s, 1H), 6.98-6.95 (m, 2H), 6.46 (s, 1H), 4.32 (s, 4H), 4.14 (apparent t, *J* = 7.6 Hz, 2H), 1.72-1.69 (m, 2H), 1.30-1.20 (m, 10H), 0.88 (t, *J* = 7.0 Hz, 3H); ^{13}C{^{1}H} NMR (125.8 MHz, $CDCl_3$): δ 143.9, 143.7, 141.3, 137.6, 128.5, 127.0, 123.0, 121.6, 120.8, 120.0, 118.7, 117.6, 110.3, 102.0, 64.8 (two signals), 44.2, 32.1, 30.3, 29.5, 29.4, 27.1, 23.0, 14.4; HRMS *m/z* ESI^{+} found 386.2091 [M+Na]$^{+}$ calculated for $C_{24}H_{29}NNaO_2$ 386.2096. Following **GP2-2** (0.6 mmol ketone, 0.63 mmol octylamine, using 1-chloro-2-iodobenzene), the title product was isolated as a brown oil (67 %). In all cases the spectral data were in agreement with the title compound.

2-(furan-2-yl)-1-octyl-1*H*-indole (2-2o)

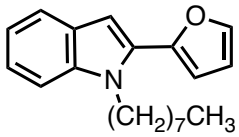

Following **GP2-1** (1.2 mmol ketone, 0.63 mmol octylamine, using 1-chloro-2-iodobenzene), the title product was isolated as a dark brown oil (72 %). An ethyl acetate: hexanes (1:100) eluent system was used for column chromatography. ^{1}H NMR (500 MHz, $CDCl_3$): δ 7.64 (d, *J* = 13.0 Hz, 1H), 7.56 (m, 1H), 7.38 (d, *J* = 13.8 Hz, 1H), 7.28-7.22 (m,

1H), 7.16-7.11 (m, 1H), 6.78 (s, 1H), 6.61 (apparent d, J = 5.6 Hz, 1H), 6.56-6.53 (m, 1H), 4.34 (apparent t, J = 12.7 Hz, 2H), 1.88-1.78 (m, 2H), 1.39-1.29 (m, 10H), 0.91 (apparent t, J = 11.6 Hz, 3H); $^{13}C\{^{1}H\}$ NMR (125.8 MHz, $CDCl_3$): δ 147.9, 142.6, 137.9, 130.9, 128.1, 122.3, 121.1, 120.2, 111.7, 110.0, 108.5, 101.9, 45.0, 32.1, 30.5, 29.6, 29.5, 27.3, 23.0, 14.4; HRMS m/z ESI^+ found 318.1828 $[M+Na]^+$ calculated for $C_{20}H_{25}NNaO$ 318.1834.

1-octyl-2-(pyridin-4-yl)-1*H*-indole (2-2p)

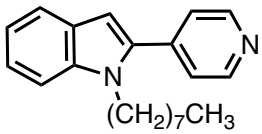

Following **GP2-1** (1.2 mmol ketone, 0.63 mmol octylamine, using 1-chloro-2-iodobenzene), the title product was isolated as a brown oil (68 %). An ethyl acetate: hexanes (1:10) eluent system was used for column chromatography. ^{1}H NMR (500 MHz, $CDCl_3$): δ 8.73-8.71 (m, 2H), 7.68 (d, J = 13.0 Hz, 1H), 7.45-7.41 (m, 3H), 7.32-7.27 (m, 1H), 7.20-7.15 (m, 1H), 6.68 (s, 1H), 4.21 (apparent t, J = 12.7 Hz, 2H), 1.77-1.67 (m, 2H), 1.30-1.20 (m, 10H), 0.88 (t, J = 11.1 Hz, 3H); $^{13}C\{^{1}H\}$ NMR (125.8 MHz, $CDCl_3$): δ 150.4, 141.3, 138.6, 138.5, 128.3, 123.8 (two signals), 122.9, 121.4, 120.6, 110.7, 104.3, 44.6, 32.0, 30.3, 29.4, 29.4, 27.1, 22.9, 14.4; HRMS m/z ESI^+ found 307.2169 $[M+H]^+$ calculated for $C_{21}H_{27}N_2$ 307.2174.

1-octyl-2-(pyridin-3-yl)-1*H*-indole (2-2q)

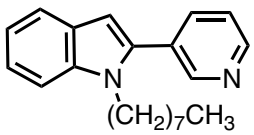

Following **GP2-1** (1.2 mmol ketone, 0.63 mmol octylamine, using 1-chloro-2-iodobenzene), the title product was isolated as a brown oil (73 %). An ethyl acetate: hexanes

(1:7.5) eluent system was used for column chromatography. ^{1}H NMR (500 MHz, $CDCl_3$): δ 8.82 (m, 1H) (s, 1H), 8.70-8.69 (m, 1H), 7.85-7.83 (m, 1H), 7.70 (d, *J* = 7.9 Hz, 1H), 7.46-7.43 (m, 2H), 7.32-7.29 (m, 1H), 7.20 (t, *J* = 7.5 Hz, 1H), 6.62 (s, 1H), 4.17 (t, *J* = 7.6 Hz, 2H), 1.75-1.72 (m, 2H), 1.31-1.21 (m, 10H), 0.90 (t, *J* = 7.1 Hz, 3H); $^{13}C\{^{1}H\}$ NMR (125.8 MHz, $CDCl_3$): δ 150.4, 149.3, 138.0, 137.7, 136.8, 129.7, 128.4, 123.6, 122.4, 121.1, 120.4, 110.5, 103.6, 44.4, 32.0, 30.4, 29.4, 29.4, 27.1, 22.9, 14.4; HRMS *m/z* ESI^+ found 307.2169 $[M+H]^+$ calculated for $C_{21}H_{27}N_2$ 307.2174. Following **GP2-2** (0.6 mmol ketone, 0.63 mmol octylamine, using 1-chloro-2-iodobenzene), the title product was isolated as a brown oil (58%). In all cases the spectral data were in agreement with the title compound.

1-octyl-2-(thiophen-2-yl)-1*H*-indole (**2-2r**)

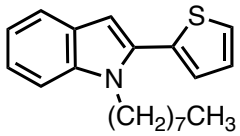

Following **GP2-1** (1.2 mmol ketone, 0.63 mmol octylamine, using 1-chloro-2-iodobenzene), the title product was isolated as a brown oil (65 %). A 100 % hexanes eluent system was used for column chromatography. ^{1}H NMR (500 MHz, $CDCl_3$): δ 7.67 (d, *J* = 8.1 Hz, 1H), 7.45-7.39 (m, 2H), 7.30-7.16 (m, 4H), 6.71 (s, 1H), 4.29 (t, *J* = 7.5 Hz, 2H), 1.87-1.81 (m, 2H), 1.35-1.30 (m, 10H), 0.94 (t, *J* = 7.1 Hz, 3H); $^{13}C\{^{1}H\}$ NMR (125.8 MHz, $CDCl_3$): δ 137.9, 134.7, 133.7, 128.2, 127.8, 127.1, 126.5, 122.3, 121.0, 120.2, 110.2, 103.6, 44.4, 32.1, 30.6, 29.5 (two signals), 27.2, 23.0, 14.4; HRMS *m/z* ESI^+ found 312.1780 $[M+H]^+$ calculated for $C_{20}H_{26}SN$ 312.1786.

1,2-diphenyl-1*H*-indole (**2-3a**)

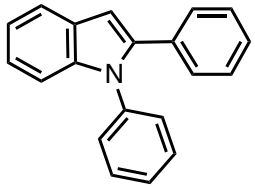

Following **GP2-2** the title product was isolated as a white powder (74 %, from 1-chloro-2-iodobenzene). A 100 % hexanes eluent system was used for column chromatography. ^{1}H NMR (500 MHz, $CDCl_3$): δ 7.76-7.72 (m, 1H), 7.48-7.45 (m, 2H), 7.41-7.38 (m, 1H), 7.36-7.27 (m, 8H), 7.25-7.21 (m, 2H), 6.86 (s, 1H); ^{13}C{^{1}H} NMR (125.8 MHz, $CDCl_3$): δ 141.1, 139.4, 138.9, 132.9, 129.6, 129.3, 128.6, 128.5, 128.4, 127.6 (two signals), 122.7, 121.1, 120.9, 111.0, 104.1. HRMS *m/z* ESI^{+} found 270.1277 [M+Na]$^{+}$ calculated for $C_{20}H_{16}N$ 270.1283.

1-octyl-2-phenyl-6-(trifluoromethyl)-1*H*-indole (**2-3b**)

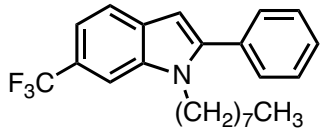

Following **GP2-2** the title product was isolated as a clear oil (57 %). A 100 % hexanes eluent system was used for column chromatography. ^{1}H NMR (500 MHz, $CDCl_3$): δ 7.70 (d, *J* = 8.3 Hz, 1H), 7.64 (s, 1H), 7.50-7.44 (m, 5H), 7.37 (d, *J* = 8.3 Hz, 1H), 6.57 (s, 1H), 4.19 (t, *J* = 7.5 Hz, 2H), 1.70-1.67 (m, 2H), 1.27-1.17 (m, 10H), 0.87 (t, *J* = 7.1 Hz, 3H); ^{13}C{^{1}H} NMR (125.8 MHz, $CDCl_3$): δ 144.4, 136.6, 133.0, 130.9, 129.8, 129.0, 128.8, 123.8 (J_{CF} = 126.6 Hz), 121.1, 116.8, 116.7, 107.8 (two signals), 102.6, 44.5, 32.0, 30.3, 29.4, 29.3, 27.0, 22.9, 14.4; HRMS *m/z* ESI^{+} found 374.2090 [M+H]$^{+}$ calculated for $C_{23}H_{27}F_3N$ 374.2096.

Chapter 3: Nickel Catalyzed Monoarylation of Ammonia in the Synthesis of Functionalized Heterocycles

3.1 Contributions

This chapter describes the nickel-catalyzed monoarylation of ammonia employing (hetero)aryl (pseudo)halides. Both projects described in this chapter were collaborative efforts incorporating a number Stradiotto group members. During the first amination project, a postdoctoral fellow Andrey Borzenko conducted the ligand screen and obtained the aryl halide scope with ammonia. During the second amination project Chris Lavoie synthesized the ligands and associated Ni^{II} complexes, as well as conducted the initial ligand screen and completed the aryl halide substrate scope investigation with ammonia. Throughout both projects my research focus was directed towards developing the first examples of nickel-catalyzed ammonia monoarylation employing (hetero)aryl halides.

3.2 Introduction

3.2.1 Introduction to Nickel Catalyzed Amination

Building on the development of nickel-catalyzed C-C cross-coupling chemistry (see Section 1.3.5), the first report of related C-N cross-coupling involving aryl halides was disclosed by Wolfe and Buchwald in 1997.[84] They found that the application of a $Ni(COD)_2$/dppf mixture affords a highly active catalyst for the coupling of aryl chlorides with primary and secondary alkylamines. While this represented a major breakthrough for nickel catalyzed C-N bond-forming reactions, it was severely limited in terms of functional group tolerance and scope of amine coupling partners. Nonetheless, it is noteworthy that a successful Ni-catalyzed amination protocol was realized only two years following the establishment of analogous palladium-catalyzed BHA protocols. However, the established

nature of palladium catalysis, including larger libraries of effective ligands and thorough mechanistic understanding, led in part to lethargic growth for nickel-catalyzed C-N bond-forming protocols. More recent emphasis on the need for more economical, earth-abundant catalysts demanded that nickel along with other base metal catalysts be explored more broadly. The use of more complex ligands including NHCs,[85] N,N-bidentate ligands,[86] and others have led to numerous nickel-catalyzed bond-forming protocols. The ability of nickel to cross-couple more challenging electrophiles has also led to a diverse range of complex heterocycles being synthesized. Important contributions from Buchwald[87] and Hartwig[88] regarding the development of bisphosphine/Ni catalysts with expanded reactivity to accommodate the cross-coupling of secondary and primary amines respectively, contributed in part to a resurgence of interest in Ni-catalyzed amination chemistry. The Buchwald group developed an air-stable (dppf)Ni(*o*-tolyl)Cl pre-catalyst for the nickel-catalyzed amination of aryl (pseudo)halides employing secondary amine nucleophiles; Hartwig and co-workers applied a BINAP ligated Ni(0) complex stabilized by a η^2-coordinated benzonitrile ligand for such transformations with expanded functional group tolerance and milder reaction conditions than featured in earlier reports. (Scheme 3-1)

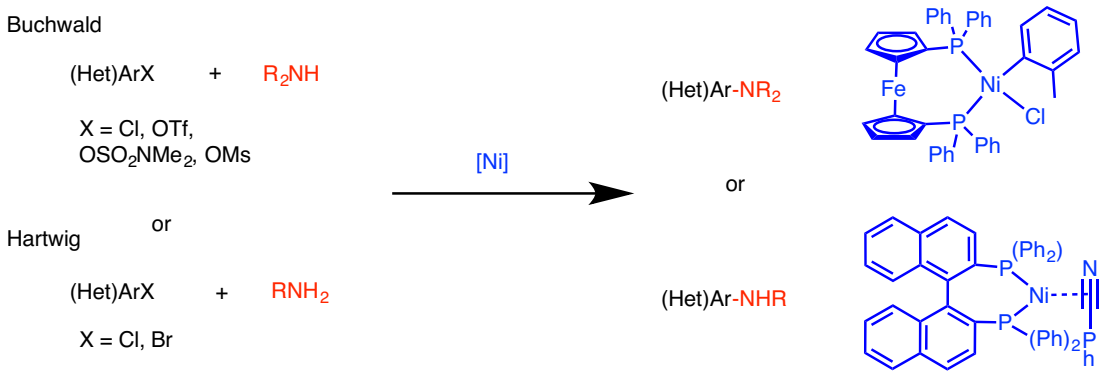

Scheme 3-1. Buchwald and Hartwig's advancement of nickel-catalyzed aminations

Each of these studies represent significant advancements in improving the scope of reactivity in applying nickel as a metal catalyst for C-N bond formation. Notwithstanding the significance of such studies, at the outset of my thesis research, several important outstanding challenges existed with respect to suitable reaction partners, including the highly abundant and inexpensive reagent ammonia. This chapter details my research efforts in accommodating ammonia for the first time in the cross-coupling of heteroaryl halides.

3.2.2 Ligand Design in Nickel-Catalyzed Aminations

In early reports of nickel-catalyzed aminations, relatively simple ligands were able to catalyze these transformations successfully, albeit typically under forcing conditions and with relatively limited substrate scope.[45] Unlike palladium, ligand design for nickel has been relatively slow, which is a product of the limited mechanistic understanding of the nickel-catalyzed amination reaction pathway. The preponderance of evidence in recent years, however, has revealed some preliminary trends regarding ideal ligand characteristics for use in nickel catalysis. Due in part to the electropositive nature of nickel, oxidative addition has been demonstrated to be a relatively facile process versus palladium. Therefore, less electron-rich ligands are typically utilized in nickel cross-coupling, in comparison to palladium.[44] Through recent mechanistic investigation involving both experimental and computational techniques, reductive elimination has been identified as the rate-limiting step in the catalytic cycle of several types of nickel-catalyzed cross-coupling reactions;[44] this benefits from employment of a sterically encumbered, electron-poor ligand. Also, due to the smaller co-ordination sphere around nickel, decomposition pathways such as β-hydride elimination, which are common in palladium-catalyzed cross-couplings, can be discouraged. This can offer another advantage of nickel over its

palladium counterpart.

3.2.3 Motivation and Research Goals

At the time of commencing my graduate research, the nickel-catalyzed monoarylation of ammonia was an unknown reaction. For many nickel-catalyzed transformations, the approach of repurposing ligands that function well in analogous Pd-catalyzed processes is commonplace, due to the lack of information pertaining to ideal ligands in nickel catalysis. Within the first half of this chapter the use of a JosiPhos-based nickel catalyst in the first ever nickel-catalyzed ammonia monoarylation with heteroaryl halides is described. The strategic design of a new class of ligands to suit the particular needs of nickel in this chemistry is detailed subsequently. This involves a discussion of a new P,P bidentate ligand PAd-DalPhos, designed and synthesized by the Stradiotto group, which is examined in the monoarylation of heteroayl halides with ammonia under mild conditions.

3.2.4 The History of Ammonia Amination and Associated Challenges

As discussed in Section 1.3.3 ammonia represents one of the most commonly utilized inorganic compounds, and is produced on a large scale via the Haber-Bosch process.[37] As such, ammonia represents an attractive synthon due to the fact that amino-functionalized compounds are commonly found in many biologically active molecules and conjugated functional organic materials.[37, 89] As well, the ensuing aniline products derived from the monoarylation of ammonia can be further functionalized to access even more value-added products. For example, shown below is crizotinib (known as Xalkori), which features a primary (hetero)aniline moiety and which has found application as an anti-cancer drug (Figure 3-1).[90] One could envision preparing primary aniline derivatives, such as

crizotinib, directly from ammonia if appropriate cross-coupling methods could be developed.

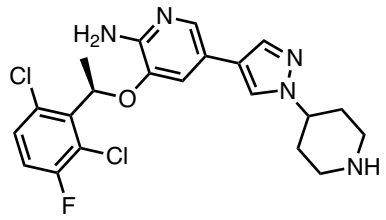

Figure 3-1. Structure of crizotinib

Despite the appeal of employing ammonia as a nucleophile for C-N cross-coupling reactions, its use is extremely challenging for several reasons. Specifically, the nucleophilic nature of ammonia can result in catalyst deactivation via amine induced ancillary ligand dissociation. Also, the ensuing aniline products derived from the initial monoarylation reaction are competing substrates, due to the favourable acidity of the generated aniline. This can result in the formation of unwanted di- and tri- substituted aniline products. The first successful use of ammonia as a coupling partner in BHA was reported by Hartwig and Shen in 2006,[39] reports by the groups of Hartwig,[40] Beller,[41] Buchwald,[42] and Stradiotto[25a] followed. These groups have been able to expand the scope of (hetero)aryl halides applied in this chemistry and also develop catalysts that can operate under very mild conditions, including at room temperature. Notably, all of these previous systems were conducted with palladium as the metal source with the exception of a single copper-catalyzed system involving harsh reaction conditions and limited substrate scope.[43b] This chapter will outline my success in developing the first nickel-catalyzed monoarylation of ammonia with heteroaryl halides.

3.2.5 Catalyst Development and Initial Substrate Scope

The initial catalyst screen by the Stradiotto group and the resulting discovery of a

ligand capable of performing this transformation is shown in Scheme 3-2. The ability to readily monitor 4-chlorobiphenyl by GC methods led to the choice of this substrate for initial screening. There exists a clear distinction between the starting material (4-chlorobiphenyl), the product (4-aminobiphenyl), and the unwanted hydrodehalogenation product (biphenyl). 4-Chlorobiphenyl as well does not contain any highly electron donating or withdrawing moieties, therefore rendering it as a "neutral" test substrate. In collaboration with Andrey Borzenko, a postdoctoral fellow working in the Stradiotto group, this ligand screen focussed initially on the use of *rac*-BINAP and dppf, given the successful prior application of nickel catalysts featuring these ligands in C-N cross-couplings of both primary and secondary amines.[84, 87-88] However, these ligands, as well as the more electron-rich D*i*PPF, proved ineffective for the nickel-catalyzed monoarylation of ammonia under the screening conditions employed. It should be noted that all values quoted in brackets represent isolated yields. Attention was then turned to the application of a selection of other commercially available ancillary ligands that have proven effective in the palladium-catalyzed monoarylation of ammonia, including Mor-DalPhos,[25a] BippyPhos,[76] and the JosiPhos ligand variant CyPF-*t*Bu.[39-40] While none were found to be particularly selective for ammonia monoarylation, the modest success achieved with CyPF-*t*Bu prompted a more exhaustive survey of structurally related JosiPhos (**3-L1** to **3-L9**), TaniaPhos (**3-L10**, **3-L11**), and WalPhos (**3-L12**, **3-L13**) ligands developed by Solvias. Gratifyingly, each of **3-L7** to **3-L10** proved highly effective, affording high conversion to 4-aminobiphenyl, **3-1**; 82% isolated yield of **3-1** was obtained using **3-L9**. The success of **3-L7** to **3-L10** cannot yet be fully rationalized, both in terms of the structural variability found within this successful set of ligands, and between these and structurally similar yet less effective

ferrocenyl ligands within the screening set. Nonetheless, the subsequent observation that **3-L9** was found to be modestly more effective than **3-L7**, **3-L8**, or **3-L10** in a small selection of nickel-catalyzed ammonia monoarylation reactions involving alternative (hetero)aryl halide electrophiles enabled the identification of **3-L9** as the ligand of choice for use in my thesis research exploring the scope of reactivity with various heteroaryl halides. My research progress in this regard is detailed in the following sections.

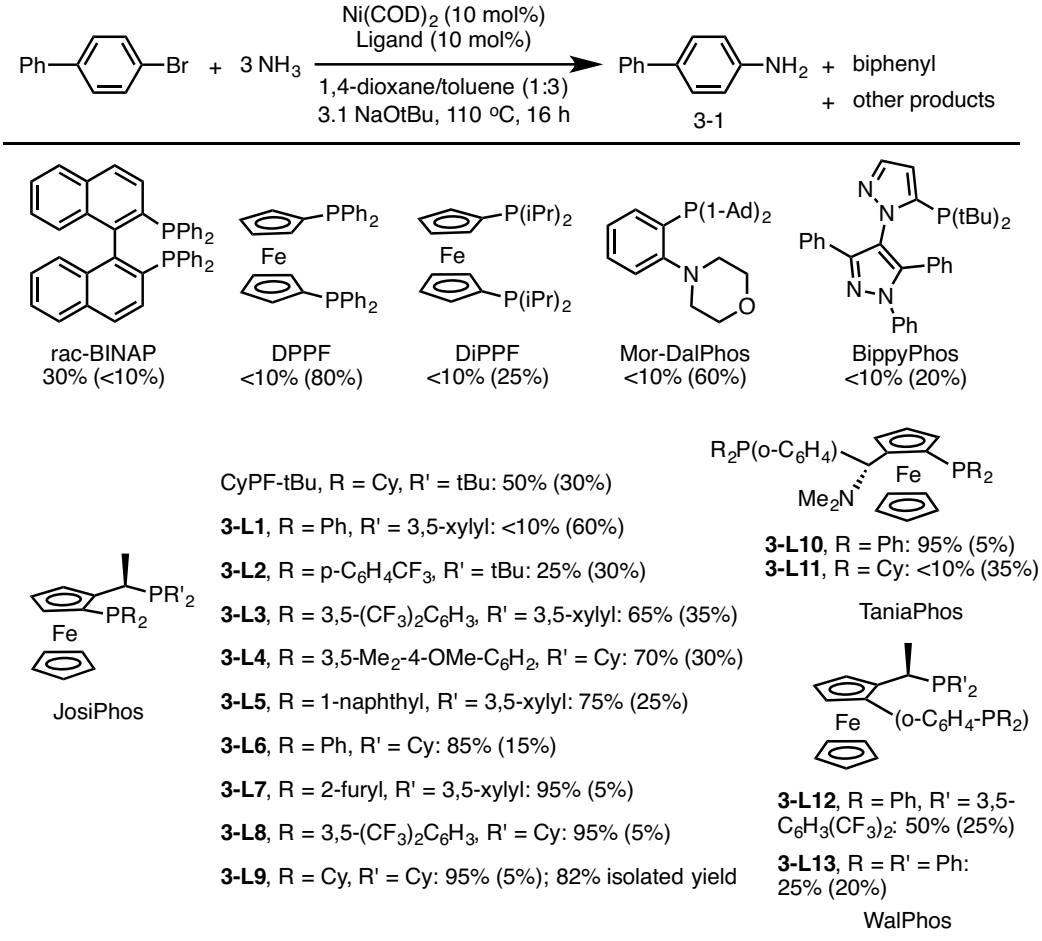

Scheme 3-2. Ligand screen for nickel-catalyzed for ammonia monoarylation

3.3 Results and Discussion

3.3.1. Heteroaryl Substrate Scope

Heteroaryl primary aniline derivatives represent particularly attractive synthons in

medicinal, biological, natural products, and materials chemistry.[91] It is for this reason that I directed my research efforts toward the application of our newly identified $Ni(COD)_2$/**3-L9** catalyst system in ammonia monoarylation reactions with heteroaryl halides. Such substrates are particularly challenging, given their ability to coordinate and inhibit reactive metal centres. This required careful screening of the reaction conditions to optimize the reaction conditions specifically for these substrates (Scheme 3-3).

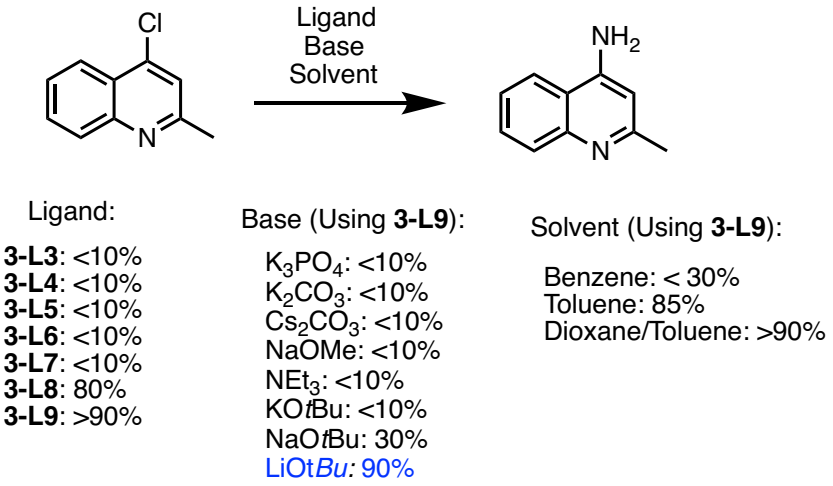

Scheme 3-3. Catalyst, base, and solvent optimization for heteroaryl halides

Typically for ammonia monoarylation, NaO*t*Bu represents the most commonly utilized base. However, upon initial observation, NaO*t*Bu proved to be ineffective for the formation of amino-functionalized heterocycles. From this point, I surveyed a number of different bases, including weak bases such as potassium phosphate, potassium carbonate, and cesium carbonate, which often represent commonly employed alternatives. Attention was then turned to other *t*-butoxide bases including LiO*t*Bu and KO*t*Bu. Although these compounds possess very similar basicity, LiO*t*Bu proved to be the only effective base for this reaction. While the source of this reactivity difference was not exhaustively explored, it is feasible that different bases exhibit favourable solubility or rates of reactivity with key

Ni catalytic intermediates. The difficulty in the synthesis of these amino-functionalized heterocycles was their sensitivity to the reaction conditions. Reproducibility became an issue and the catalyst conditions had to be modified slightly to accommodate each substrate. It is worth noting that for every reaction that failed when using **3-L9**, I retried with **3-L8** to confirm the competency of the catalyst. After careful and arduous optimization, a range of amino-functionalized pyridine (**3-2**), pyrimidine (**3-3**), quinaldine (**3-4**, **3-5**), isoquinoline (**3-6**), quinoline (**3-7**, **3-8**), quinoxaline (**3-9**, **3-10**), benzothiophene (**3-11**), and benzothiazole (**3-12**) heterocycles were prepared utilizing our nickel-catalyzed ammonia monoarylation protocols (Scheme 3-4, 68-85% yield). Only in the case of 6-chloroquinoline, leading to **3-8**, did we observe that the performance of **3-L9** was inferior to that of **3-L8**.

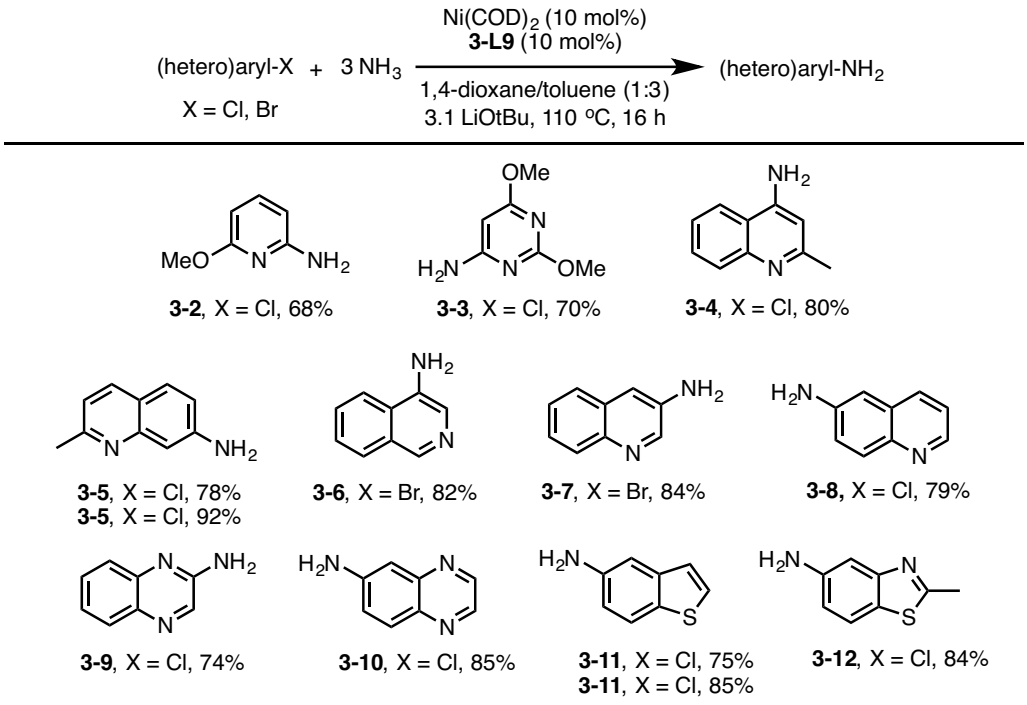

Scheme 3-4. Heteroaryl substrate scope with ammonia

The exploration into ammonia monoarylation thus far makes use of a commercially available 0.5 M solutions of ammonia in 1,4-dioxane. Although this is a practical methodology for use in small-scale laboratory synthesis, the use of ammonia gas would appear to be a more scalable protocol. Notably, a PhD candidate in the Stradiotto group (Preston MacQueen) was able to apply this methodology to allow the successful formation of amino-functionalized heterocycles using this ammonia gas protocol.

Upon successful publication of our results, Hartwig published a concurrent paper describing ammonia monoarylation involving a similar JosiPhos catalyst system.[92] Mechanistic insight was provided that was supportive of a Ni(0)/Ni(II) reaction pathway. At the outset of the investigation they were able to synthesize a series of Ni^{II} pre-catalysts, which were active for the cross-coupling to access their target substrate, although with poor conversion for neutral and electron rich substrates. Addition of excess benzonitrile increased the yield of each reaction, therefore lending the conclusion that the reaction proceeds through a Ni^0/Ni^{II} catalytic cycle, whereby the active Ni^0 species in stabilized by the benzonitrile ligand. They also examined the possibility of radical formation in the reaction protocol. However, only the target product formed upon completion with the radical trap remaining unchanged. This also supports the evidence for a Ni(0)/Ni(II) catalytic cycle. In this vein, we proceeded with the development of bisphosphine ligands specifically tuned for nickel catalysis as well as Ni^{II} pre-catalysts, which will be discussed in Section 3.5.1.

3.4 Limitations and Ligand Design Moving Forward

Our approach of "repurposing" commercially available ligands led to the discovery of a JosiPhos/$Ni(COD)_2$ catalyst system, which established the first successful

incorporation of nickel in the monoarylation of ammonia. Although this catalyst system accommodated a diverse substrate scope, several outstanding limitations and challenges remained. Although the economic benefit of using nickel versus palladium is clear, the use of expensive, extremely air and moisture sensitive $Ni(COD)_2$ restricts the advantage of this methodology for application in bench-top chemistry. As well, JosiPhos, a redundantly chiral ligand for our purposes, represents an expensive ligand motif for this type of chemistry. Other issues in this chemistry including long reaction times, forcing conditions (110 ^{o}C), and the requirement for an excess of ammonia. In this regard, the Stradiotto group set out to address these challenges and develop a class of sterically encumbered, relatively electron-poor phenylene bridged P,P-ligands that can accommodate this type of reactivity, as well as to develop P_2Ni(*o*-tolyl)Cl pre-catalysts that would represent an attractive catalytic alternative, being air stable, easy to synthesize and activate under catalytic conditions.

3.5 Results and Discussion

3.5.1 Initial Catalyst screen and development

To place my thesis work focused on ammonia cross-coupling involving heteroaryl halides in context, I provide here details of the initial catalyst screen by the Stradiotto group and the resulting discovery of a ligand capable of performing this transformation (Scheme 3-5). Chris Lavoie, a PhD student working in the Stradiotto group, carried out this ligand screen where he initially pursued bulky electron-poor bisphosphine ligands that would fit the motif of ligand design for nickel-catalyzed C-N bond-forming reactions. The screen began with the application of *o*-phenylene bisphosphines incorporating the 1,3,5,7-tetramethyl-2,4,8-trioxa-6-phosphadamantane (CgP) group with an adjacent phosphorus

donor fragment that could be easily modified. A number of mono- and bis-phosphines featuring this CgP moiety were synthesized utilizing this structural motif. A catalyst screening with these ligands was conducted utilizing L/Ni(COD)$_2$ to determine the competency of each ligand in the monoarylation of ammonia (Scheme 3-5, **b**). The test substrate, 4-chlorobiphenyl, was chosen for the reasons stated in Section 3.2.5. However, the ability to utilize an aryl chloride versus an aryl bromide represents a significant synthetic advantage as chlorides are more widely available than their bromide counterparts. Several trends became clear, the first being that bisphosphines were superior to their monophosphine counterparts. The resulting bis-ligation of the bisphosphine ligands may help stabilize the active nickel species as it undergoes the catalytic transformation. As well, the electron poor, bulky phosphines showed the highest turnover in the screening reaction chosen. Phenylene bridged P(Cg)/P(*o*-tol)$_2$ (**3-L14**, PAd-DalPhos) was the chosen candidate to continue forward with this reaction protocol. It should be noted that P(*t*Bu)$_2$/P(*o*-tol)$_2$ showed competent reactivity in this reaction supporting the idea that ligand sterics play a large role in reaction efficiency. To circumvent the use of Ni(COD)$_2$ the (PAd-DalPhos)Ni(*o*-tol)Cl (**3-C2**) complex was synthesized, which is air stable for months on the benchtop, and can be readily entered into the catalytic cycle without the need for an external reductant. It should also be noted that a [Pd(cinnamyl)Cl]$_2$/**3-L14** reaction was conducted, which performed poorly. This intrinsically shows the specificity of this ligand for nickel catalysis.

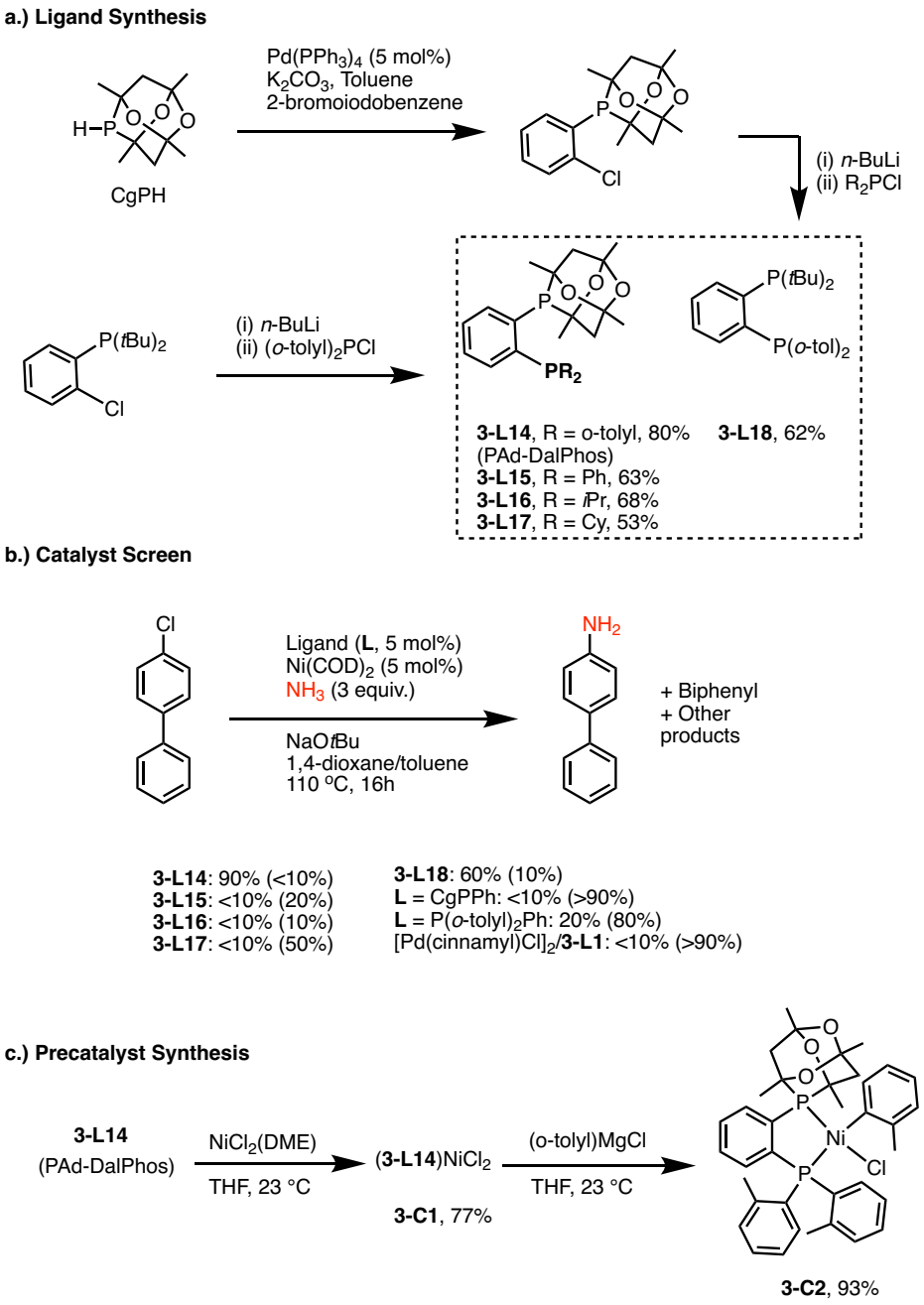

Scheme 3-5. Ligand, pre-catalyst synthesis, and optimization of PAd-DalPhos variant

3.5.2 Substrate Scope with (Hetero)aryl Halides

In this vein, I was able to apply **3-C2** in ammonia monoarylation with particularly challenging heteroaryl halides. Given the importance of biologically active (hetero)anilines in pharmaceutical chemistry it was encouraging to observe that quinolone (**3-8**),

isoquinoline (**3-6**), quinaldine (**3-4**), pyrimidine (**3-13**), quinoxaline (**3-9**), quinazoline (**3-15**), benzothiophene (**3-11**), and benzothiazole (**3-12**) core structures each proved compatible in this chemistry, as outlined in Scheme 3-6. Notably the quinazoline (**3-14**) represents the core structure found within a series of commercialized drugs including doxazosin which is employed for the treatment of symptoms associated with benign prostatic hyperplasia. Moreover, the quinoline (**3-15**) (tacrine) has been used as a cholinesterase inhibitor for the treatment of Alzheimer's disease, whereas 3-aminoestrone (**3-16**) has been identified as a key synthon for the of non-natural C-18 seroids for use in the treatment of prostate and other breast cancers.[93] In the case of benzothiophene (**3-11**) and quinoxaline (**3-14**) these products were synthesized via the ammonia gas protocol outlined earlier.

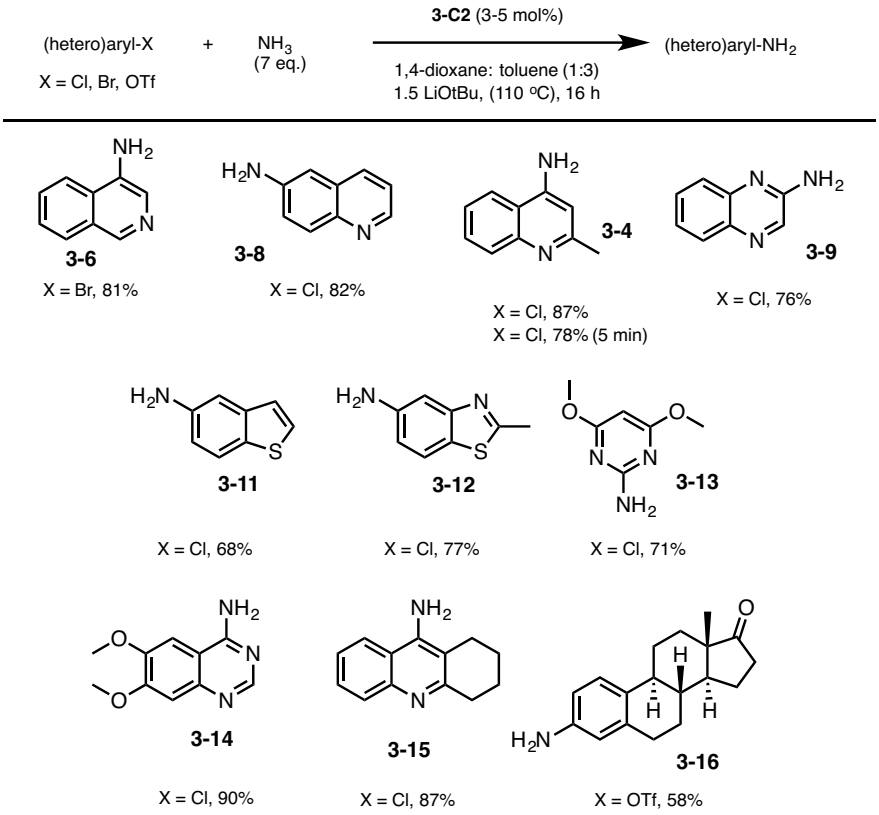

Scheme 3-6. Ammonia monoarylation of heteroaryl halides with **3-C2**

3.5.3 (Hetero)ArylAnilines: Challenges and Limitations

There were several challenges associated with utilizing this catalyst system. The first was the difficulty in separating the ligand from the target products to acquire purified products. A vast number of TLC techniques and complex solvent systems were required to isolate clean products. Although this seems trivial, several products of successful cross-couplings could not be obtained in pure form as result of poor separation from the ligand. At the outset of the PAd-DalPhos ammonia project we looked to address certain limitations associated with the JosiPhos catalyst system although several could not be overcome. (PAd-DalPhos)Ni(*o*-tol)Cl was able to accommodate the room-temperature ammonia coupling of a number of aryl halides as well as primary amines with heteroaryl halides. However, when trying to apply room-temperature protocols to ammonia monoarylation with heteroaryl halides there was no observed product formation. As well, 7 eq. of ammonia were required for these reactions, which represents a limitation of utilizing this catalytic system on a large scale.

3.5.4 Conclusions

In summary, my thesis research established the first nickel-catalyzed ammonia cross-coupling chemistry. Structurally diverse heteroaryl chloride and bromide electrophiles (e.g., pyridine, pyrimidine, quinaldine, isoquinoline, quinolone, quinoxaline, benzothiophene, benzothiazole) were accommodated with success. Such broad reaction scope, when coupled with the demonstrated efficacy of the reported JosiPhos/Ni(COD)$_2$ catalyst system, as well as the air-stable (PAd-DalPhos)Ni(*o*-tol)Cl system, when using either commercially available stock solutions of ammonia or ammonia gas, serves to underscore the versatility and potential scalability of the newly developed protocol. The

breadth of reaction scope in ammonia monoarylation reactions achieved by use of these nickel catalyst systems is unprecedented in first-row metal catalysis. The results presented herein establish for the first time the viability of nickel catalysts functioning as first-row competitors to state-of-the-art palladium catalysts with regard to substrate scope in ammonia monoarylation chemistry.

3.6 Experimental: General Procedures and Characterization Data

3.6.1 General Considerations

Unless otherwise stated, all reactions were setup inside a nitrogen-filled inert atmosphere glovebox and worked up in air using benchtop procedures. Toluene was deoxygenated by sparging with dinitrogen followed by passage through an mBraun double column solvent purification system packed with alumina and copper-Q5 reactant and storage over activated 4 Å molecular sieves. All reagents, solvents and materials were used as received from commercial sources. Column chromatography was carried out using Silicycle SiliaFlash 60 silica (particle size 40-63 μm; 230-400 mesh) or using neutral alumina (150 mesh; Brockmann-III; activated), as indicated. Preparatory TLC was carried out on the Silicycle plates (TLG-R1001B-341, silica, glass backed TLC Extra Hard Layer, 60 angstrom, thickness 1 mm, indicator F-254). All ^{1}H NMR (500 MHz or 300 MHz) and ^{13}C NMR (125.8 MHz or 75.4 MHz) spectra were recorded at 300 K. Chemical shifts are expressed in parts per million (ppm) using the solvent signal $CHCl_3$ (^{1}H 7.26 ppm, ^{13}C 77.2 ppm) as an internal reference. Splitting patterns are indicated as follows: br, broad; s, singlet; d, doublet; t, triplet; q, quartet; m, multiplet. All coupling constants (*J*) are reported in Hertz (Hz). Mass spectra were obtained using ion trap (ESI) instruments operating in

positive mode, and GC data were obtained on an instrument equipped with a SGE BP-5 column (30 m, 0.25 mm i.d.).

3.6.2 General Synthetic Protocols

General Protocol for the Coupling of Heteroaryl Halides with Ammonia Utilizing Ni(COD)/3-L9 (GP3-1). Unless specified otherwise in the text, $Ni(COD)_2$ (9.9 mg, 0.036 mmol, 10.0 mol%), **3-L9** (21.8 mg, 0.036 mmol, 10.0 mol%), NaO*t*Bu (103.8 mg, 1.12 mmol, 3.1 eq) and toluene (4 ml) were added to a screw-capped vial containing a magnetic stir-bar, to which was added subsequently aryl (pseudo)halide (0.36 mmol, 1.0 eq) followed by the addition of NH_3 as a 0.5 M solution in 1,4-dioxane (2.16 mL, 1.08 mmol, 3.0 eq). The vial was sealed with a cap containing a PTFE septum, removed from the glovebox and placed in a temperature-controlled aluminum heating block set at 110 °C for 16 h. Reactions were monitored using both TLC and GC methods. After complete consumption of the starting aryl (pseudo)halide, the vial was removed from the heating block and left to cool to ambient temperature. The product was isolated by using **Workup Method 1**.

General Protocol for the Coupling of Heteroaryl Halides with Ammonia Utilizing Ni(COD)/3-L9 (GP3-2): Unless specified otherwise in the text, $Ni(COD)_2$ (10.4 mg, 0.05 mmol, 10.0 mol%), **3-L9** (30.3 mg, 0.05 mmol, 10.0 mol%), LiO*t*Bu (120.1 mg, 1.6 mmol, 3.1 eq) and toluene (8.3 mL) were added to a screw-capped vial containing a magnetic stir-bar, to which was added subsequently aryl (pseudo)halide (0.5 mmol, 1.0 eq), followed by the addition of NH_3 as a 0.5 M solution in 1,4-dioxane (3.13 mL, 1.5 mmol, 3.0 eq). The vial was sealed with a cap containing a PTFE septum, removed from the glovebox and placed in a temperature-controlled aluminum heating block set at 110 °C for

16 h. Reactions were monitored using both TLC and GC methods. After complete consumption of the starting aryl (pseudo)halide, the vial was removed from the heating block and left to cool to ambient temperature. Unless otherwise stated the product was isolated by using **Workup Method 2**.

General Protocol for the Coupling of Heteroaryl Halides with Ammonia Gas Utilizing 3-L9/Ni(COD)$_2$ (GP3-3). A vial (1 dram, 3.696 mL) containing a magnetic stir-bar was charged with Ni(COD)$_2$ (3.3 mg, 0.012 mmol, 10.0 mol%), **3-L9** (7.3 mg, 0.012 mmol, 10.0 mol%), NaO*t*Bu (34.6 mg, 0.36 mmol, 3.0 eq), toluene (1.0 mL), aryl chloride (0.36 mmol, 1.0 eq), and 1,4-dioxane (0.72 mL). The resulting solution was stirred briefly and then was sealed with a cap containing a PTFE septum; the septum was then punctured with a 26G1/2 PrecisionGlide needle and the needle was not removed until the final workup. The reaction vial was placed in a high-pressure reaction chamber purchased from the Parr Instrument Company (type 316 stainless steel, equipped with a thermocouple immersed in oil to allow for accurate external temperature monitoring within the reaction chamber proximal to the placement of the reaction vial), and the reaction chamber was sealed under dinitrogen within the glovebox. The reaction chamber was removed from the glovebox, and was placed in an oil bath at room temperature that was mounted on top of a hot-plate/magnetic stirrer. The reaction chamber was fitted with a braided and PTFE-lined stainless steel hose designed for use with corrosive gases that was connected to a tank of anhydrous ammonia gas. Magnetic stirring was initiated and the reaction chamber was purged with ammonia for approximately five minutes, after which time the reaction chamber was pressurized with ammonia (114 psi maintained for 30 minutes at room temperature). The reaction chamber was then sealed, disconnected from the ammonia tank,

and was heated at 105 °C for 18 h; pressure was built up to 150 psi over the course of the reaction. The reaction chamber was allowed to cool to room temperature, after which the contents of the reaction chamber were vented slowly within a fumehood. The products were isolated using **Workup Method 2** with the exception that these products were not run through a silica plug.

General Protocol for the Coupling of Heteroaryl Halides with Ammonia Utilizing 3-C2 (GP3-4): Unless specified otherwise in the text, PAd-DalPhosNi(*o*-tol)Cl, **3-C2** (10.4 mg, 0.015 mmol, 3 mol %), aryl halide (0.5 mmol, 1 eq.), and LiO*t*Bu (60.0 mg, 0.75 mmol, 1.5 eq) were added to a screw-capped vial containing a magnetic stir-bar, followed by the addition of toluene (4.2 mL) and NH_3 as a 0.5M solution in 1,4-dioxane (3.5 mmol, 7 eq.). The vial was sealed with a cap containing a PTFE septum, removed from the glovebox, placed in a temperature-controlled aluminum heating block set at 25 °C or 110 °C for 16 h. Reactions were monitored using both TLC and GC methods. After complete consumption of the starting aryl (pseudo)halide, the vial was removed from the heating block and left to cool to ambient temperature. The crude reaction mixture was dissolved in ethyl acetate (10 mL) and poured onto brine (10 mL). The layers were separated and the aqueous layer was extracted with ethyl acetate (2 x 10 mL). The organic fractions were combined, dried over Na_2SO_4 and concentrated under reduced pressure. The crude residue was purified by use of column chromatography over silica.

General Protocol for the Coupling of Heteroaryl Halides with Ammonia Gas Utilizing 3-C2 (GP3-5): Unless specified otherwise in the text, A vial (1 dram, 3.696 mL) containing a magnetic stir-bar was charged with PAd-DalPhosNi(*o*-tol)Cl, **3-C2** (0.018 mmol, 5 mol%), LiO*t*Bu (43.2 mg, 0.54 mmol, 1.5 eq), toluene (1.0 mL), and aryl chloride

(0.36 mmol, 1.0 eq). For full details of parr bomb instrumentation and methdology see **GP3-2**.

Workup Methods:

Workup Method 1: The reaction mixture was concentrated *in vacuo* and filtered through an alumina plug with ethyl acetate (~30 mL)**.** The solvent was removed and the compound was either used for tosylation without purification, or purified by column chromatography on alumina or preparatory TLC (EtOAc/hexanes) and allowed to dry *in vacuo* to afford the desired product.

Workup Method 2: The reaction mixture was concentrated *in vacuo*, dissolved in dichloromethane (~ 20 mL), and extracted with 1 M HCl (3 x 10 mL). The combined aqueous layers were then washed with dichloromethane (3 x 10 mL). A concentrated solution of sodium bicarbonate was added to the acidic aqueous layer until it was fully neutralized (monitored with pH paper). The aqueous layer was then extracted with dichloromethane (3 x 10 mL). The organic layers were combined, dried over anhydrous sodium sulfate, and filtered through a silica plug with ethyl acetate (~30 mL). The residual solvent was removed *in vacuo* and the product was allowed to dry overnight.

3.6.3 Characterization Data

2-amino-6-methoxypyridine (**3-2**)

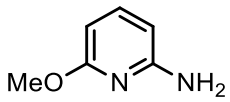

Following **GP3-2** (0.5 mmol aryl halide, 2.5 mmol ammonia, 65 °C): The title product **3-2** was isolated as a brown oil in 68% yield from the corresponding chloride. ^{1}H NMR (500 MHz, $CDCl_3$): δ 7.34 (t, J = 7.9 Hz, 1H), 6.10-6.05 (m, 2H), 4.28 (br s, 2H), 3.84 (s, 3H);

$^{13}C\{^{1}H\}$ NMR (125.8 MHz, $CDCl_3$): δ 164.2, 157.6, 140.6, 100.0, 99.0, 53.6. Agrees with data previously reported in the literature.[94]

6-amino-2,4-dimethoxypyrimidine (**3-3**)

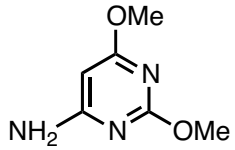

Following **GP3-2** (0.5 mmol aryl halide, 2.5 mmol ammonia, 65 ºC): The title product **3-3** was isolated as a beige solid in 70% yield from the corresponding chloride. ^{1}H NMR (500 MHz, $CDCl_3$): δ 5.44 (s, 1H), 4.69 (br s, 2H), 3.89 (6H); $^{13}C\{^{1}H\}$ NMR (125.8 MHz, $CDCl_3$): δ 172.6, 166.1, 165.8, 81.1, 54.7, 53.9. HRMS ESI^+ (*m/z*) found 178.0593 $[M+Na]^+$ calculated for $C_6H_9N_3NaO_2$ was 178.1443.

4-aminoquinaldine (**3-4**)

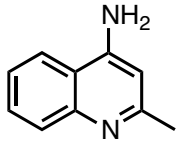

Following **GP3-1** (0.5 mmol aryl halide, 1.5 mmol ammonia): Purified by column chromatography on alumina (100:1, EtOAc/diisopropylamine) the title product **3-4** was isolated as a light brown solid in 80% yield from the corresponding chloride. ^{1}H NMR (500 MHz, $CDCl_3$): δ 7.92 (d, J = 8.5 Hz, 1H), 7.71 (d, J = 8.3 Hz, 1H), 7.61 (t, J = 7.5 Hz, 1H), 7.38 (t, J = 7.5 Hz, 1H), 6.50 (s, 1H), 4.68 (br s, 2H), 2.58 (s, 3H); $^{13}C\{^{1}H\}$ NMR (125.8 MHz, $CDCl_3$): δ 159.7, 149.9, 149.1, 129.7, 129.5, 124.5, 120.3, 117.8, 104.4, 25.7. Agrees with data previously reported in the literature.[95] Following **GP3-5**: Purified by column chromatography (7:2:1, hexanes/EtOAc/NH*i*Pr_2). The title product **3-4** was isolated as an

off-yellow solid in 87% yield from the corresponding chloride. Agrees with data previously reported in the literature.[96]

7-aminoquinaldine (**3-5**)

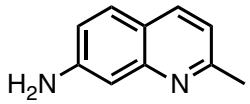

Following **GP3-1** (0.5 mmol aryl halide, 1.5 mmol ammonia): Purified by column chromatography on alumina (6:4:1, EtOAc/hexanes/triethylamine) the title product **3-5** was isolated as a yellow solid in 78% yield from the corresponding chloride. ^{1}H NMR (500 MHz, $CDCl_3$): δ 7.86 (d, *J* = 8.2 Hz, 1H), 7.55 (d, *J* = 8.7 Hz, 1H), 7.14 (m, 1H), 7.02 (d, *J* = 8.2 Hz, 1H), 6.90 (d of d, *J* = 8.6 Hz, *J* = 2.2 Hz, 1H), 4.02 (br s, 2H), 2.66 (s, 3H); ^{13}C{^{1}H} NMR (125.8 MHz, $CDCl_3$): δ 159.6, 150.0, 148.0, 136.1, 129.0, 120.8, 119.0, 117.9, 109.4, 25.7. HRMS ESI$^+$ (*m/z*) found 159.0911 $[M+H]^+$ calculated for $C_{10}H_{11}N_2$ was 159.2077. Following **GP3-3** the title product **3-5** was isolated as a yellow solid in 92% yield from the corresponding chloride. Agrees with data previously reported in the literature.[96]

4-aminoisoquinoline (**3-6**)

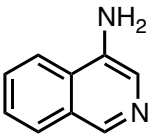

Following **GP3-2** (0.5 mmol aryl halide, 2.5 mmol ammonia): The title product **3-6** was isolated as a beige solid in 82% yield from the corresponding bromide. ^{1}H NMR (500 MHz, $CDCl_3$): δ 8.74 (s, 1H), 8.03 (s, 1H), 7.91 (d, *J* = 8.2 Hz, 1H), 7.80 (d, *J* = 8.5, 1H), 7.66 (t, *J* = 7.6 Hz, 1H), 7.57 (t, *J* = 7.7 Hz, 1H), 4.11 (br s, 2H); ^{13}C{^{1}H} NMR (125.8 MHz, $CDCl_3$): δ 143.7, 137.1, 129.4, 129.0, 128.6, 128.2, 127.4, 126.5, 120.3. Agrees with data previously reported in the literature.[39] Following **GP3-4** (25 °C): Purified by column

chromatography (10:1:0.1, hexanes/EtOAc/NH*i*Pr$_2$) the title product **3-6** was isolated as a light brown solid in 81% yield from the corresponding bromide. Agrees with data previously reported in the literature.[96]

3-aminoquinoline (**3-8**)

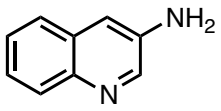

Following **GP3-2** (0.5 mmol aryl halide, 1.5 mmol ammonia): The title product **3-8** was isolated as a beige solid in 84% yield from the corresponding chloride. ^{1}H NMR (500 MHz, $CDCl_3$): δ 8.51 (m, 1H), 7.96 (d, *J* = 7.6 Hz, 1H), 7.60-7.58 (m, 1H), 7.46-7.41 (m, 2H), 7.24-7.23 (m, 1H), 3.92 (br s, 2H); ^{13}C{^{1}H} NMR (125.8 MHz, $CDCl_3$): δ 143.4, 143.1, 140.1, 129.5, 129.4, 127.3, 126.2, 126.0, 115.4; Agrees with data previously reported in the literature.[94]

6-aminoquinoline (**3-8**)

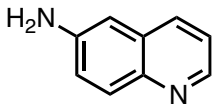

Following **GP3-1** (0.5 mmol aryl halide, 1.5 mmol ammonia): Purified by column chromatography on alumina (5:5:1, EtOAc/hexanes/triethylamine) the title product **3-8** was isolated as a light brown solid in 79% yield from the corresponding chloride. ^{1}H NMR (500 MHz, $CDCl_3$): δ 8.69 (m, 1H), 7.93 (t, *J* = 9.4 Hz, 2H), 7.30-7.28 (m, 1H), 7.18 (d of d, *J* = 8.9 Hz, *J* = 2.6 Hz, 1H), 6.93-6.92 (m, 1H), 4.01 (s, 2H); ^{13}C{^{1}H} NMR (125.8 MHz, $CDCl_3$): δ 147.2, 144.9, 143.8, 134.1, 130.9, 130.1, 122.0, 121.7, 107.8. Agrees with data previously reported in the literature.[97] Following **GP3-4**: Purified by preparatory TLC (7:2:1, hexanes/EtOAc/NH*i*Pr$_2$) the title product **3-8** was isolated as a white solid in 82%

yield from the corresponding chloride. Agrees with data previously reported in the literature.[96]

2-aminoquinoxaline (**3-9**)

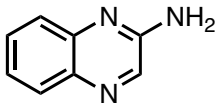

Following **GP3-2** (0.5 mmol aryl halide, 1.5 mmol ammonia; 65 ºC): The title product **3-9** was isolated as a beige solid in 74% yield from the corresponding chloride. ^{1}H NMR (500 MHz, $CDCl_3$): δ 8.33 (s, 1H), 7.92 (d, *J* = 8.3 Hz, 1H), 7.67 (d, *J* = 8.3 Hz, 1H), 7.61 (t, *J* = 7.4 Hz, 1H), 7.45 (t, *J* = 7.6 Hz, 1H); 4.93 (br s, 2H); ^{13}C{^{1}H} NMR (125.8 MHz, $CDCl_3$): δ 152.1, 141.9, 138.1, 137.9, 130.7, 129.4, 126.5, 125.6. Agrees with data previously reported in the literature.[94] Following **GP3-5**: Purified by column chromatography (8:2:0.2, hexanes/EtOAc/NH*i*Pr_2) the title product **3-9** was isolated as a yellow solid in 76% yield from the corresponding chloride. Agrees with data previously reported in the literature.[96]

6-aminoquinoxaline (**3-10**)

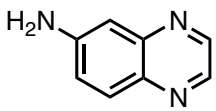

Following **GP3-2** (0.5 mmol aryl halide, 1.5 mmol ammonia): The title product **23** was isolated as a yellow solid in 85% yield from the corresponding chloride. ^{1}H NMR (500 MHz, $CDCl_3$): δ 8.66 (m, 1H), 8.55 (m, 1H), 7.88 (d, *J* = 9.1 Hz, 1H), 7.20-7.18 (m, 1H), 7.14 (m, 1H), 4.22 (br s, 2H); ^{13}C{^{1}H} NMR (125.8 MHz, $CDCl_3$): δ 148.3, 145.5, 145.3, 141.5, 138.5, 130.9, 122.4, 108.5. Agrees with data previously reported in the literature.[94]

5-aminobenzo[*b*]thiophene (**3-11**)

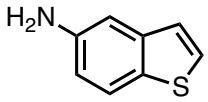

Following **GP3-2** (0.5 mmol aryl halide, 1.5 mmol ammonia): The title product **3-11** was isolated as a red-brown solid in 75% yield from the corresponding chloride. ^{1}H NMR (500 MHz, $CDCl_3$): δ 7.63 (d, J = 8.5 Hz, 1H), 7.38 (d, J = 5.3 Hz, 1H), 7.15 (d, J = 5.5 Hz, 1H), 7.11-7.10 (m, 1H), 6.78 (dd, J = 8.5 Hz, J = 2 Hz, 1H), 3.70 (br s, 2H); ^{13}C{^{1}H} NMR (125.8 MHz, $CDCl_3$): δ 143.9, 141.3, 130.8, 127.4, 123.4, 123.3, 115.2, 108.6. Agrees with data previously reported in the literature.[94] Following **GP3-3** the title product was isolated as a red-brown solid in 85% yield from the corresponding chloride. Following **GP3-5**: Purified by column chromatography (9:1:0.1, hexanes/EtOAc/NH*i*Pr_2) the title compound **3-11** was isolated as a white solid in 68% yield from the corresponding chloride. Agrees with data previously reported in the literature.[96]

5-amino-2-methylbenzothiazole (**3-12**)

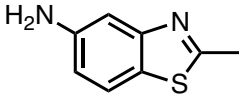

Following **GP3-2** (0.5 mmol aryl halide, 1.5 mmol ammonia): The title product **3-12** was isolated as a red-brown solid in 84% yield from the corresponding chloride. ^{1}H NMR (500 MHz, $CDCl_3$): δ 7.53 (d, J = 8.5 Hz, 1H), 7.23 (m, 1H), 6.74 (d of d, J = 8.5 Hz, J = 2.2 Hz, 1H), 3.58 (br s, 2H), 2.77 (s, 3H); ^{13}C{^{1}H} NMR (125.8 MHz, $CDCl_3$): δ 168.1, 155.1, 145.6, 125.7, 122.0, 114.8, 107.8, 20.4; Agrees with data previously reported in the literature.[94] Following **GP3-4** (5 mol% **3-C2**) Purified by column chromatography (5:5:0.1, hexanes/EtOAc/NH*i*Pr_2) the title product **3-12** was isolated as a white solid in 77%

yield from the corresponding chloride. Agrees with data previously reported in the literature. [96]

2-Amino-4,6-dimethoxypyrimidine (**3-13**)

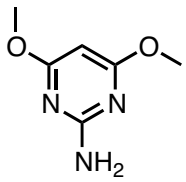

Following **GP3-4**: Purified by preparatory TLC (10% NH*i*Pr$_2$/hexanes) the title product **3-14** was isolated as a white solid in 71% yield from the corresponding chloride. ^{1}H NMR (500 MHz, $CDCl_3$): δ 5.49 (s, 1H), 4.96 (br s, 2H), 3.87 (s, 6H); $^{13}C\{^1H\}$ NMR (125.8 MHz, $CDCl_3$): δ 172.7, 162.5, 79.9, 53.9; Agrees with data previously reported in the literature.[94]

4-amino-6,7-dimethoxyquinazoline (**3-14**)

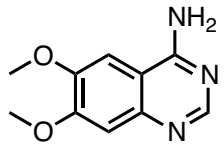

Following **GP3-5**: Purified by column chromatography (5:5:1, hexanes/EtOAc/NH*i*Pr$_2$) the title product **3-15** was isolated as a beige-yellow solid in 90% yield from the corresponding chloride. ^{1}H NMR (500 MHz, DMSO): δ 8.25 (s, 1H), 7.67 (s, 1H), 7.46 (br s, 2H), 7.06 (s, 1H), 3.89 (s, 3H), 3.88 (s, 3H); $^{13}C\{^1H\}$ NMR (125.8 MHz, DMSO): δ 160.4, 154.0, 153.8, 148.1, 146.6, 108.0, 106.7, 102.9, 56.1, 55.6; Agrees with data previously reported in the literature.[94]

9-amino-1,2,3,4-tetrahydroacridine (**3-15**)

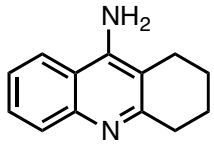

Following **GP3-4**: (5 mol% **3-C2**) Purified by column chromatography (6:4:1, EtOAc/hexanes/NH*i*Pr$_2$) the title compound **3-16** was isolated as a beige solid in 87% yield from the corresponding chloride. ^{1}H NMR (500 MHz, $CDCl_3$): δ 7.91-7.88 (m, 1H), 7.72-7.69 (m, 1H), 7.59-7.53 (m, 1H), 7.39-7.33 (m, 1H), 4.72 (br s, 2H), 3.05-3.01 (m, 2H), 2.63-2.59 (m, 2H), 1.99-1.88 (m, 4H); ^{13}C{^{1}H} NMR (125.8 MHz, $CDCl_3$): δ 158.6, 146.8, 146.5, 128.8, 128.7, 124.1, 119.9, 117.3, 110.6, 34.1, 23.9, 23.0, 22.9; Agrees with data previously reported in the literature.[98]

3-aminoestrone (**3-16**)

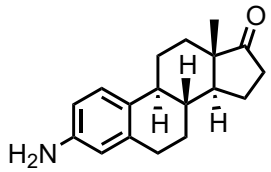

Following **GP3-4**: Purified by column chromatography (30% EtOAc/hexanes) the title product **3-17** was isolated as a white solid in 58% yield from the corresponding triflate. ^{1}H NMR (500 MHz, $CDCl_3$): δ 7.12 (d, J = 8.3 Hz, 1H), 6.57-6.55 (m, 1H), 6.49-6.48 (m, 1H), 3.56 (br s, 2H), 2.89-2.86 (m, 2H), 2.56-2.51 (m, 1H), 2.43-2.39 (m, 1H), 2.28-2.23 (m, 1H), 2.21-2.13 (m, 1H), 2.11-2.06 (m, 1H), 2.04-1.96 (m, 2H), 1.70-1.41 (m, 7H), 0.94 (s, 3H); ^{13}C{^{1}H} NMR (125.8 MHz, $CDCl_3$): δ 221.2, 144.4, 137.6, 130.3, 126.4, 115.6, 113.3, 50.7, 48.3, 44.2, 38.7, 36.1, 31.8, 29.7, 26.8, 26.2, 21.8, 14.1; Agrees with data previously reported in the literature.[93]

Chapter 4: Exploring the Influence of Phosphine Ligation on the Gold-Catalyzed Hydrohydrazination of Terminal Alkynes at Room Temperature

4.1 Contributions

This chapter describes the gold-catalyzed hydrohydrazination of alkynes utilizing a series of $(PR_3)AuCl$ complexes. The project described herein was a collaborative effort involving several members of the Stradiotto group. Preston MacQueen (PhD candidate) and Alicia Chisholm were responsible for the synthesis, characterization, and catalytic application of complex **4-C8** and **4-C9**. Single crystal X-ray diffraction analysis was carried out by Dr. Robert McDonald and Michael Ferguson (University of Alberta)

4.2 Introduction

4.2.1 Metal-Catalyzed Hydroaminations and Hydrohydrazinations

Hydroamination, the addition of an N-H bond to an unsaturated substrate, represents an atom-economical methodology for the formation of carbon-nitrogen bonds.[53] This methodology can lead to the formation of amine, enamine, and imine products, which can undergo further functionalization and have found application in agrochemical, pharmaceutical and other industrial processes.[53d] Many metal-catalyzed hydroamination methodologies have emerged to accommodate this type of reactivity incorporating a range of N-H substrates. However, the ability to accommodate the hydroamination of particularly challenging nitrogen nucleophiles, including hydrazine, remains a challenge.

Several methodologies involving both early and late-metal catalysts have been developed for the hydrohydrazination of substituted hydrazine reaction partners. The groups of Beller[99] and Zhurilo[100] have developed zinc-catalyzed hydrohydrazination protocols to synthesize highly substituted indoles and triazole products with substituted

hydrazines, which represent important intermediates in the formation of pharmaceutical compounds. Other protocols involving rhodium,[101] platinum,[102] as well as titanium[103] have been developed to access products via substituted hydrazine sources. While these protocols represent important strides in advancing the state-of-the-art for metal-catalyzed hydrohydrazination, these surrogates of hydrazine represent less attractive and less atom economical routes to access N-functionalized products. In this vein, the pursuit of catalysts to perform hydrohydrazinations with free hydrazine represents an important challenge.

4.2.2 Gold-Catalyzed Hydrohydrazination Utilizing NHC-Ligated Catalysts

Hydrazine is synthesized on multi-tonne scale each year.[104] It represents an important building block in many organic frameworks, including in the formation of heterocyclic frameworks in pharmaceutical products,[104] Although this represents an industrially significant starting material, limited reactivity has been achieved utilizing hydrazine as a reaction partner in metal chemistry. Only exiguous examples of hydrazine cross-coupling have been explored. In 2010, a report from the Stradiotto group utilizing a Mor-DalPhos/Pd[25b] catalyst system disclosed the cross-coupling of hydrazine with aryl chlorides and tosylates. As well, a continuous flow methodology developed by Buchwald[105] was able to facilitate this challenging cross-coupling. This relative lack of attention may be attributed to the difficulties associated with utilizing hydrazine as a starting material. Hydrazine, in a similar vain to ammonia, can form stable Werner complexes,[89, 106] which typically represent catalytically inactive species. It is also a strong reductant, which can lead to the formation of inactive metal particles.[107] Hydrazine can also generate hydrogen, leading to the unwanted metal-catalyzed reduction of unsaturated

bonds,[108]. As well, the N-N bond of hydrazine can be cleaved leading to undesired reaction pathways and generation of catalytically inactive species.

In 2008, Bertrand and coworkers were able to successfully catalyze the first-ever hydroamination of alkynes with ammonia.[109] They were able to utilize a cationic cyclic (alkyl)(amino)carbene (CAAC) gold complex to accommodate this unprecedented reaction. These CAAC type carbenes vary from traditional carbenes in their ability for π-back donation. Traditional carbenes are excellent σ-donors but notoriously poor π-acceptors. This modification allows for the complexation of the C-C multiple bond to gold and thus facilitate the nucleophilic attack from the nitrogen nucleophile. Bertrand was able to show that their CAAC-Au(I) pre-catalyst (Figure 4-1, **A**) was able to form Werner-type complexes (Figure 4-1, **B**), which when subjected to excess alkyne allowed the formation of the target hydroamination product.

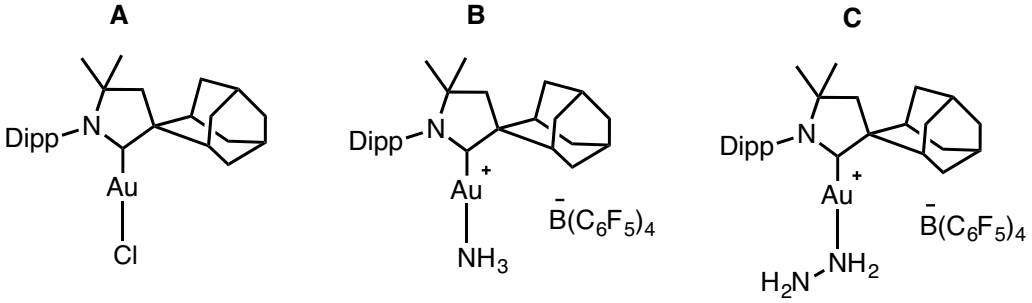

Figure 4-1. CAAC complexes for ammonia hydroamination

The unique reactivity of this AuCl pre-catalyst (Figure 4-1, **A**) for the hydroamination of alkynes with ammonia led to the its application in the first-ever hydrohydrazination of alkynes with free hydrazine.[110] Analogous hydrazine-bound Werner complexes were synthesized (Figure 4-1, **C**), which also exhibited catalytic turnover in this

reaction protocol. Over the proceeding five years several different NHC classes were developed for the hydrohydrazination of terminal alkynes. Bertrand and co-workers were able to develop anti-Bredt NHCs (Figure 4-2, ***pyr*NHC**),[111] which demonstrated the first example of room-temperature hydrohydrazinations; however this catalyst type lacked a diverse substrate scope (three examples). Hashmi was able to overcome these limitations with the development of saturated abnormal NHC-Au pre-catalysts (Figure 4-2, **saNHC**) to develop a broader scope of reactivity for the room-temperature hydrohydrazination of terminal alkynes.[112] In 2015, Bertrand developed a 1,2,3-triazol-5-ylidene, also known as a mesoionic carbene (MIC) for application in hydrohydrazination (Figure 4-2, **MIC**).[113] These (MIC)AuCl complexes were then utilized in the bis-hydrohydrazination of alkynes to form symmetrical and unsymmetrical azine-type products.

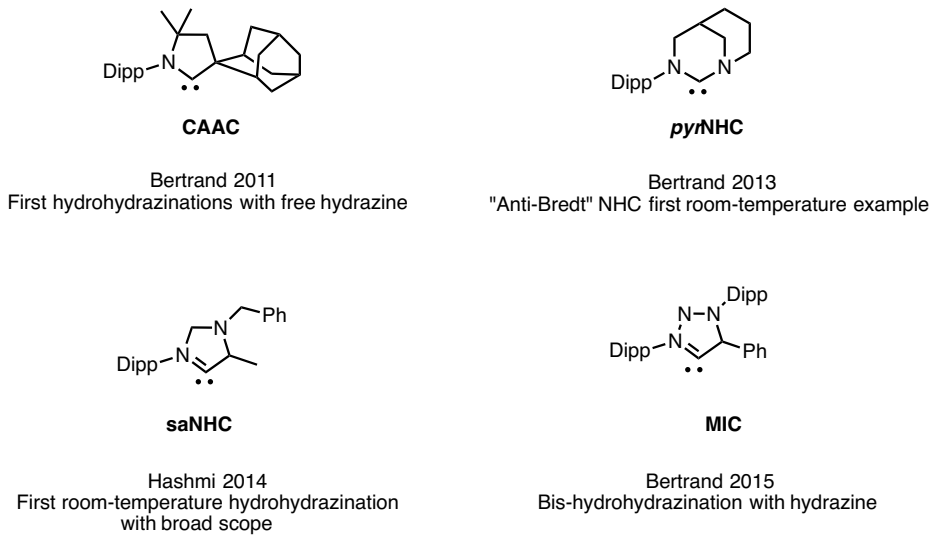

Figure 4-2. NHC catalysts for gold-mediated hydrohydrazination

In 2017, the group of Mendoza-Espinosa was able to synthesize a series of (MIC)Au^{I} complexes and upon exposure to light they observed disproportionation to a Au^{III} species.[114] They were able to conduct successful screenings of both Au^{I} and Au^{III} catalysts in the hydrohydrazination of terminal alkynes at elevated temperatures (80 °C). Their

observations reveal initially that (MIC)Au^{I} complexes outperform the (MIC)Au^{III} complexes although the addition of additives (e.g., $KB(C_6F_5)_4$) is a key factor. All of these published reports have employed the use of modified carbenes, which usually represent notoriously difficult materials to handle on the benchtop in their free carbene form. In this regard the development of alternative classes of gold pre-catalysts featuring more easily handled ligands represents a useful area of inquiry in the pursuit of new hydrohydrazination chemistry.

4.2.3 Mechanism of Gold-Mediated Hydrohydrazination

The mechanism of late-metal hydroamination is still highly contested.[115] The debate of inner vs. outer-sphere mechanism, as seen Chapter One of this document, is ongoing. Mechanistic evidence has been provided for an outer-sphere mechanism by Maier and co-workers for gold-catalyzed hydroaminations.[68] In 2014, Ujaque, Lledós and co-workers conducted a mechanistic investigation into the hydrohydrazination of both terminal and internal alkynes with aforementioned NHC catalysts (Scheme 4-2) to identify a potential mechanism for gold-catalyzed hydrohydrazination.[116]

Before the catalytic cycle can be initiated, the formation of a catalytically active, cationic gold species must be generated via the addition of a halide abstractor (MX), as shown in Scheme 4-1.

$$[(NHC)AuCl] \xrightarrow{M\text{-}X} [(NHC)Au]^{+}X^{-} + MCl$$

Scheme 4-1. Activation of AuCl pre-catalyst with a halide abstractor (MX)

Commonly applied activators include the silver compounds $Ag(SbF_6)$, AgOTf, $AgBF_4$, and $AgB(C_6F_5)_4$ as well as their potassium and lithium analogues, featuring low or non-co-ordinating anions. These are common for all gold-catalyzed hydrohydrazinations

and allow the formation of highly active catalysts. Tuning the additive can lead to higher conversion and a more diverse substrate scope.

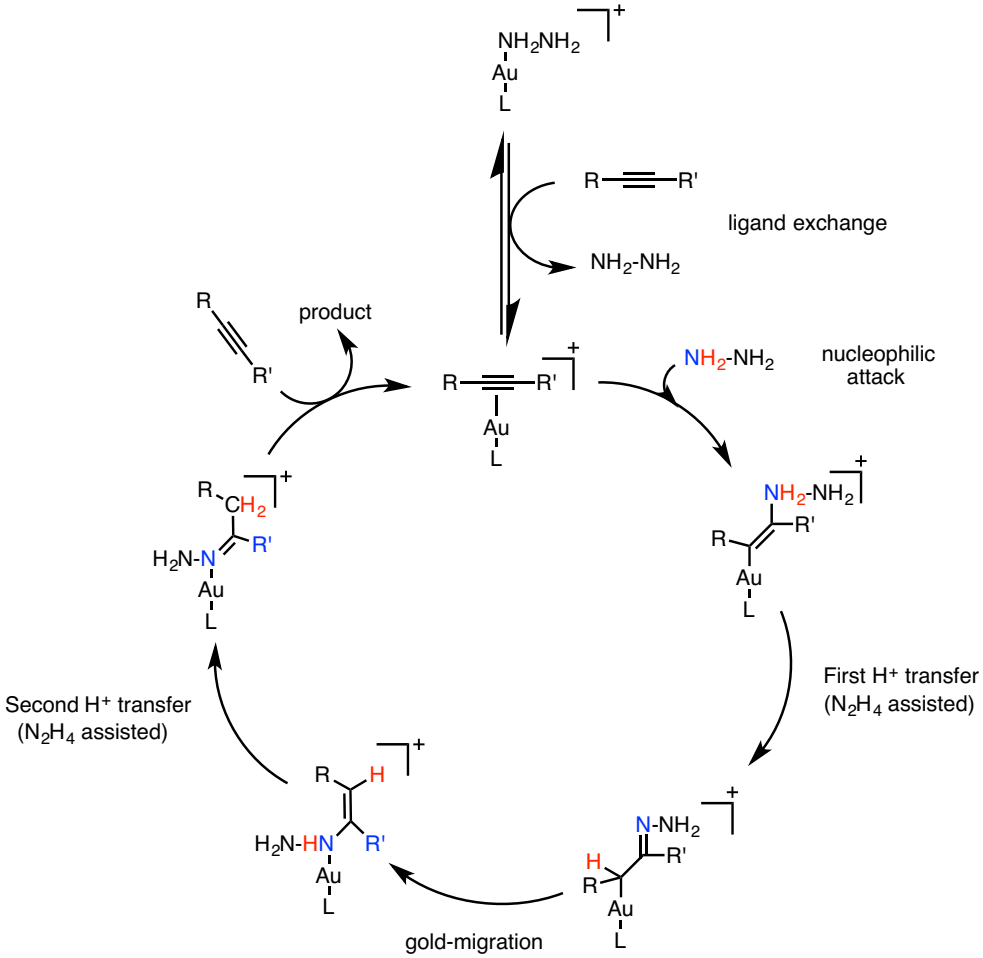

Scheme 4-2. Proposed mechanistic pathway for gold-mediated hydrohydrazination

Upon successful generation of the amine-bound cationic gold complex (Scheme 4-2, as adapted from reference 113), a ligand substitution must take place to form a π-bound alkyne. The ability for the alkyne to π-donate into the gold complex allows for the nucleophilic attack of the hydrazine in an outer sphere approach. A proton transfer followed by migration of gold to the nitrogen of the hydrazine synthon allows for the formation of an enamine intermediate,[117] which can undergo a second proton transfer to generate the target imine product. Ligand substitution of the starting alkyne then regenerates the active

catalytic species, which can further undergo catalytic turnover. Computational studies along with isolation of key intermediates confirm the viability of this pathway. As well, Ujaque and Lledós found that hydrohydrazination is highly thermodynamically favourable process. DFT calculations reveal that the hydrazone product, resulting from the reaction between hydrazine and phenylacetylene, is more than 30 kcal mol^{-1} more stable than the reactants.[116] The ability to specifically tune the ligand to meet the requirements of gold in such reactions, including possibly enforcing low co-ordination, as well as providing the right halide abstractor, may lead to more active catalysts in the hydrohydrazination of alkynes, particularly for challenging internal alkynes.

4.3 Motivation and Research Goals

As outlined above, all previously developed methodologies for the hydrohydrazination of alkynes with free hydrazine have been conducted with modified NHC ligands. This would appear to preclude the ability of other ligands, most notably phosphines, to perform this reaction type. Indeed, Hashmi and co-workers have examined the use of a $(PPh_3)AuCl$ complex for the room-temperature hydrohydrazination of terminal alkynes, operating with negligible turnover.[112] To test this idea further, my thesis research focused on the development of a series of readily synthesized $(PR_3)AuCl$ complexes for the room-temperature hydrohydrazination of terminal alkynes with parent hydrazine.

4.4 Results and Discussion

4.4.1 Ligand Choice and Catalyst Development

In selecting phosphines to employ in the survey, we envisioned that sterically demanding ligands might work best in supporting reactive, low-coordinate, cationic Au(I) centers, in part by discouraging bimolecular decomposition. With this in mind, the

following ligands were chosen (Figure 4-3): BippyPhos (**4-L1**); *t*BuJohnPhos (**4-L2**); AdJohnPhos (**4-L3**); OTips-DalPhos (**4-L4**) and the new variant **4-L5**; cataCXium-A (**4-L6**); Mor-DalPhos (**4-L7**); and PAd-DalPhos (**4-L8**). This set of ligands was chosen intentionally to span monophosphines featuring or lacking a secondary donor moiety (i.e. (hetero)aryl, O, N), as well as a bisphosphine. From a practical perspective, each of **4-L1** to **4-L8** is air-stable, and with the exception of **4-L5**, is commercially available, thus making protocols developed herein viable for end-users. The ability to utilize readily available ligands, especially those which have proven excellent catalysts for myriad other transformations represents a significant synthetic advantage (see Section 4.2.3).

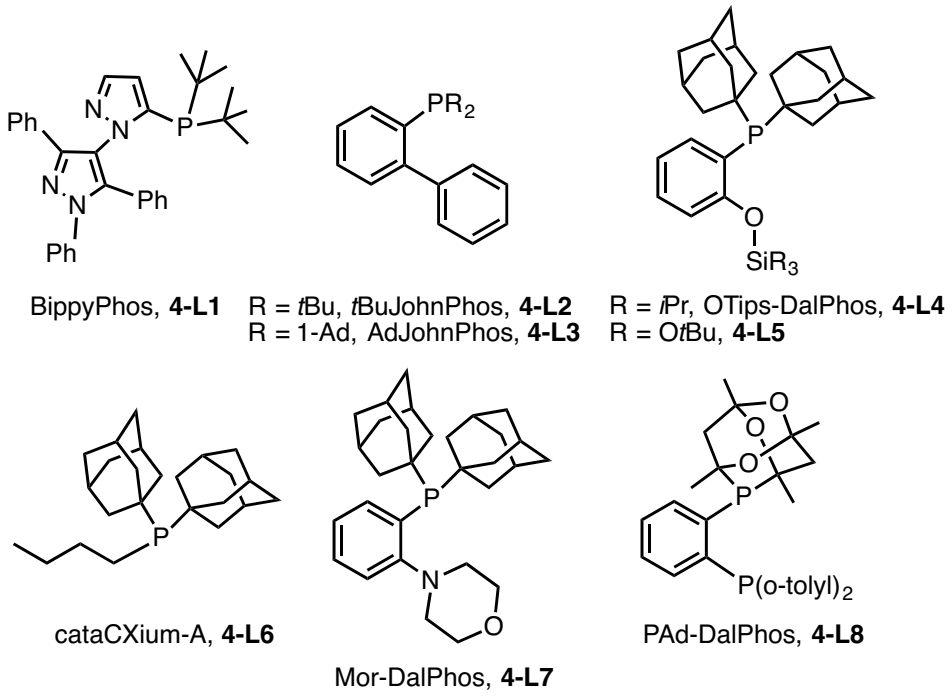

Figure 4-3. Phosphine ligands applied screened for activity in hydrohydrazination

Whereas (**4-L2**)AuCl (**4-C2**) and (**4-L7**)AuCl (**4-C7**) were obtained from commercial sources, and (**4-L3**)AuCl (**4-C3**)[67] and (**4-L6**)AuCl (**4-C6**)[118] were prepared using litereature methods. the otherwise new (**L**)AuCl complexes derived from **4-L1** (**4-**

C1), **4-L4** (**4-C4**), **4-L5** (**4-C5**) and **4-L8** (**4-C8**) were prepared in high yield either via displacement of dimethylsulfide from $AuCl(SMe_2)$ or from $HAuCl_4 \cdot H_2O$ under reducing conditions (Scheme 4-3, see Section 4.5.2). The presence of two phosphorus atoms in **4-L8** was exploited in the preparation of the digold species, (**4-L8**)$(AuCl)_2$ (**4-C9**). It should be noted that the choice of synthetic protocol was not ligand-specific. Both methodologies afforded the target AuCl pre-catalysts in high yield and the selection of synthetic protocol in some cases was based simply upon the availability of appropriate starting materials in the laboratory.

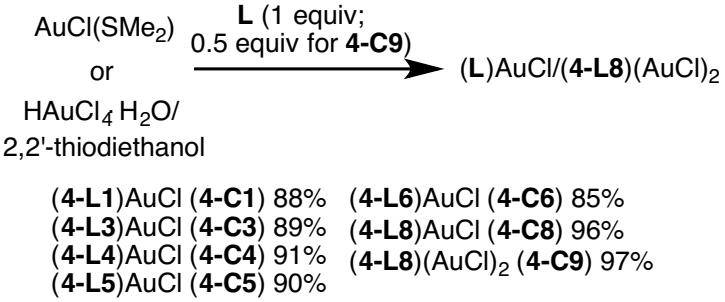

Scheme 4-3. Synthesis of AuCl pre-catalysts

Each of the new complexes reported herein was identified on the basis of NMR and elemental analysis data, as well as single-crystal X-ray diffraction data (Figure 4-4); X-ray data for C3 are also provided. The metrical parameters found within the solid state structures of these complexes (See Appendix 3) are neither unusual nor vary significantly, with Au-P (2.23-2.26 Å), Au-Cl (2.28-2.30 Å), and nearly linear P-Au-Cl linkages (170-179˚) observed that are in agreement with previously reported compounds including the catacXium A and Mor-DalPhos complexes **4-C6**[118] and **4-C7**,[67] and (carbene)AuCl complexes[111, 113] that have been employed previously in alkyne hydrohydrazination with hydrazine. The Au-Au distance (2.9700(3) Å) in **4-C9** is within the common range observed for aurophilic interactions.[119]

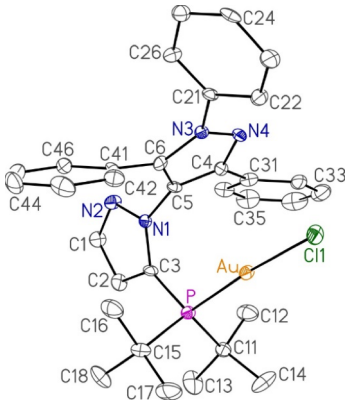

4-C1

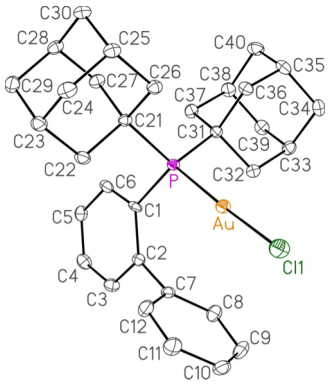

4-C3

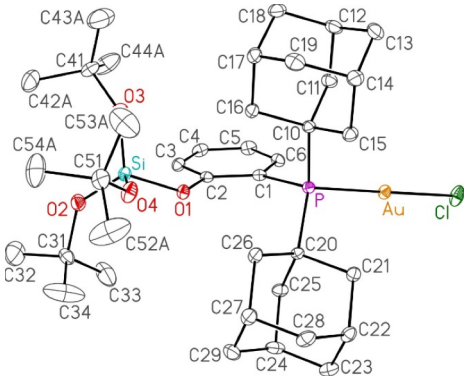

4-C4

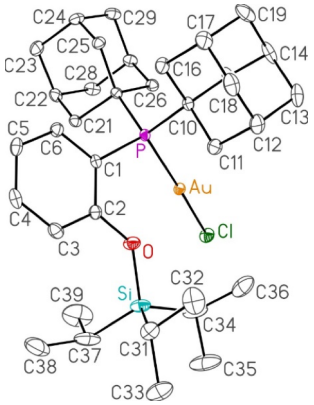

4-C5

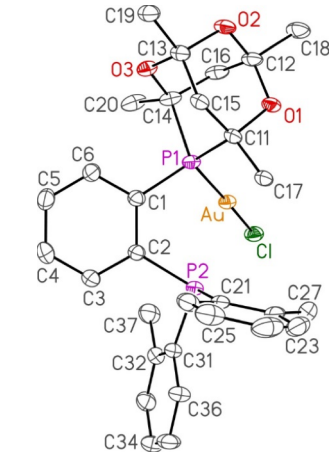

4-C8

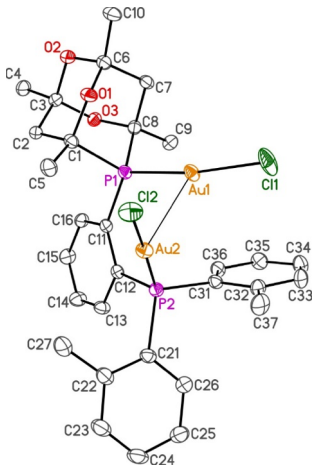

4-C9

Figure 4-4. Single-crystal X-ray structures of new gold pre-catalyst complexes

4.4.2 Optimization and Substrate Scope for Au-Catalyzed Hydrohydrazination

With a collection of phosphine-ligated Au(I) pre-catalysts in hand (i.e. **4-C1** to **4-C9**) we conducted a competitive screen involving the hydrohydrazination of phenylacetylene with hydrazine hydrate to give **4-1**, employing $LiB(C_6F_5)_4 \cdot 2.5Et_2O$ as a halide abstraction agent under mild conditions (4 h, 25 ˚C, 1 mol% pre-catalyst; Scheme 4-4). Although a number of other halide abstracting agents were utilized, $LiB(C_6F_5)_4 \cdot 2.5Et_2O$, a commercially available reagent, proved to be the most efficient for this transformation. While most of the pre-catalysts surveyed afforded low consumption of the starting materials and ≤ 20% conversion to **4-1**, each of **4-C5** and **4-C6** afforded high conversion to the target hydrazine product, with **4-C6** proving to be marginally superior. The success of **4-C5** and **4-C6** in enabling this reaction is noteworthy, given that the groups of Bertrand[110-111] and Hashmi[120] have each demonstrated the inability of otherwise effective (carbene)AuCl complexes to catalyze such a transformation under these mild conditions. Furthermore, the observation that the Mor-DalPhos ligated pre-catalyst **4-C7** is highly effective for the stereoselective hydroamination of internal aryl alkynes with dialkylamines,[67] but is ineffective for the test transformation leading to **4-1** (Scheme 4-4), confirms that the ancillary ligand plays an important role in determining the successful outcome of Au-catalyzed hydroaminations in a substrate-dependent manner.

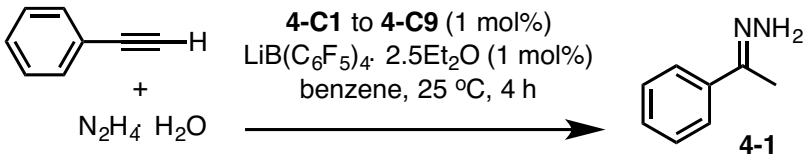

Scheme 4-4. Optimization table for the hydrohydrazination of phenylacetylene

Having discovered that the cataCXium-A ligated complex **4-C6** is a capable pre-catalyst for the hydrohydrazination of phenylacetylene with hydrazine hydrate under mild conditions (4 h, 25 ˚C, 1 mol% Au), we then turned our attention to examining the scope of reactivity (Scheme 4-5). A range of substituted terminal aryl alkynes were accommodated successfully under these conditions; *para*-alkyl, methoxy, and halide substituents were well-tolerated and the desired product in each case was generated in high yield **4-C2** to **4-C6** (87-98%). While the presence of an *ortho*-amino group within the phenylacetylene framework did somewhat inhibit conversion, the successful formation of **4-8** (52%) was nonetheless achieved at room temperature. Conversely, the *para*-trifluoromethyl substituted phenylacetylene substrate leading to **4-7** proved to be particularly challenging, requiring more forcing conditions in order to achieve suitable conversion (94%; 14 h, 90 ˚C, 5 mol% Au), whereas by use of a saturated abnormal NHC ligand this transformation was enabled under more mild conditions (71%; 7 h, 20 ˚C, 5 mol% Au).[112] Attempts to employ 1-phenyl-2-trimethylsilylacetylene in place of phenylacetylene afforded high conversion (87%) to the desilylated product **4-1**. Suitably high conversion was also achieved when using 3-phenyl-1-propyne leading to **4-9** (70%), or terminal (hetero)aryl alkynes based on pyridine or thiophene, leading to **4-10** and **4-11** (98 and 75%, respectively). Although not explored broadly, the ability of the (**4-C6**)-based catalyst system to effect hydrohydrazinations of internal alkynes was established in the transformation of diphenylacetylene (14 h, 90 ˚C, 5 mol% Au), leading to **4-12** (83%).

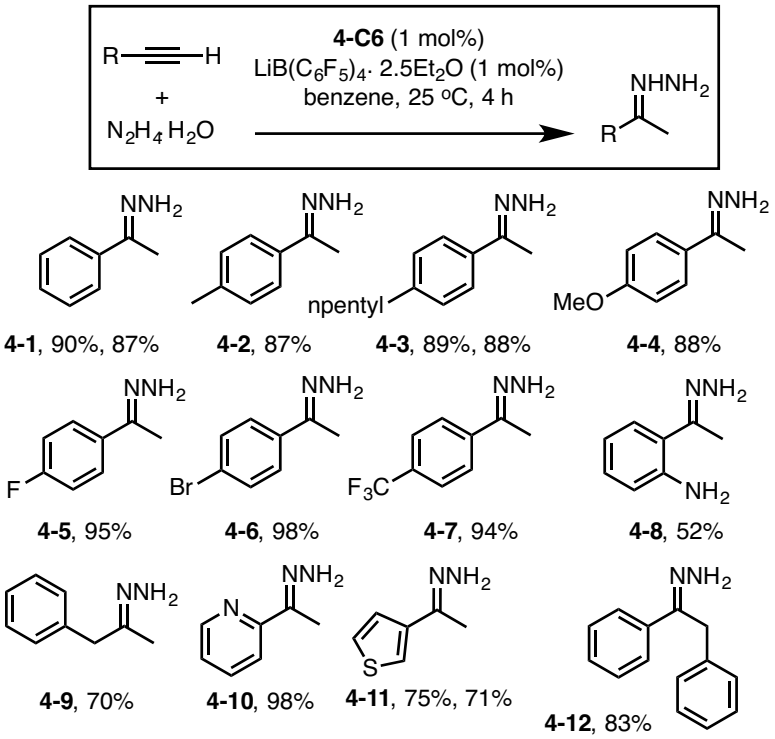

Scheme 4-5. Substrate scope for the (**4-C6**)-catalyzed hydrohydrazination of alkynes

4.4.3 Attempts at a Multicomponent Synthesis of Indazoles and Catalytic Limitations

Indazoles represent a privileged heterocyclic core structure in many pharmaceutical applications. Particularly attractive is the bioactivity exhibited by many indazole containing substrates. These have demonstrated efficacy in many treatments including anti-cancer,[121] anti-inflammatory,[122] anti-platelet drugs,[123] as well as serotonin 5-HT3 receptor antagonist activities.[124] As well, the ability to synthesize C3-monosubstitued indazoles is attractive, as these represent a biologically relevant class of indazole products[125] (Figure 4-5).

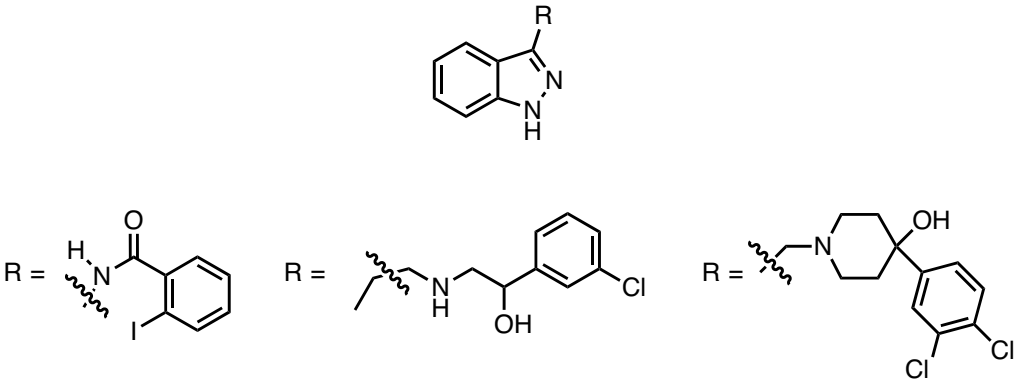

Figure 4-5. Biologically relevant C3-monosubtituted indazoles

Utilizing our knowledge of gold-catalyzed hydrohydrazination (Section 4.4.2), as well as our previously developed amination catalysts with both nickel and palladium (Chapters Two and Three) we envisioned a one-pot synthetic protocol to access the core of these biologically relevant substrates. The process would involve a first-step gold-catalyzed hydrohydrazination of an *o*-alkynyl haloarene followed a by a subsequent intramolecular arylation of the intermediate hydrazone to generate a C3-substituted indazole product (Scheme 4-6).

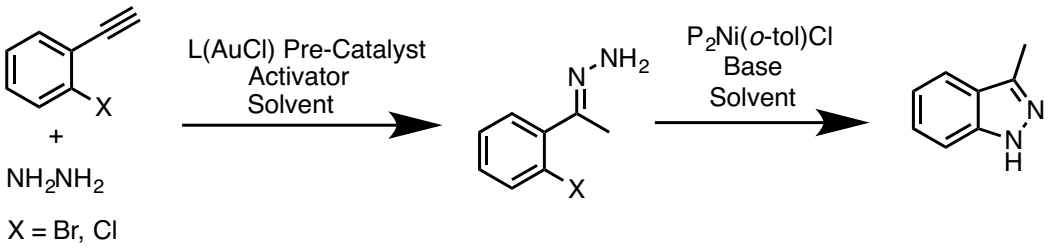

Scheme 4-6. Multicomponent synthesis of indazoles

This represents an attractive protocol which precludes the need to isolate a potentially unstable hydrazone intermediate, which can undergo degradation to form the corresponding azine product. The first attempts at this synthesis involved a first-step, Au-catalyzed hydrohydrazination, which was allowed to react for four hours at room temperature, in keeping with our established protocol. Unfortunately, the ortho-substitution

of the alkynes seemed to hinder room-temperature reactivity with poor substrate conversion observed. The reaction was then conducted at 90 ˚C over 4 hours, whereby the formation of hydrazone intermediate was monitored by the use NMR spectroscopy. Once the hydrohydrazination reaction was complete, the reaction mixture was then filtered through magnesium sulfate and Celite into a second vial containing the nickel pre-catalyst, base (NaO*t*Bu), and solvent. This reaction was allowed to continue for sixteen hours. Unfortunately, after many attempts at a one pot synthesis including the use of a plethora of nickel sources, bases, solvent combinations and temperatures turnover to the desired indazole product was not observed (Scheme 4-7).

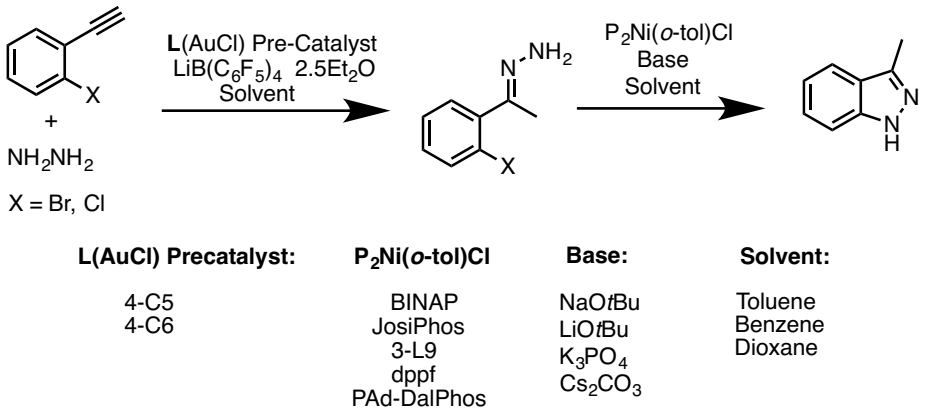

Scheme 4-7. Attempts at a one-pot indazole synthesis

As well, Mor-DalPhos/[Pd(cinnamyl)Cl]$_2$ was also utilized as a catalyst for the intramolecular amination under a number of varied reactions conditions, to no avail. Although this is a promising reaction protocol it will require further optimization and a deeper understanding of the interaction between the ligands and metal centres in the reaction mechanism to afford a successful system.

Although the successful reactions detailed in Scheme 4-5 represent the first examples of a phosphine-based Au catalyst conducting room-temperature

hydrohydrazinations, there were limitations associated with the reaction protocol. Many of the hydrazone products proved unstable under work-up conditions. This made isolation particularly difficult, with some of the products requiring isolation as the azine product (see Section 4.5.3). The use of ortho-containing substrates was limited to one example with a fairly low yield (Scheme 4-5, **4-8**). The inability to incorporate alkynes with alkyl functional groups remains a challenge, as these products are difficult to isolate and degrade rapidly. The lack of internal alkyne products also represents a significant limitation of this chemistry. Internal alkynes remain a particular challenge in the field hydrohydrazination, requiring forcing conditions and affording a very limited substrate scope.

4.4.4 Conclusions

In conclusion, the results of a screening process involving a crystallographically characterized series of phosphine-ligated and $LiB(C_6F_5)_4 \cdot 2.5Et_2O$-activated (**L**)AuCl pre-catalysts in the hydrohydrazination of terminal aryl alkynes with hydrazine hydrate establish (**4-L6**)AuCl (**4-L6** = cataCXium-A) as being highly effective for these reactions. The ability of (**4-L6**)AuCl to effect such transformations under mild conditions (25 ˚C, 1 mol% Au) distinguishes this pre-catalyst from previously reported pre-catalysts for alkyne hydrohydrazination with unsubstituted hydrazine, which are exclusively of the type (carbene)AuCl and operate under somewhat more forcing conditions (> 80 ˚C and/or 5 mol% Au). In addition to establishing for the first time the beneficial role of appropriately configured phosphine ancillary ligands in Au-catalyzed alkyne hydrohydrazination chemistry, we view our results as expanding the catalyst "tool box" for chemists who seek to apply this methodology in chemical synthesis.

4.5 Experimental: General Procedures and Characterization Data

4.5.1 General Considerations

Unless otherwise stated, all reactions were set-up inside a nitrogen-filled inert atmosphere glovebox and worked up in air using benchtop procedures. When used within the glovebox solvents were deoxygenated by sparging with nitrogen gas followed by passage through a double column solvent purification system packed with alumina and copper-Q5 reactant (toluene and benzene), or alumina (dichloromethane), and storage over activated 4 Å molecular sieves. Ligands **4-L4**[126] and **4-L8**[127] and complexes **4-C3**[67] and **4-C6**[118] were prepared using literature methods; ligands **4-L1**, **4-C2** and **4-C7** were used as received from commercial sources. Column chromatography was carried out using neutral Silicycle Siliaflash 60 silica (particle size 40-63 μm; 230-400 mesh). NMR spectra were recorded at 300 K and referenced internally to the solvent employed. Splitting patterns are indicated as follows: br, broad; s, singlet; d, doublet; t, triplet; q, quartet; m, multiplet. All coupling constants (*J*) are reported in Hertz (Hz). Mass spectra were obtained using ion trap (ESI) instruments operating in positive mode, and GC data were obtained on an instrument equipped with a SGE BP-5 column (30 m, 0.25 mm i.d.).

4.5.2 General Procedures and Crystallographic Refinement Details

General Procedures for the Synthesis of Au Complexes (4-GP1). In air, a 100 mL round-bottom Schlenk flask was charged with a magnetic stir-bar, phosphine ligand (0.41 mmol), and dichloromethane (30 mL). To this mixture was added a mixture of $AuCl(SMe_2)$ (0.41 mmol, 120.8 mg) in dichloromethane (50 mL). The reaction vessel was covered in Al foil to circumvent light-induced decomposition and was connected to a Schlenk apparatus. The headspace of the reaction flask was evacuated briefly, back-filled

with nitrogen gas, and magnetic stirring was initiated. After 2 h, the reaction mixture was concentrated *in vacuo*. In air, the resulting residue was washed with acetone (2 x 10 mL), and was dried *in vacuo* to afford the target product. **4-GP2.** Under a nitrogen atmosphere, a 50 mL round-bottom Schlenk flask was charged with a magnetic stir-bar, $HAuCl_4 \cdot H_2O$ (1.45 mmol, 0.492 g), and water (1.5 mL), and magnetic stirring was initiated. To this mixture was added dropwise 2,2'-thiodiethanol (4.4 mmol) over the course of 0.5 h, during which time the solution changed from an orange-yellow emulsion to a clear and colorless. The Schlenk flask was then opened and against a counter-flow of nitrogen the phosphine ligand (1.45 mmol) was added in a single portion, followed by the addition of ethanol (4.5 mL). The Schlenk flask was then re-sealed under nitrogen and magnetic stirring was continued for 3 h. The resulting mixture was then filtered in air, and was washed with acetone (2 x 15 mL), diethyl ether (15 mL), and pentane (15 mL). The remaining solid was then dried *in vacuo* to afford the target product.

General Catalytic Procedure for the Formation of Imines from Terminal Alkynes (GP3). Unless specified otherwise in the text, **4-C6** (0.002 mmol) and $LiB(C_6F_5)_4 \cdot 2.5Et_2O$ (0.002 mmol) were added as a stock solution in C_6D_6 (200 μL total delivered) to a screw capped vial containing alkyne (0.2 mmol), hydrazine hydrate (0.24 mmol), C_6D_6 (400 μL), and a small magnetic stir-bar. The vial was sealed with a cap containing a PTFE septum, removed from the glovebox, placed in a temperature-controlled aluminum heating block set at 25 °C, and vigorous magnetic stirring was initiated for 4 h.

General Catalytic Procedure for the Formation of Imines from Internal Alkynes (GP4). Unless specified otherwise in the text, **4-C6** (0.02 mmol), $LiB(C_6F_5)_4 \cdot 2.5Et_2O$ (0.02 mmol), alkyne (0.4 mmol), hydrazine hydrate (0.48 mmol), and

benzene (1.2 mL) were added to a screw capped vial containing a small magnetic stir-bar. The vial was sealed with a cap containing a PTFE septum, removed from the glovebox, placed in a temperature-controlled aluminum heating block set at 90 °C, and vigorous magnetic stirring was initiated for 16 h.

Workup Methods:

Workup Method A (purification via chromatography). Upon completion following **GP3** or **GP4**, the reaction vial was cooled to room temperature (if needed). The reaction mixture was filtered through a Celite/silica plug and washed with dichloromethane (3 x 20 mL). From the collected eluent, the solvent was removed *in vacuo* via rotary evaporation and the compound was purified by flash column chromatography on silica gel.

Workup Method B (procedure for the preparation of samples for NMR quantification). Upon completion following **GP3** or **GP4**, the reaction vial was removed from the heating block and cooled to 4 °C, whereby an internal standard of trimethoxybenzene (0.04 mmol) was added to the reaction mixture. The reaction mixture was then filtered through Celite, and the eluent was collected and subjected to NMR analysis, with yields of product reported relative to the internal standard on the basis of integrated ^{1}H NMR signals.

Crystallographic solution and refinement details. Crystallographic data for were obtained between 193-213 K on a Bruker D8/APEX II CCD diffractometer equipped with a CCD area detector using graphite-monochromated Mo Kα (α = 0.71073 Å) or Cu Kα (α = 1.54178 Å) radiation employing a sample that was mounted in inert oil and transferred to a cold gas stream on the diffractometer. Data reduction, correction Lorentz polarization, and absorption correction (Gaussian integration; face-indexed) were each performed.

Structure solution by using direct methods, Patterson methods, or intrinsic phasing was carried out, followed by least-squares refinement on F^2. All non-hydrogen atoms were refined with anisotropic displacement parameters, while all hydrogen atoms were added at calculated positions and refined by use of a riding model employing isotropic displacement parameters based on the isotropic displacement parameter of the attached atom. Additional information is contained in the deposited CIFs (CCDC 1550225-1550231).

4.5.2 Characteriztion Data for Ligands and Gold Complexes

Synthesis of 4-L5

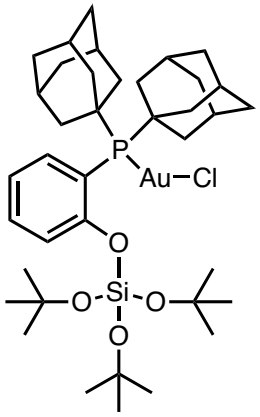

A method directly analogous to that employed in the preparation of OTips-DalPhos (**4-L4**)[16] was used, whereby ClSi(O*t*Bu)$_3$ was used in place of ClSi(*i*Pr)$_3$. The crude product was purified by column chromatography using a 1:100 (EtOAc:hexanes) eluent system to afford the target product as a white powder (90 %). ^{1}H NMR (500 MHz, $CDCl_3$): δ 7.66-7.65 (m, 1H), 7.27-7.24 (m, 1H), 7.23-7.19 (m, 1H), 6.91-6.88 (m, 1H), 1.98-1.96 (m, 6H), 1.87-1.86 (m, 12H), 1.65 (s, 12H), 1.37 (s, 27H); ^{13}C{^{1}H} NMR (125.8 MHz, $CDCl_3$): δ 160.4 (d, J_{CP} = 22.6 Hz), 137.1, 129.4, 124.6 (d, J_{CP} = 27 Hz), 119.4, 119.2, 73.6, 42.0 (d, J_{CP} = 14 Hz), 37.3, 37.0, 36.8, 31.5, 29.0 (d, J_{CP} = 8.7 Hz); ^{31}P{^{1}H} NMR (202.4 MHz,

$CDCl_3$): δ 11.7; HRMS *m/z* ESI^+ found 641.4149 $[M+H]^+$ calculated for $C_{38}H_{62}O_4P_1Si_1$ 641.4155.

Complex 4-C1.

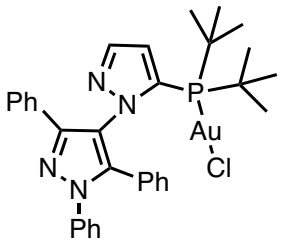

The title complex was synthesized via **4-GP2** from **4-L1** and was isolated as a white solid in 88% yield. A single crystal suitable for X-ray diffraction was obtained via vapor diffusion of pentane into a dichloromethane solution of **4-C1.** ^1H NMR (500 MHz, $CDCl_3$): δ 8.11 (d, *J* = 2.1 Hz, 1H), 7.74-7.72 (m, 2H), 7.55-7.53 (m, 2H), 7.39-7.36 (m, 3H), 7.35-7.27 (m, 4H), 7.23-7.16 (m, 4H), 6.79 (d, *J* = 2.1 Hz, 1H), 0.90 (d, *J* = 16.6 Hz, 9H), 0.79 (d, *J* = 16.5 Hz, 9H); $^{13}C\{^1H\}$ NMR (125.8 MHz, $CDCl_3$): δ 149.4, 141.5, 140.2, 140.1, 133.0-126.0 (overlapping signals), 120.0, 114.7, 37.3 (overlapping signals), 29.5 (overlapping signals); $^{31}P\{^1H\}$ NMR (202.4 MHz, $CDCl_3$): δ 48.2. Anal. Calcd for $C_{32}H_{35}Au_1Cl_3N_4P_1$: C, 52.01; H, 4.77; N, 7.58. Found: C, 51.87; H, 4.62; N 7.68.

Complex 4-C4.

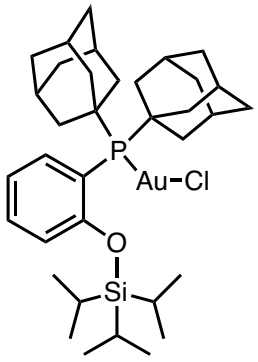

The title complex was synthesized via **4-GP2** from **4-L4** and was isolated as a white solid in 91% yield. A single crystal suitable for X-ray diffraction was obtained via vapor diffusion of pentane into a dichloromethane solution of **4-C4**. ^{1}H NMR (500 MHz, $CDCl_3$): δ 7.73-7.68 (m, 1H), 7.38-7.28 (m, 1H), 7.03-6.96 (m, 2H), 2.23-2.19 (m, 12H), 2.02 (s, 6H), 1.85-1.80 (m, 3H), 1.71 (s, 12H), 1.20-1.18 (m, 18H); ^{13}C{^{1}H} NMR (125.8 MHz, $CDCl_3$): δ 135.3, 132.1, 120.0, 118.8 (d, J_{CP} = 12.6 Hz), 112.9, 42.5-42.0 (overlapping signals), 36.3, 28.5 (d, J_{CP} = 16.4 Hz), 18.2, 13.6; ^{31}P{^{1}H} NMR (202.4 MHz, $CDCl_3$): δ 51.1. Anal. Calcd for $C_{35}H_{55}Au_1Cl_1O_1P_1Si_1$: C, 53.65; H, 7.08; N, 0. Found: C, 53.49; H, 7.17; N < 0.5.

Complex 4-C5.

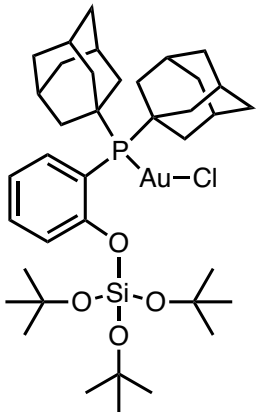

The title complex was synthesized via **4-GP2** from **4-L5** and was isolated as a white solid in 90% yield. A single crystal suitable for X-ray diffraction was obtained via vapor diffusion of pentane into a dichloromethane solution of **4-C5**. ^{1}H NMR (500 MHz, $CDCl_3$): δ 8.56-8.51 (m, 1H), 7.56-7.54 (m, 1H), 7.43-7.40 (m, 1H), 7.06 (t, J = 7.5 Hz, 1H), 2.34-2.32 (br m, 6H), 2.21 (br s, 6H), 2.02 (br s, 6H), 1.75-1.69 (br m, 12H), 1.40 (s, 27H); ^{13}C{^{1}H} NMR (125.8 MHz, $CDCl_3$): δ 156.1, 146.4 (d, J_{CP} = 23.9 Hz), 132.9, 121.2 (d, J_{CP} = 14.4 Hz), 120.6 (d, J_{CP} = 4.7 Hz), 116.0 (d, J_{CP} = 41.5 Hz), 74.9, 42.1 (d, J_{CP} = 23.9 Hz),

41.8, 36.5, 31.9, 28.9 (d, J_{CP} = 10.3 Hz); $^{31}P\{^{1}H\}$NMR (202.4 MHz, $CDCl_3$): δ 97.4. Anal. Calcd for $C_{38}H_{61}Au_1Cl_1O_4P_1Si_1$: C, 52.26; H, 7.04; N, 0. Found: C, 52.31; H, 7.44; N < 0.5.

Complex 4-C8.

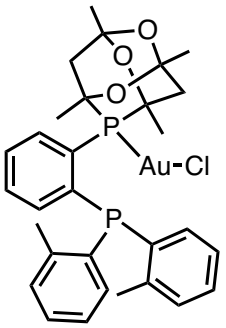

The title complex was synthesized via **4-GP1** from **4-L8** and was isolated as a white solid in 96% yield. A single crystal suitable for X-ray diffraction was obtained via vapor diffusion of diethyl ether into a dichloromethane solution of **4-C8**. The NMR spectra of **4-L8** and derived complexes are rendered complex due to a combination of second order phenomena and dynamic behavior involving the chiral phosphaadamantyl cage (CgP)/P(*o*-tolyl)$_2$ moiety.[127] ^{1}H NMR (CD_2Cl_2, 500 MHz): 8.62-8.58 (m, 1H), 7.65-7.62 (m, 1H), 7.55-7.52 (m, 1H), 7.37-7.31 (m, 4H), 7.28-7.25 (m, 1H), 7.16-7.11 (m, 2H), 6.75 (m, 2H), 2.90-2.88 (m, 1H), 2.63 (br, 3H), 2.33 (s, 3H), 2.12-1.84 (m, 4H), 1.57 (s, 2H), 1.45 (s, 4H), 1.31 (s, 3H), 0.94-0.89 (m, 2H). $^{31}P\{^{1}H\}$ NMR (CD_2Cl_2, 202.4 MHz): 9.22 (d, J_{PP} = 207 Hz), 4.92 (d, J_{PP} = 207 Hz). Anal. Calcd for $C_{30}H_{34}Au_1Cl_1O_3P_2$: C, 48.87; H, 4.65; N, 0. Found: C, 48.61; H, 4.73; N < 0.5.

Complex 4-C9.

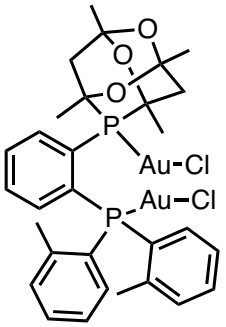

The title complex was synthesized via **4-GP1** from **L8** (using two equiv $AuCl(SMe_2)$) and was isolated as a yellow solid in 97% yield. A single crystal suitable for X-ray diffraction was obtained via vapor diffusion of diethyl ether into a dichloromethane solution of **C9**. The NMR spectra of **L8** and derived complexes are rendered complex due to a combination of second order phenomena and dynamic behavior involving the chiral phosphaadamantyl cage (CgP)/P(*o*-tolyl)$_2$ moiety.[127] ^{1}H NMR (CD_2Cl_2, 500 MHz): 8.89-8.85 (m, 1H), 7.82-7.78 (m, 1H), 7.60-7.55 (m, 3H), 7.54-7.51 (m, 1H), 7.47-7.45 (m, 1H), 7.29-7.26 (m, 1H), 7.22-7.15 (m, 2H), 6.95-6.91 (m, 1H), 6.38-6.33 (m, 1H), 2.89-2.88 (m, 3H), 2.80 (s, 3H), 2.35-2.32 (m, 1H), 2.05-1.90 (m, 5H), 1.60-1.56 (m, 4H), 1.49-1.43 (m, 6H); ^{31}P{^{1}H} NMR (CD_2Cl_2, 202.4 MHz): 9.10 (d, J_{PP} = 51 Hz), 4.47 (d, J_{PP} = 51 Hz). Anal. Calcd for $C_{30}H_{34}Au_2Cl_2O_3P_2$: C, 37.15; H, 3.54; N, 0. Found: C, 37.33; H, 3.72; N < 0.5.

4.4 Characterization Data for Hydrohydrazination Products

(1-(phenyl)ethylidene)hydrazine (**4-1**).

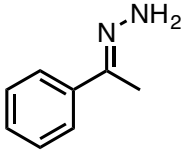

The title compound was synthesized from the corresponding alkyne according to **4-GP3**. Utilizing workup method **B** with trimethoxybenzene as an internal standard a yield of 90%

was obtained. Utilizing **GP3** from 1-phenyl-2-trimethylsilylacetylene (5 mol% catalyst loading) and following workup method **B** with trimethoxybenzene as an internal standard a yield of 87%. ^{1}H NMR (500 MHz, C_6D_6): δ 7.74-7.72 (m, 2H), 7.19-7.15 (m, 2H), 7.11-7.08 (m, 1H), 4.78 (br, 2H), 1.56-1.55 (m, 3H). Agrees with data previously reported in the literature.[112]

(1-(p-tolyl)ethylidene)hydrazine (**4-2**).

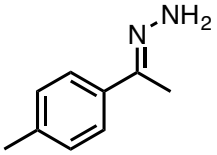

The title compound was synthesized from the corresponding alkyne according to **4-GP3**. Utilizing workup method **B** with trimethoxybenzene as an internal standard a yield of 87% was obtained. ^{1}H NMR (500 MHz, C_6D_6): δ 7.70-7.69 (m, 2H), 7.02-7.01 (d, *J* = 8.1 Hz, 2H), 4.82-4.75 (m, 2H), 2.11 (s, 3H), 1.60-1.59 (m, 3H). Agrees with data previously reported in the literature.[112]

(1-(4-pentylphenyl)ethylidene)hydrazine (**4-3**).

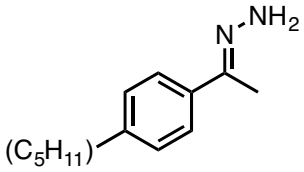

The title compound was synthesized from the corresponding alkyne according to **4-GP3**. Utilizing workup method **B** with trimethoxybenzene as an internal standard a yield of 89% was obtained. ^{1}H NMR (500 MHz, C_6D_6): δ 7.73 (d, *J* = 8.2 Hz, 2H), 7.08 (d, *J* = 8.3 Hz, 2H), 4.75 (br, 2H), 2.47 (t, *J* = 7.9 Hz, 2H), 1.62-1.61 (m, 3H), 1.56-1.49 (m, 3H), 1.26-1.19 (m, 5H), 0.86-0.83 (m, 3H). Product identity confirmed via isolation of the corresponding azine (**4-3'**).

(1,2-bis(1-(4-pentylphenyl)ethylidene)hydrazine (**4-3'**).

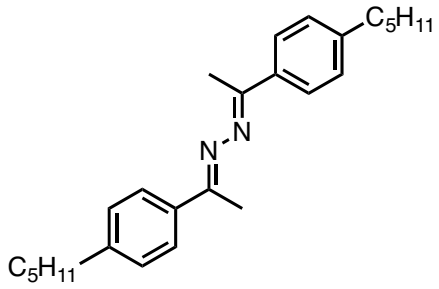

The title compound was synthesized from the corresponding alkyne according to **4-GP3** utilizing workup method **A**. Purified by column chromatography (1 % EtOAc/hexanes) to yield as a yellow solid in 88% yield. ^{1}H NMR (500 MHz, $CDCl_3$): δ 7.87 (d, *J* = 8.2 Hz, 4H), 7.28 (d, *J* = 8.2 Hz, 4H), 2.69 (t, *J* = 7.7 Hz, 4H), 2.35 (s, 6H), 1.72-1.66 (m, 4H), 1.40-1.37 (m, 8H), 0.95 (t, *J* = 6.9 Hz, 6H); ^{13}C NMR: ($CDCl_3$, 125.8 MHz): δ 158.3, 145.0, 136.2, 128.6, 126.8, 36.0, 31.7, 31.2, 22.8, 15.2, 14.2. HRMS *m/z* ESI^{+} found 377.2951[M+H]$^{+}$ calculated for $C_{26}H_{37}N_2$ 377.2957.

(1-(4-methoxyphenyl)ethylidene)hydrazine (**4-4**).

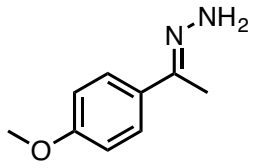

The title compound was synthesized from the corresponding alkyne according to **4-GP3**. Utilizing workup method **B** with trimethoxybenzene as an internal standard a yield of 88% was obtained. ^{1}H NMR (500 MHz, C_6D_6): δ 7.71-7.70 (d, *J* = 8.9 Hz, 2H), 6.79 (d, *J* = 8.9 Hz, 2H), 4.75 (br, 2H), 3.30 (s, 3H), 1.60 (s, 3H). Agrees with data previously reported in the literature.[112]

(1-(4-fluorophenyl)ethylidene)hydrazine (**4-5**).

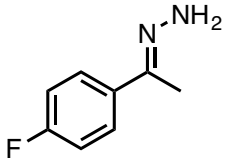

The title compound was synthesized from the corresponding alkyne according to **4-GP3**. Utilizing workup method **B** with trimethoxybenzene as an internal standard a yield of 95% was obtained. ^{1}H NMR (500 MHz, C_6D_6): δ 7.52-7.49 (m, 2H), 6.83-6.79 (m, 2H), 4.72 (br, 2H), 1.46 (m, 3H). Agrees with data previously reported in the literature.[112]

(1-(4-bromophenyl)ethylidene)hydrazine (**4-6**)

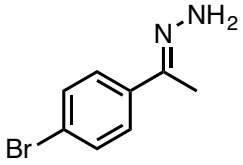

The title compound was synthesized from the corresponding alkyne according to **GP3**. Utilizing workup method **B** with trimethoxybenzene as an internal standard a yield of 98% was obtained. ^{1}H NMR (500 MHz, C_6D_6): δ 7.38-7.36 (m, 2H), 7.28-7.27(m, 2H), 4.74 (br, 2H), 1.40-1.39 (m, 3H). Agrees with data previously reported in the literature.[112]

(1-(4-trifluoromethyl)phenyl)ethylidene)hydrazine (**4-7**).

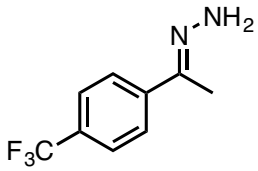

The title compound was synthesized from the corresponding alkyne according to **4-GP3**. Utilizing workup method **B** with trimethoxybenzene as an internal standard a yield of 94% was obtained. ^{1}H NMR (500 MHz, C_6D_6): δ 7.51 (d, J = 13.7 Hz, 2H), 7.37-7.34 (m, 2H), 4.80 (br, 2H), 1.39 (s, 3H). Agrees with data previously reported in the literature.[112]

2-(1-hydrazonoethyl)aniline (**4-8**).

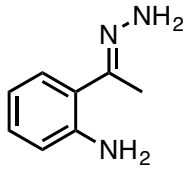

The title compound was synthesized from the corresponding alkyne according to **4-GP3**. Utilizing workup method **B** with trimethoxybenzene as an internal standard a yield of 52% was obtained. ^{1}H NMR (500 MHz, C_6D_6): δ 7.11-7.09 (m, 1H), 7.08-7.04 (m, 2H), 6.32-6.30 (m, 1H), 4.74 (br, 2H), 2.89 (br s, 2H), 1.59 (s, 3H). Agrees with data previously reported in the literature.[112]

(1-phenylpropan-2-ylidene)hydrazine (**4-9**).

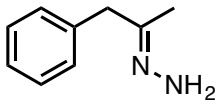

The title compound was synthesized from the corresponding alkyne according to **4-GP3**. Utilizing workup method **B** with trimethoxybenzene as an internal standard a yield of 70% was obtained. ^{1}H NMR (500 MHz, C_6D_6): δ 7.11-7.07 (m, 5H), 4.46 (br, 2H), 3.41 (s, 2H), 1.22-1.20 (m, 3H). Agrees with data previously reported in the literature.[112]

2-(1-hydrazonoethyl)pyridine (**4-10**).

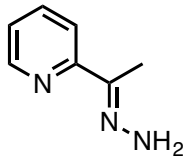

The title compound was synthesized from the corresponding alkyne according to **4-GP3**. Utilizing workup method **B** with trimethoxybenzene as an internal standard a yield of 98% was obtained. ^{1}H NMR (300 MHz, C_6D6): δ 8.44-8.42 (m, 1H), 8.16 (d, J = 13.6 Hz, 1H),

7.11-7.08 (m, 1H), 6.64-6.60 (m, 1H), 4.96 (s, 2H), 2.07 (s, 3H). Agrees with data previously reported in the literaure.[128]

(1-(thiophen-3-yl)ethylidene)hydrazine (**4-11**).

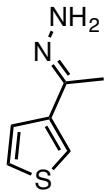

The title compound was synthesized from the corresponding alkyne according to **4-GP3**. Utilizing workup method **B** with trimethoxybenzene as an internal standard a yield of 75% was obtained. ^{1}H NMR (300 MHz, C_6D_6): δ 7.69-7.67 (m, 1H), 6.89-6.85 (m, 2H), 4.46 (br, 2H), 1.51-1.49 (m, 3H). Product identity confirmed via isolation of the corresponding azine (**4-11'**).

(1,2-bis(1-thiophen-3-yl)ethylidene)hydrazine (**4-11'**).

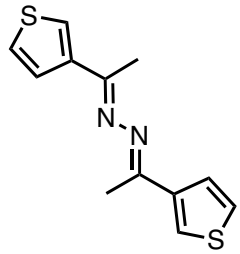

The title compound was synthesized from the corresponding alkyne according to **4-GP3** utilizing workup method **A**. Purified by column chromatography (3 % EtOAc/hexanes) to yield as a yellow solid in 71% yield. ^{1}H NMR (500 MHz, $CDCl_3$): δ 7.75-7.74 (m, 2H), 7.70-7.69 (m, 2H), 7.37-7.36 (m, 2H), 2.37 (s, 6H); $^{13}C\{^{1}H\}$ NMR: ($CDCl_3$, 125.8 MHz): δ 156.4, 141.7, 126.5, 126.4, 126.1, 16.1. HRMS *m/z* ESI^{+} found 249.0515 $[M+H]^{+}$ calculated for $C_{12}H_{13}N_2S_2$ 249.0520.

(1,2-diphenylethylidene)hydrazine (**4-12**).

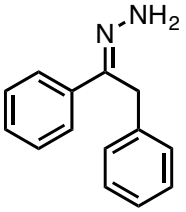

The title compound was synthesized from the corresponding alkyne according to **4-GP4** utilizing workup method **A**. Purified by column chromatography (5 % EtOAc/hexanes) to yield as a white solid in 83% yield. ^{1}H NMR (500 MHz, $CDCl_3$): δ 7.65 (d, J = 7.3 Hz, 2H, ArH), 7.32-7.25 (m, 5H), 7.21-7.20 (m, 3H), 5.34 (s, 2H), 4.01 (s, 2H). $^{13}C\{^{1}H\}$ NMR ($CDCl_3$, 125.8 MHz): δ 148.8, 139.4, 135.6, 130.0, 129.3, 128.9, 128.8, 128.6, 128.4, 128.2, 127.7, 127.1, 125.8, 32.6. Agrees with data previously reported in the literature.[129]

Chapter 5: Conclusions

5.1 Chapter 2: Summary and Conclusions

Chapter Two outlines the multicomponent synthesis of indoles utilizing a Mor-DalPhos/Pd catalyst system. This catalytic protocol allowed the formation of 29 unique indole products in both one and two-step multicomponent reactions utilizing a Buchwald-Hartwig amination/α-arylations pathway to generate the target indoles. Section 2.4.1 establishes the reaction pathway as a two-step, one-pot multicomponent synthesis utilizing N-octylamine and acetone as the primary coupling partners. This protocol established the first multicomponent synthesis of indoles utilizing acetone as a starting material. This methodology was extended in Section 2.4.2 to establish substrate scope with acetone (10 eq.), while varying the amine coupling partner. It should be noted that this class of 2-methylindoles represent a pharmaceutically relevant class of compounds. Section 2.4.3 demonstrates the ability to utilize methyl ketones (2 eq.) while keeping the amine coupling partner constant to generate a diverse array of N-octyl, 2-substituted indole products. This methodology was also extended to a one-step one-pot reaction sequence under non-inert conditions (Section 2.4.4). All reactants, catalysts and solvent could be added at the outset of the reaction sequence, subsequently exposed to air, and react to afford the target indole products, albeit with lower yields. This ability to conduct these reactions in a "true one pot" synthetic protocol under benchtop conditions offers a synthetic advantage over previously identified indole syntheses.

We were also able to conduct several mechanistic investigations as to the elementary steps involved in this catalytic protocol. Both GC and NMR monitoring of the reaction led to a proposed involving a first-step Buchwald-Hartwig amination, followed by

an α-arylation of the ketone and a rapid condensation to generate the target indole. This mechanism is in contrast to a previously identified reaction pathway proposed by Kurth and coworkers.[81] Although this catalyst system demonstrated excellent reactivity and selectivity, there still exist several outstanding challenges that must be addressed in future work.

5.2 Chapter 2: Future Work

Section 2.4.6 outlines some of the limitations of this catalyst system including the inability to accommodate ammonia as a coupling partner. The ability to accommodate more challenging amine coupling partners in multicomponent syntheses represents an important challenge to be addressed. With appropriate tuning of the ligand and metal centre, the ability to accommodate ammonia as coupling partner in this synthetic protocol represents a useful multicomponent reaction to access substituted NH indoles. The development of such reactions should be explored further.

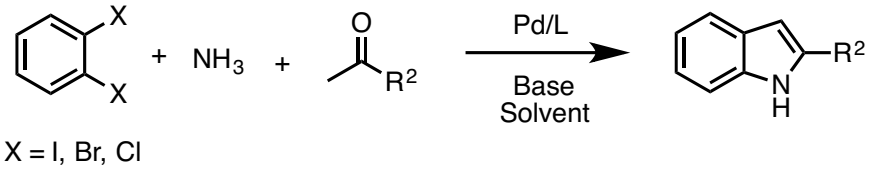

Scheme 5-1. Multicomponent indole synthesis applying ammonia

In a similar vein the inability to accommodate heteroaryl coupling partners in this reaction protocol represented a limitation, given the demand for highly substituted heterocyclic indoles by synthetic and medicinal chemists. The need for more strategically designed catalysts to accommodate this type of reactivity represents an important area of future work.

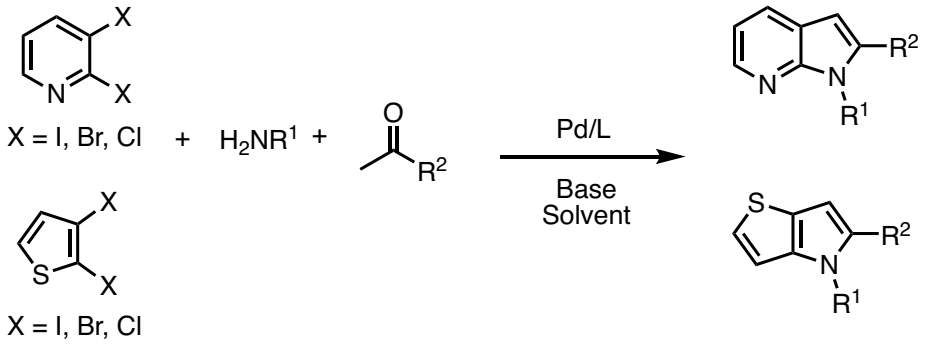

Scheme 5-2. Multicomponent synthesis of heterocyclic indoles

The identification of a possible BHA/α-arylation reaction pathway offers a powerful synthetic tool to access a number of other highly functionalized products. The ability to combine these two critical cross-coupling methods, especially under non-inert conditions could lead the simplification of synthesis to access functionalized products. The number of combination reactions that could emerge from this reaction pathway could offer a route to a plethora of different products via these multicomponent reaction pathways.

5.3 Chapter 3: Summary and Conclusions

Chapter Three examines the application of "repurposed" commercial ligands as well as the development of strategically tuned pre-catalysts for the nickel-catalyzed monoarylation of ammonia with (heteroaryl)halides. The ligand screen in Section 3.2 reveals that successful ligands previously utilized for palladium-catalyzed ammonia monoarylation do not translate to their nickel analogues. A set of JosiPhos-type ligands were examined and a successful catalyst system was developed for a test substrate (4-chlorobiphenyl). The application of this JosiPhos required further optimization for the ammonia monoarylation of heteroaryl halides (Section 3.3.1). Once optimized, a substrate scope was developed including a diverse range of heteroaryl halides. The limitations of the JosiPhos catalyst system were addressed in Section 3.4 including the need for an air-stable

pre-catalyst, the use of an expensive $Ni(COD)_2$, and the application of an unnecessarily chiral and extremely expensive ligand class. The efforts of the following project were directed toward the development of ligands specifically designed for nickel catalyzed C-N bond-forming reactions

In this regard, Section 3.2.2 examines the development of a class of sterically encumbered, relatively electron poor bisphosphine ligands. PAd-DalPhos (**L14**) became the ligand of choice in this reaction after an exhaustive ligand screen. It is noteworthy that this ligand does not perform ammonia monoarylation in the presence of palladium, therefore showing its steric and electronic properties are tuned specifically for nickel catalysis. A successful pre-catalyst (**3-C2**) of this ligand was developed, which represents an air stable and easily activated catalyst source. Section 3.5.2 outlines the application of (PAd-DalPhos)Ni(*o*-tol)Cl (**3-C2**) in the ammonia monoarylation of a range of heteroaryl halides including quinolone (**3-8**), isoquinoline (**3-6**), quinaldine (**3-4**), pyrimidine (**3-14**), quinoxaline (**3-9**), quinazoline (**3-15**), benzothiophene (**3-11**), and benzothiazole (**3-12**). The ability to accommodate both aqueous ammonia as well as ammonia gas demonstrated the robust nature of the catalyst system. Although (PAd-DalPhos)Ni(*o*-tol)Cl) (**3-C2**) was able to accommodate a range of heteroaryl halides, there exists a wealth of work to be done with regard to the application of this pre-catalyst in more challenging aminations as well as other nickel-catalyzed bond-forming reactions.

5.4 Chapter 3: Future Work

The discovery of the commercially available JosiPhos ligands, the development of the novel (PAd-DalPhos) ligand (**3-L14**) and its associated pre-catalyst (PAd-DalPhos)Ni(*o*-tol)Cl (**3-C2**) will hopefully allow for further and more complex aminations

to be conducted. First of all the unique ability of nickel to activate particularly challenging electrophiles remains relatively unexplored in the realm of ammonia monoarylation. There are few examples of heteroaryl (pseudo)halides in ammonia cross-coupling with nickel. The ability to access these amino-functionalized heterocycles from environmentally friendly reagents, including mesylates, carbamates, and imidazolylsulfonates, is a subject of further exploration. Moving beyond amination, the ability for nickel to accommodate further reactivity in the formation of other C-E bonds is highly sought after in many pharmaceutical applications.[130] We have conducted some preliminary investigations into this chemistry.

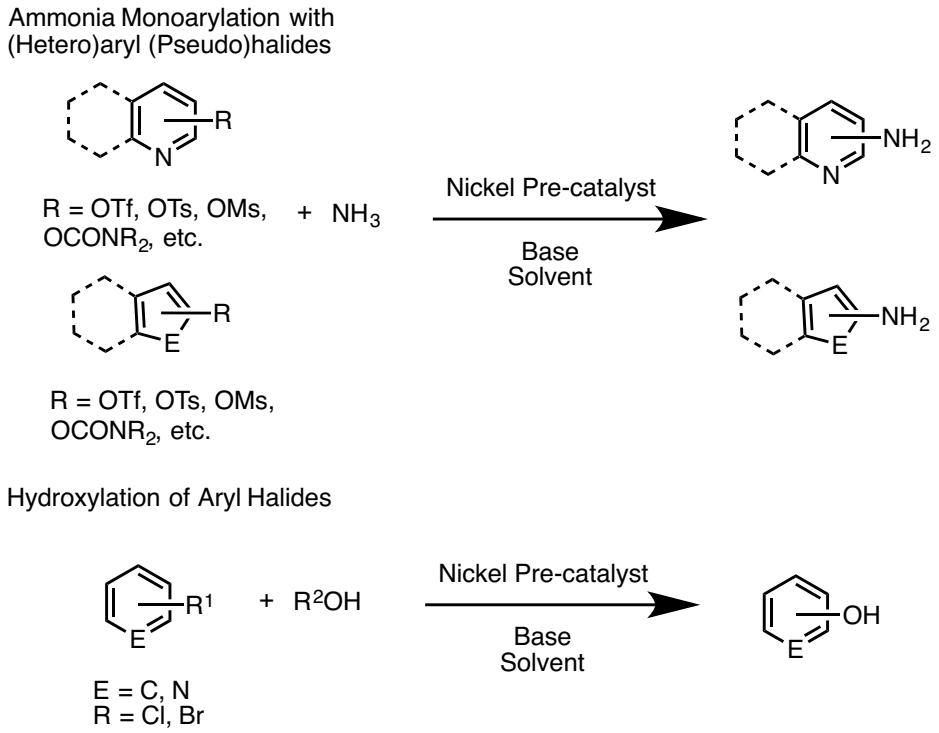

Scheme 5-3. Nickel-catalyzed amination and hydroxylation

As well, further understanding of the reaction mechanism must also be undertaken. Although we presume a Ni^0/Ni^{II} catalytic cycle for nickel-catalyzed amination, in part based on preliminary studies by Hartwig,[92] the propensity for nickel to conduct radical type

pathways can not be ruled out. Therefore, much more effort must be placed into understanding the nuances of ligand design in nickel-catalyzed amination, and subsequently apply that knowledge to further challenging and possibly unexplored reactions.

5.5 Chapter 4: Summary and Conclusions

Chapter Four outlines the synthesis and application of a series of $(PR_3)AuCl$ complexes in the room-temperature hydrohydrazination of terminal alkynes. Section 4.4.1 outlines the choice of ligands for these gold-catalyzed utilized in this survey. A range of monophosphines was chosen with variation in the secondary donor fragment, which can alter the chemical properties of the corresponding complex. Subsequently a series of air-stable gold complexes were synthesized via two analogous protocols to access a variety of structurally characterized **L**AuCl complexes.

These complexes were then applied in the hydrohydrazination of terminal alkynes with hydrazine hydrate. Section 4.4.2 outlines the screening test reaction for the hydrohydrazination of phenylacetylene with hydrazine. (cataCXium A)AuCl (**4-C6**) proved to the be the most effective Au complex for this transformation. Upon identification of the most competent catalyst a substrate scope was developed applying a number of different aryl alkynes with hydrazine. Complex **4-C6** was able to accommodate a fairly diverse range of alkynes including *para*-alkyl (**4-2**, **4-3**), methoxy (**4-4)**, halide substituents (**4-5**, **4-6**), as well as ortho-amino functionality (**4-8**) albeit with lower yield (52%). 3-Phenyl-1-propyne leading to **4-9** as well as terminal (hetero)aryl alkynes based on pyridine or thiophene, leading to **4-10** and **4-11** were also accommodated. There is also one example of an internal alkyne (**4-12**), however requiring higher catalyst loading and temperatures (5

mol%, 90 ˚C). This project represents the first demonstrated example of a (PR_3)AuCl complex being able to catalyze the hydrohydrazination of alkynes with parent hydrazine. Although this is competitive with the state-of-the-art NHC catalysts several limitations exist with this catalytic protocol.

5.6 Chapter 4: Future Work

The substrate scope with terminal alkynes must be expanded to incorporate more functional group tolerance. The focus of future research will also be the application of a gold catalyst toward the regioselective hydrohydrazination of internal alkynes. The ability to design a catalyst to accommodate the hydrohydrazination of unsymmetrical, internal alkynes would represent a major advancement for gold-catalyzed hydroaminations.

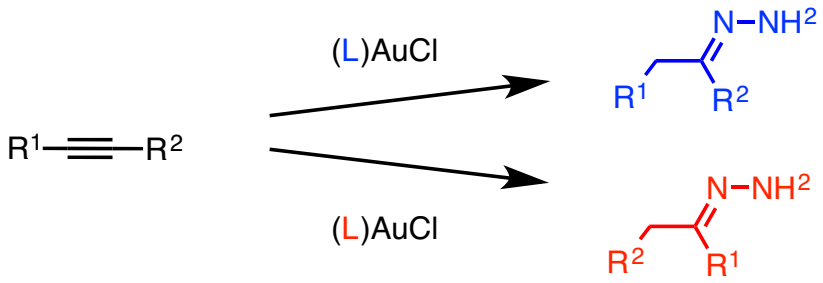

Scheme 5-4. Regioselective hydrohydrazination of unsymmetrical internal alkynes

Building on the themes of previous chapters, including first-row catalysis and multicomponent reactivity, we began exploration into the multicomponent synthesis of indazoles via a one-pot synthetic protocol. This methodology would involve a first-step hydrohydrazination of an alkyne followed by an intramolecular nickel-catalyzed amination to cyclize and form the target indazole product. This reaction requires further optimization however preliminary results indicate that it is a feasible reaction pathway.

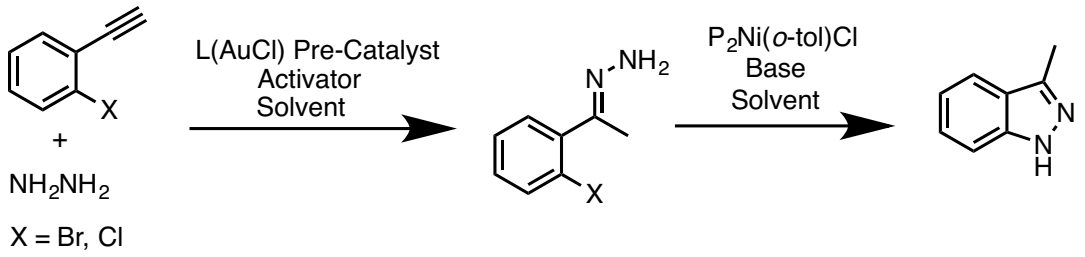

Scheme 5-5. Targeted multicomponent synthesis of indazoles

The ability to combine the themes of every chapter outlined in this thesis document allow for more powerful synthetic protocols to be established. The need to utilize inexpensive and abundant feedstock chemicals, multicomponent reactivity, strategic ligand design to increase the economy of late-metal catalyzed C-C and C-Het bond forming reactions remains the ultimate goal of this future work.

References

[1] D. Astruc, in *Organometallic Chemistry and Catalysis*, Springer, **2007**, pp. 351-355.

[2] J. Hagen, in *Industrial Catalysis: A Practical Approach*, Wiley, **1999**, pp. 1-15.

[3] H. Gröger, Y. Asano, in *Enzyme Catalysis in Organic Synthesis*, Wiley, **2012**, pp. 1-42.

[4] H. Doucet, T. Ohkuma, K. Murata, T. Yokozawa, M. Kozawa, E. Katayama, A. F. England, T. Ikariya, R. Noyori, *Angew. Chem. Int. Ed.* **1998**, *37*, 1703-1707.

[5] R. Schlogl, *Angew. Chem. Int. Ed.* **2015**, *54*, 3465-3520.

[6] a.) G. V. Smith, F. Notheisz, in *Heterogeneous Catalysis in Organic Chemistry*, Academic Press, San Diego, **1999**, pp. 1-28; b.) J. K. Norskov, F. Studt, F. Abild-Pedersen, T. Bligaard, Editors, *Fundamental Concepts in Heterogeneous Catalysis*, Wiley, **2014**.

[7] R. Noyori, M. Yamakawa, S. Hashiguchi, *J. Org. Chem.* **2001**, *66*, 7931-7944.

[8] a.) R. H. Grubbs, *Angew. Chem. Int. Ed.* **2006**, *45*, 3760-3765; b.) R. R. Schrock, *Prix Nobel.* **2006**, 216-237.

[9] X.-F. Wu, P. Anbarasan, H. Neumann, M. Beller, *Angew. Chem. Int. Ed.* **2010**, *49*, 9047-9050.

[10] C. C. C. Johansson, M. O. Kitching, T. J. Colacot, V. Snieckus, *Angew. Chem. Int. Ed.* **2012**, *51*, 5062-5085.

[11] K. Tamao, K. Sumitani, M. Kumada, *J. Am. Chem. Soc.* **1972**, *94*, 4374-4376.

[12] A. M. Echavarren, J. K. Stille, *J. Am. Chem. Soc.* **1987**, *109*, 5478-5486.

[13] K. Sonogashira, Y. Tohda, N. Hagihara, *Tetrahedron Lett.* **1975**, 4467-4470.

[14] R. F. Heck, *Acc. Chem. Res.* **1979**, *12*, 146-151.

[15] R. J. Lundgren, M. Stradiotto, *Chem. Eur. J.* **2012**, *18*, 9758-9769.

[16] B.-J. Li, S.-D. Yang, Z.-J. Shi, *Synlett* **2008**, 949-957.

[17] D. A. Culkin, J. F. Hartwig, *Acc. Chem. Res.* **2003**, *36*, 234-245.

[18] M. F. Semmelhack, B. P. Chong, R. D. Stauffer, T. D. Rogerson, A. Chong, L. D. Jones, *J. Am. Chem. Soc.* **1975**, *97*, 2507-2516.

[19] C. C. C. Johansson, T. J. Colacot, *Angew. Chem. Int. Ed.* **2010**, *49*, 676-707.

[20] a.) T. Mino, T. Matsuda, K. Maruhashi, M. Yamashita, *Organometallics* **1997**, *16*, 3241-3242; b.) J. Morgan, J. T. Pinhey, B. A. Rowe, *J. Chem. Soc. Perkin Trans. 1* **1997**, 1005-1008.

[21] B. C. Hamann, J. F. Hartwig, *J. Am. Chem. Soc.* **1997**, *119*, 12382-12383.

[22] M. Palucki, S. L. Buchwald, *J. Am. Chem. Soc.* **1997**, *119*, 11108-11109.

[23] T. Satoh, Y. Kawamura, M. Miura, M. Nomura, *Angew. Chem. Int. Ed.* **1997**, *36*, 1740-1742.

[24] K. D. Hesp, R. J. Lundgren, M. Stradiotto, *J. Am. Chem. Soc.* **2011**, *133*, 5194-5197.

[25] a.) R. J. Lundgren, B. D. Peters, P. G. Alsabeh, M. Stradiotto, *Angew. Chem. Int. Ed.* **2010**, *49*, 4071-4074; b.) R. J. Lundgren, M. Stradiotto, *Angew. Chem. Int. Ed.* **2010**, *49*, 8686-8690; c.) P. G. Alsabeh, R. J. Lundgren, L. E. Longobardi, M. Stradiotto, *Chem. Commun.* **2011**, *47*, 6936-6938; d.) P. G. Alsabeh, R. J. Lundgren, R. McDonald, C. C. C. Johansson, T. J. Colacot, M. Stradiotto, *Chem. Eur. J.* **2013**, *19*, 2131-2141.

[26] a.) D. Ma, Q. Cai, H. Zhang, *Org. Lett.* **2003**, *5*, 2453-2455; b.) S. E. Creutz, K. J. Lotito, G. C. Fu, J. C. Peters, *Science* **2012**, *338*, 647-651.

[27] a.) A. S. Guram, R. A. Rennels, S. L. Buchwald, *Angew. Chem. Int. Ed.* **1995**, *34*, 1348-1350; b.) J. Louie, J. F. Hartwig, *Tetrahedron Lett.* **1995**, *36*, 3609-3612.

[28] K. H. Hoi, S. Calimsiz, R. D. J. Froese, A. C. Hopkinson, M. G. Organ, *Chem. Eur. J.* **2011**, *17*, 3086-3090.

[29] L. M. Klingensmith, E. R. Strieter, T. E. Barder, S. L. Buchwald, *Organometallics* **2006**, *25*, 82-91.

[30] J. P. Wolfe, S. Wagaw, S. L. Buchwald, *J. Am. Chem. Soc.* **1996**, *118*, 7215-7216.

[31] D. S. Surry, S. L. Buchwald, *Chem. Sci.* **2011**, *2*, 27-50.

[32] G. J. Withbroe, R. A. Singer, J. E. Sieser, *Org. Process Res. Dev.* **2008**, *12*, 480-489.

[33] a.) M. G. Organ, M. Abdel-Hadi, S. Avola, I. Dubovyk, N. Hadei, E. A. B. Kantchev, C. J. O'Brien, M. Sayah, C. Valente, *Chem. Eur. J.* **2008**, *14*, 2443-2452; b.) C. Valente, S. Calimsiz, K. H. Hoi, D. Mallik, M. Sayah, M. G. Organ, *Angew. Chem. Int. Ed.* **2012**, *51*, 3314-3332.

[34] H.-U. Blaser, W. Brieden, B. Pugin, F. Spindler, M. Studer, A. Togni, *Top. Catal.* **2002**, *19*, 3-16.

[35] a.) T. Ogata, J. F. Hartwig, *J. Am. Chem. Soc.* **2008**, *130*, 13848-13849; b.) R. A. Green, J. F. Hartwig, *Org. Lett.* **2014**, *16*, 4388-4391.

[36] R. J. Lundgren, K. D. Hesp, M. Stradiotto, *Synlett* **2011**, 2443-2458.

[37] J. Kim, H. J. Kim, S. Chang, *Eur. J. Org. Chem.* **2013**, 3201-3213.

[38] A. P. Taylor, R. P. Robinson, Y. M. Fobian, D. C. Blakemore, L. H. Jones, O. Fadeyi, *Org. Biomol. Chem.* **2016**, *14*, 6611-6637.

[39] Q. L. Shen, J. F. Hartwig, *J. Am. Chem. Soc.* **2006**, *128*, 10028-10029.

[40] G. D. Vo, J. F. Hartwig, *J. Am. Chem. Soc.* **2009**, *131*, 11049-11061.

[41] T. Schulz, C. Torborg, S. Enthaler, B. Schaffner, A. Dumrath, A. Spannenberg, H. Neumann, A. Borner, M. Beller, *Chem. Eur. J.* **2009**, *15*, 4528-4533.

[42] D. S. Surry, S. L. Buchwald, *J. Am. Chem. Soc.* **2007**, *129*, 10354-10355.

[43] a.) F. R. Lang, D. Zewge, I. N. Houpis, R. P. Volante, *Tetrahedron Lett.* **2001**, *42*, 3251-3254; b.) P. Ji, J. H. Atherton, M. I. Page, *J. Org. Chem.* **2012**, *77*, 7471-7478.

[44] S. Z. Tasker, E. A. Standley, T. F. Jamison, *Nature* **2014**, *509*, 299-309.

[45] M. Marin, R. J. Rama, M. C. Nicasio, *Chem. Rec.* **2016**, *16*, 1819-1832.

[46] R. J. P. Corriu, J. P. Masse, *Chem. Commun.* **1972**, 144.

[47] S. Ge, J. F. Hartwig, *Angew. Chem. Int. Ed.* **2012**, *51*, 12837-12841.

[48] S. D. Ramgren, L. Hie, Y. Ye, N. K. Garg, *Org. Lett.* **2013**, *15*, 3950-3953.

[49] M. Mohadjer Beromi, A. Nova, D. Balcells, A. M. Brasacchio, G. W. Brudvig, L. M. Guard, N. Hazari, D. J. Vinyard, *J. Am. Chem. Soc.* **2017**, *139*, 922-936.

[50] a.) M. Baghbanzadeh, C. Pilger, C. O. Kappe, *J. Org. Chem.* **2011**, *76*, 1507-1510; b.) S. D. Ramgren, A. L. Silberstein, Y. Yang, N. K. Garg, *Angew. Chem. Int. Ed.* **2011**, *50*, 2171-2173; c.) P. Leowanawat, N. Zhang, V. Percec, *J. Org. Chem.* **2012**, *77*, 1018-1025; d.) M. R. Harris, L. E. Hanna, M. A. Greene, C. E. Moore, E. R. Jarvo, *J. Am. Chem. Soc.* **2013**, *135*, 3303-3306.

[51] a.) P. Maity, D. M. Shacklady-McAtee, G. P. A. Yap, E. R. Sirianni, M. P. Watson, *J. Am. Chem. Soc.* **2013**, *135*, 280-285; b.) Q. Zhou, H. D. Srinivas, S. Dasgupta, M. P. Watson, *J. Am. Chem. Soc.* **2013**, *135*, 3307-3310; c.) J. Zhang, G. Lu, J. Xu, H. Sun, Q. Shen, *Org. Lett.* **2016**, *18*, 2860-2863.

[52] S. L. Zultanski, G. C. Fu, *J. Am. Chem. Soc.* **2013**, *135*, 624-627.

[53] a.) R. A. WidenHoefer, X. Han, *Eur. J. Org. Chem.* **2006**, 4555-4563; b.) R. Severin, S. Doye, *Chem. Soc. Rev.* **2007**, *36*, 1407-1420; c.) T. E. Mueller, K. C. Hultzsch, M. Yus, F. Foubelo, M. Tada, *Chem. Rev.* **2008**, *108*, 3795-3892; d.) L.

Huang, M. Arndt, K. Goossen, H. Heydt, L. J. Goossen, *Chem. Rev.* **2015**, *115*, 2596-2697.

[54] J. Barluenga, F. Aznar, R. Liz, R. Rodes, *J. Chem. Soc. Perkin Trans. 1* **1980**, 2732-2737.

[55] J. Barluenga, F. Aznar, *Synthesis* **1977**, 195-196.

[56] P. J. Walsh, A. M. Baranger, R. G. Bergman, *J. Am. Chem. Soc.* **1992**, *114*, 1708-1719.

[57] L. Ackermann, R. G. Bergman, *Org. Lett.* **2002**, *4*, 1475-1478.

[58] J. Sun, S. A. Kozmin, *Angew. Chem. Int. Ed.* **2006**, *45*, 4991-4993.

[59] K. Iritani, S. Matsubara, K. Uchimoto, *Tetrahedron Lett.* **1988**, *29*, 1799-1802.

[60] J.-J. Brunet, N. C. Chu, O. Diallo, S. Vincendeau, *J. Mol. Catal. A: Chem.* **2005**, *240*, 245-248.

[61] M. Utsunomiya, R. Kuwano, M. Kawatsura, J. F. Hartwig, *J. Am. Chem. Soc.* **2003**, *125*, 5608-5609.

[62] M. Tokunaga, M. Eckert, Y. Wakatsuki, *Angew. Chem. Int. Ed.* **1999**, *38*, 3222-3225.

[63] Y. Fukuda, K. Uchimoto, H. Nozaki, *Heterocycles* **1987**, *25*, 297-300.

[64] a.) X.-Y. Liu, Z. Guo, S. S. Dong, X.-H. Li, C.-M. Che, *Chem. Eur. J.* **2011**, *17*, 12932-12945; b.) A. Stephen, K. Hashmi, *Top. Organomet. Chem.* **2013**, *44*, 143-164.

[65] E. Mizushima, T. Hayashi, M. Tanaka, *Org. Lett.* **2003**, *5*, 3349-3352.

[66] Y. Luo, Z. Li, C.-J. Li, *Org. Lett.* **2005**, *7*, 2675-2678.

[67] K. D. Hesp, M. Stradiotto, *J. Am. Chem. Soc.* **2010**, *132*, 18026-18029.

[68] A. Zhdanko, M. E. Maier, *Angew. Chem. Int. Ed.* **2014**, *53*, 7760-7764.

[69] G. Van der Heijden, E. Ruijter, R. V. A. Orru, *Synlett* **2013**, *24*, 666-685.

[70] C. J. Ball, M. C. Willis, *Eur. J. Org. Chem.* **2013**, 425-441.

[71] D. M. D'Souza, T. J. J. Mueller, *Chem. Soc. Rev.* **2007**, *36*, 1095-1108.

[72] D. A. Horton, G. T. Bourne, M. L. Smythe, *Chem. Rev.* **2003**, *103*, 893-930.

[73] N. K. Kaushik, N. Kaushik, P. Attri, N. Kumar, C. H. Kim, A. K. Verma, E. H. Choi, *Molecules* **2013**, *18*, 6620-6662.

[74] a.) R. J. Melander, M. J. Minvielle, C. Melander, *Tetrahedron* **2014**, *70*, 6363-6372; b.) V. Sharma, P. Kumar, D. Pathak, *J. Heterocycl. Chem.* **2010**, *47*, 491-502.

[75] B. Robinson, *Chem. Rev.* **1963**, *63*, 373-401.

[76] S. M. Crawford, C. B. Lavery, M. Stradiotto, *Chem. Eur. J.* **2013**, *19*, 16760-16771.

[77] S. Cacchi, G. Fabrizi, *Chem. Rev.* **2005**, *105*, 2873-2920.

[78] a.) R. C. Larock, E. K. Yum, M. D. Refvik, *J. Org. Chem.* **1998**, *63*, 7652-7662; b.) A. Takeda, S. Kamijo, Y. Yamamoto, *J. Am. Chem. Soc.* **2000**, *122*, 5662-5663; c.) L. T. Kaspar, L. Ackermann, *Tetrahedron* **2005**, *61*, 11311-11316; d.) S. G. Newman, M. Lautens, *J. Am. Chem. Soc.* **2010**, *132*, 11416-11417.

[79] D. W. Old, M. C. Harris, S. L. Buchwald, *Org. Lett.* **2000**, *2*, 1403-1406.

[80] a.) S. M. Crawford, P. G. Alsabeh, M. Stradiotto, *Eur. J. Org. Chem.* **2012**, 6042-6050; b.) B. J. Tardiff, R. McDonald, M. J. Ferguson, M. Stradiotto, *J. Org. Chem.* **2012**, *77*, 1056-1071.

[81] J. M. Knapp, J. S. Zhu, D. J. Tantillo, M. J. Kurth, *Angew. Chem. Int. Ed.* **2012**, *51*, 10588-10591.

[82] Indomethacin (non-steroidal anti-inflammatory), Oxypertine (antipsychotic), and Panobinostat (anti-cancer) represent a selection of drug molecules that feature the 2-methylindole core

[83] T. C. Barden, *Top. Heterocycl. Chem.* **2010**, *26*, 31-46.

[84] J. P. Wolfe, S. L. Buchwald, *J. Am. Chem. Soc.* **1997**, *119*, 6054-6058.

[85] a.) M. J. Iglesias, J. F. Blandez, M. R. Fructos, A. Prieto, E. Alvarez, T. R. Belderrain, M. C. Nicasio, *Organometallics* **2012**, *31*, 6312-6316; b.) M. J. Iglesias, A. Prieto, M. C. Nicasio, *Adv. Synth. Catal.* **2010**, *352*, 1949-1954; c.) B. R. Dible, M. S. Sigman, *J. Am. Chem. Soc.* **2003**, *125*, 872-873; d.) K. Matsubara, K. Ueno, Y. Shibata, *Organometallics* **2006**, *25*, 3422-3427.

[86] a.) G. Manolikakes, A. Gavryushin, P. Knochel, *J. Org. Chem.* **2008**, *73*, 1429-1434; b.) H.-J. Cristau, J.-R. Desmurs, *Ind. Chem. Libr.* **1995**, *7*, 240-263.

[87] N. H. Park, G. Teverovskiy, S. L. Buchwald, *Org. Lett.* **2014**, *16*, 220-223.

[88] S. Ge, R. A. Green, J. F. Hartwig, *J. Am. Chem. Soc.* **2014**, *136*, 1617-1627.

[89] J. L. Klinkenberg, J. F. Hartwig, *Angew. Chem. Int. Ed.* **2011**, *50*, 86-95.

[90] A. T. Shaw, D.-W. Kim, K. Nakagawa, T. Seto, L. Crinó, M.-J. Ahn, T. De Pas, B. Besse, B. J. Solomon, F. Blackhall, Y.-L. Wu, M. Thomas, K. J. O'Byrne, D. Moro-Sibilot, D. R. Camidge, T. Mok, V. Hirsh, G. J. Riely, S. Iyer, V. Tassell, A. Polli, K. D. Wilner, P. A. Jänne, *N. Engl. J. Med.* **2013**, *368*, 2385-2394.

[91] a.) A. G. MacDiarmid, *Angew. Chem. Int. Ed.* **2001**, *40*, 2581-2590; b.) S. A. Lawrence, *Amines: Synthesis, Properties and Applications*, Cambridge University Press, Cambridge., **2006**; c.) M. Liang, J. Chen, *Chem. Soc. Rev.* **2013**, *42*, 3453-3488.

[92] R. A. Green, J. F. Hartwig, *Angew. Chem. Int. Ed.* **2015**, *54*, 3768-3772.

[93] U. Schoen, J. Messinger, M. Buchholz, U. Reinecker, H. Thole, M. K. S. Prabhu, A. Konda, *Tetrahedron Lett*. **2005**, *46*, 7111-7115.

[94] C. W. Cheung, D. S. Surry, S. L. Buchwald, *Org*. *Lett*. **2013**, *15*, 3734-3737.

[95] H. H. Xu, C. Wolf, *Chem Commun* **2009**, 3035-3037.

[96] A. Borzenko, N. L. Rotta-Loria, P. M. MacQueen, C. M. Lavoie, R. McDonald, M. Stradiotto, *Angew*. *Chem*. *Int*. *Ed*. **2015**, *54*, 3773-3777.

[97] S. Ahammed, A. Saha, B. C. Ranu, *J*. *Org*. *Chem*. **2011**, *76*, 7235-7239.

[98] Y.-H. Lou, J.-S. Wang, G. Dong, P.-P. Guo, D.-D. Wei, S.-S. Xie, M.-H. Yang, L.-Y. Kong, *Toxicol*. *Res*. **2015**, *4*, 1465-1478.

[99] a.) K. Alex, A. Tillack, N. Schwarz, M. Beller, *Org*. *Lett*. **2008**, *10*, 2377-2379; b.) K. Alex, A. Tillack, N. Schwarz, M. Beller, *Angew*. *Chem*. *Int*. *Ed*. **2008**, *47*, 2304-2307.

[100] A. Lukin, T. Vedekhina, D. Tovpeko, N. Zhurilo, M. Krasavin, *RSC Adv*. **2016**, *6*, 57956-57959.

[101] a.) Y. Fukumoto, A. Ohmae, M. Hirano, N. Chatani, *Asian J*. *Org*. *Chem*. **2013**, *2*, 1036-1039; b.) Y. Fukumoto, Y. Tamura, Y. Iyori, N. Chatani, *J*. *Org*. *Chem*. **2016**, *81*, 3161-3167.

[102] J. M. Hoover, A. DiPasquale, J. M. Mayer, F. E. Michael, *J*. *Am*. *Chem*. *Soc*. **2010**, *132*, 5043-5053.

[103] A. D. Schwarz, C. S. Onn, P. Mountford, *Angew*. *Chem*. *Int*. *Ed*. **2012**, *51*, 12298-12302.

[104] J.-P. Schirmann, P. Bourdauducq, in *Ullmann's Encyclopedia of Industrial Chemistry*, Wiley, **2000**, pp. 79-96.

[105] A. DeAngelis, D.-H. Wang, S. L. Buchwald, *Angew*. *Chem*. *Int*. *Ed*. **2013**, *52*, 3434-3437.

[106] J. I. van der Vlugt, *Chem. Soc. Rev.* **2010**, *39*, 2302-2322.

[107] a.) P. P. Cellier, J.-F. Spindler, M. Taillefer, H.-J. Cristau, *Tetrahedron Lett.* **2003**, *44*, 7191-7195; b.) B. A. Roden, in *Encyclopedia of Reagents for Organic Synthesis*, Wiley, **2001**; c.) J. P. Chen, L. L. Lim, *Chemosphere* **2002**, *49*, 363-370.

[108] a.) C. Smit, M. W. Fraaije, A. J. Minnaard, *J. Org. Chem.* **2008**, *73*, 9482-9485; b.) A. Dhakshinamoorthy, M. Alvaro, H. Garcia, *Adv. Synth. Catal.* **2009**, *351*, 2271-2276.

[109] V. Lavallo, G. D. Frey, B. Donnadieu, M. Soleilhavoup, G. Bertrand, *Angew. Chem. Int. Ed.* **2008**, *47*, 5224-5228.

[110] R. Kinjo, B. Donnadieu, G. Bertrand, *Angew. Chem. Int. Ed.* **2011**, *50*, 5560-5563.

[111] M. J. Lopez-Gomez, D. Martin, G. Bertrand, *Chem. Commun.* **2013**, *49*, 4483-4485.

[112] R. Manzano, T. Wurm, F. Rominger, A. S. K. Hashmi, *Chem. Eur. J.* **2014**, *20*, 6844-6848.

[113] D. R. Tolentino, L. Q. Jin, M. Melaimi, G. Bertrand, *Chem. Asian J.* **2015**, *10*, 2139-2142.

[114] D. Mendoza-Espinosa, D. Rendon-Nava, A. Alvarez-Hernandez, D. Angeles-Beltran, G. E. Negron-Silva, O. R. Suarez-Castillo, *Chem. Asian J.* **2017**, *12*, 203-207.

[115] A. S. K. Hashmi, *Angew. Chem. Int. Ed.* **2010**, *49*, 5232-5241.

[116] A. Couce-Rios, G. Kovacs, G. Ujaque, A. Lledos, *ACS Catal.* **2015**, *5*, 815-829.

[117] G. Kovacs, A. Lledos, G. Ujaque, *Angew. Chem. Int. Ed.* **2011**, *50*, 11147-11151.

[118] U. Monkowius, M. Zabel, H. Yersin, *Inorg. Chem. Commun.* **2008**, *11*, 409-412.

[119] H. Schmidbaur, A. Schier, *Chem. Soc. Rev.* **2012**, *41*, 370-412.

[120] R. Manzano, T. Wurm, F. Rominger, A. S. K. Hashmi, *Chem. Eur. J.* **2014**, *20*, 6844-6848.

[121] M. De Lena, V. Lorusso, A. Latorre, G. Fanizza, G. Gargano, L. Caporusso, M. Guida, A. Catino, E. Crucitta, D. Sambiasi, A. Mazzei, *Eur. J. Cancer* **2001**, *37*, 364-368.

[122] C. Runti, L. Baiocchi, *Int. J. Tissue React.* **1985**, *7*, 175-186.

[123] F.-Y. Lee, J.-C. Lien, L.-J. Huang, T.-M. Huang, S.-C. Tsai, C.-M. Teng, C.-C. Wu, F.-C. Cheng, S.-C. Kuo, *J. Med. Chem.* **2001**, *44*, 3746-3749.

[124] a.) C. Spiteri, S. Keeling, J. E. Moses, *Org. Lett.* **2010**, *12*, 3368-3371; b.) P. Li, C. Wu, J. Zhao, D. C. Rogness, F. Shi, *J. Org. Chem.* **2012**, *77*, 3149-3158.

[125] A. Schmidt, A. Beutler, B. Snovydovych, *Eur. J. Org. Chem.* **2008**, 4073-4095.

[126] C. B. Lavery, R. McDonald, M. Stradiotto, *Chem. Commun.* **2012**, *48*, 7277-7279.

[127] C. M. Lavoie, P. M. MacQueen, N. L. Rotta-Loria, R. S. Sawatzky, A. Borzenko, A. J. Chisholm, B. K. V. Hargreaves, R. McDonald, M. J. Ferguson, M. Stradiotto, *Nat. Commun.* **2016**, *7*, 11073.

[128] T. Kleine, R. Froehlich, B. Wibbeling, E.-U. Wuerthwein, *J. Org. Chem.* **2011**, *76*, 4591-4599.

[129] J. L. Peltier, R. Jazzar, M. Melaimi, G. Bertrand, *Chem. Commun.* **2016**, *52*, 2733-2735.

[130] a.) D. A. Alonso, C. Najera, I. M. Pastor, M. Yus, *Chem. Eur. J.* **2010**, *16*, 5274-5284; b.) S. Enthaler, A. Company, *Chem. Soc. Rev.* **2011**, *40*, 4912-4924.

Appendix 1. Utilizing Mor-DalPhos/Palladium-Catalyzed Monoarylation in the Multicomponent One-Pot Synthesis of Indoles

^{1}H NMR Spectrum of *N*-(2-chlorophenyl)octylamine, **B** ($CDCl_3$, 500.1 MHz)

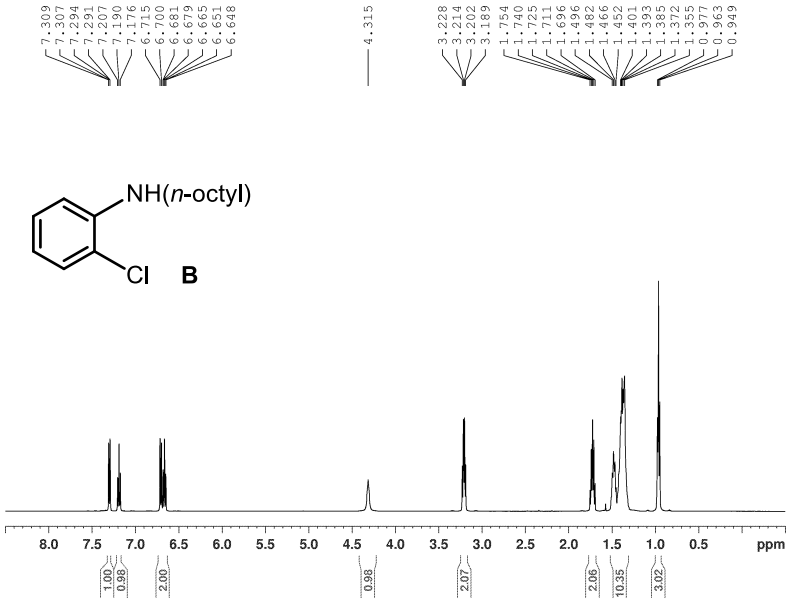

^{13}C{^{1}H} NMR Spectrum of *N*-(2-chlorophenyl)octylamine, **B** ($CDCl_3$, 125.8 MHz)

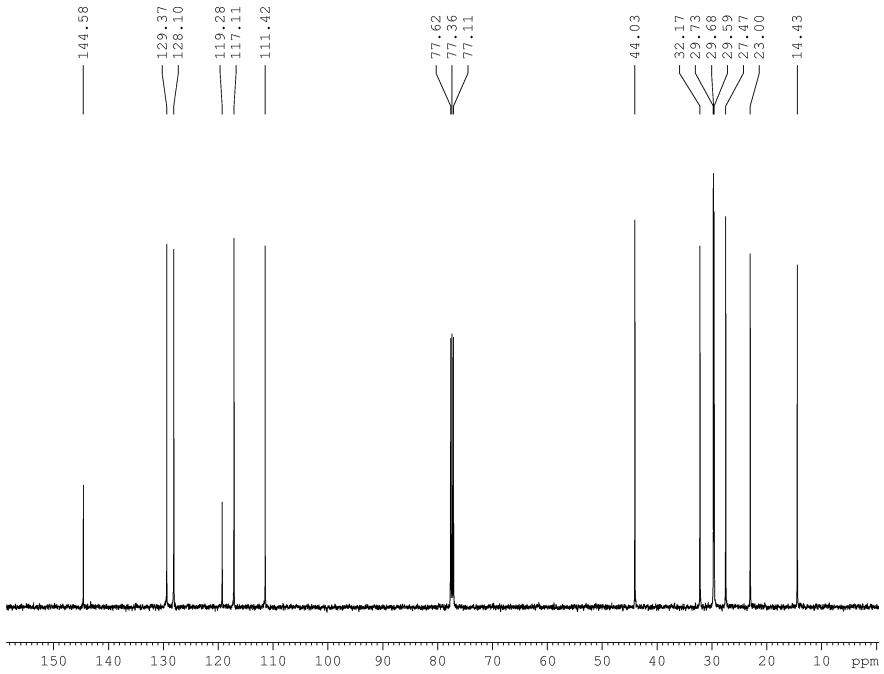

^{1}H NMR Spectrum of 1-octyl-2-methyl-1*H*-indole, **2-1a** ($CDCl_3$, 500.1 MHz)

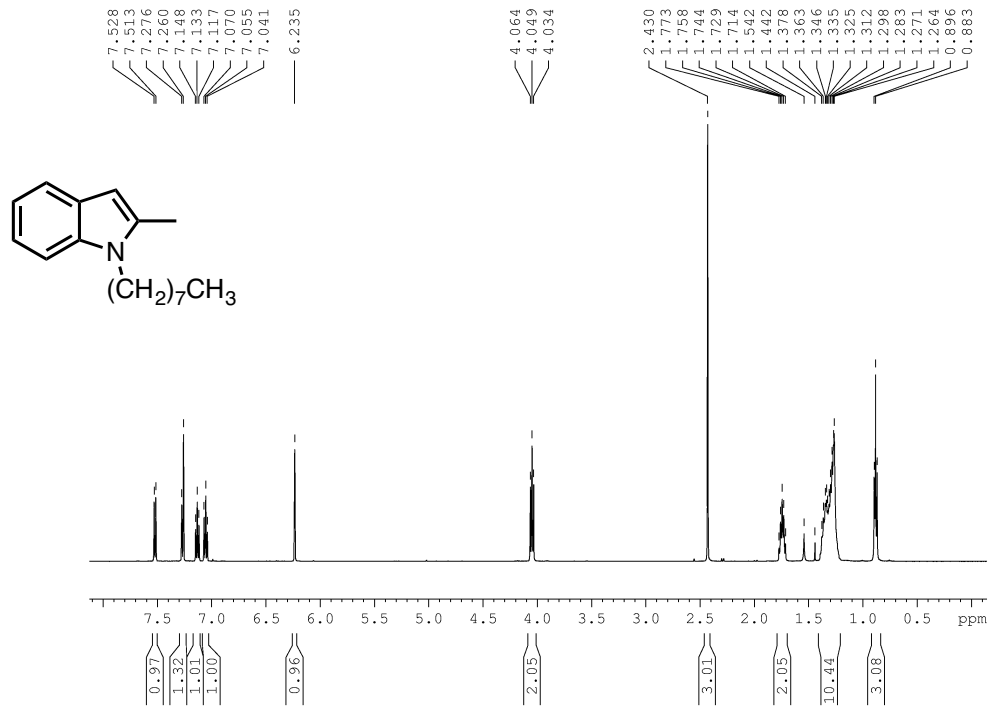

^{13}C{^{1}H} NMR Spectrum of 1-octyl-2-methyl-1*H*-indole, **2-1a** ($CDCl_3$, 125.8 MHz)

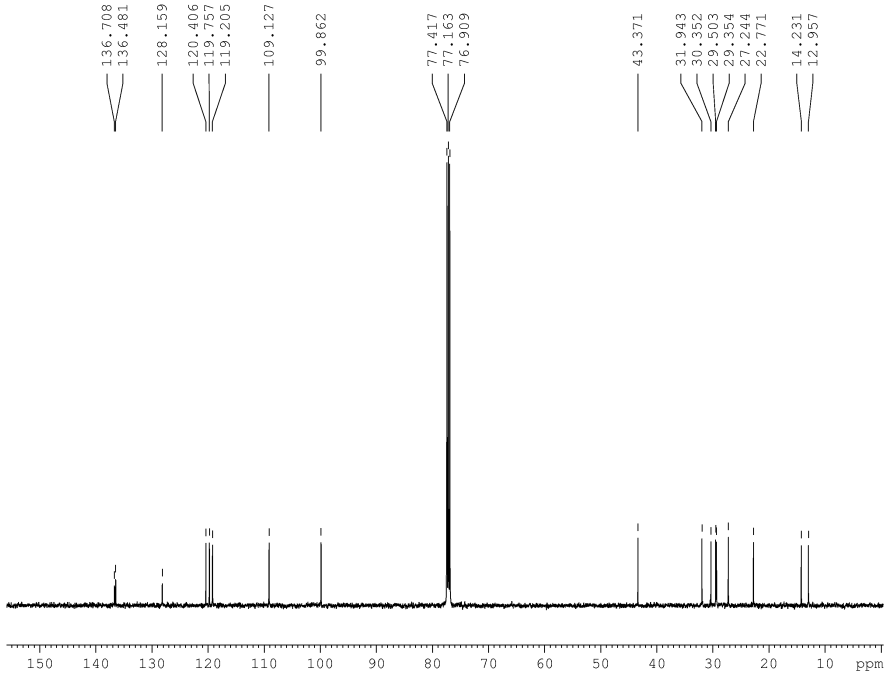

^{1}H NMR Spectrum of 1-cyclohexyl-2-methyl-1*H*-indole, **2-1b** ($CDCl_3$, 500.1 MHz)

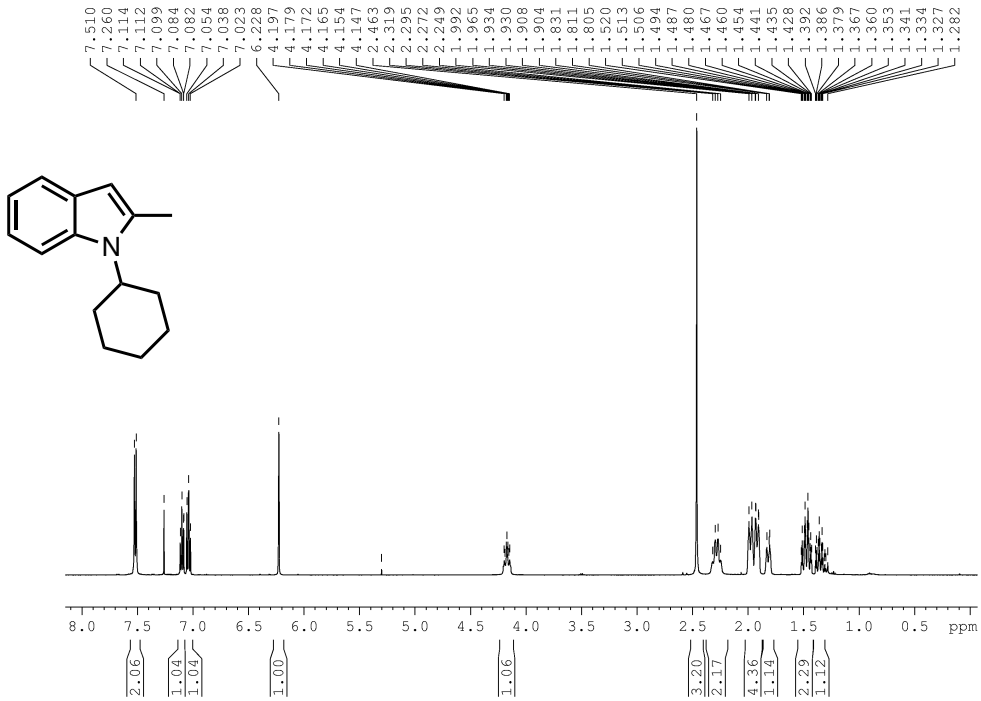

^{13}C{^{1}H} NMR Spectrum of 1-cyclohexyl-2-methyl-1*H*-indole, **2-1b** ($CDCl_3$, 125.8 MHz)

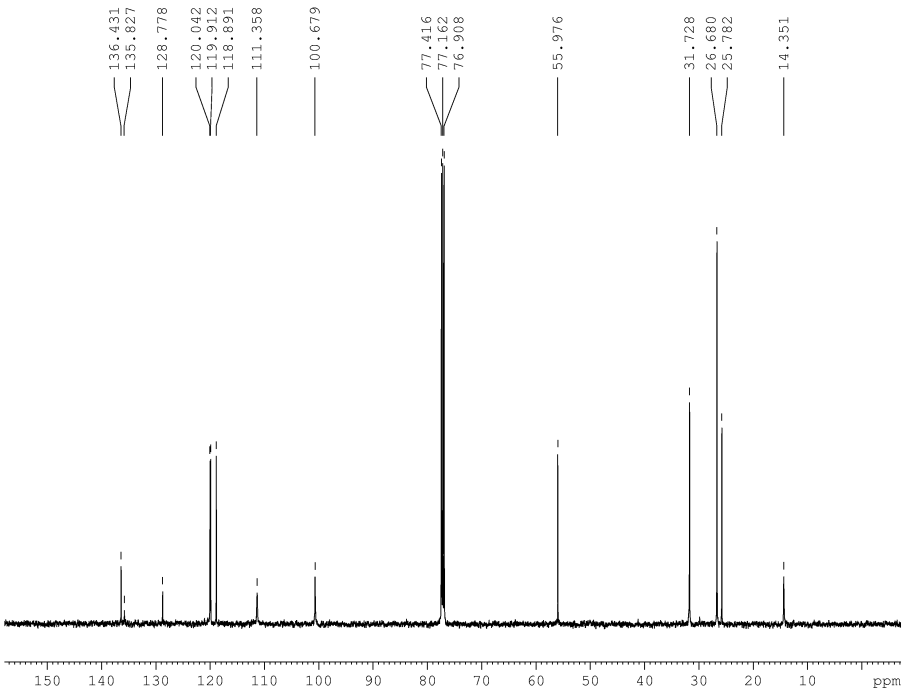

^{1}H NMR Spectrum of 1-*sec*-butyl-2-methyl-1*H*-indole, **2-1c** ($CDCl_3$, 500.1 MHz)

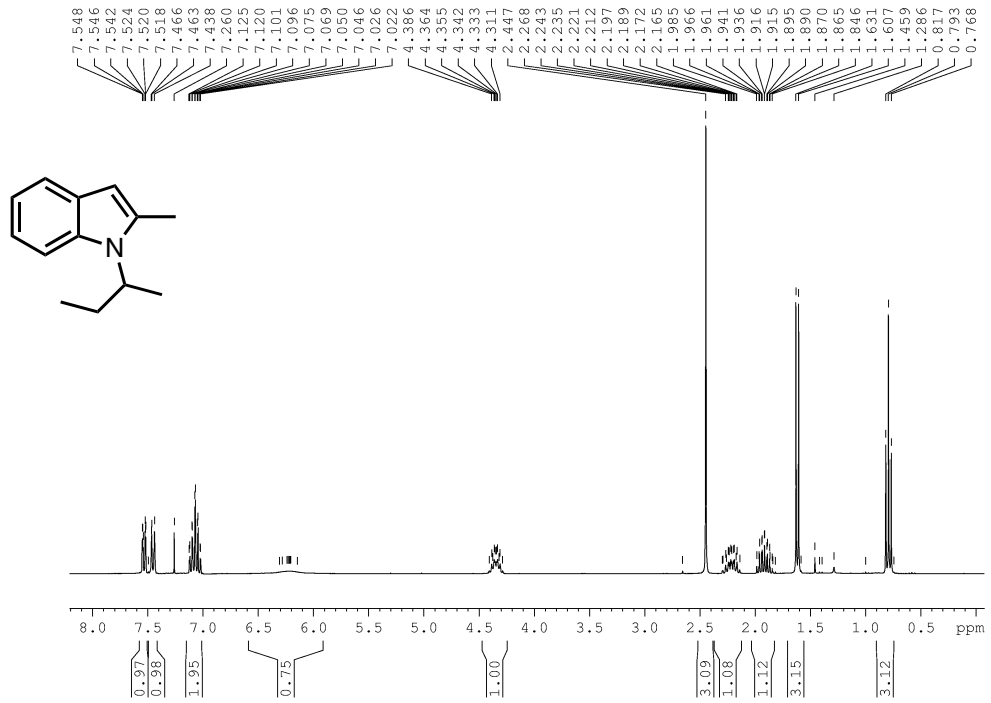

^{13}C{^{1}H} NMR Spectrum of 1-*sec*-butyl-2-methyl-1*H*-indole, **2-1c** ($CDCl_3$, 125.8 MHz)

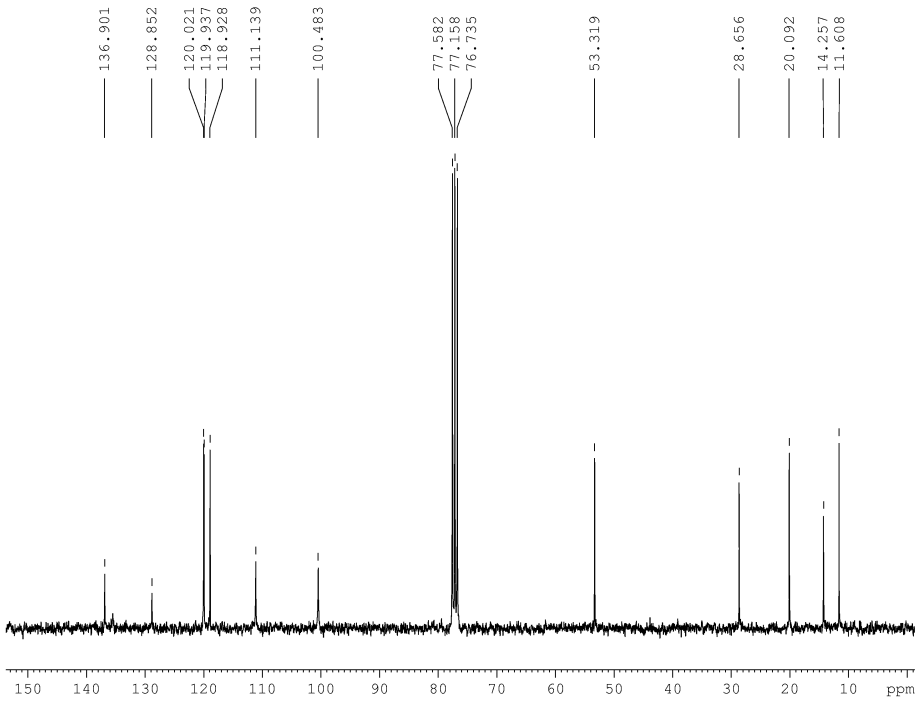

^{1}H NMR Spectrum of benzyl-2-methyl-1*H*-indole, **2-1d** ($CDCl_3$, 500.1 MHz)

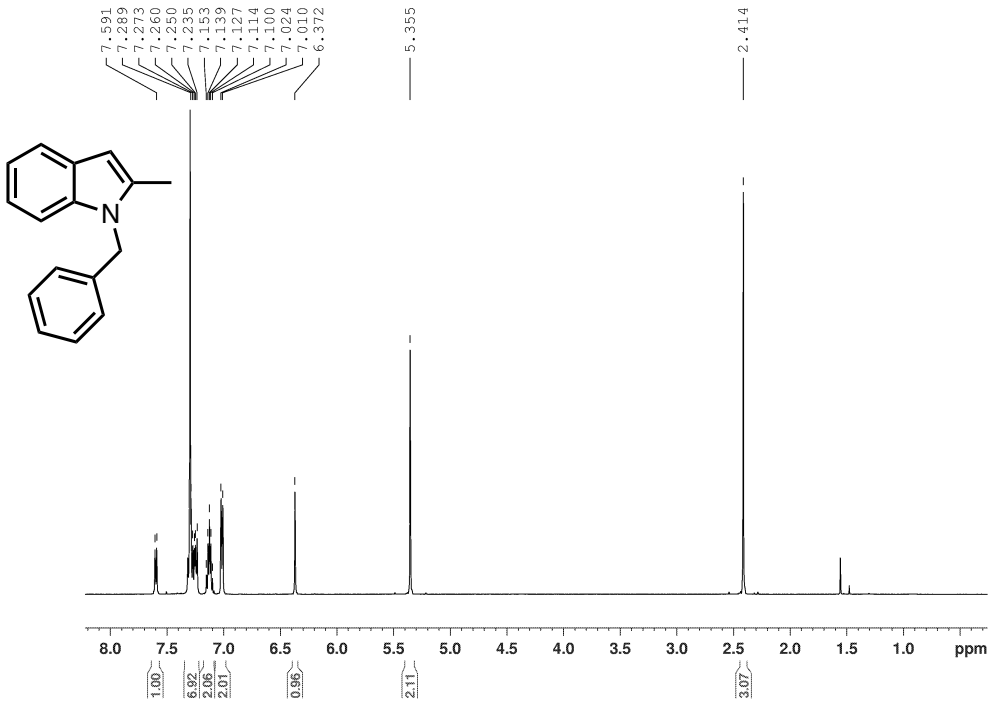

^{13}C{^{1}H} NMR Spectrum of benzyl-2-methyl-1*H*-indole **2-1d** ($CDCl_3$, 125.8 MHz)

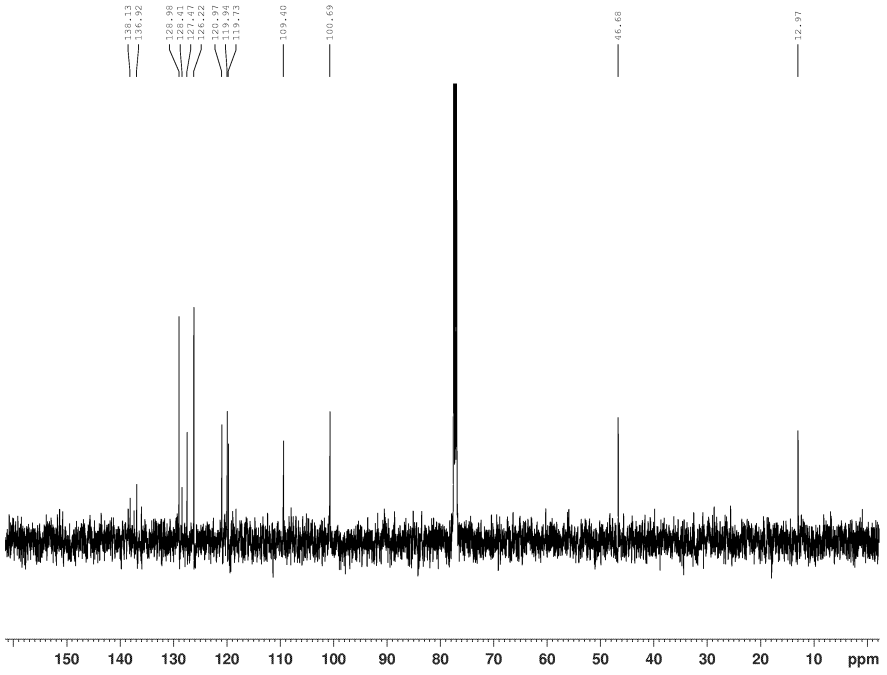

^{1}H NMR Spectrum of 1-phenyl-2-methyl-1*H*-indole, **2-1e** ($CDCl_3$, 500.1 MHz)

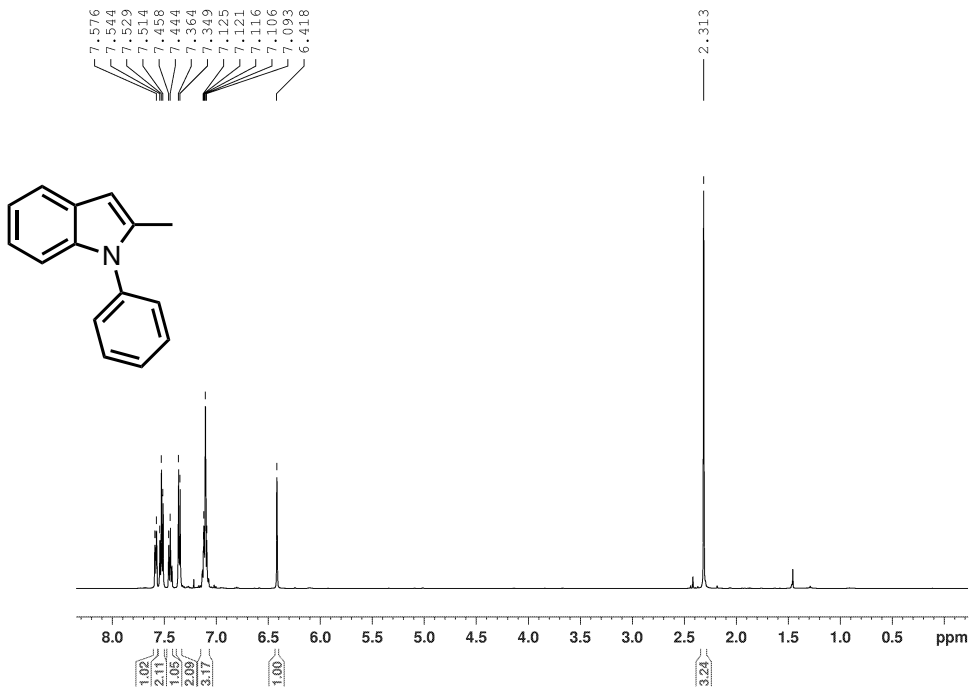

^{13}C{^{1}H} NMR Spectrum of 1-phenyl-2-methyl-1*H*-indole, **2-1e** ($CDCl_3$, 125.8 MHz)

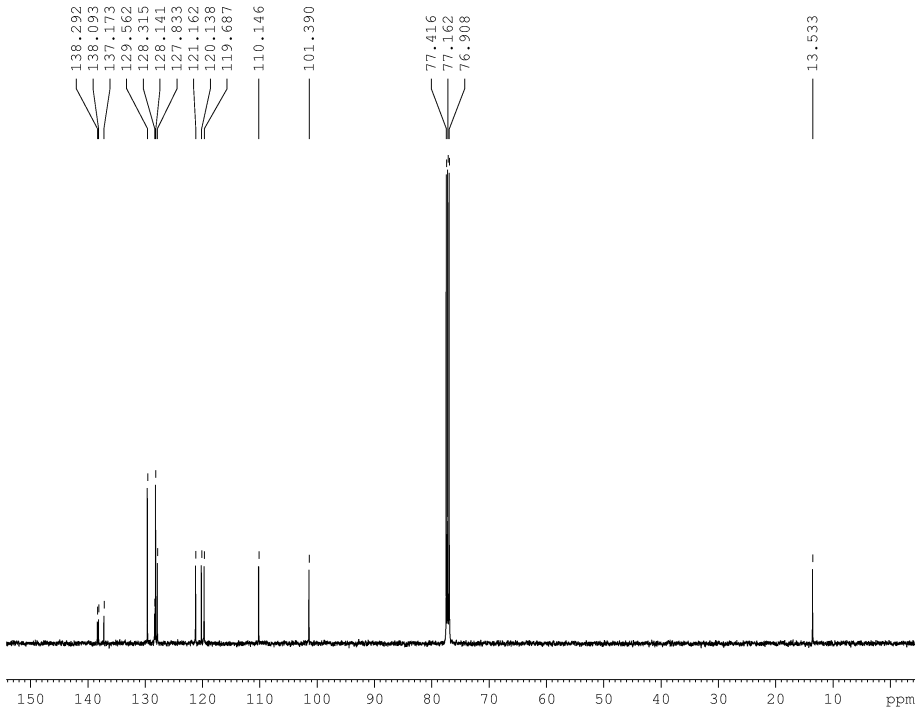

^{1}H NMR Spectrum of 2-methyl-1-*p*-tolyl-1*H*-indole, **2-1f** ($CDCl_3$, 500.1 MHz)

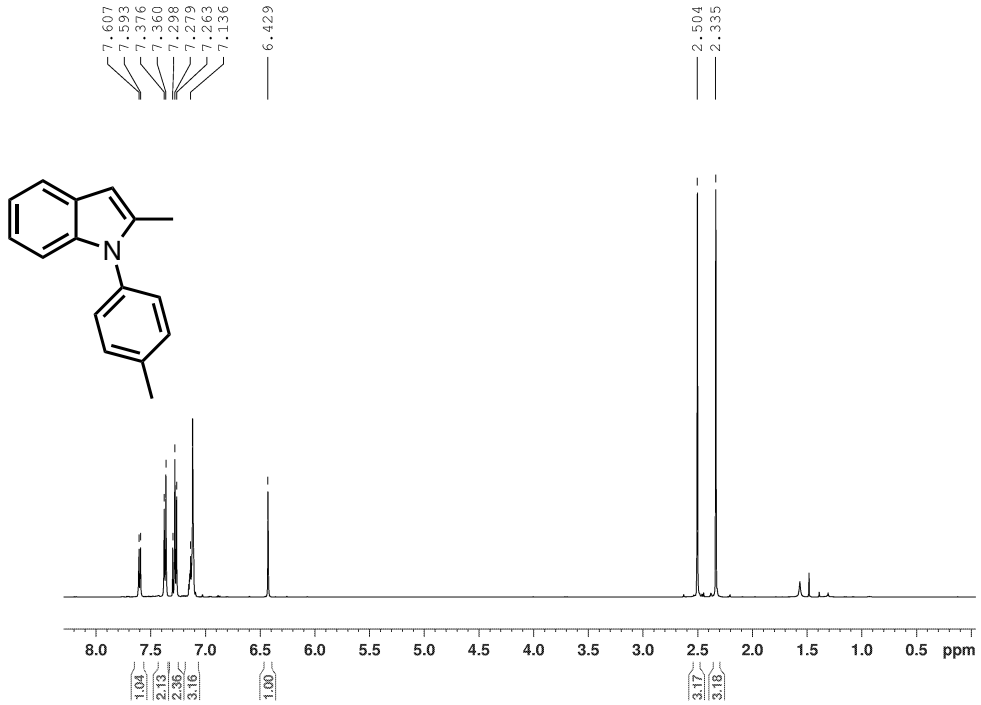

^{13}C{^{1}H} NMR Spectrum of 2-methyl-1-*p*-tolyl-1*H*-indole, **2-1f** ($CDCl_3$, 125.8 MHz)

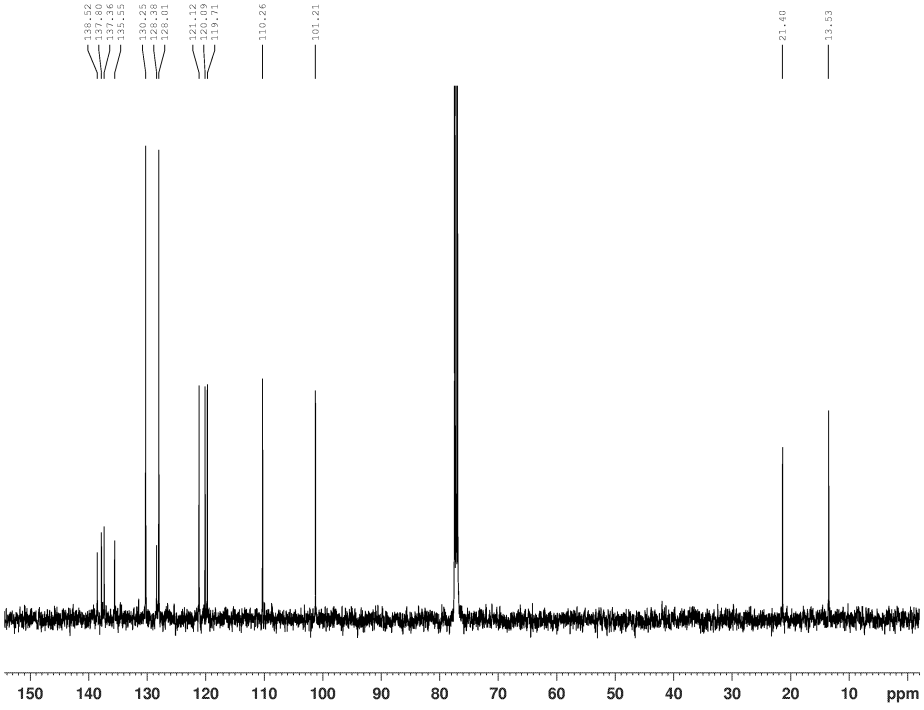

^{1}H NMR Spectrum of 1-(3,5-dimethylphenyl)-2-methyl-1H-indole, **2-1g** ($CDCl_3$, 500.1 MHz)

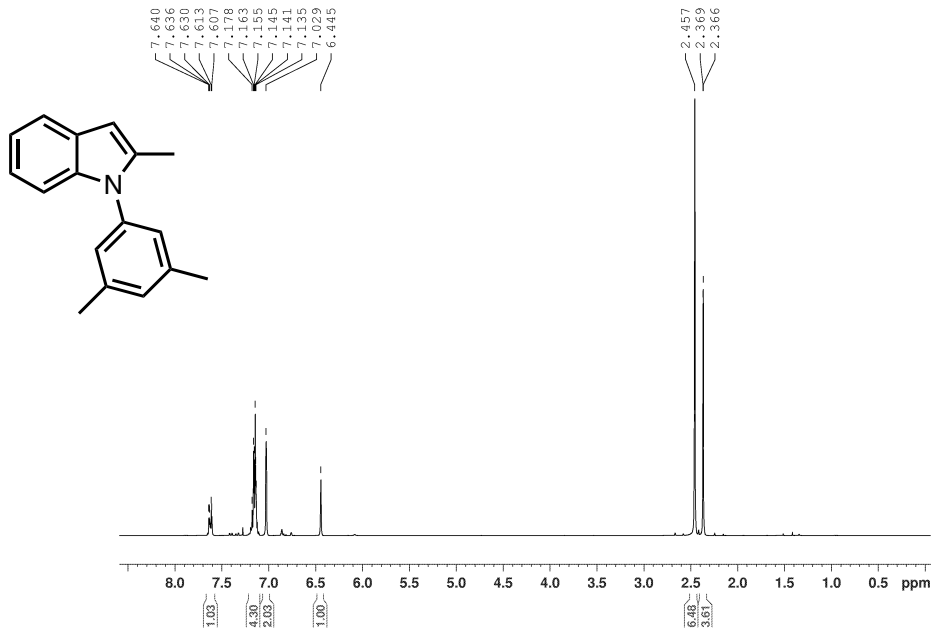

^{13}C{^{1}H} NMR Spectrum of 1-(3,5-dimethylphenyl)-2-methyl-1H-indole, **2-1g** ($CDCl_3$, 125.8 MHz)

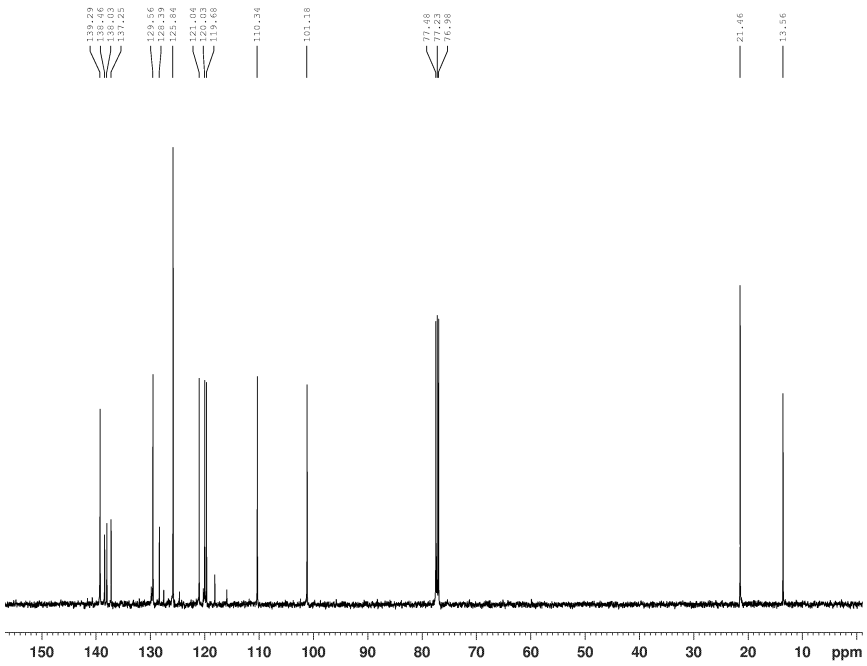

^{1}H NMR Spectrum of 1-(2-isopropylphenyl)-2-methyl-1H-indole, **2-1h** ($CDCl_3$, 500.1 MHz)

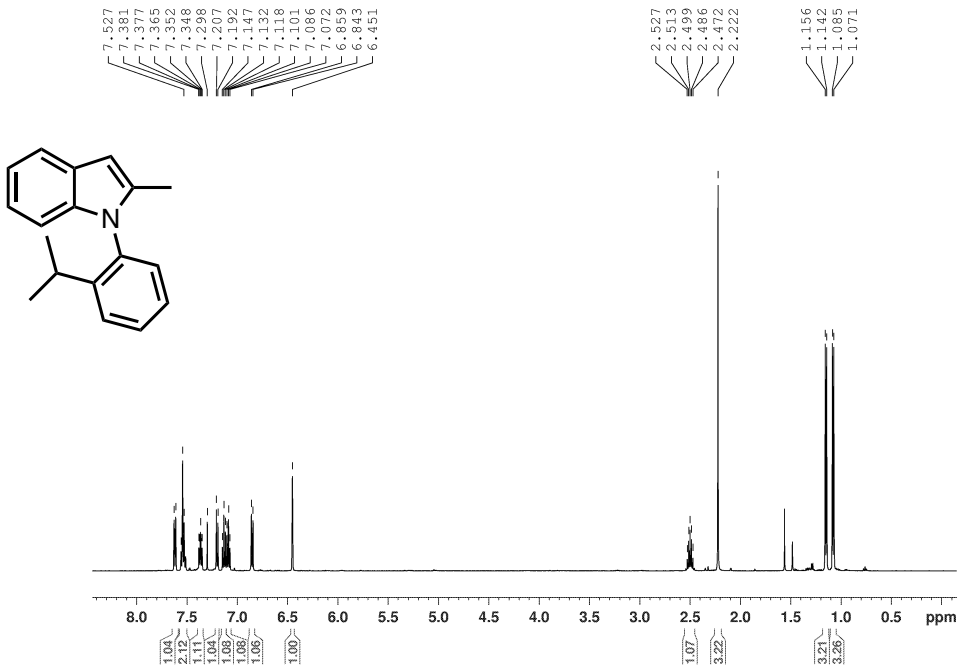

^{13}C{^{1}H} NMR Spectrum of 1-(2-isopropylphenyl)-2-methyl-1H-indole, **2-1h** ($CDCl_3$, 125.8 MHz)

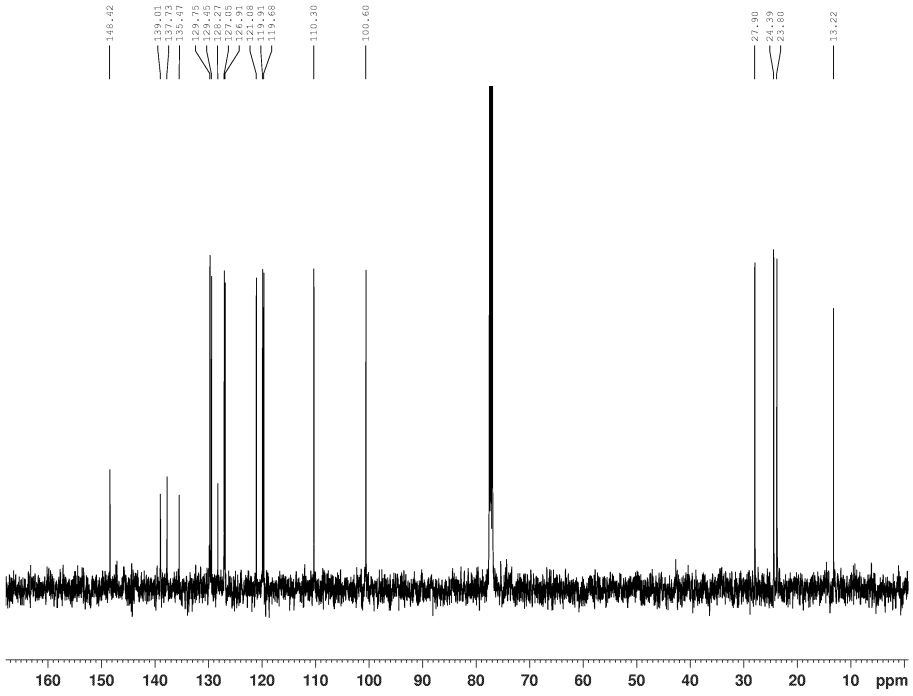

^{1}H NMR Spectrum of 2-methyl-1-(3-(trifluoromethyl)phenyl)-1*H*-indole, **2-1i** ($CDCl_3$, 500.1 MHz)

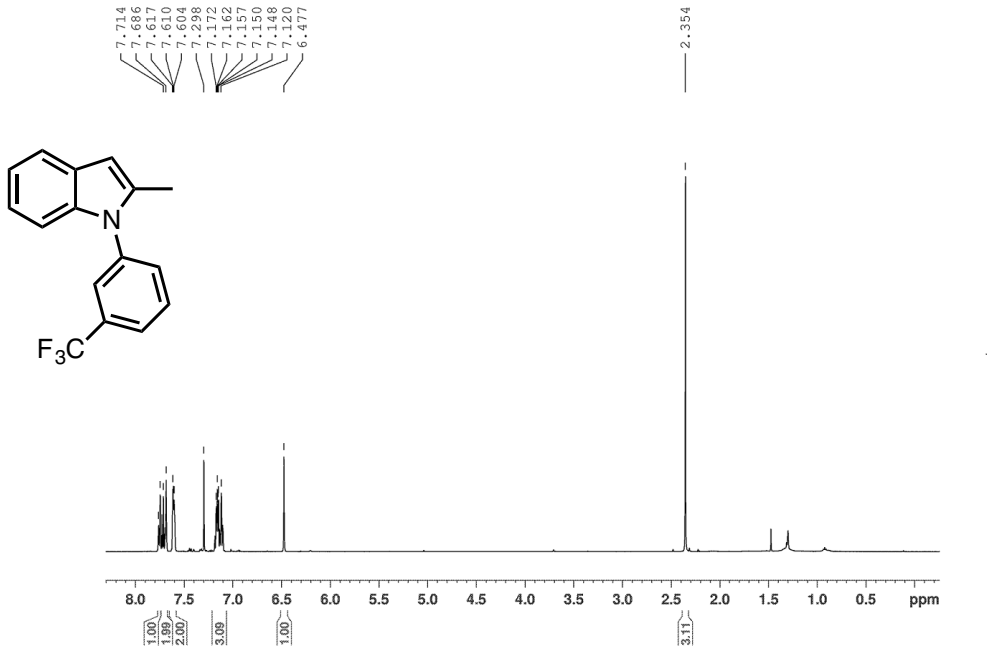

^{13}C{^{1}H} NMR Spectrum of 2-methyl-1-(3-(trifluoromethyl)phenyl)-1*H*-indole, **2-1i** ($CDCl_3$, 125.8 MHz)

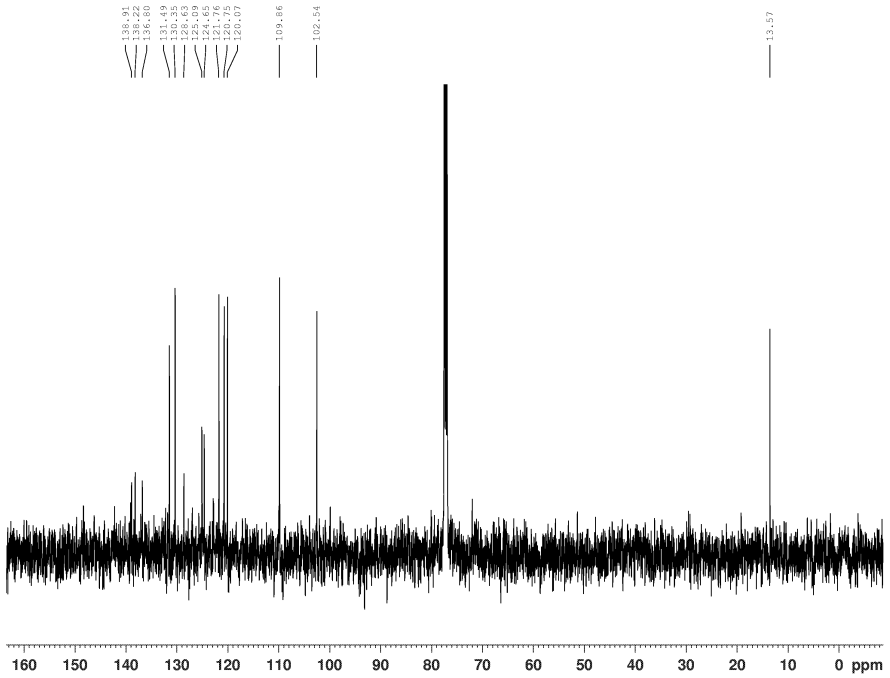

^{1}H NMR Spectrum of 1-octyl-2-phenyl-1*H*-indole, **2-2a** ($CDCl_3$, 500.1 MHz)

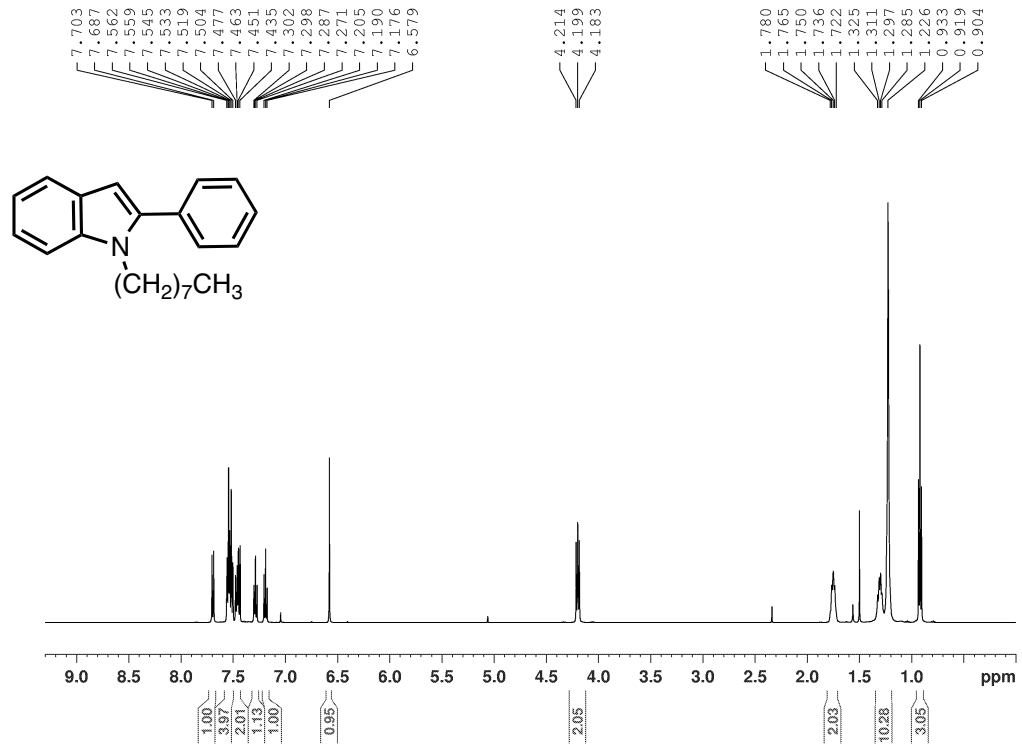

^{13}C{^{1}H} NMR Spectrum of 1-octyl-2-phenyl-1*H*-indole, **2-2a** ($CDCl_3$, 125.8 MHz)

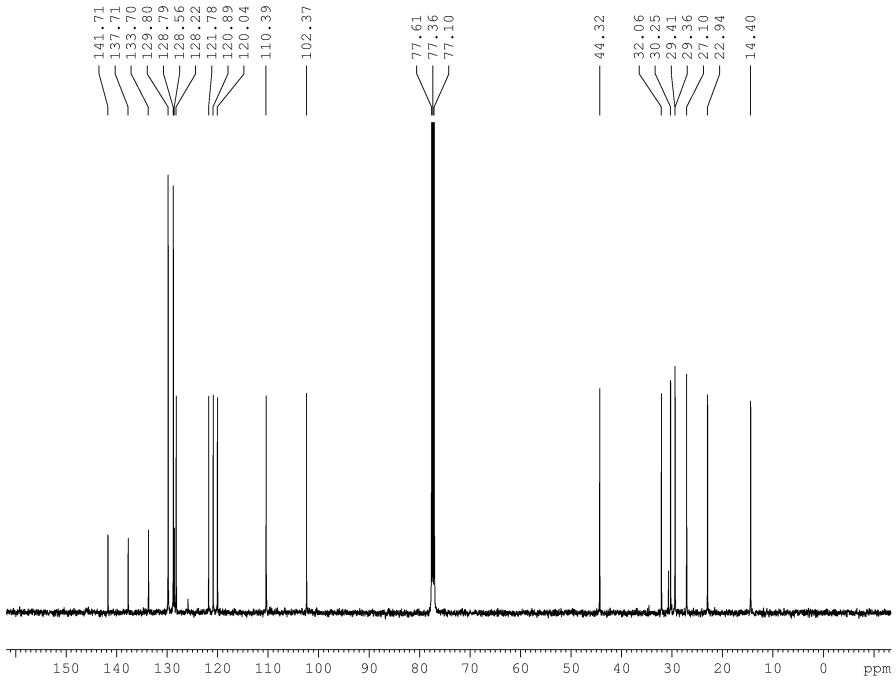

^{1}H NMR Spectrum of 1-octyl-2-(*o*-tolyl)-1*H*-indole, **2-2b** ($CDCl_3$, 500.1 MHz)

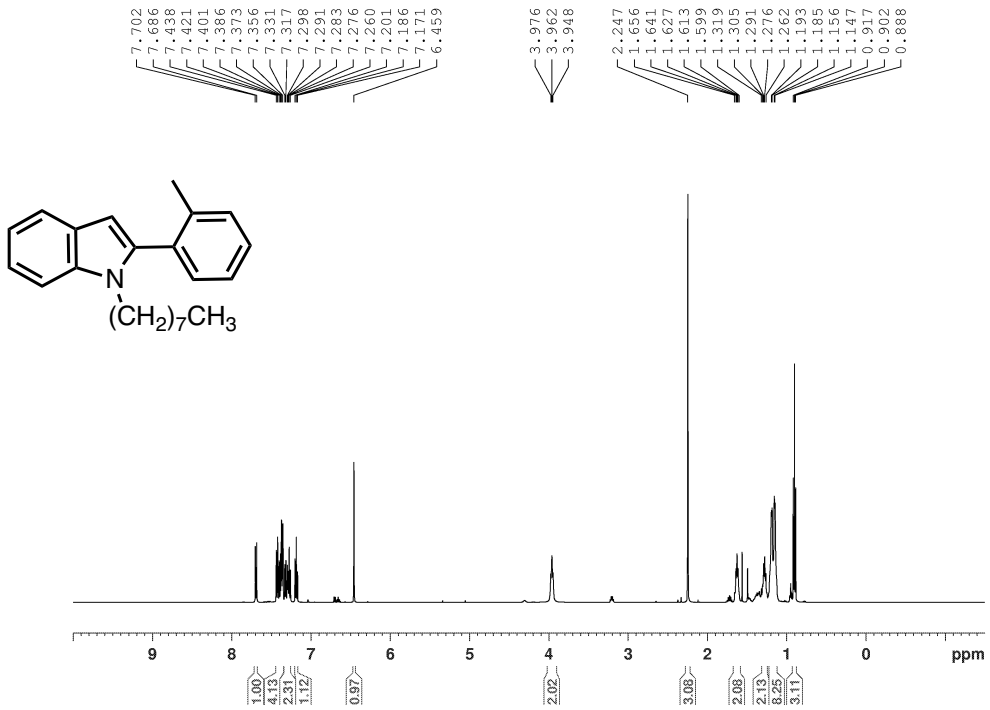

^{13}C{^{1}H} NMR Spectrum of 1-octyl-2-(*o*-tolyl)-1*H*-indole, **2-2b** ($CDCl_3$, 125.8 MHz)

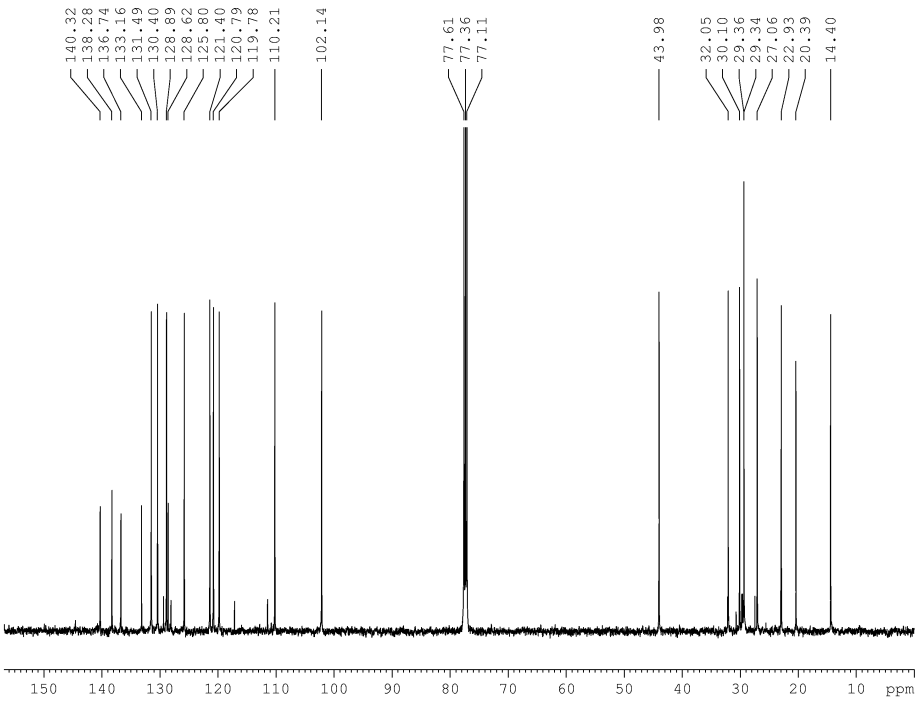

^{1}H NMR Spectrum of 1-octyl-2-(*p*-tolyl)-1*H*-indole, **2-2c** ($CDCl_3$, 500.1 MHz)

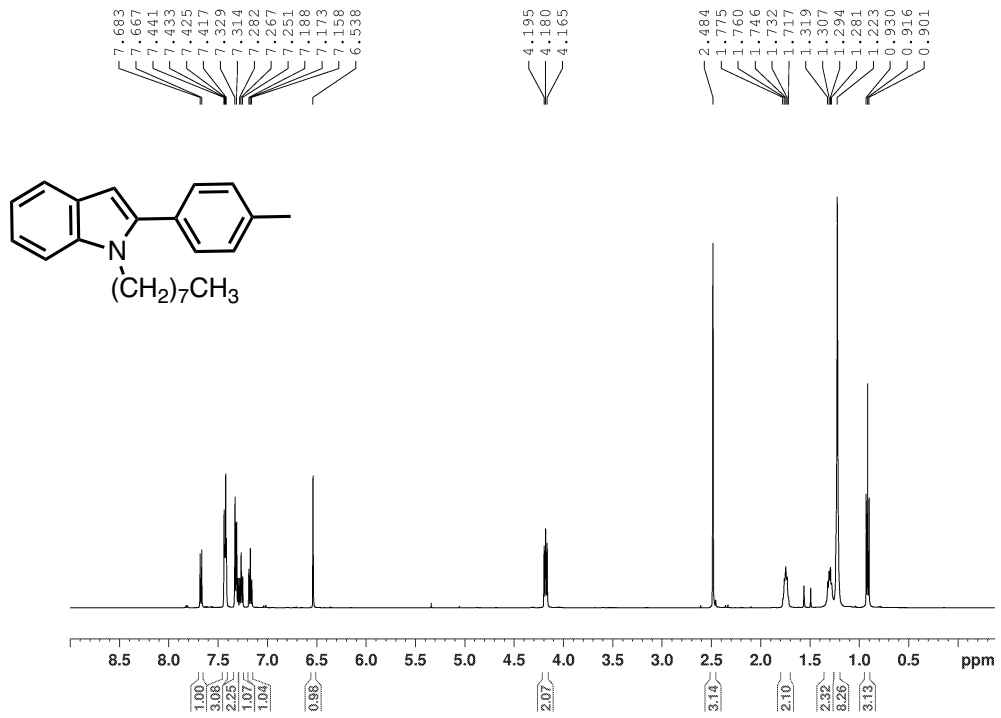

^{13}C{^{1}H} NMR Spectrum of 1-octyl-2-(*p*-tolyl)-1*H*-indole, **2-2c** ($CDCl_3$, 125.8 MHz)

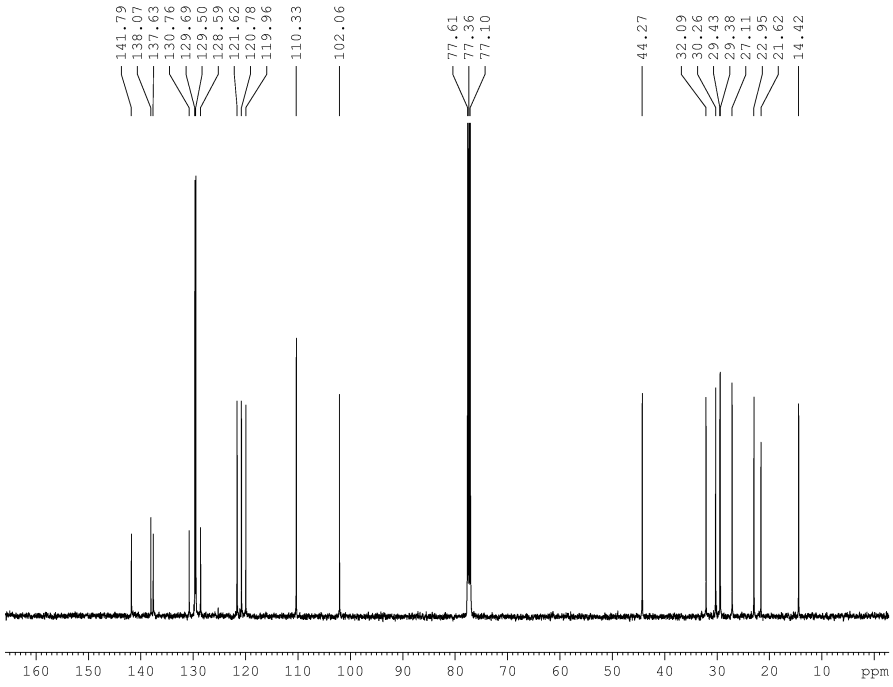

^{1}H NMR Spectrum of 2-(3-methoxyphenyl)-1-octyl-1*H*-indole, **2-2d** ($CDCl_3$, 500.1 MHz)

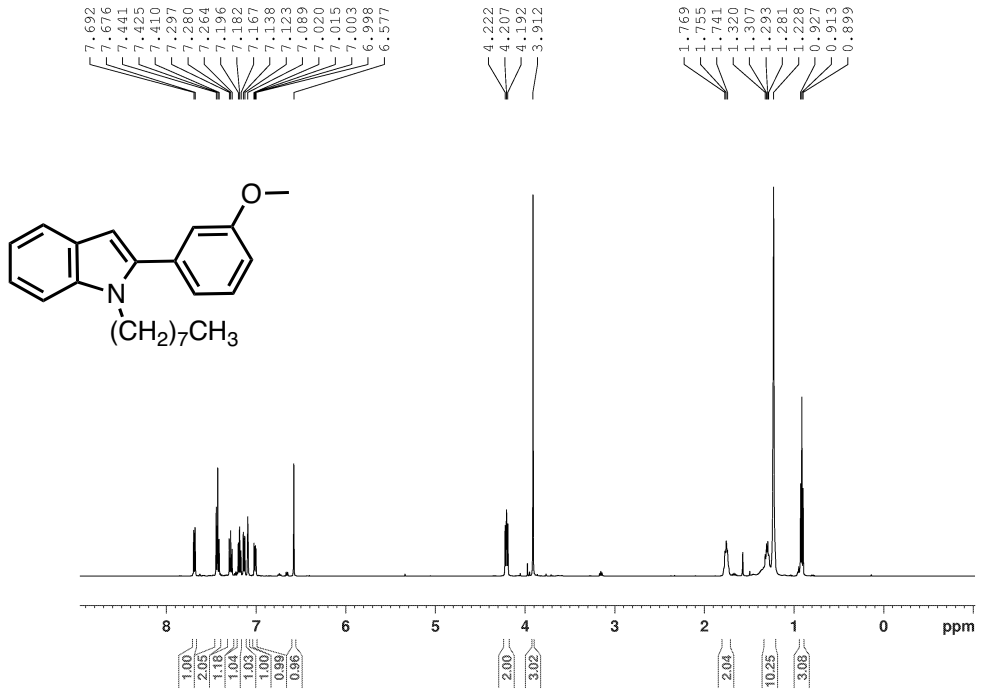

^{13}C{^{1}H} NMR Spectrum of 2-(3-methoxyphenyl)-1-octyl-1*H*-indole, **2-2d** ($CDCl_3$, 125.8 MHz)

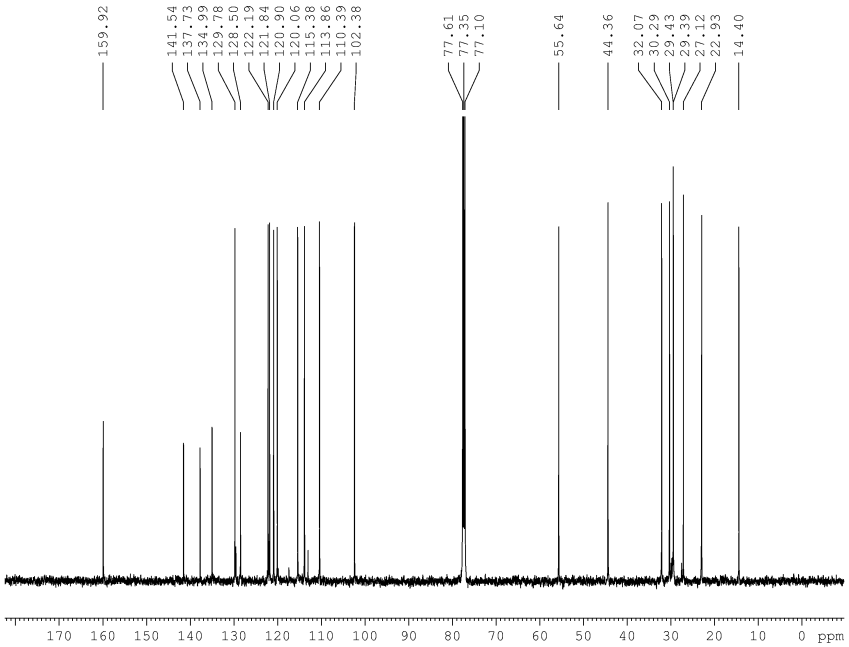

^{1}H NMR Spectrum of 2-(4-methoxyphenyl)-1-octyl-1*H*-indole, **2-2e** ($CDCl_3$, 500.1 MHz)

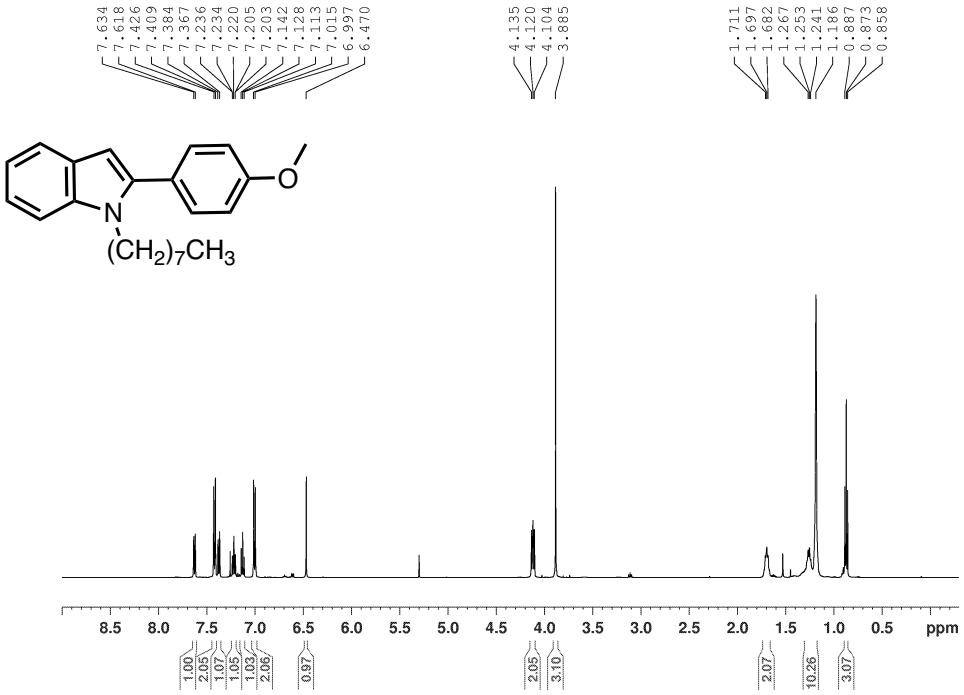

^{13}C{^{1}H} NMR Spectrum of 2-(4-methoxyphenyl)-1-octyl-1*H*-indole, **2-2e** ($CDCl_3$, 125.8 MHz)

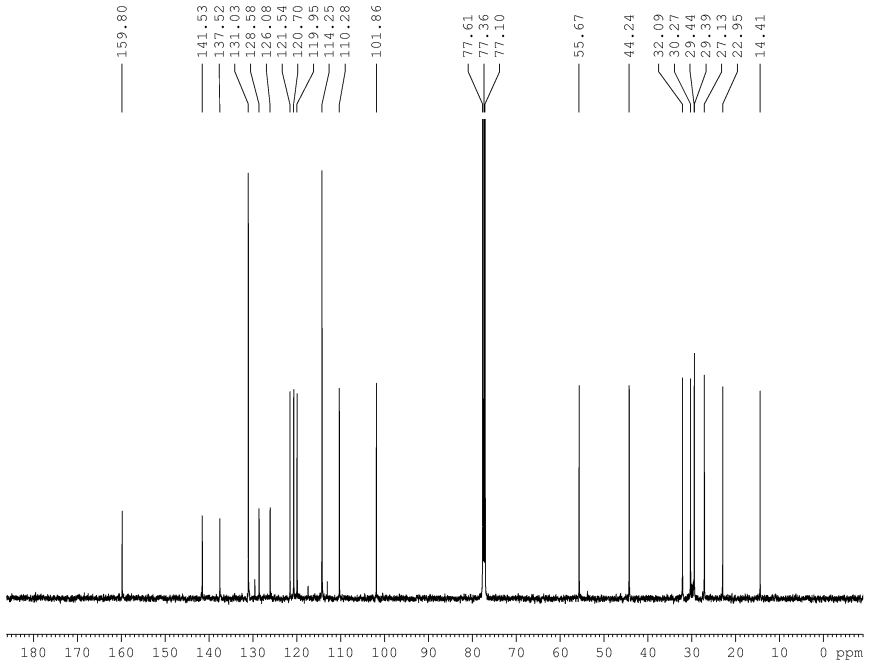

^{1}H NMR Spectrum of 2-(2-methoxyphenyl)-1-octyl-1*H*-indole, **2-2f** ($CDCl_3$, 500.1 MHz)

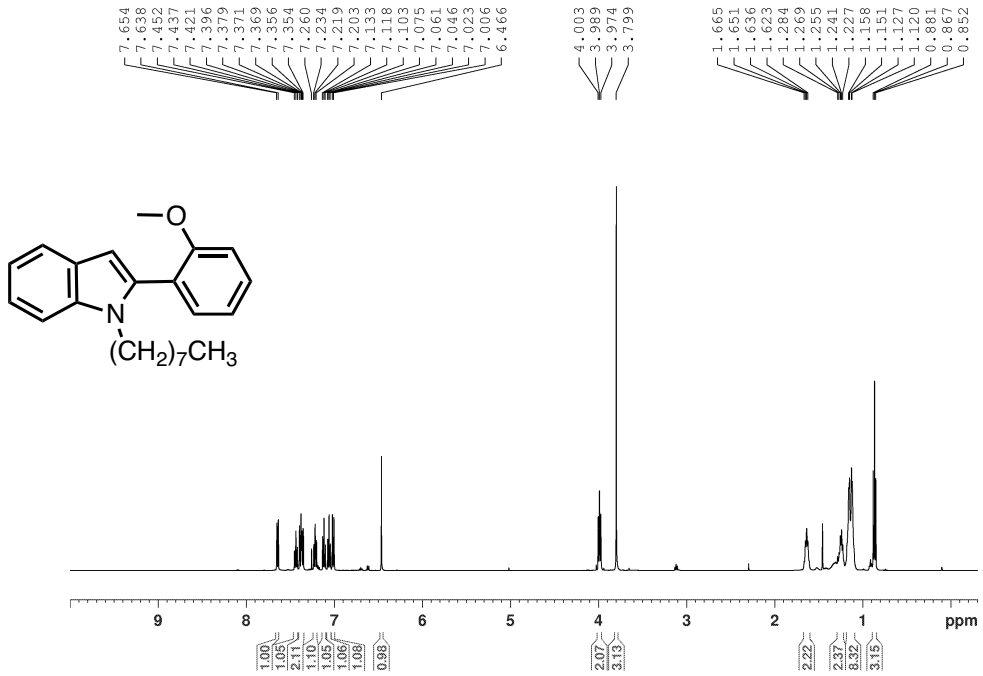

^{13}C{^{1}H} NMR Spectrum of 2-(2-methoxyphenyl)-1-octyl-1*H*-indole, **2-2f** ($CDCl_3$, 125.8 MHz)

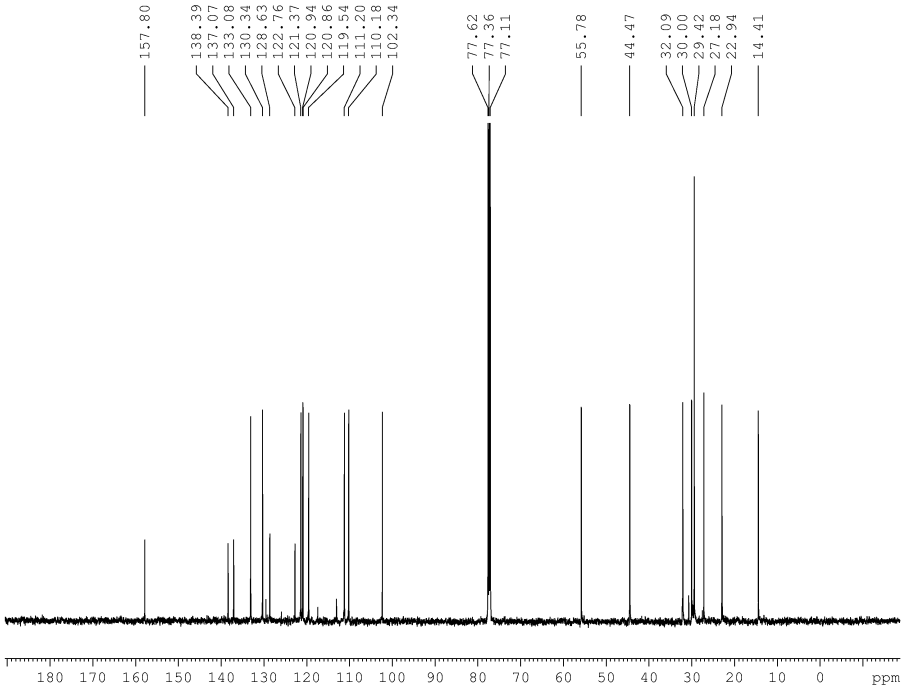

^{1}H NMR Spectrum of 2-(4-fluorophenyl)-1-octyl-1*H*-indole, **2-2g** ($CDCl_3$, 500.1 MHz)

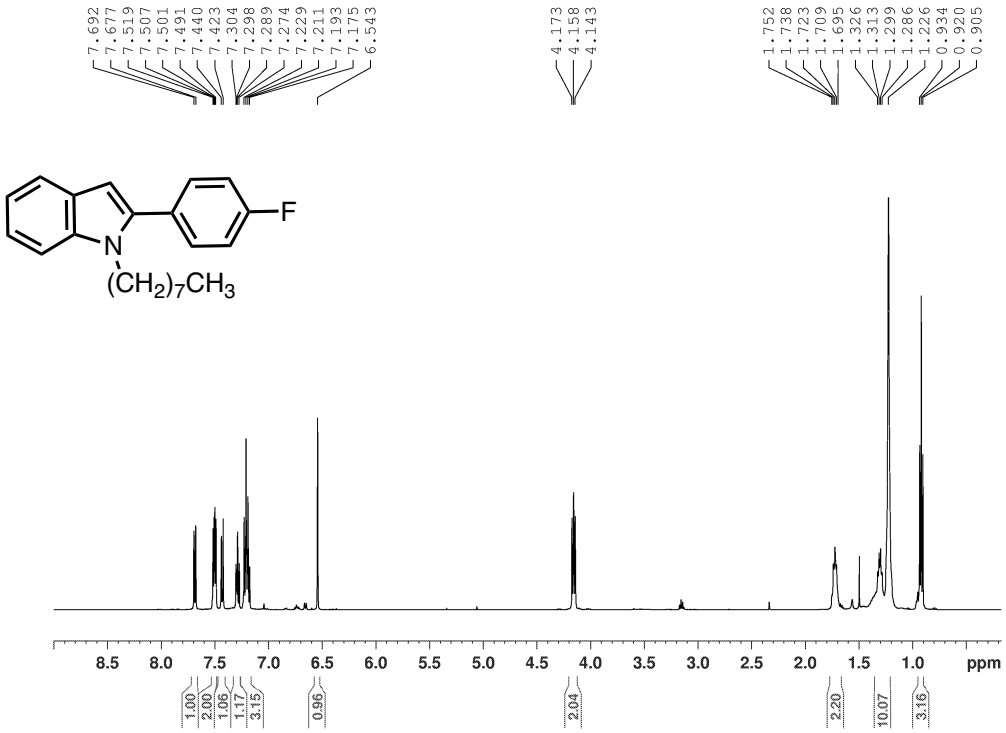

^{13}C{^{1}H} NMR Spectrum of 2-(4-fluorophenyl)-1-octyl-1*H*-indole, **2-2g** ($CDCl_3$, 125.8 MHz)

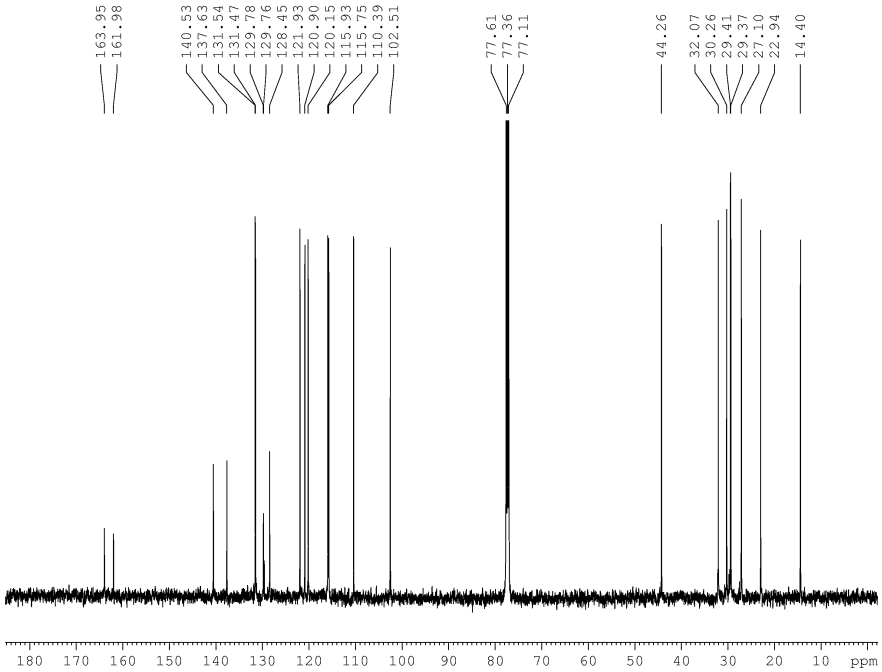

^{1}H NMR Spectrum of 2-cyclobutyl-1-octyl-1*H*-indole, **2-2h** ($CDCl_3$, 500.1 MHz)

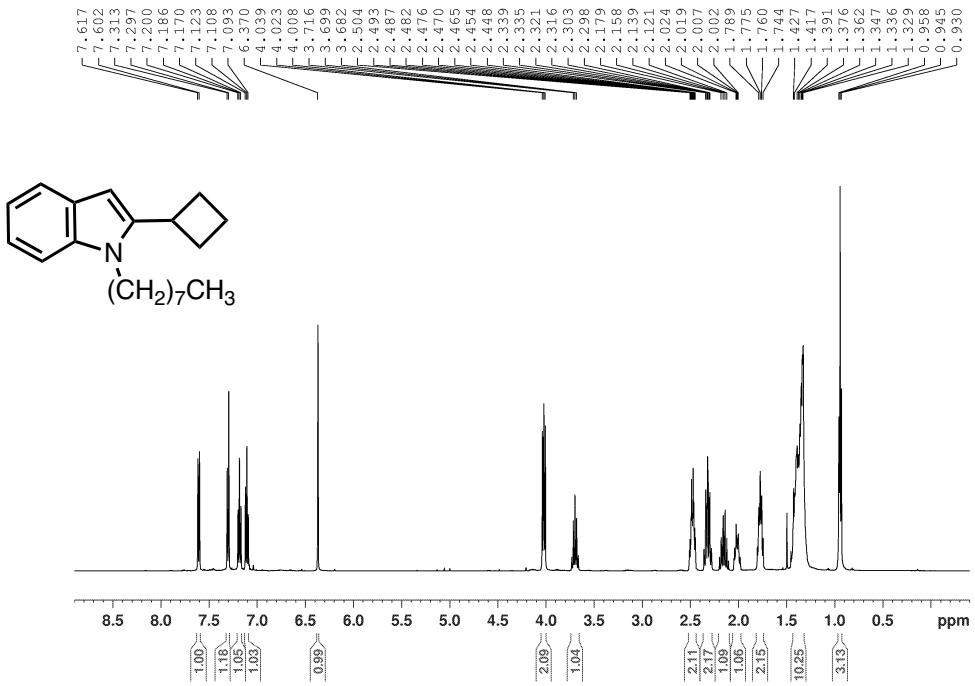

^{13}C{^{1}H} NMR Spectrum of 2-cyclobutyl-1-octyl-1*H*-indole, **2-2h** ($CDCl_3$, 125.8 MHz)

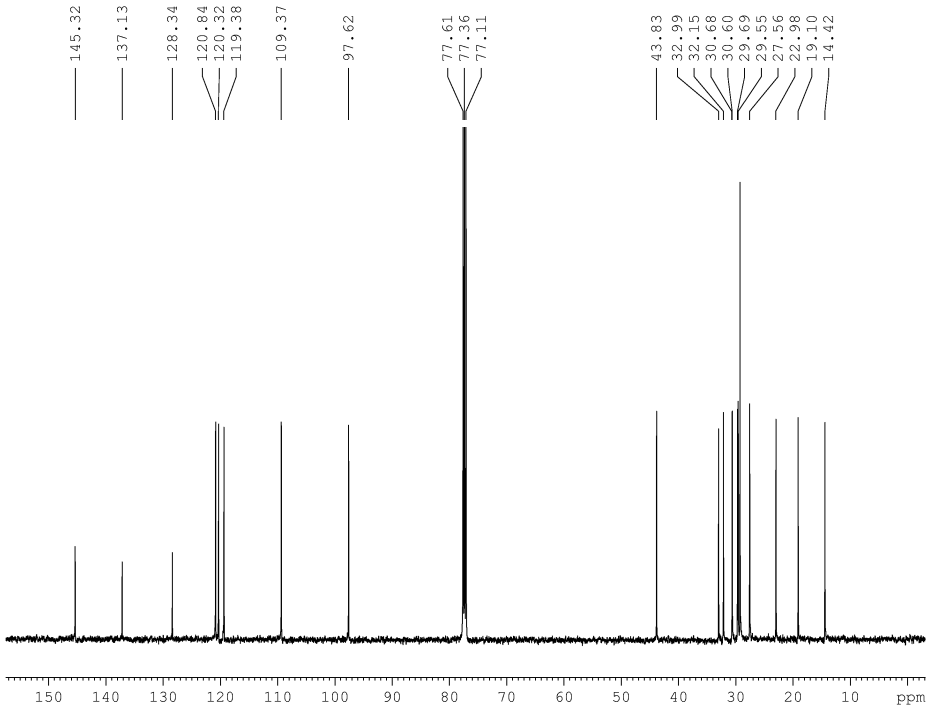

^{1}H NMR Spectrum of 2-hexyl-1-octyl-1*H*-indole, **2-2i** ($CDCl_3$, 500.1 MHz)

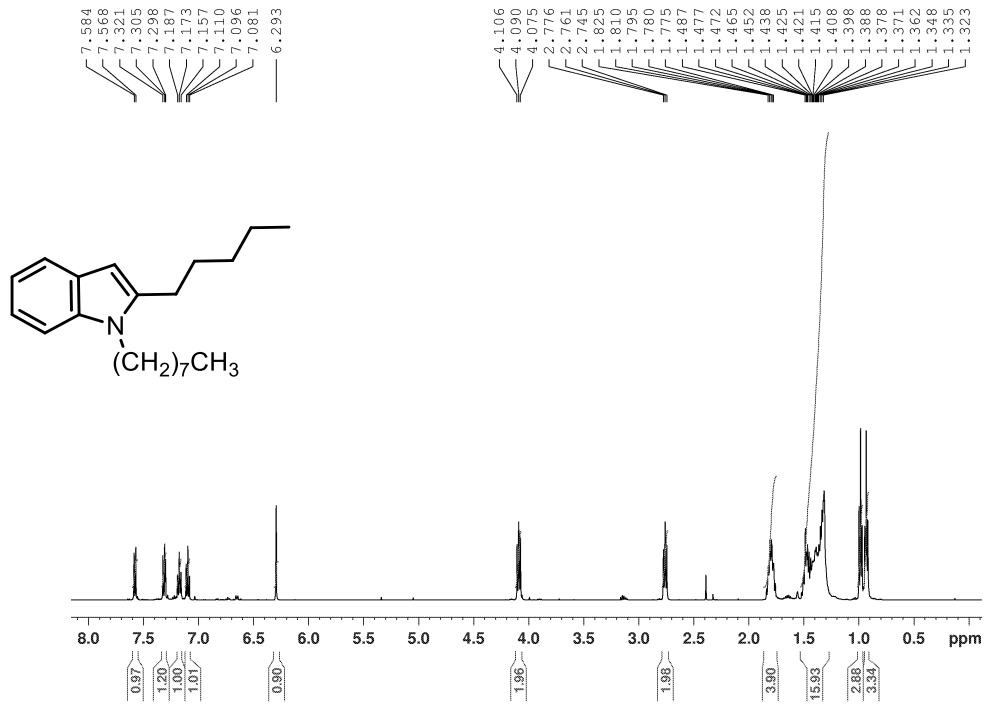

^{13}C{^{1}H} NMR Spectrum of 2-hexyl-1-octyl-1*H*-indole, **2-2i** ($CDCl_3$, 125.8 MHz)

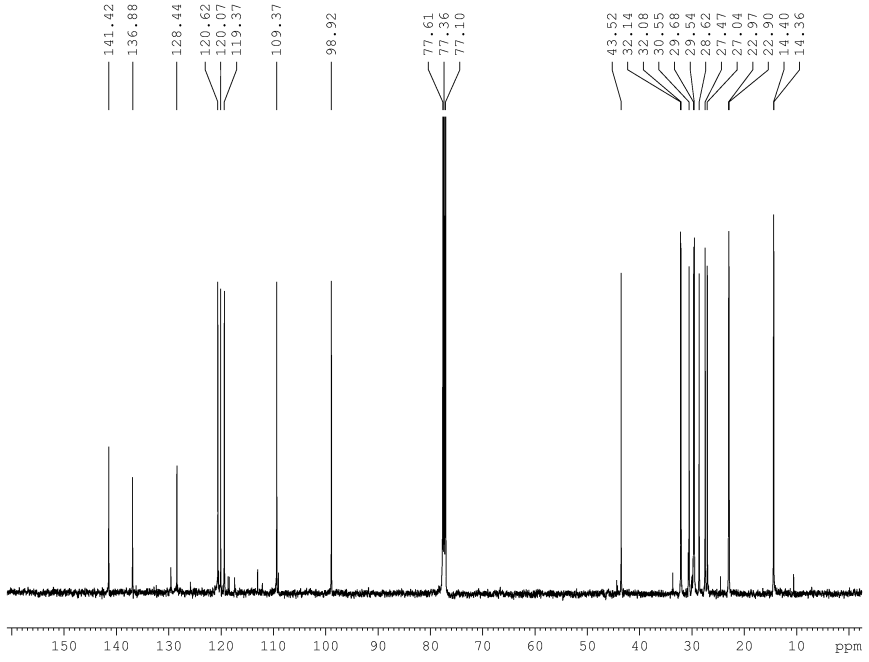

^{1}H NMR Spectrum of 2-(naphthalene-2-yl)-1-octyl-1*H*-indole, **2-2j** ($CDCl_3$, 500.1 MHz)

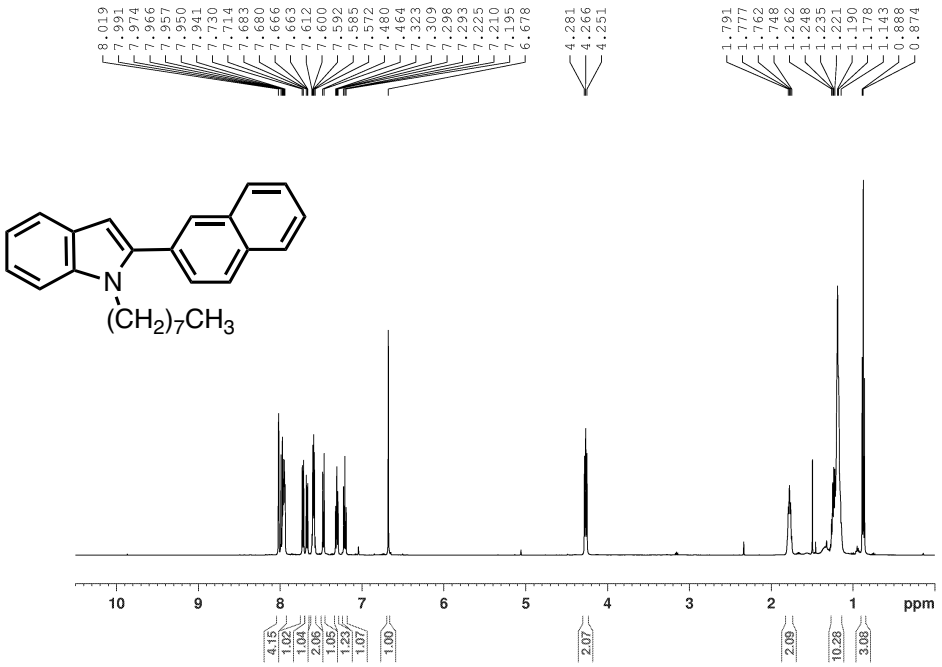

^{13}C{^{1}H} NMR Spectrum of 2-(naphthalene-2-yl)-1-octyl-1*H*-indole, **2-2j** ($CDCl_3$, 125.8 MHz)

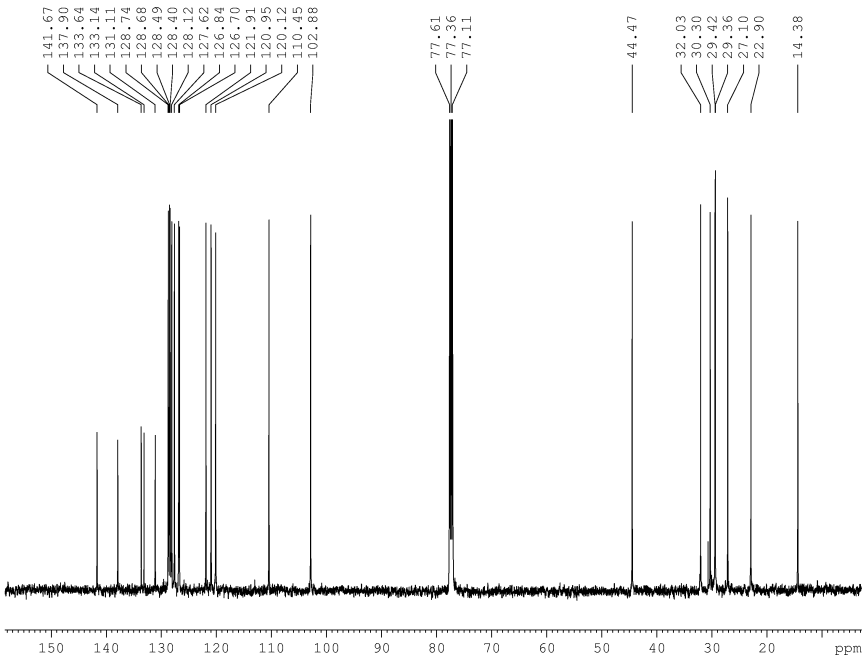

^{1}H NMR Spectrum of 11-octyl-6,11-dihydro-5*H*-benzo[*a*]carbazole, **2-2k** ($CDCl_3$, 500.1 MHz)

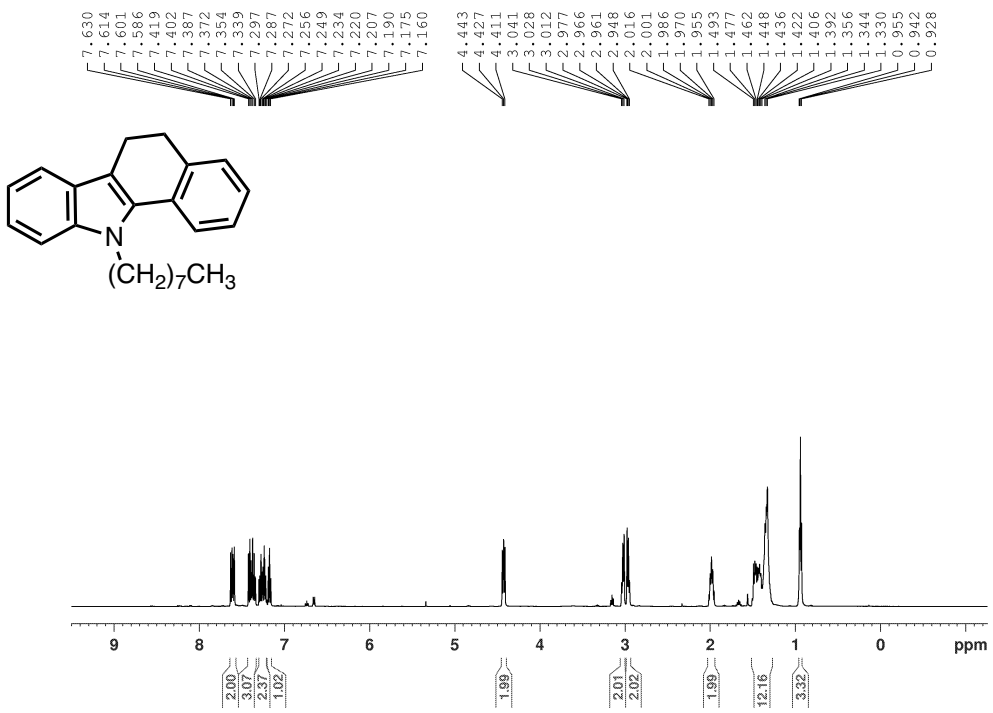

^{13}C{^{1}H} NMR Spectrum of 11-octyl-6,11-dihydro-5*H*-benzo[*a*]carbazole, **2-2k** ($CDCl_3$, 125.8 MHz)

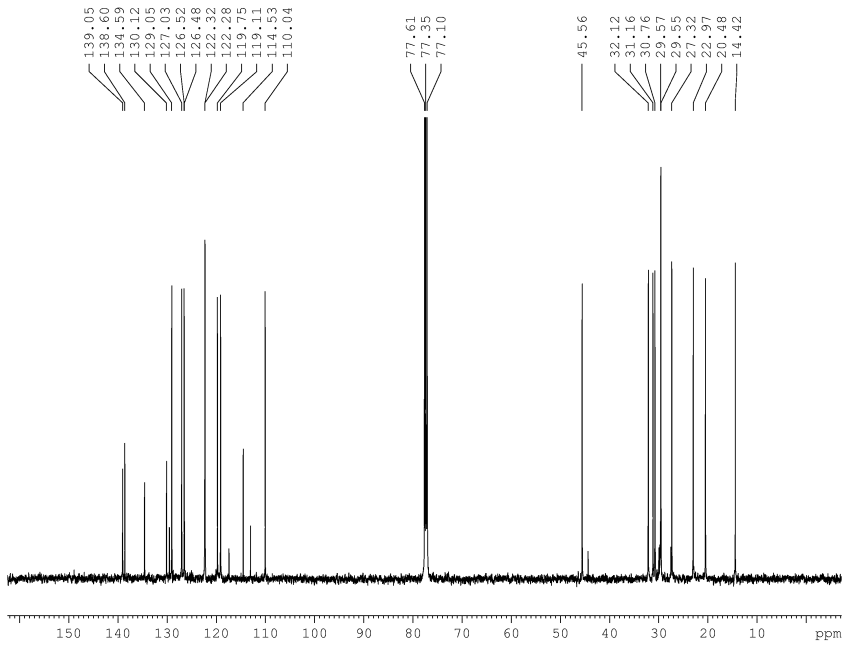

^{1}H NMR Spectrum of 9-octyl-2,3,4,9-tetrahydro-1*H*-carbazole, **2-2l** ($CDCl_3$, 500.1 MHz)

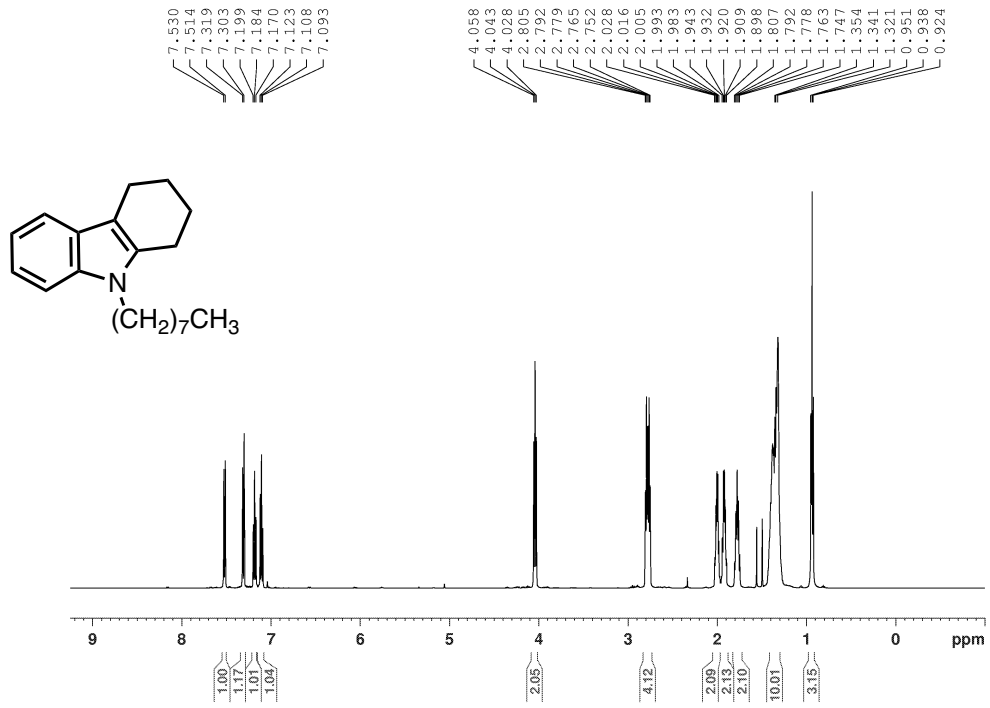

^{13}C{^{1}H} NMR Spectrum of 9-octyl-2,3,4,9-tetrahydro-1*H*-carbazole, **2-2l** ($CDCl_3$, 125.8 MHz)

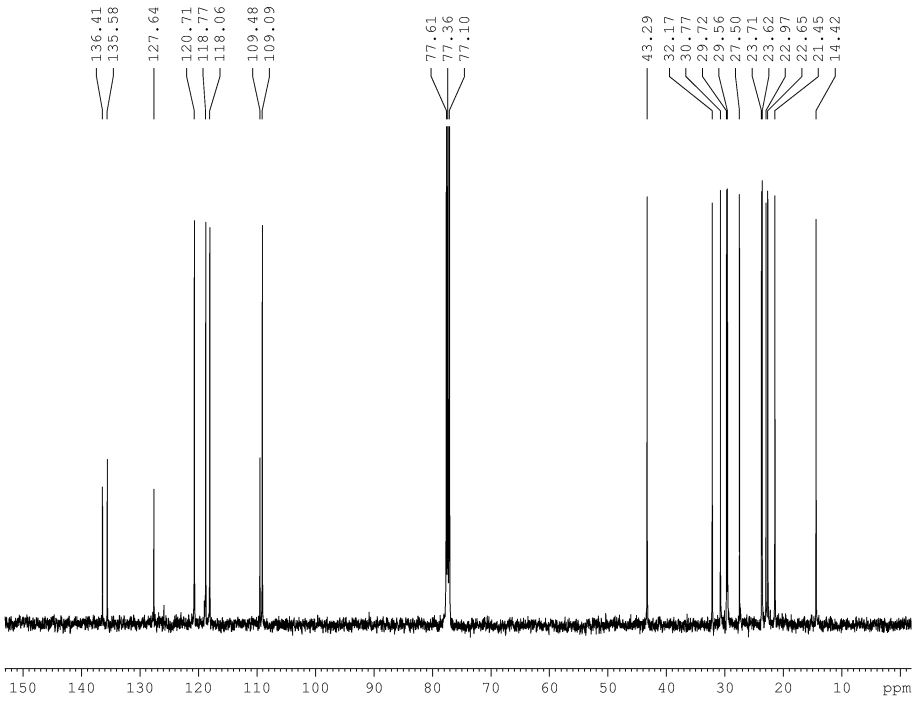

^{1}H NMR Spectrum of Methyl 4-(1-octyl-1*H*-indol-2-yl)benzoate, **2-2m** ($CDCl_3$, 500.1 MHz)

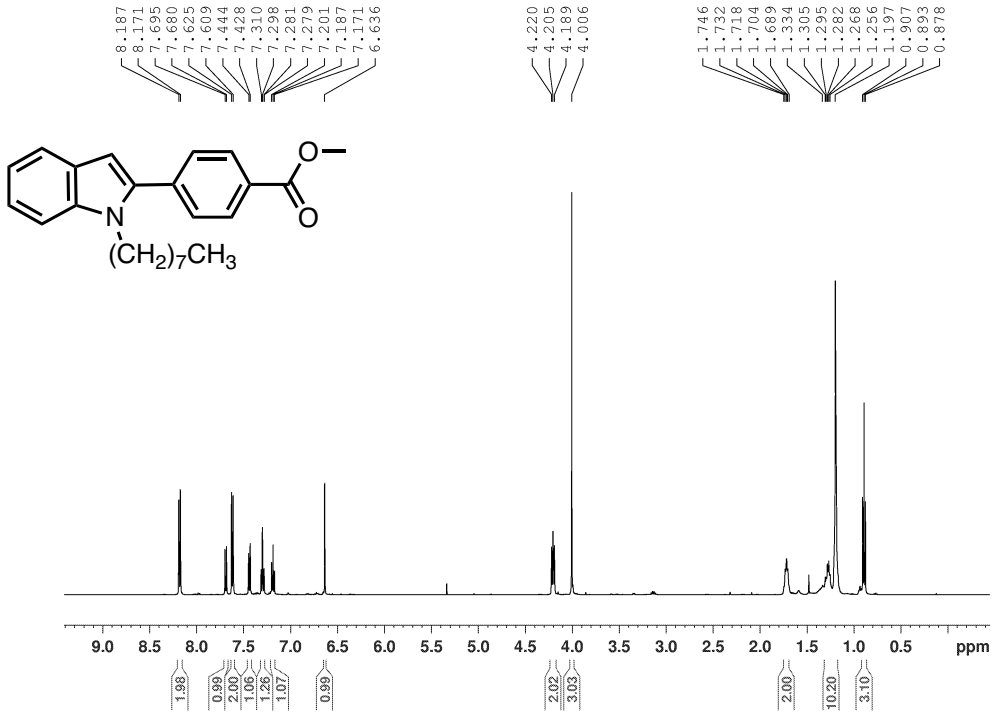

^{13}C{^{1}H} NMR Spectrum of Methyl 4-(1-octyl-1*H*-indol-2-yl)benzoate, **2-2m** ($CDCl_3$, 125.8 MHz)

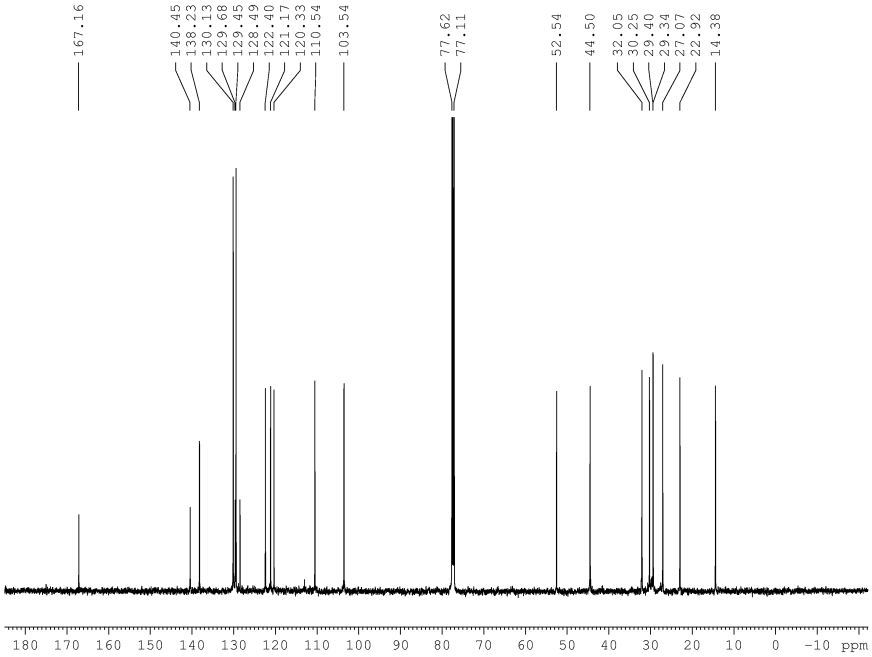

^{1}H NMR Spectrum of 2-(2,3-dihydrobenzo[*b*][1,4]dioxin-6-yl)-1-octyl-1*H*-indole, **2-2n** ($CDCl_3$, 500.1 MHz)

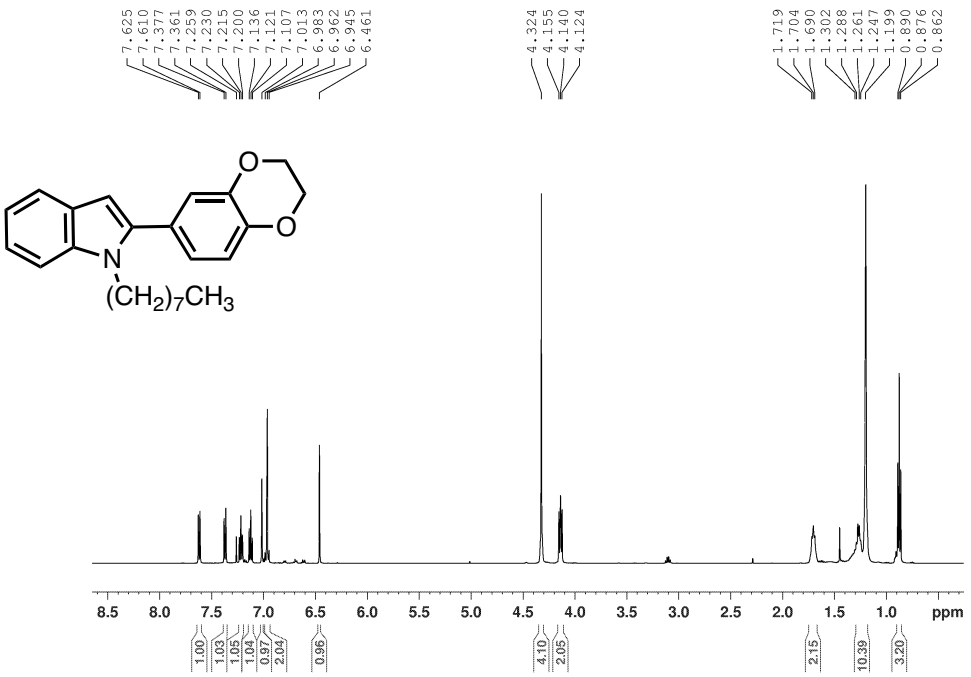

^{13}C{^{1}H} NMR Spectrum of 2-(2,3-dihydrobenzo[*b*][1,4]dioxin-6-yl)-1-octyl-1*H*-indole, **2-2n** ($CDCl_3$, 125.8 MHz)

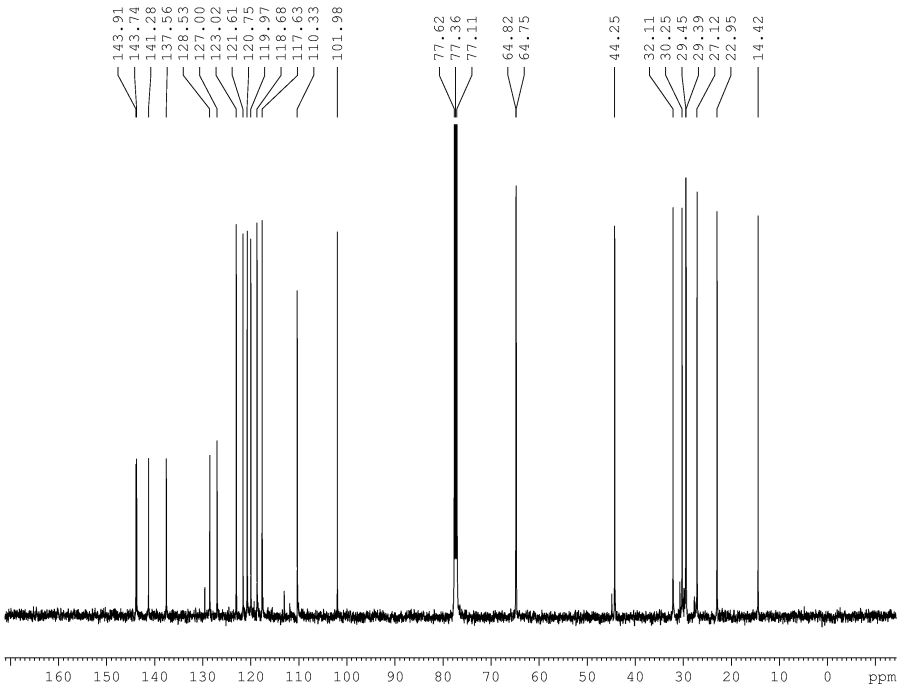

^{1}H NMR Spectrum of 2-(furan-2-yl)-1-octyl-1*H*-indole, **2-2o** ($CDCl_3$, 500.1 MHz)

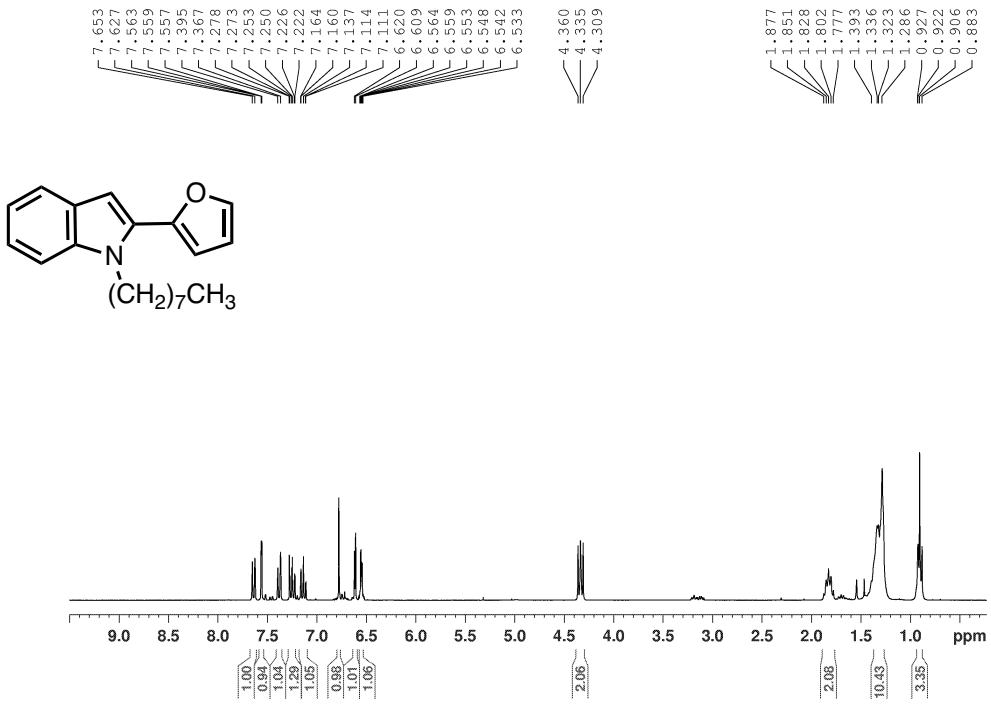

^{13}C{^{1}H} NMR Spectrum of 2-(furan-2-yl)-1-octyl-1*H*-indole, **2-2o** ($CDCl_3$, 125.8 MHz)

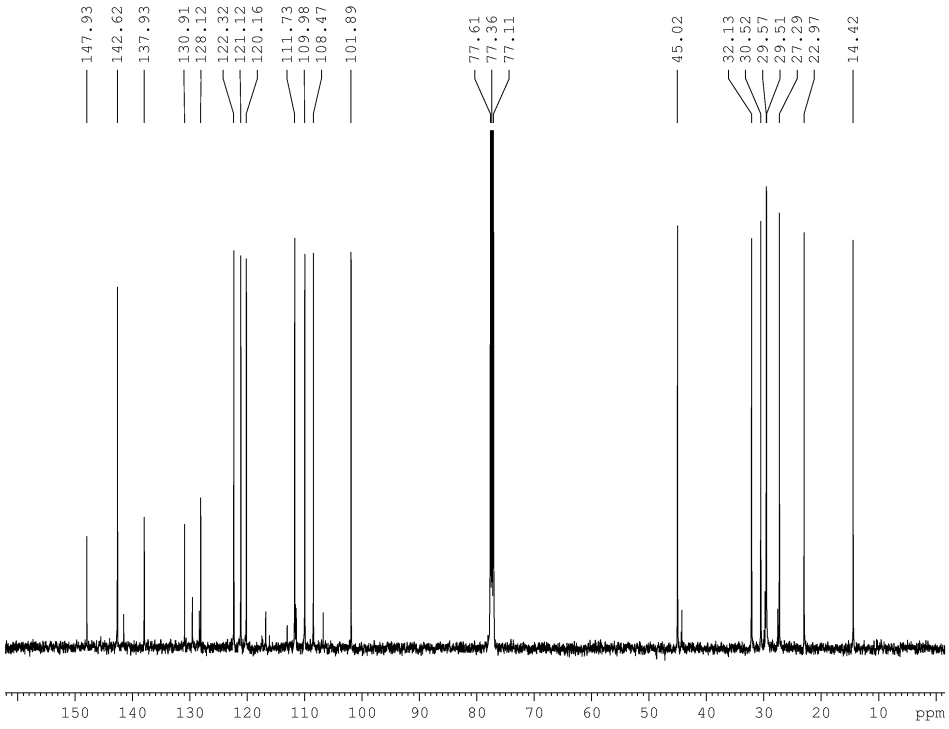

^{1}H NMR Spectrum of 1-octyl-2-(pyridin-4-yl)-1*H*-indole, **2-2p** ($CDCl_3$, 500.1 MHz)

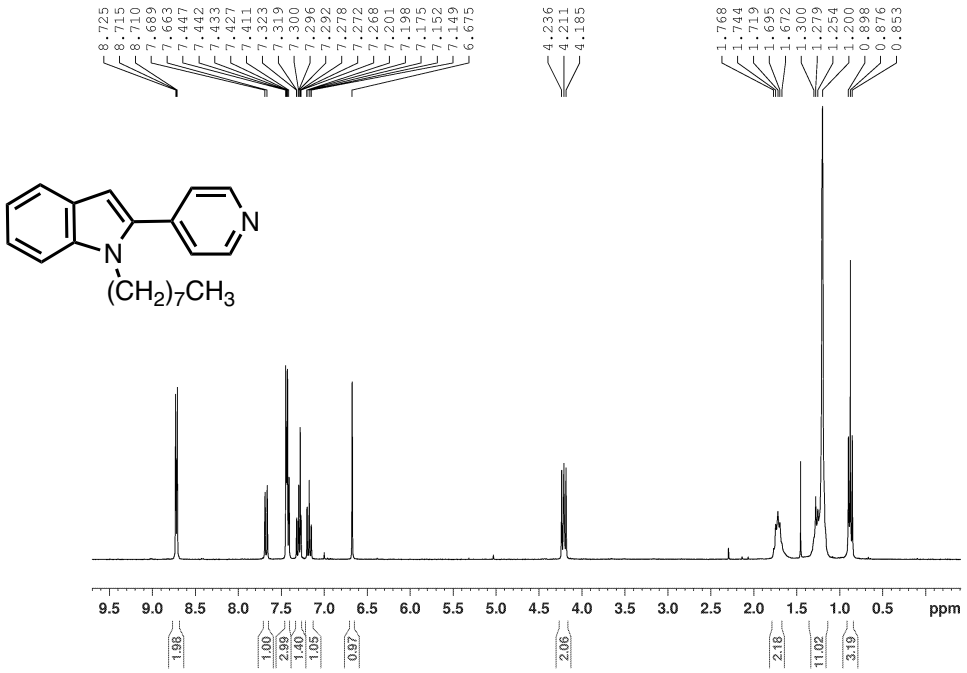

^{13}C{^{1}H} NMR Spectrum of 1-octyl-2-(pyridin-4-yl)-1*H*-indole, **2-2p** ($CDCl_3$, 125.8 MHz)

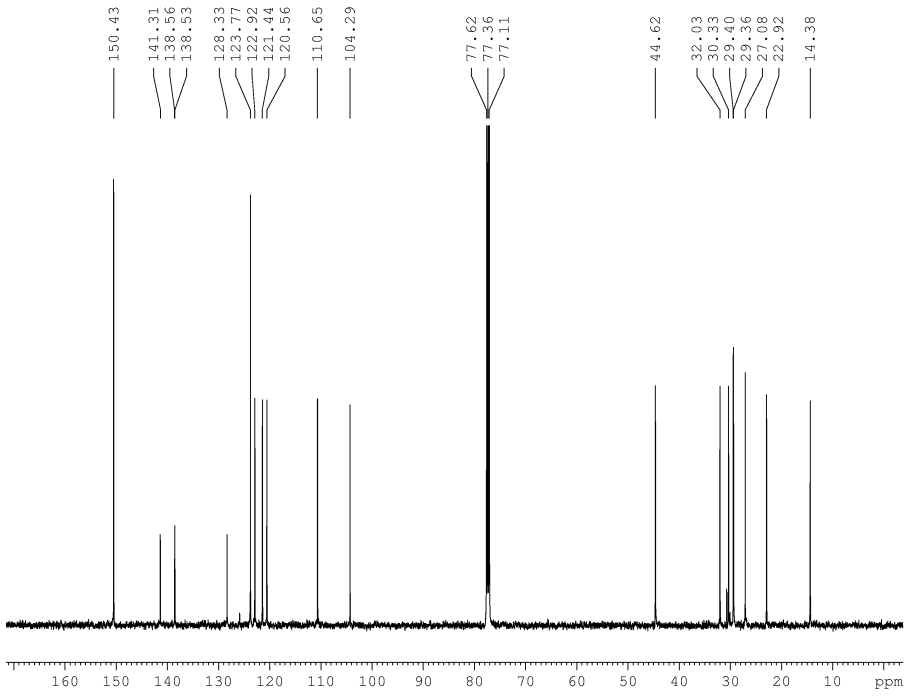

^{1}H NMR Spectrum of 1-octyl-2-(pyridin-3-yl)-1*H*-indole, **2-2q** ($CDCl_3$, 500.1 MHz)

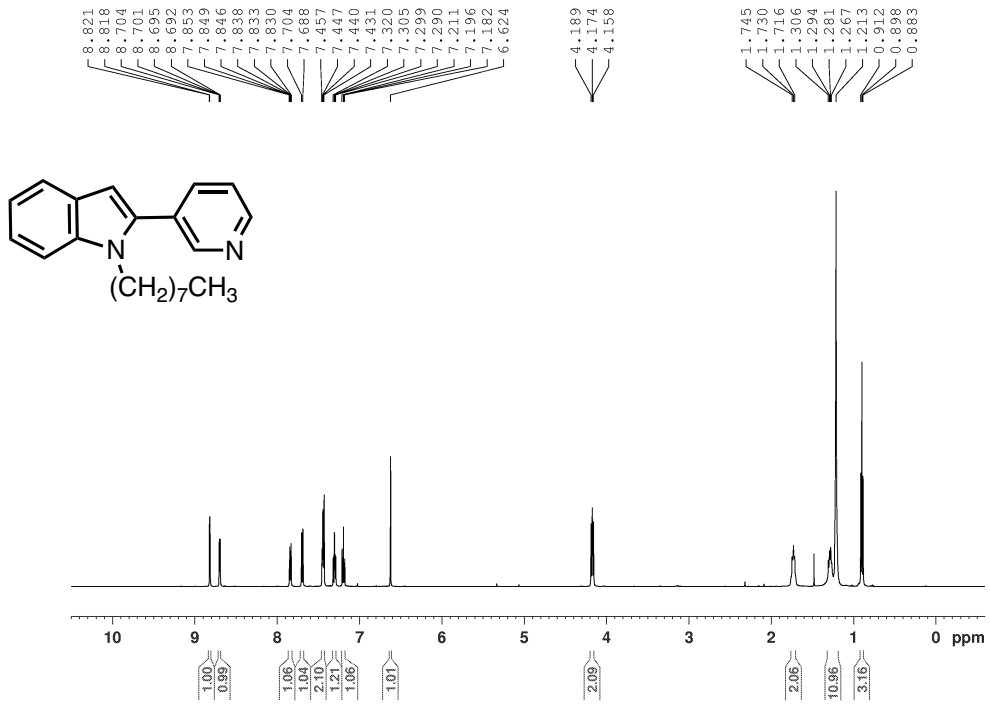

^{13}C{^{1}H} NMR Spectrum of 1-octyl-2-(pyridin-3-yl)-1*H*-indole, **2-2q** ($CDCl_3$, 125.8 MHz)

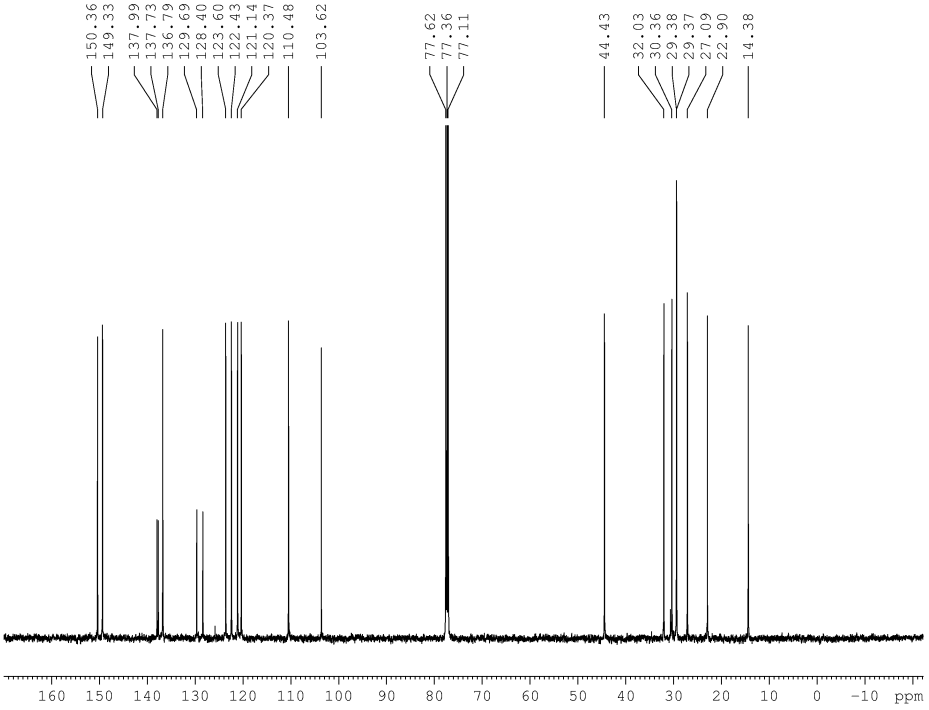

^{1}H NMR Spectrum of 1-octyl-2-(thiophen-2-yl)-1*H*-indole, **2-2r** ($CDCl_3$, 500.1 MHz)

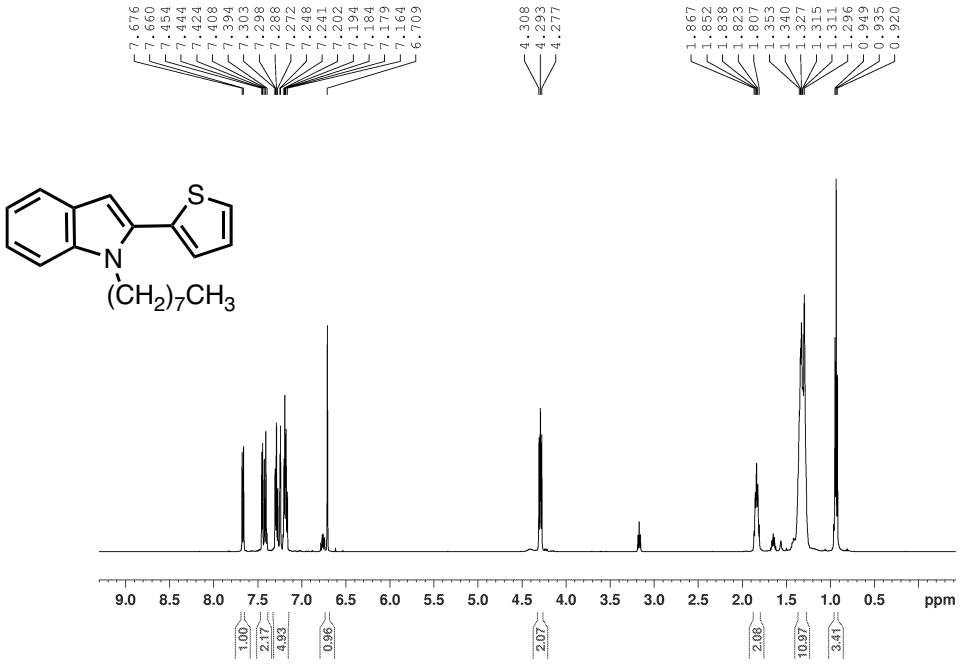

^{13}C{^{1}H} NMR Spectrum of 1-octyl-2-(thiophen-2-yl)-1*H*-indole, **2-2r** ($CDCl_3$, 125.8 MHz)

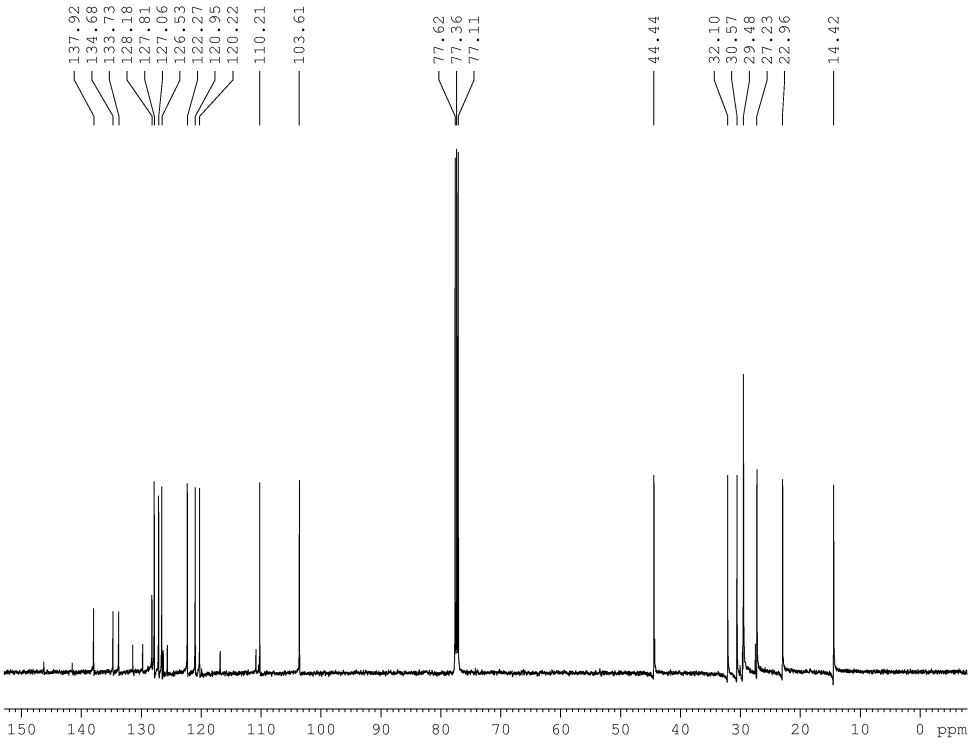

^{1}H NMR Spectrum of 1,2-diphenyl-1*H*-indole, **2-3a** ($CDCl_3$, 500.1 MHz)

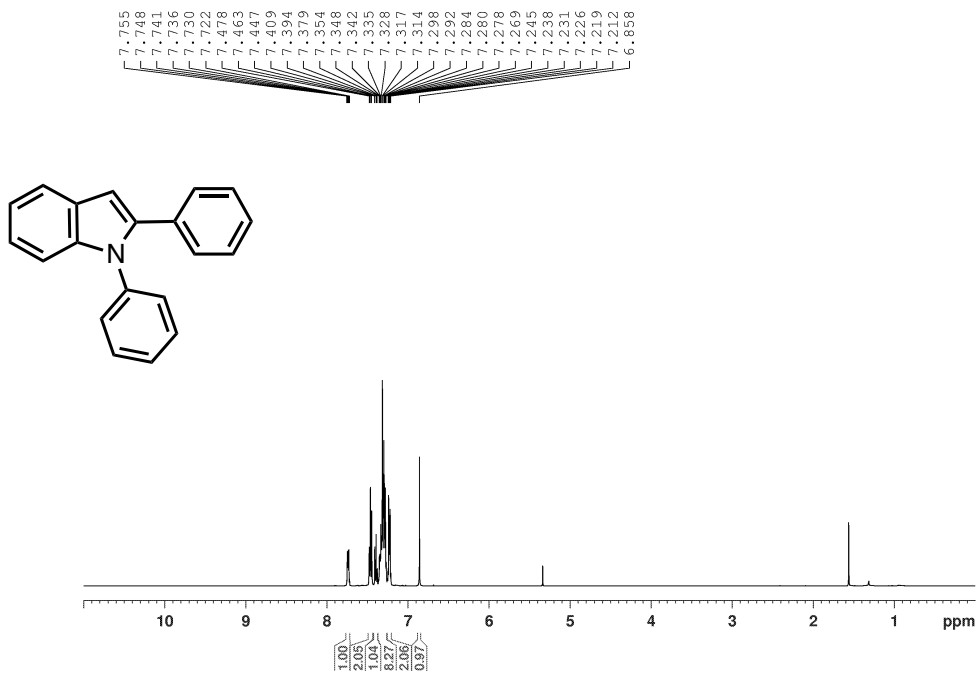

^{13}C{^{1}H} NMR Spectrum of 1,2-diphenyl-1*H*-indole, **2-3a** ($CDCl_3$, 125.8 MHz)

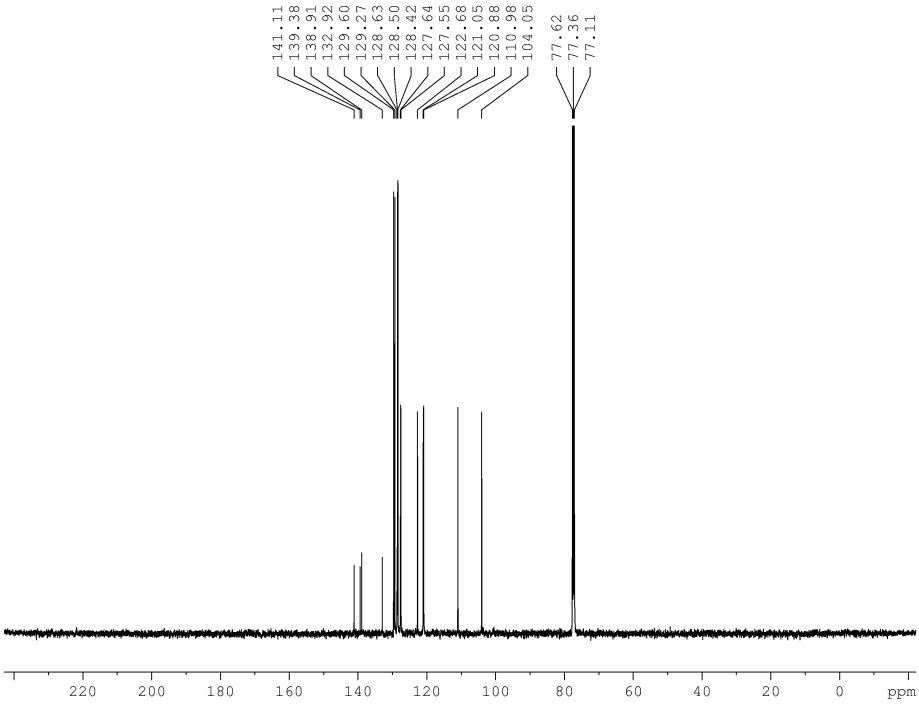

^{1}H NMR Spectrum of 1-octyl-2-phenyl-6-(trifluoromethyl)-1*H*-indole, **2-3b** ($CDCl_3$, 500.1 MHz)

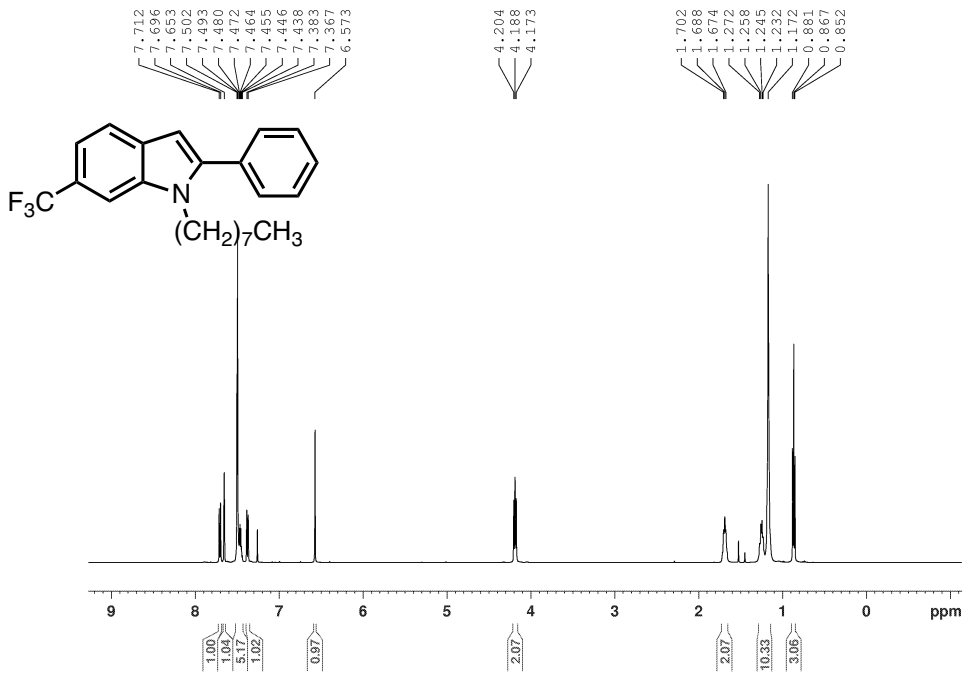

^{13}C{^{1}H} NMR Spectrum of 1-octyl-2-phenyl-6-(trifluoromethyl)-1*H*-indole, **2-3b** ($CDCl_3$, 125.8 MHz)

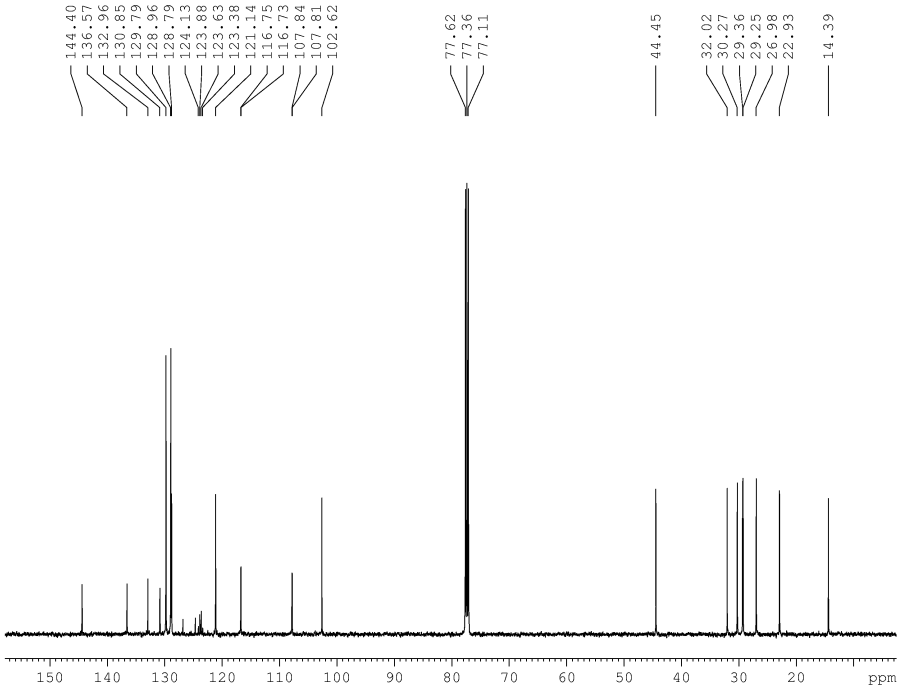

Appendix 2. Nickel-Catalyzed Monoarylation of Ammonia in the Synthesis of Funcitonalized Heterocycles

^{1}H NMR Spectrum of 2-amino-6-methoxypyridine, **3-2** ($CDCl_3$, 500.1 MHz)

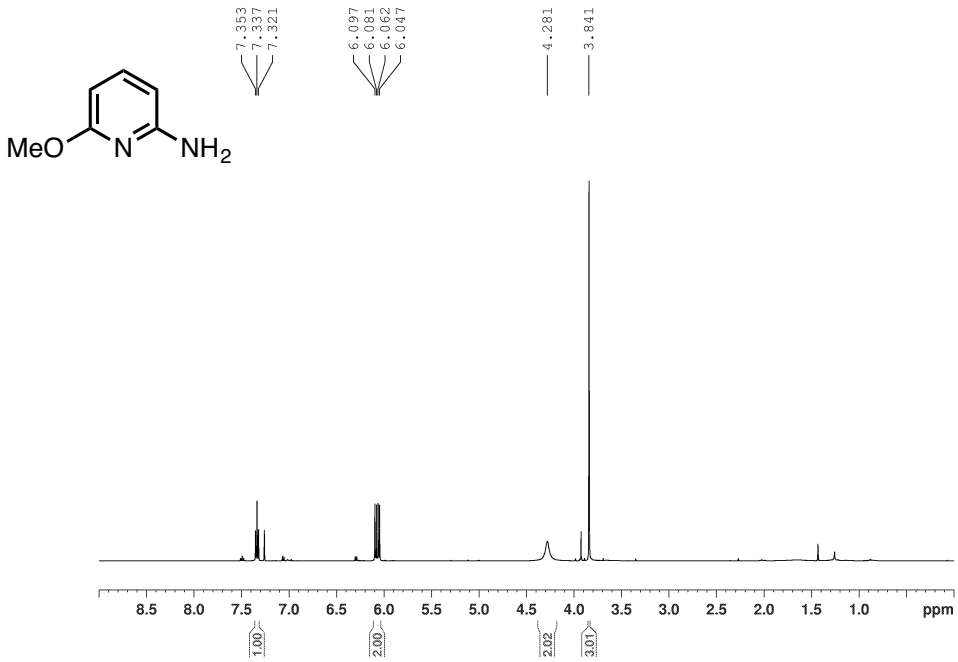

^{13}C{^{1}H} NMR Spectrum of 2-amino-6-methoxypyridine, **3-2** ($CDCl_3$, 125.8 MHz)

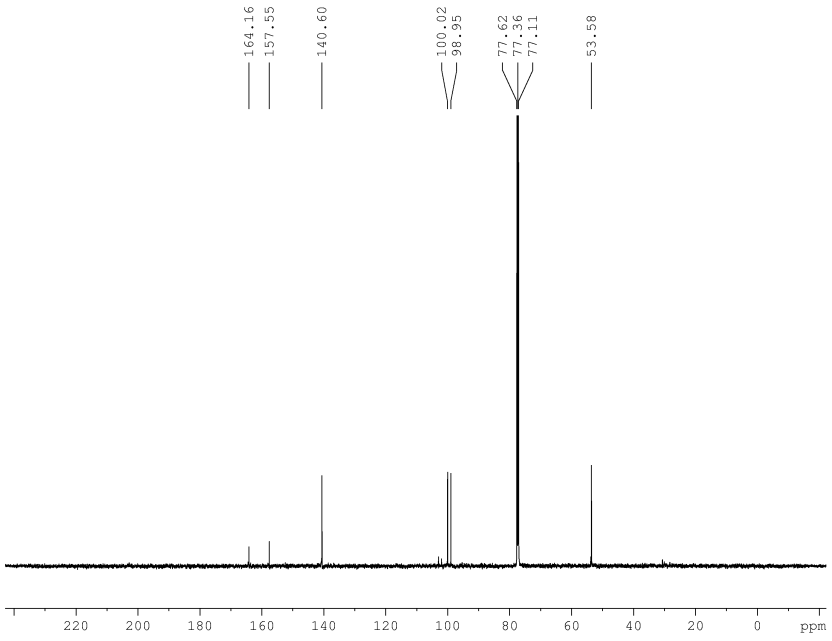

^{1}H NMR Spectrum of 6-amino-2,4-dimethoxypyrimidine, **3-3** ($CDCl_3$, 500.1 MHz)

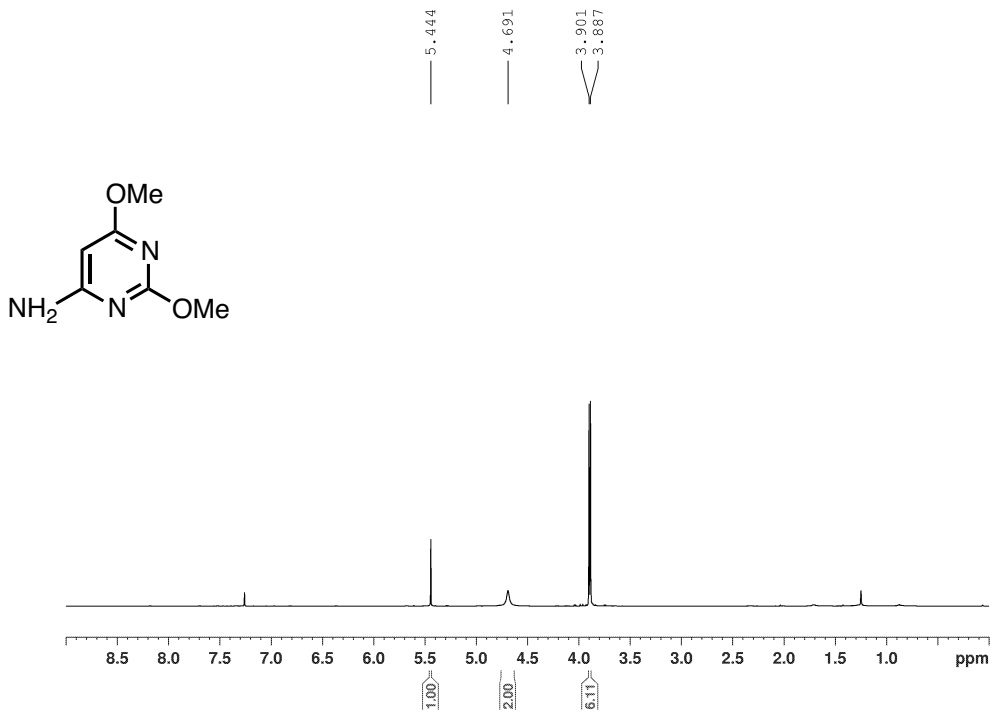

^{13}C{^{1}H} NMR Spectrum of 6-amino-2,4-dimethoxypyrimidine, **3-3** ($CDCl_3$, 125.8 MHz)

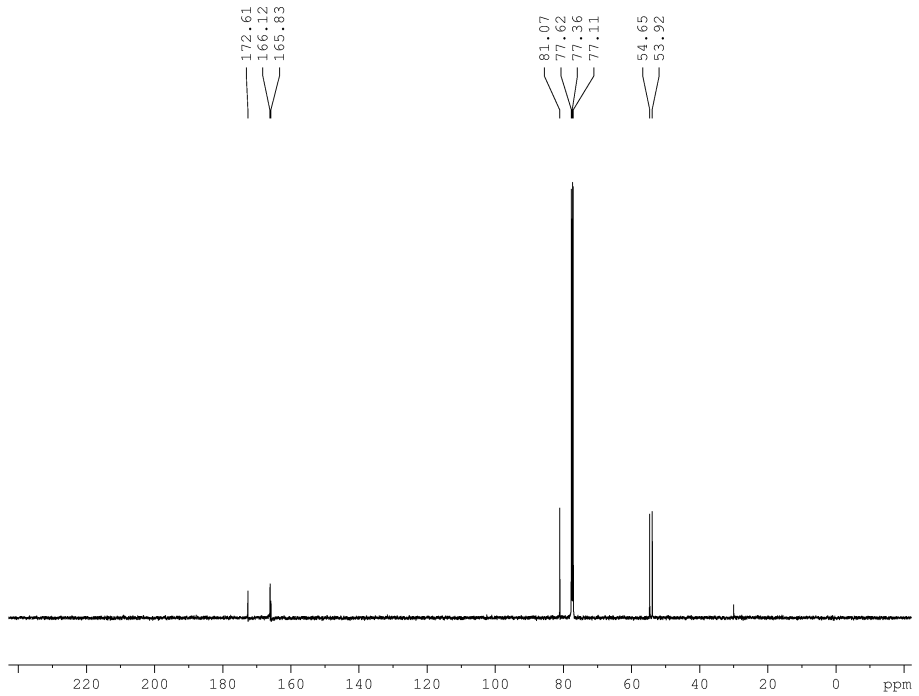

^{1}H NMR Spectrum of 4-amino-2-methylquinoline, **3-4** ($CDCl_3$, 500.1 MHz)

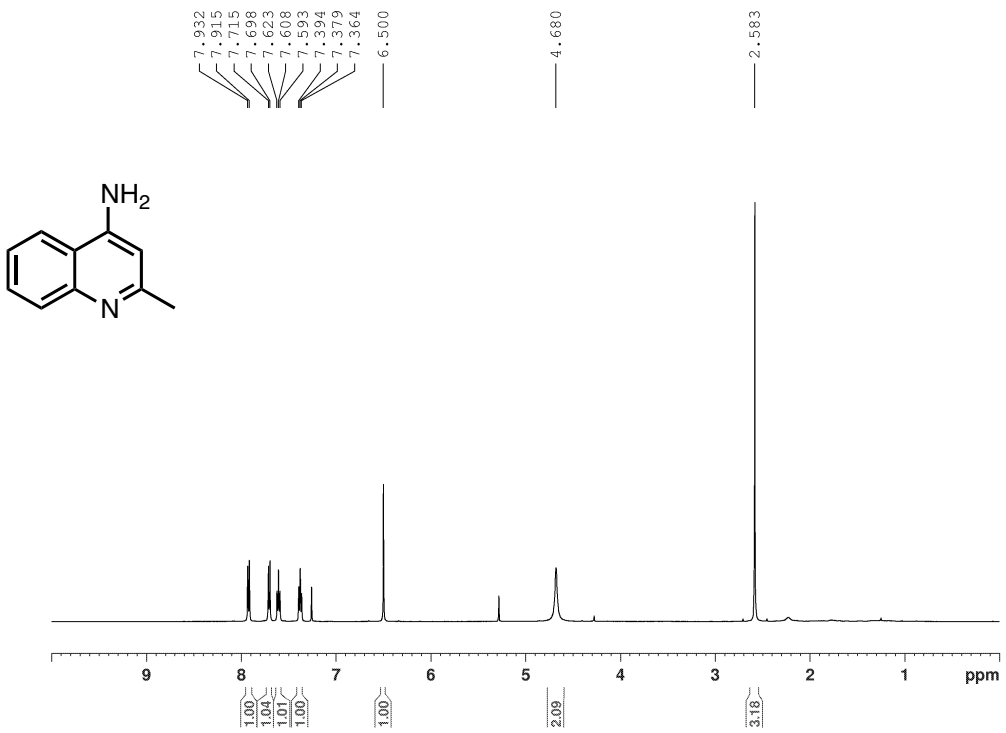

^{13}C{^{1}H} NMR Spectrum of 4-amino-2-methylquinoline, **3-4** ($CDCl_3$, 125.8 MHz)

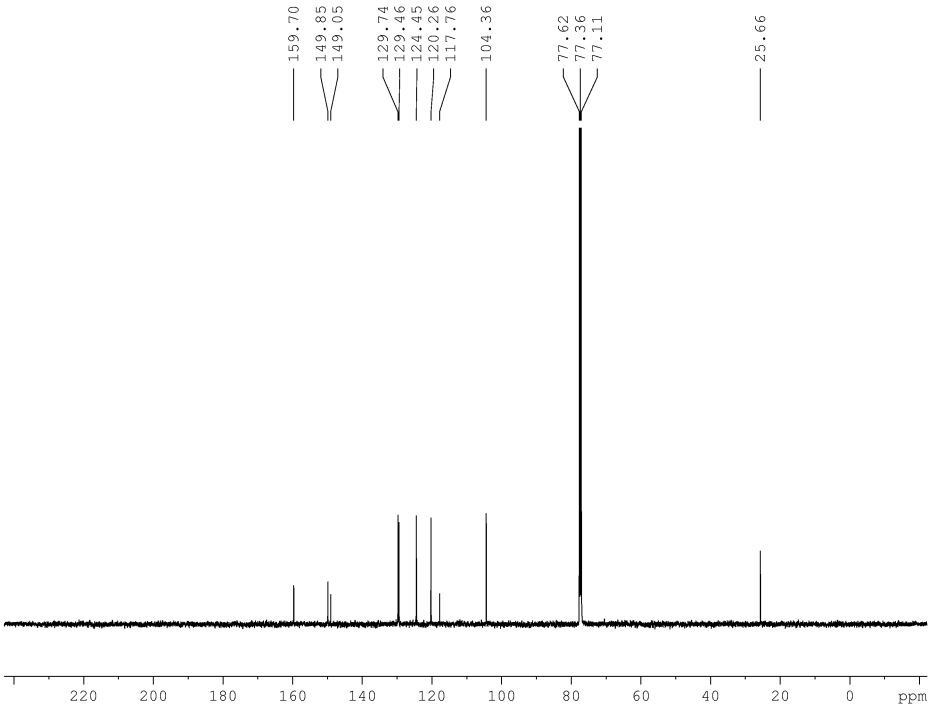

^{1}H NMR Spectrum of 7-amino-2-methylquinoline, **3-5** ($CDCl_3$, 500.1 MHz)

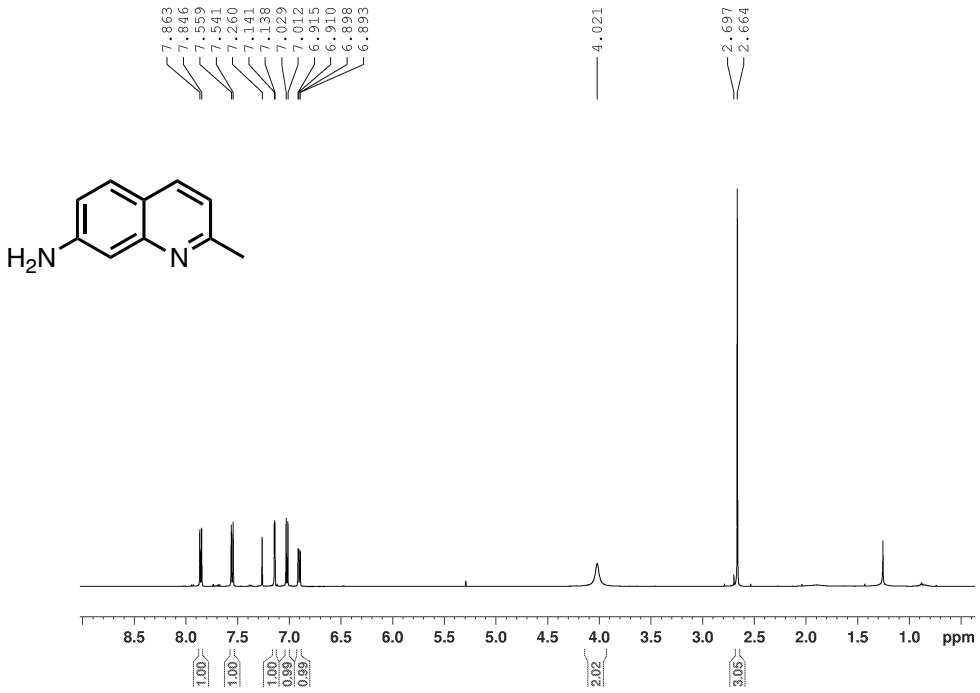

^{13}C{^{1}H} NMR Spectrum of 7-amino-2-methylquinoline, **3-5** ($CDCl_3$, 125.8 MHz)

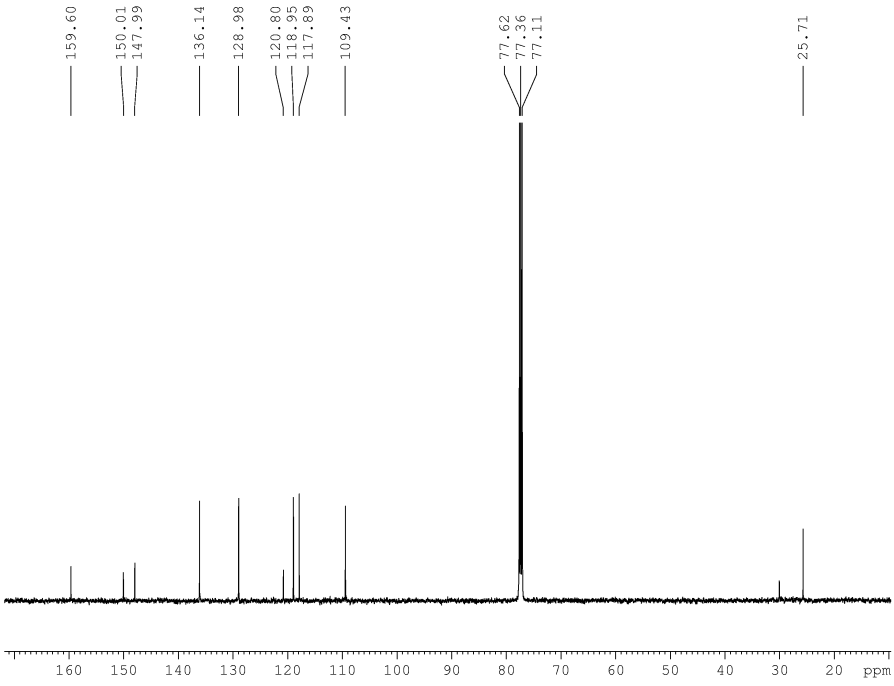

^{1}H NMR Spectrum of 4-aminoisoquinoline, **3-6** ($CDCl_3$, 500.1 MHz)

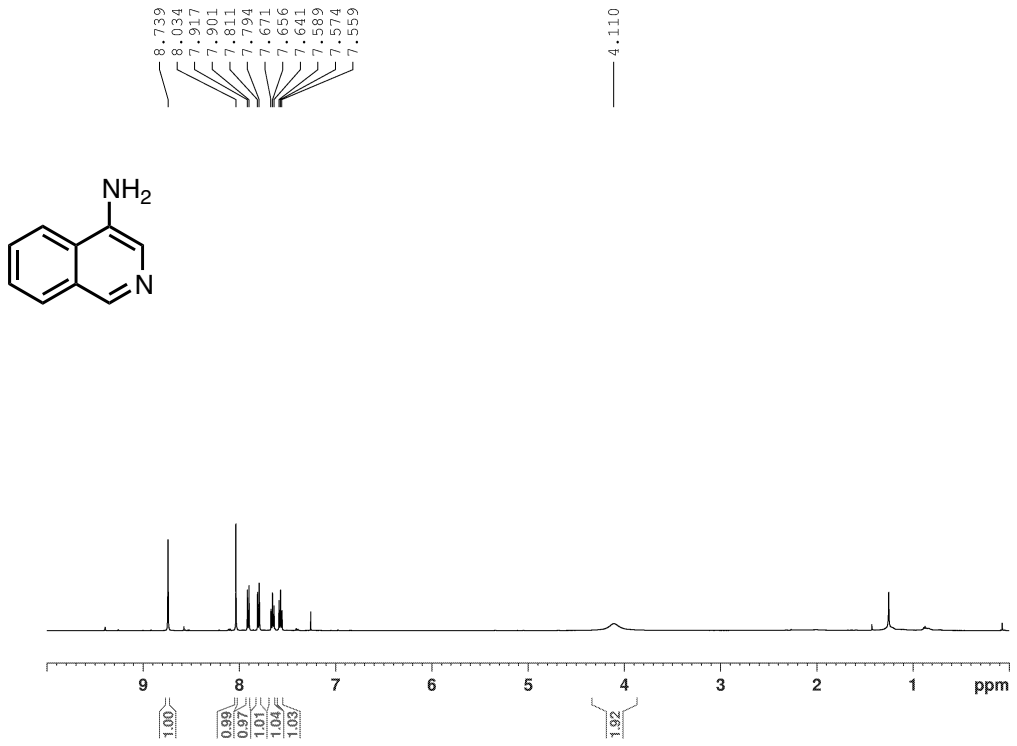

^{13}C{^{1}H} NMR Spectrum of 4-aminoisoquinoline, **3-6** ($CDCl_3$, 125.8 MHz)

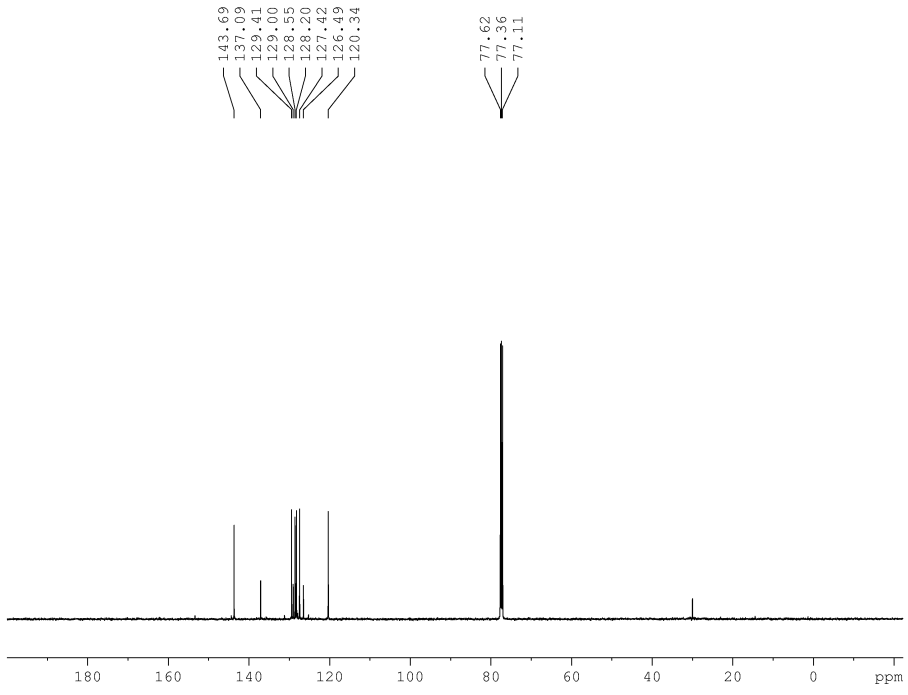

^{1}H NMR Spectrum of 3-aminoquinoline, **3-7** ($CDCl_3$, 500.1 MHz)

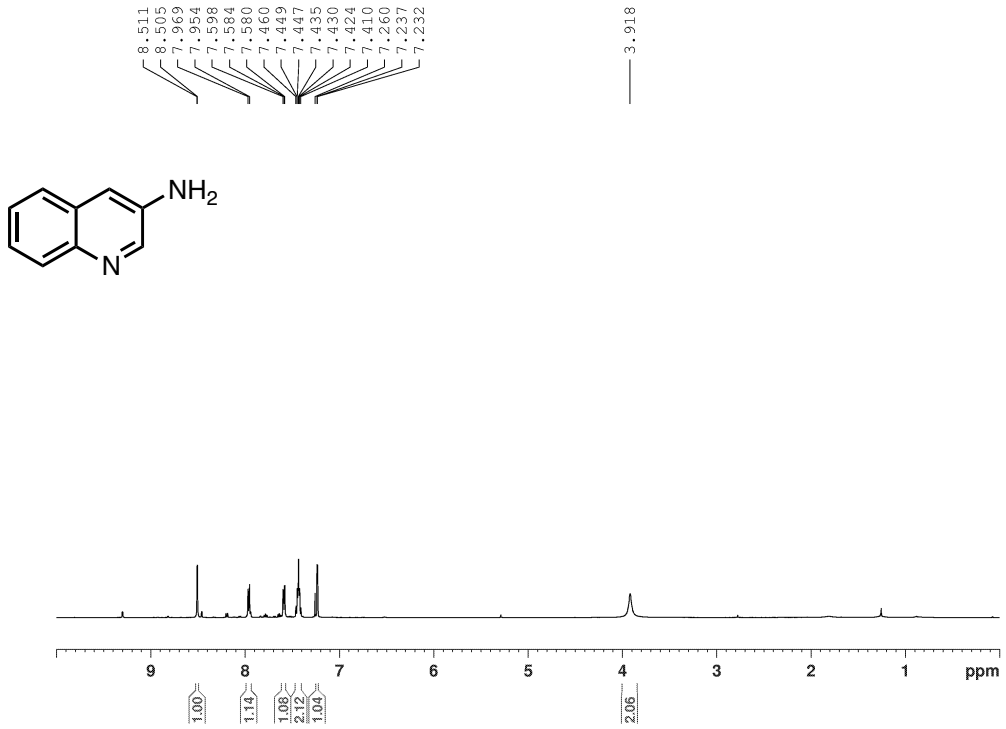

^{13}C{^{1}H} NMR Spectrum of 3-aminoquinoline, **3-7** ($CDCl_3$, 125.8 MHz)

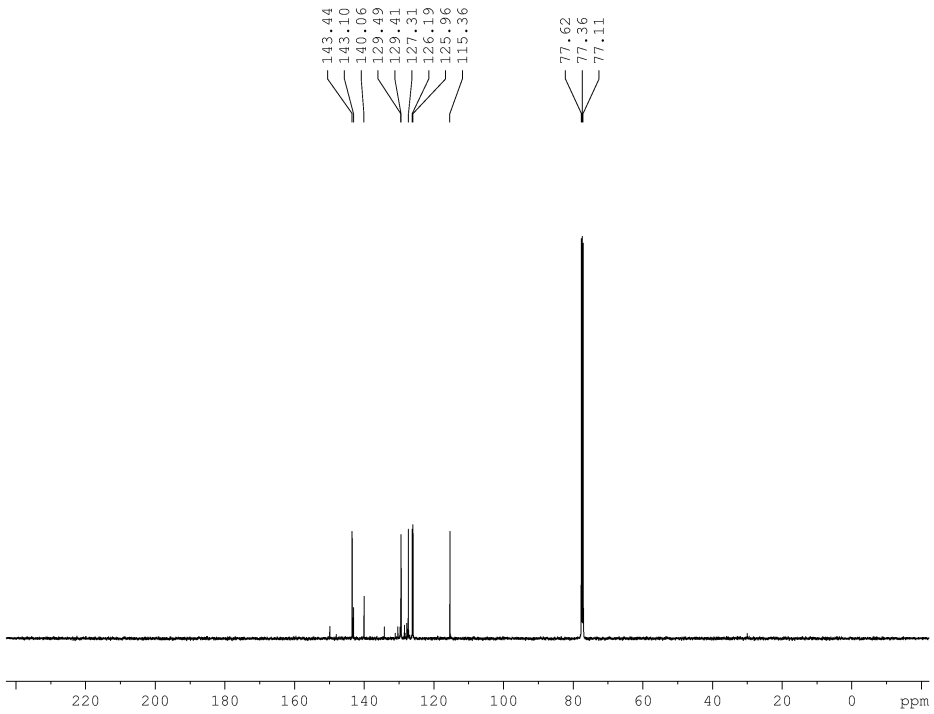

^{1}H NMR Spectrum of 6-aminoquinoline, **3-8** ($CDCl_3$, 500.1 MHz)

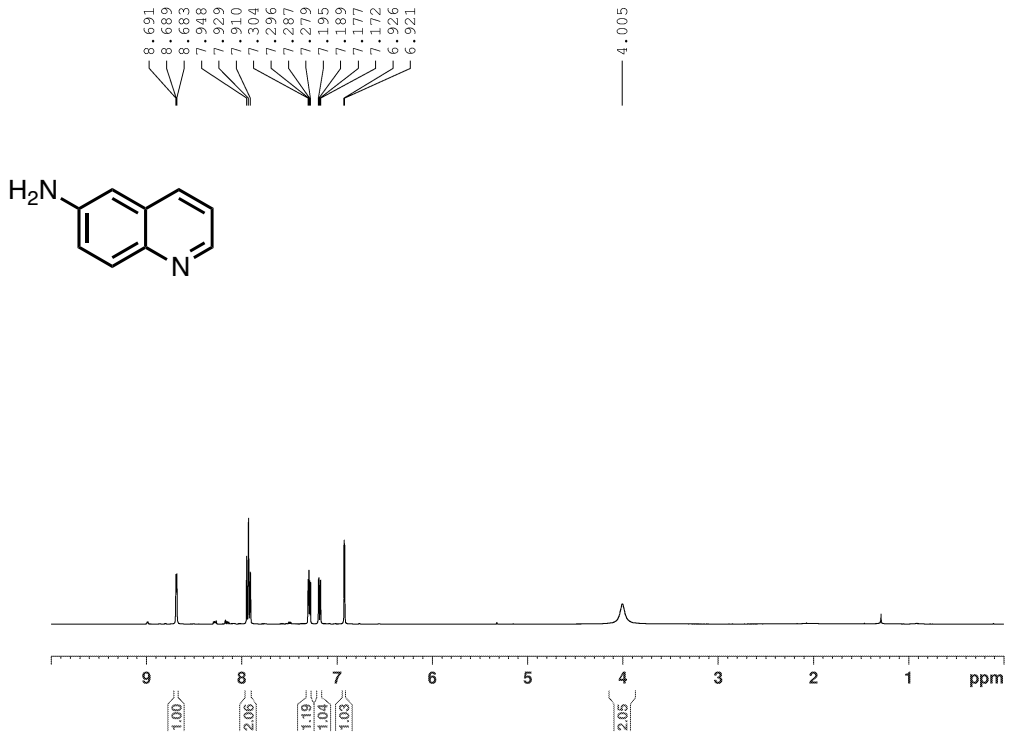

^{13}C{^{1}H} NMR Spectrum of 6-aminoquinoline, **3-8** ($CDCl_3$, 125.8 MHz)

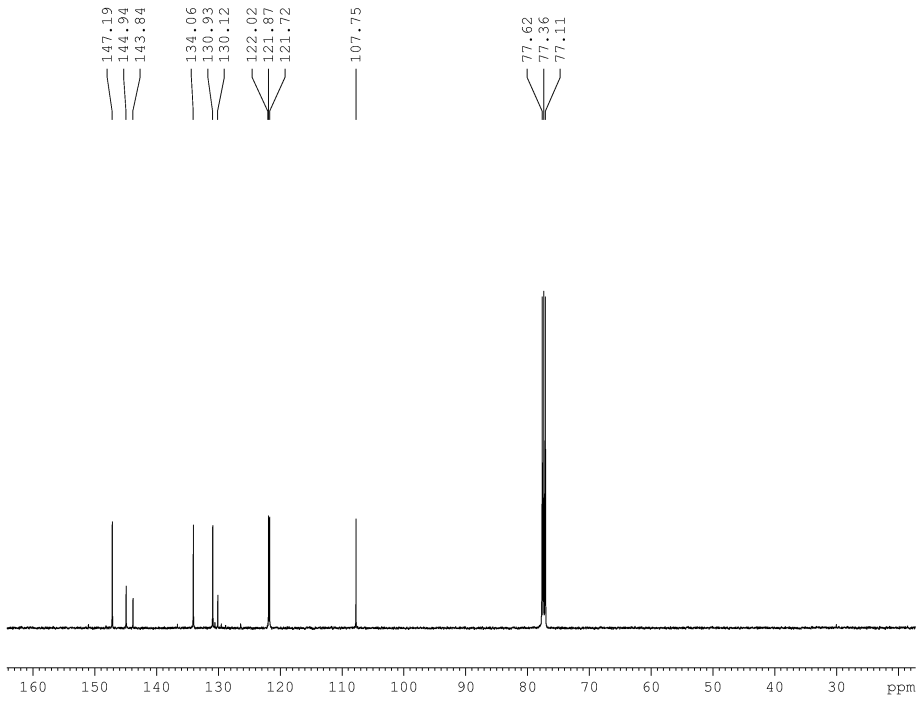

^{1}H NMR Spectrum of 2-aminoquinoxaline, **3-9** ($CDCl_3$, 500.1 MHz)

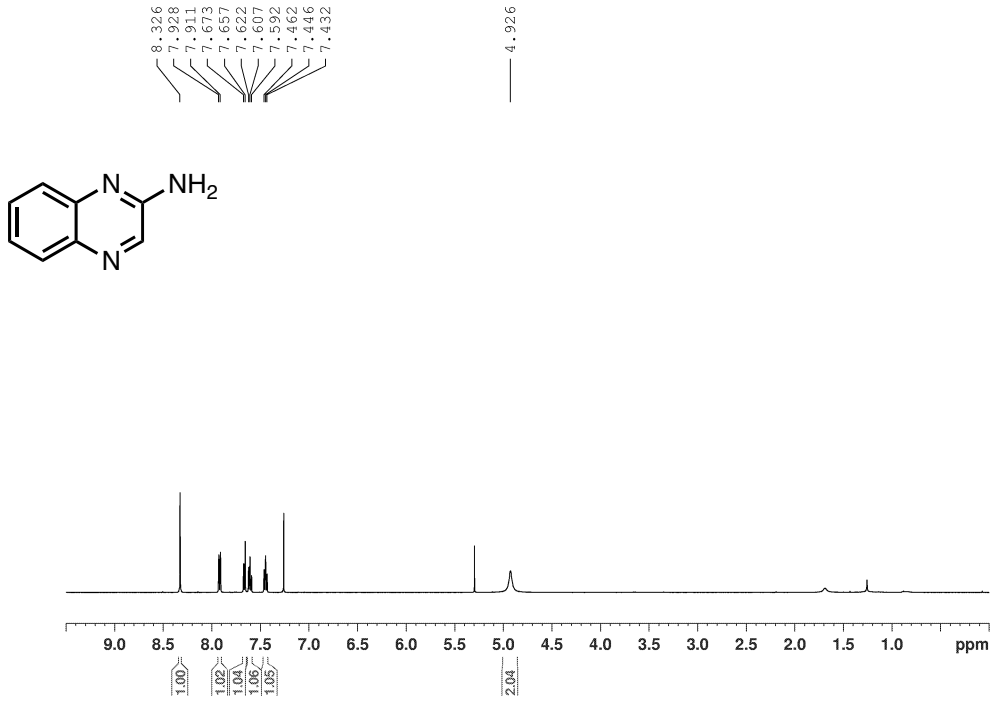

^{13}C{^{1}H} NMR Spectrum of 2-aminoquinoxaline, **3-9** ($CDCl_3$, 125.8 MHz)

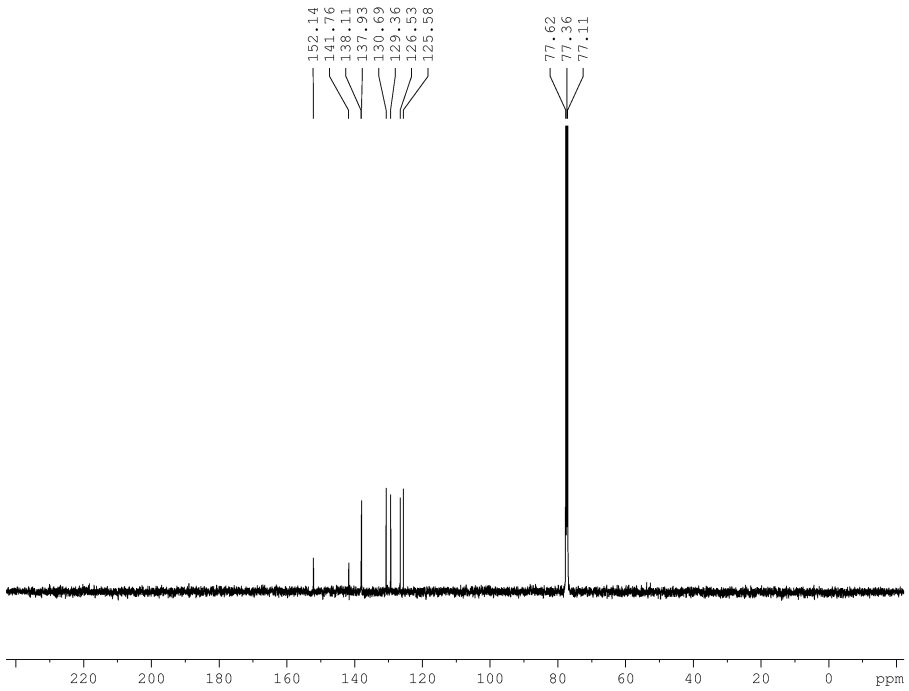

^{1}H NMR Spectrum of 6-aminoquinoxaline, **3-10** ($CDCl_3$, 500.1 MHz)

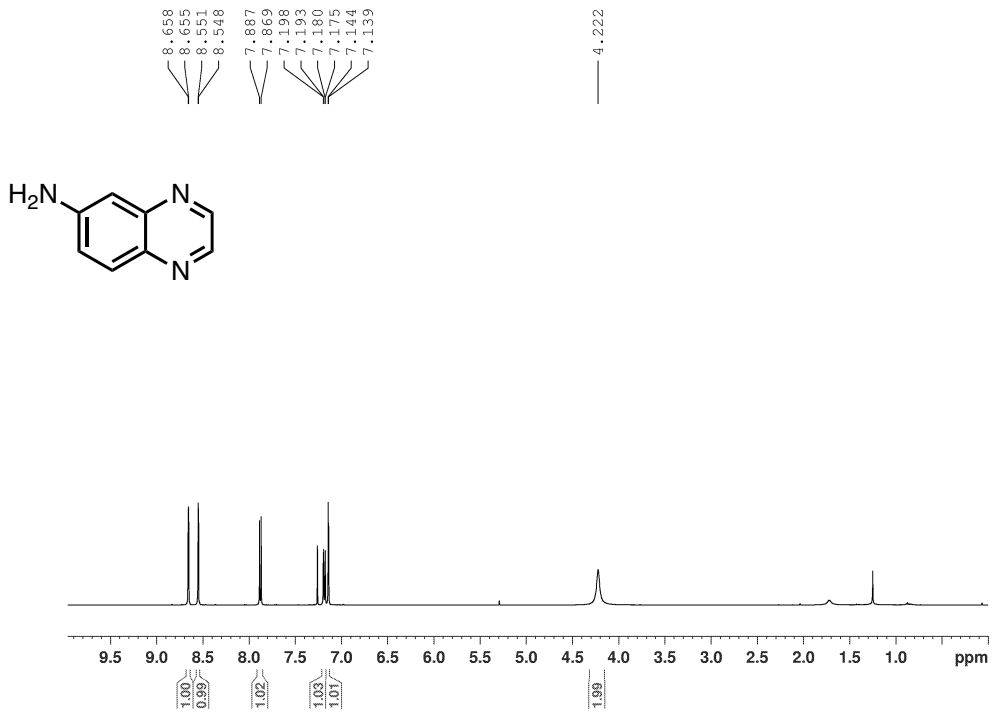

^{13}C{^{1}H} NMR Spectrum of 6-aminoquinoxaline, **3-10** ($CDCl_3$, 125.8 MHz)

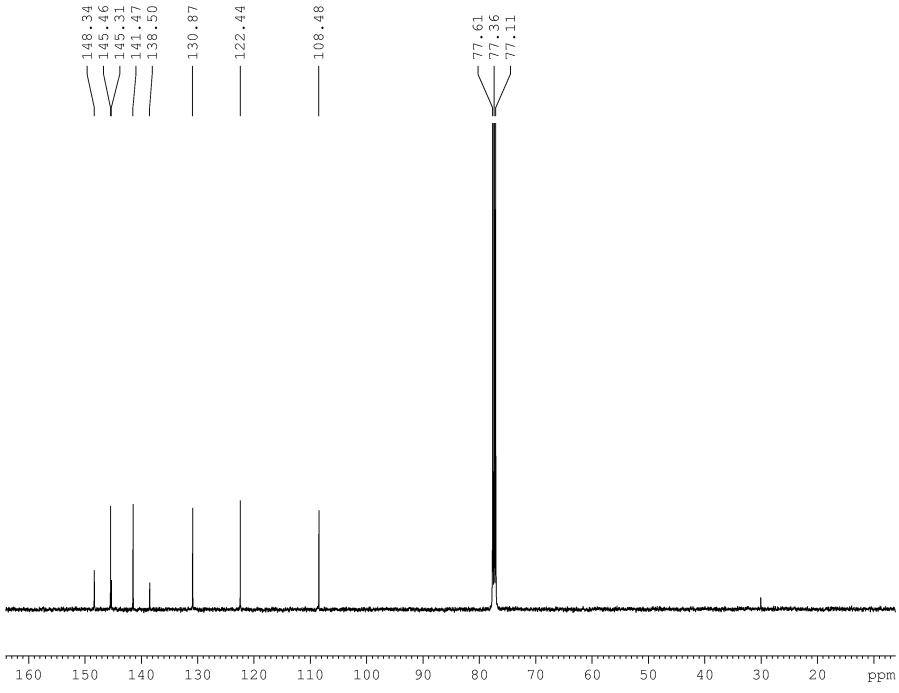

^{1}H NMR Spectrum of 5-aminobenzo[*b*]thiophene, **3-11** ($CDCl_3$, 500.1 MHz)

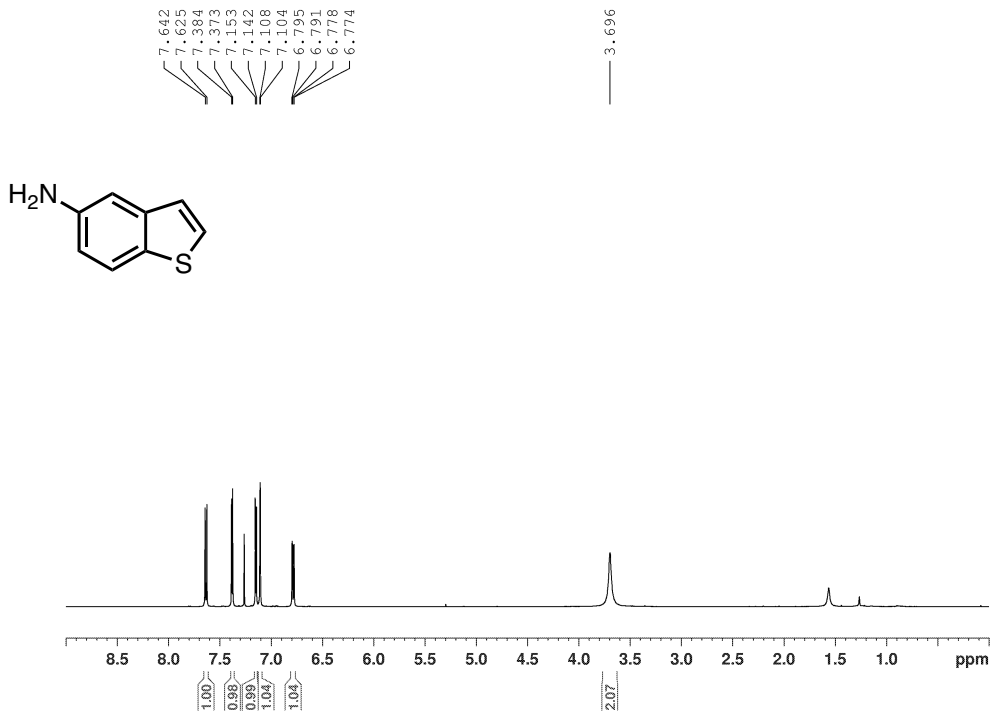

^{13}C{^{1}H} NMR Spectrum of 5-aminobenzo[*b*]thiophene, **3-11** ($CDCl_3$, 125.8 MHz)

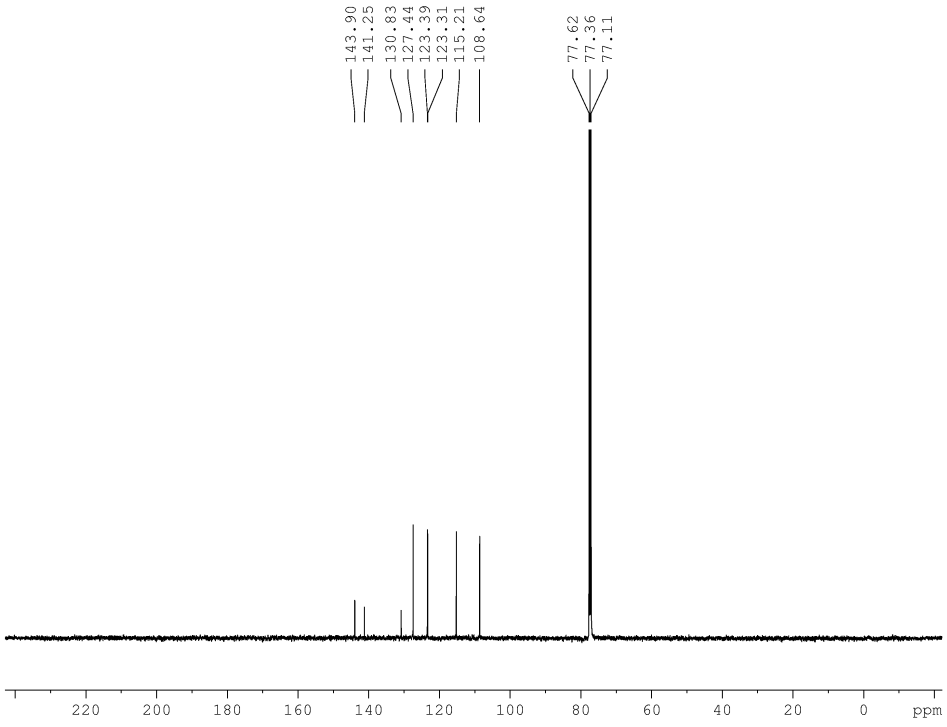

^{1}H NMR Spectrum of 5-amino-2-methylbenzothiazole, **3-12** ($CDCl_3$, 500.1 Mhz)

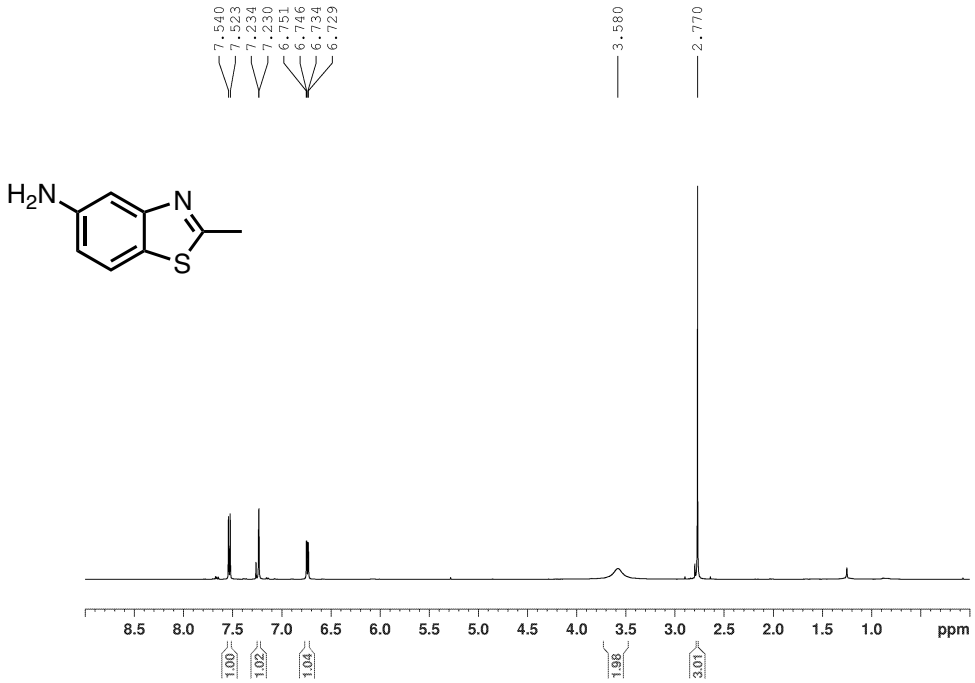

^{13}C{^{1}H} NMR Spectrum of 5-amino-2-methylbenzothiazole, **3-12** ($CDCl_3$, 125.8 MHz)

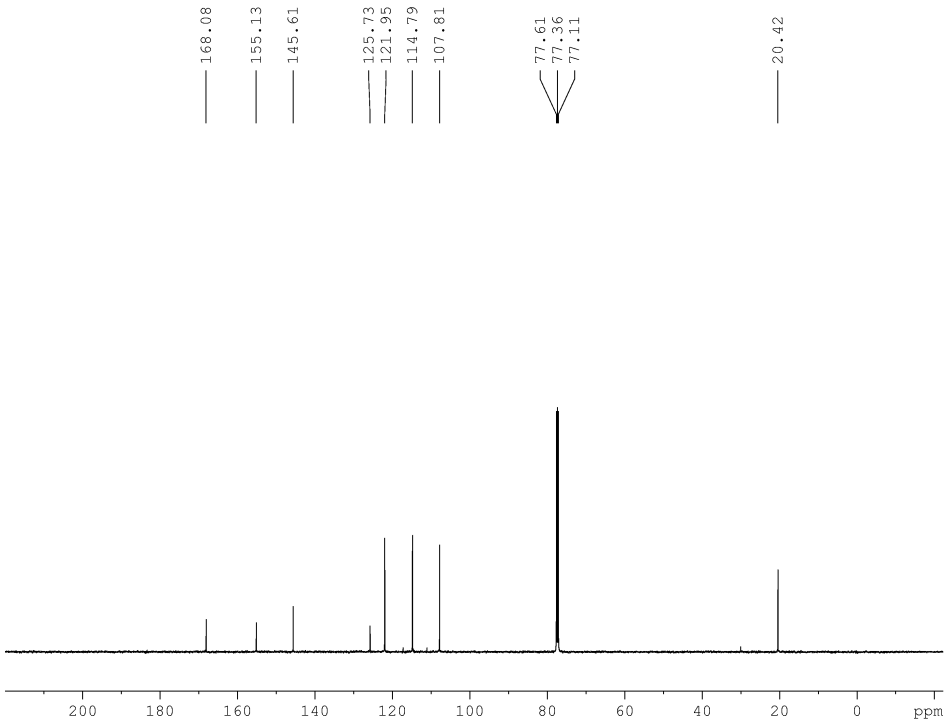

^{1}H NMR Spectrum of 2-amino-4,6-dimethoxypyrimidine, **3-13** ($CDCl_3$, 500.1 MHz)

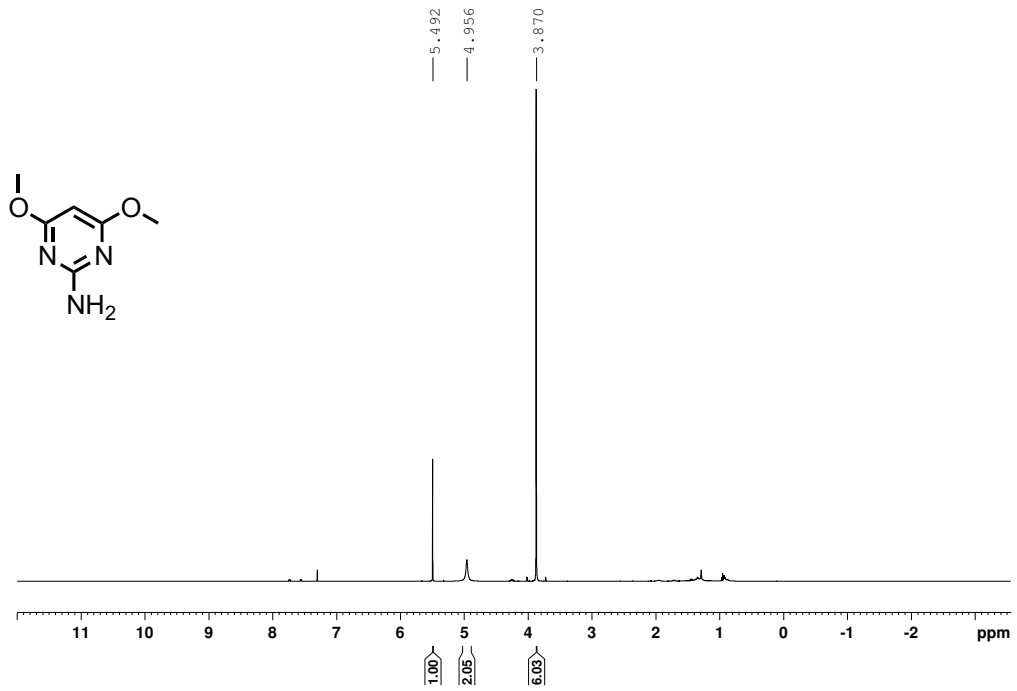

^{13}C{^{1}H} NMR Spectrum of 2-amino-4,6-dimethoxypyrimidine, **3-13** ($CDCl_3$, 125.8 MHz)

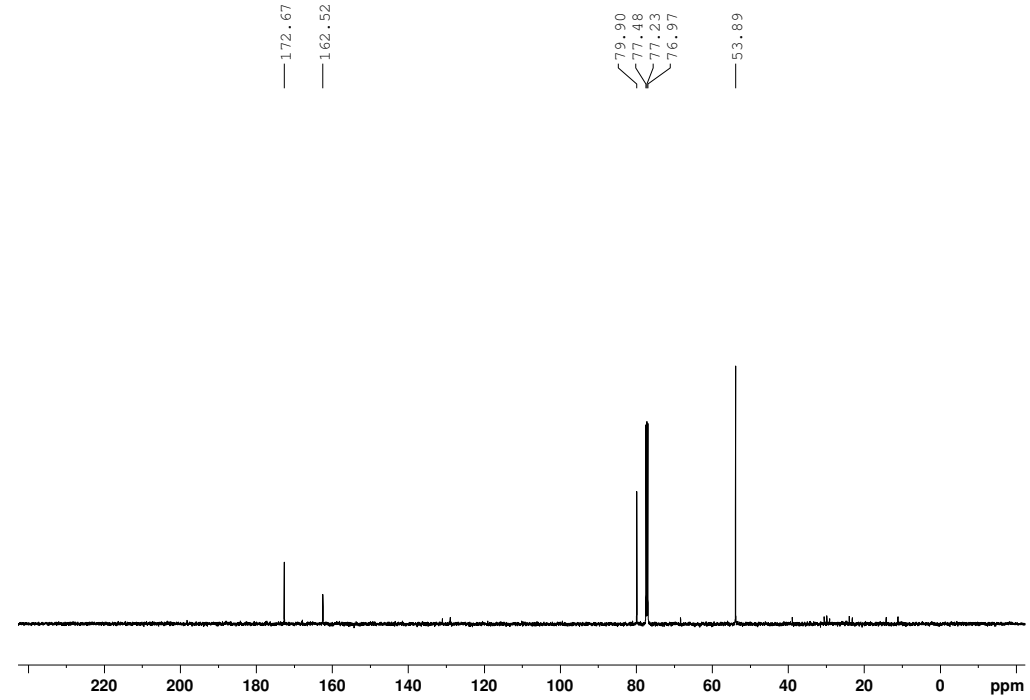

^{1}H NMR Spectrum of 2-amino-6,7-dimethoxyquinazoline, **3-14** ($CDCl_3$, 500.1 MHz)

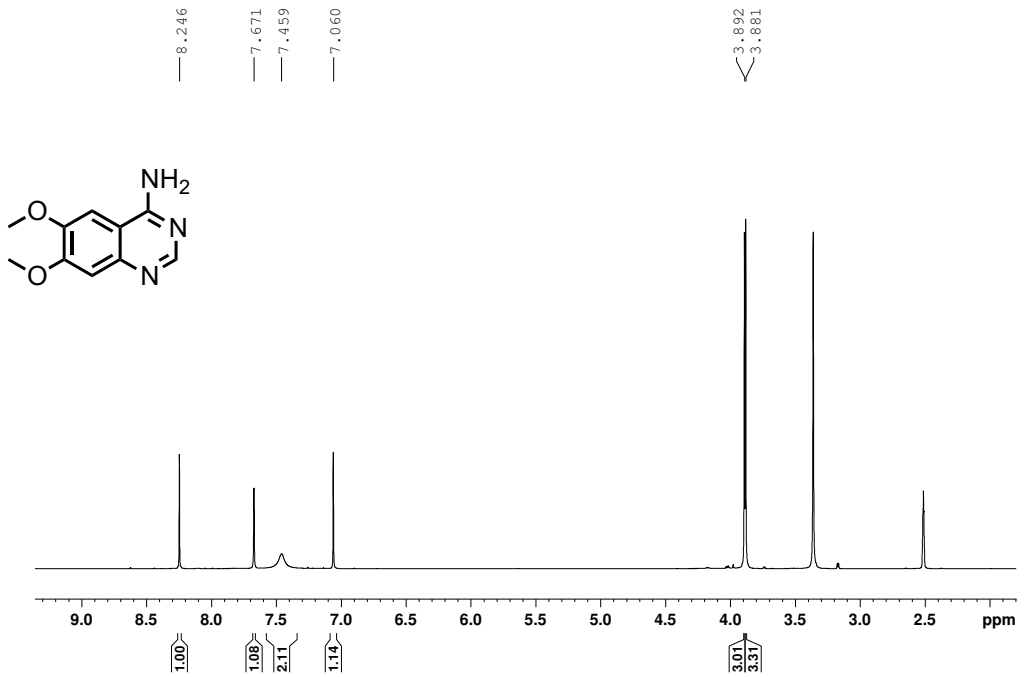

^{13}C{^{1}H} NMR Spectrum of 2-amino-6,7-dimethoxyquinazoline, **3-14** ($CDCl_3$, 125.8 MHz)

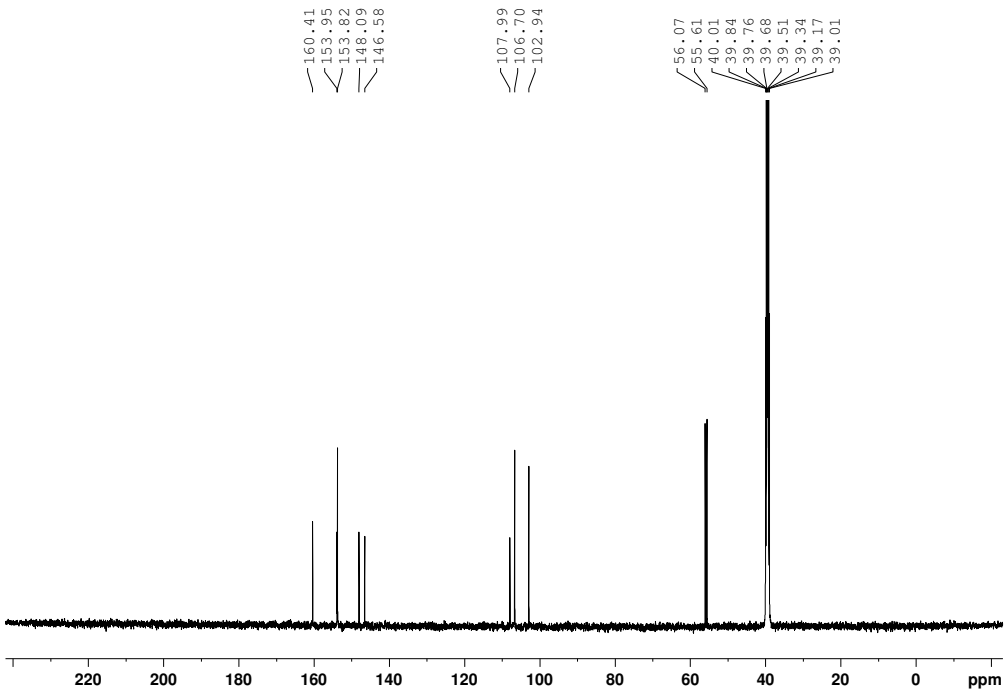

^{1}H NMR Spectrum of 9-amino-1,2,3,4-tetrahydroacridine, **3-15** ($CDCl_3$, 500.1 MHz)

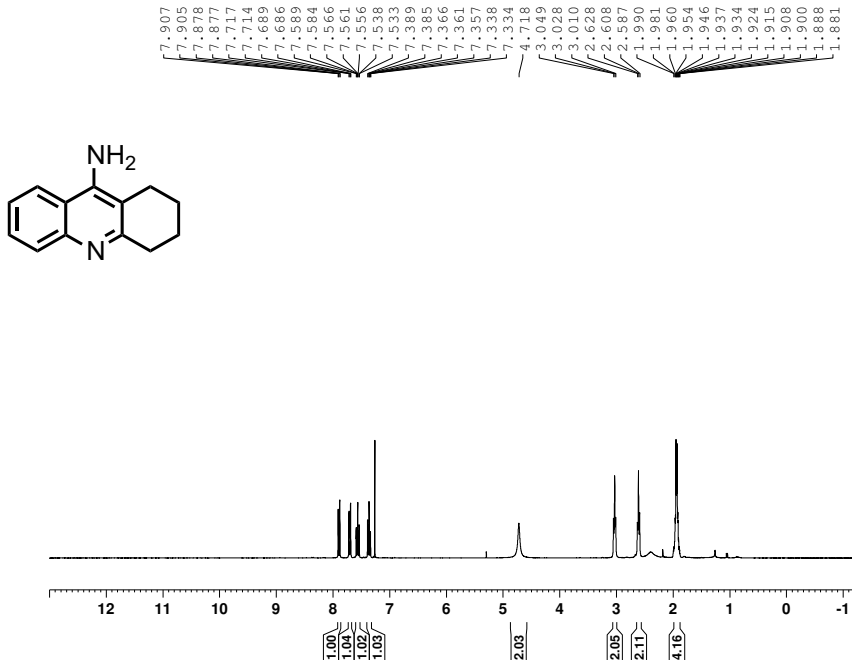

^{13}C{^{1}H} NMR Spectrum of 9-amino-1,2,3,4-tetrahydroacridine, **3-15** ($CDCl_3$, 125.8 MHz)

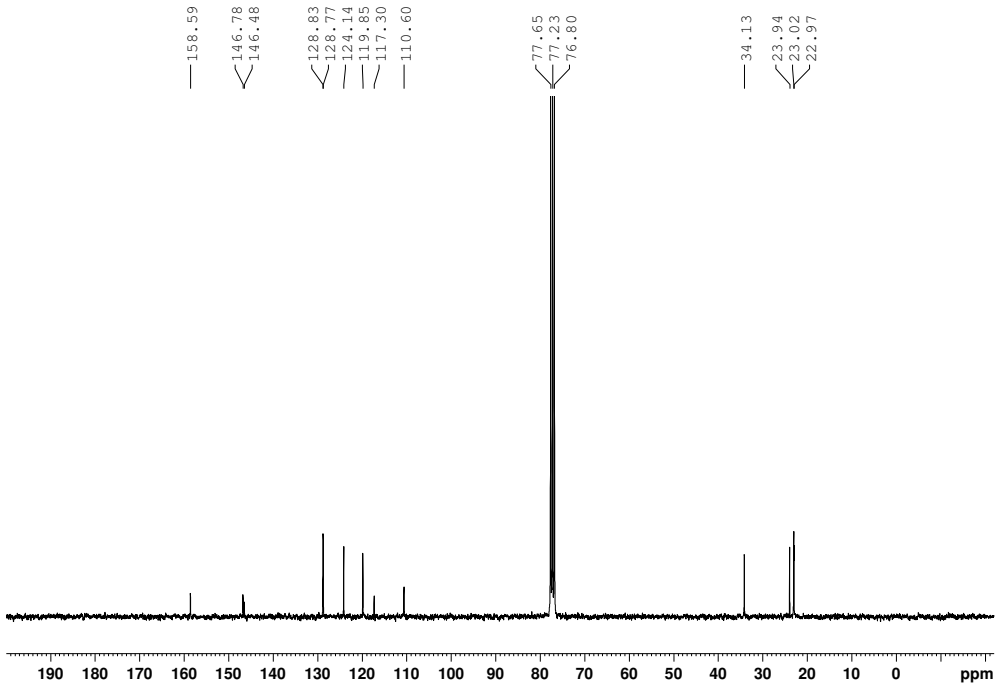

^{1}H NMR Spectrum of 3-aminoestrone, **3-16** ($CDCl_3$, 500.1 MHz)

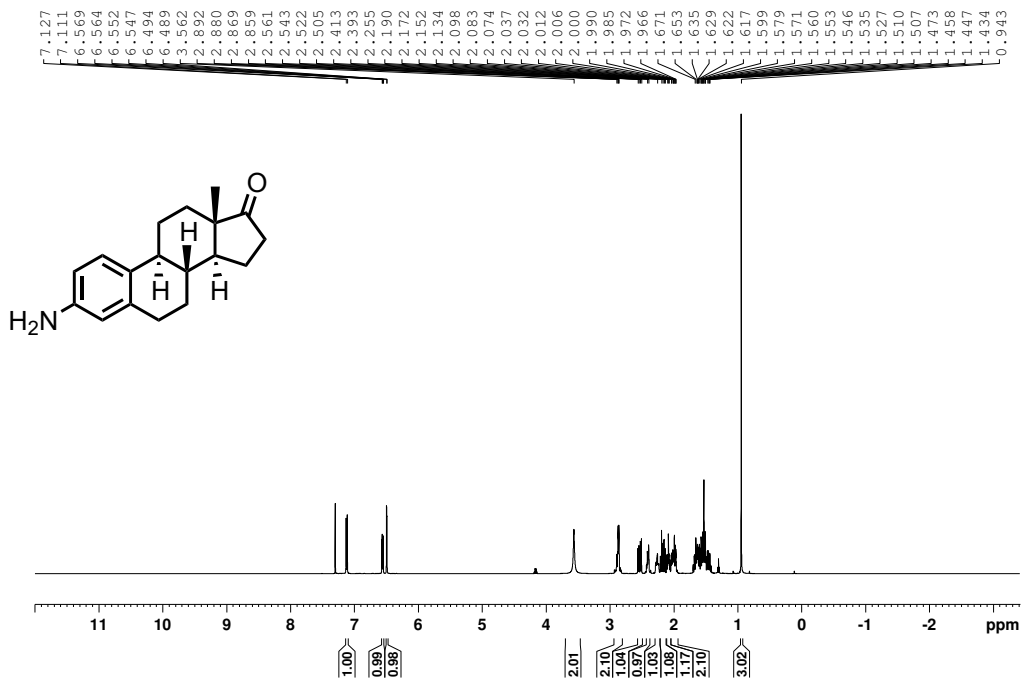

^{13}C{^{1}H} NMR Spectrum of 3-aminoestrone, **3-16** ($CDCl_3$, 125.8 MHz)

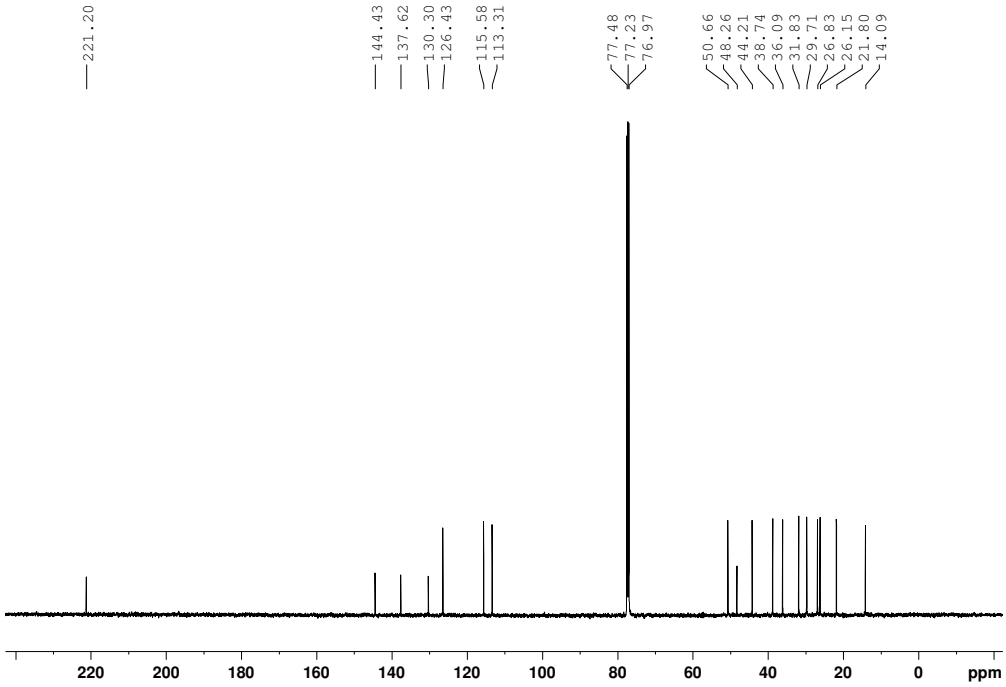

Appendix 3. Exploring the Influence of Phosphine Ligation on the Gold-Catalyzed Hydrohydrazination of Terminal Alkynes at Room Temperature

^{1}H NMR Spectrum of Complex **4-C1** ($CDCl_3$, 500.1 MHz)

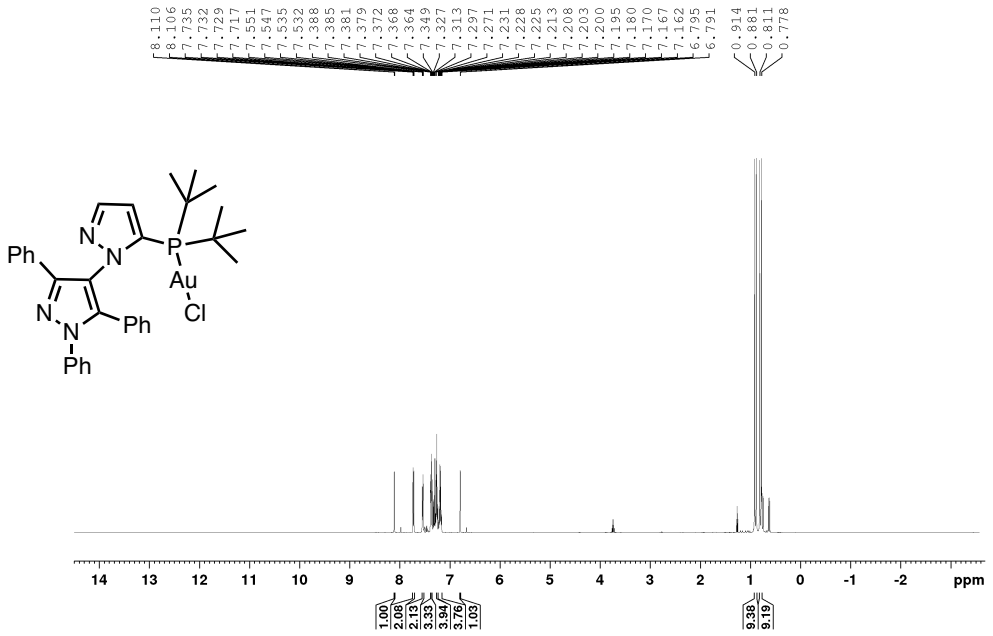

^{13}C{^{1}H} NMR Spectrum of Complex **4-C1** ($CDCl_3$, 125.8 MHz)

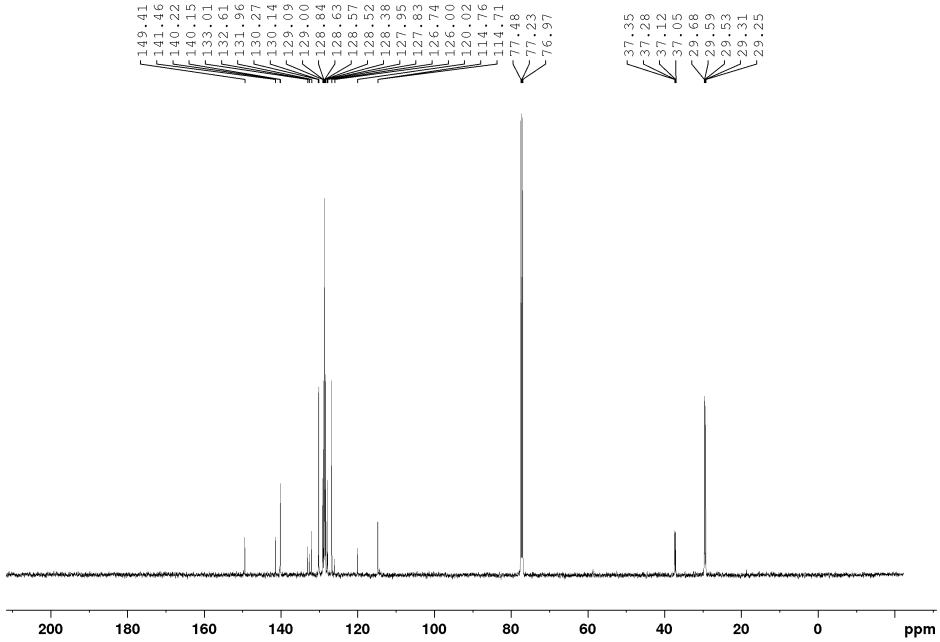

$^{31}P\{^{1}H\}$ NMR Spectrum of Complex **4-C5** ($CDCl_3$, 202 MHz)

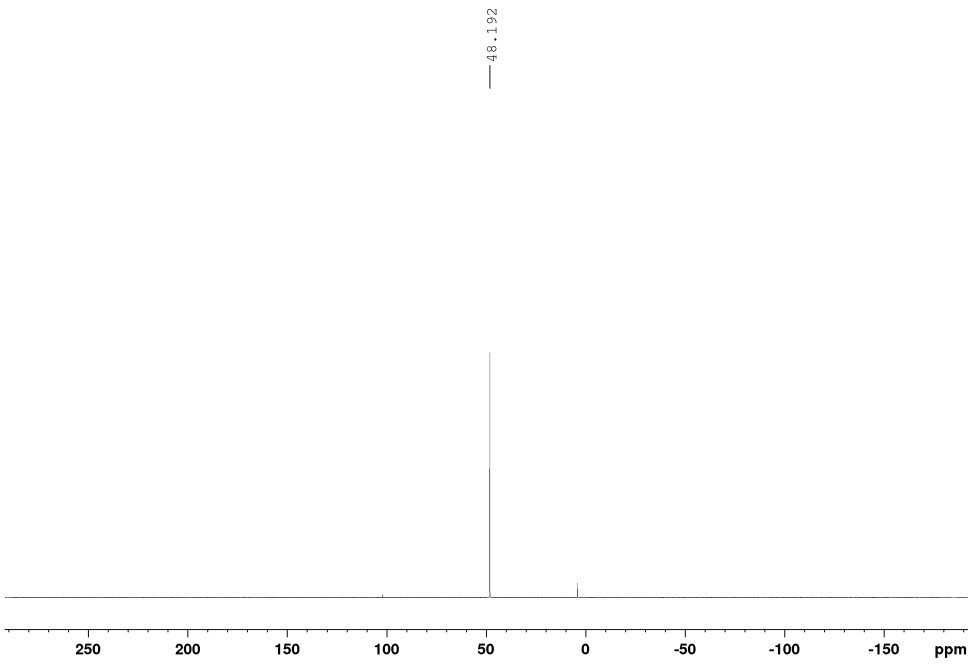

^{1}H NMR Spectrum of Complex **4-C5** ($CDCl_3$, 500.1 MHz)

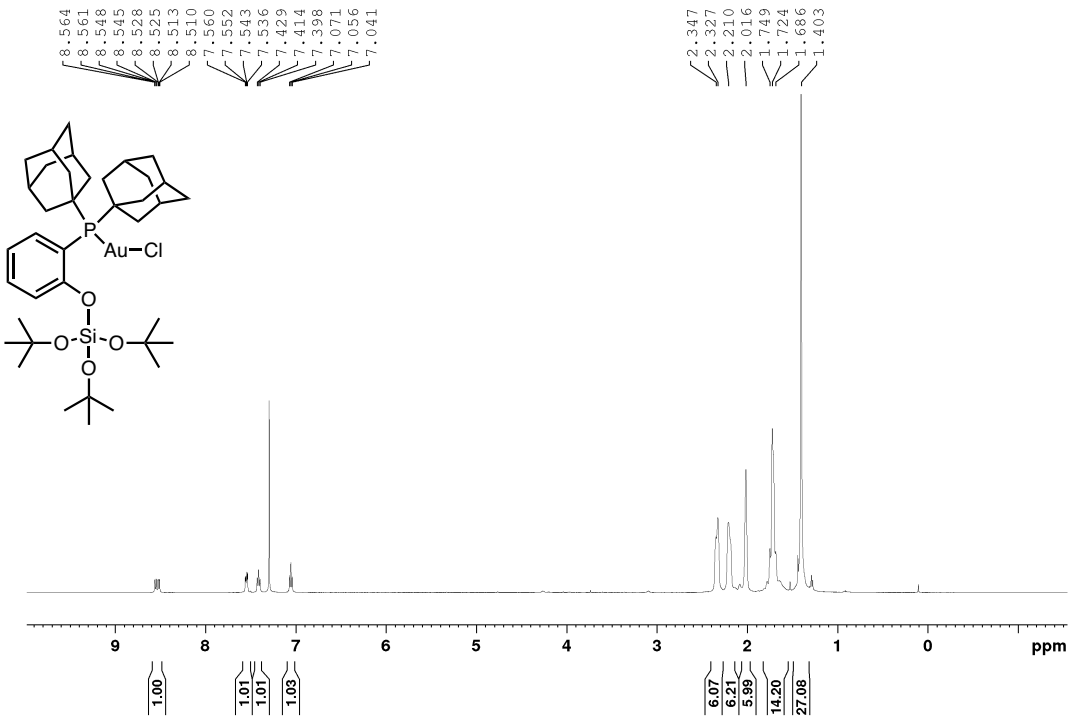

$^{13}C\{^{1}H\}$ NMR Spectrum of Complex **4-C5** ($CDCl_3$, 125.8 MHz)

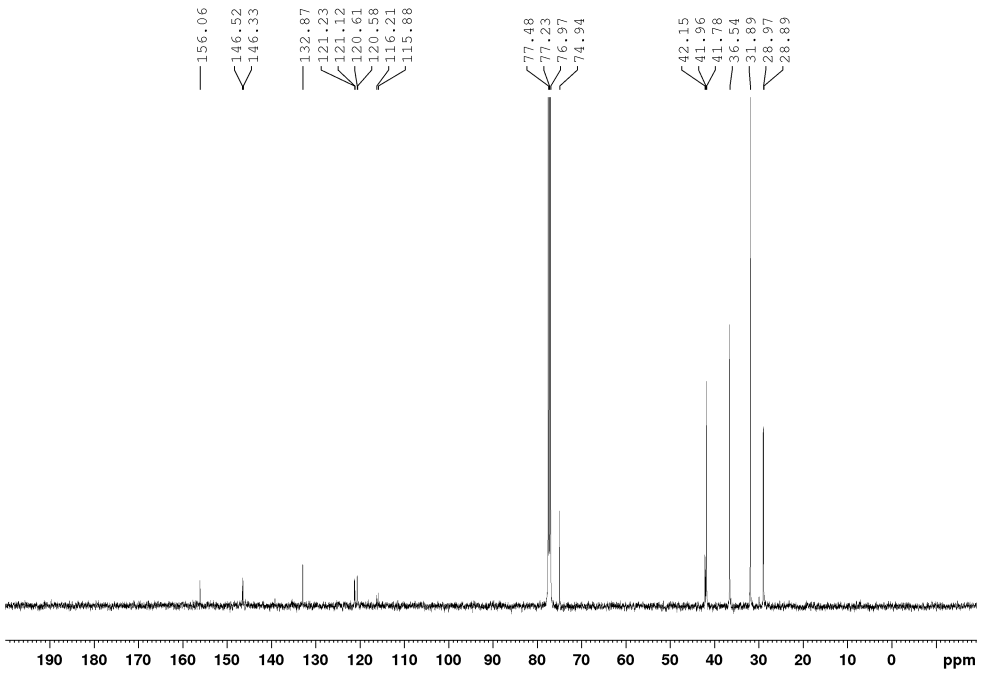

$^{31}P\{^{1}H\}$ NMR Spectrum of Complex **4-C5** ($CDCl_3$, 202 MHz)

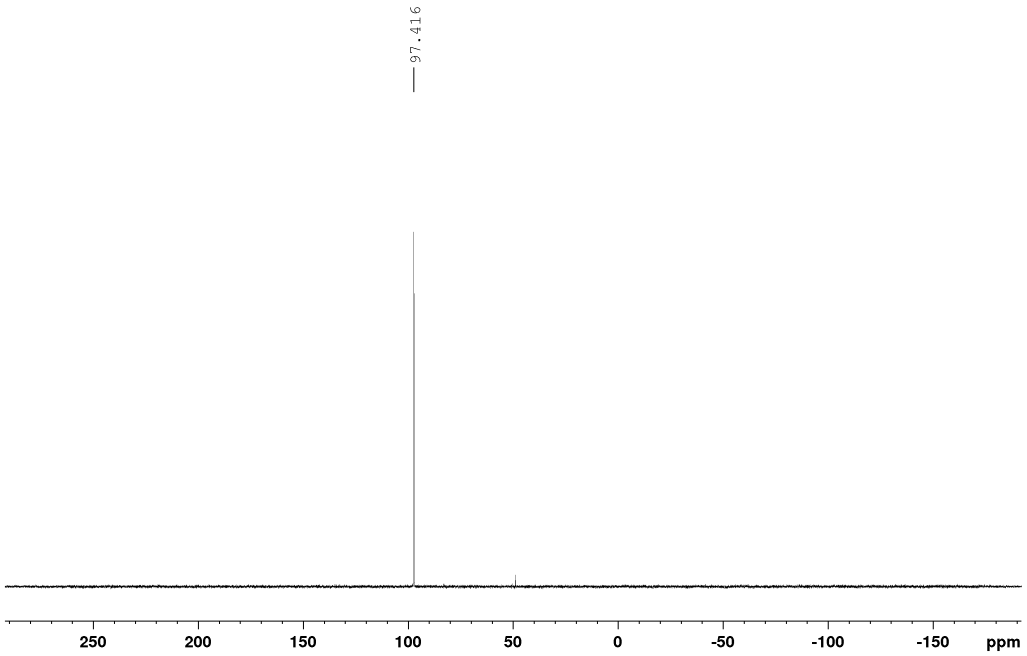

^{1}H NMR Spectrum of Complex **4-C4** ($CDCl_3$, 500.1 MHz)

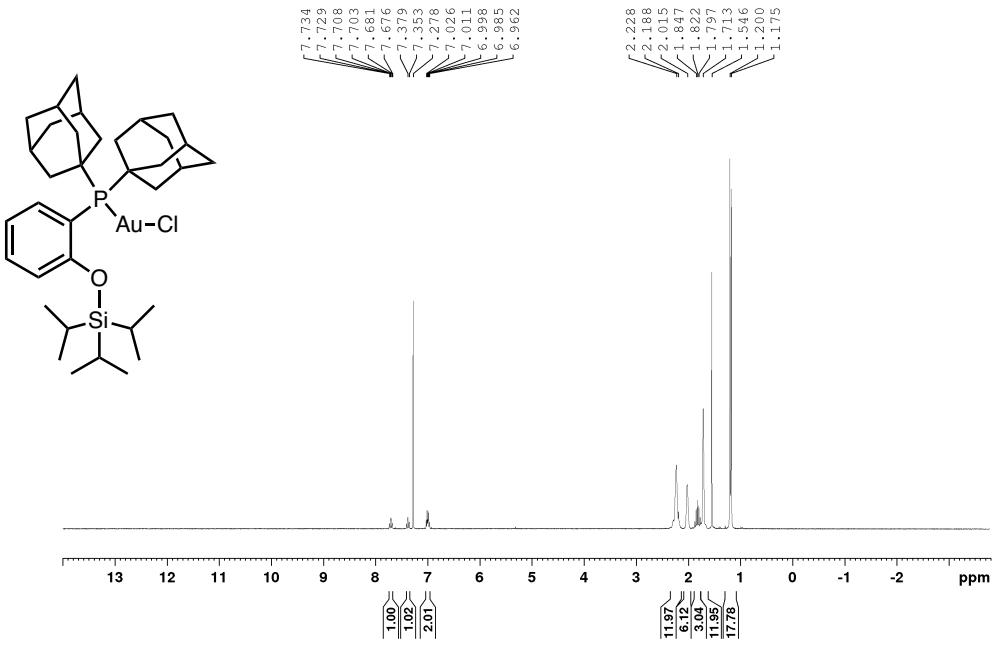

^{13}C{^{1}H} NMR Spectrum of Complex **4-C4** ($CDCl_3$, 125.8 MHz)

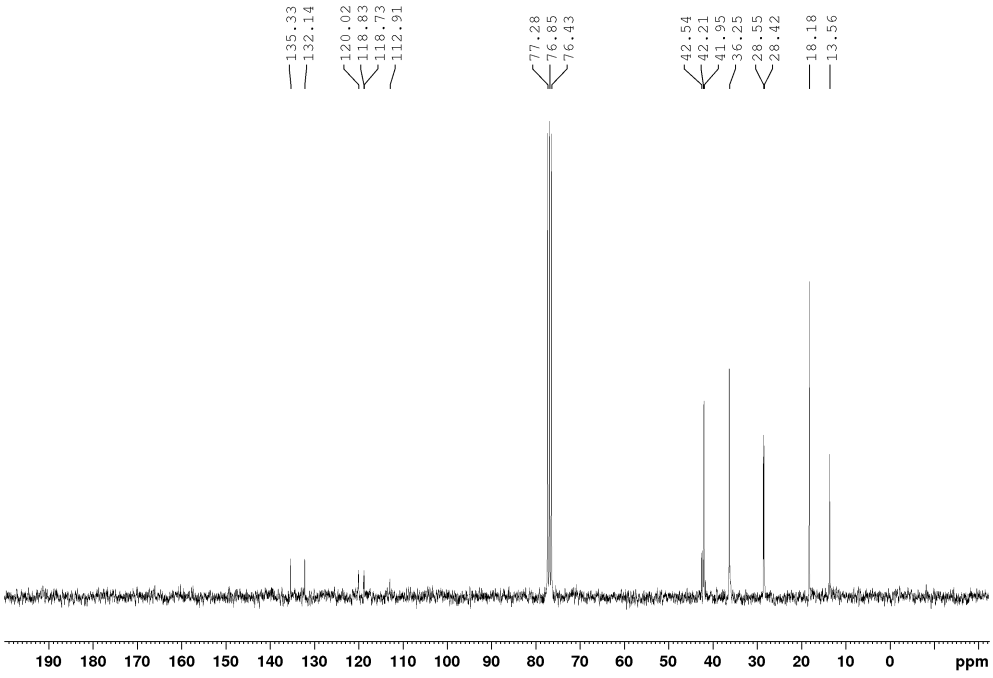

$^{31}P\{^{1}H\}$ NMR Spectrum of Complex **4-C4** ($CDCl_3$, 202 MHz)

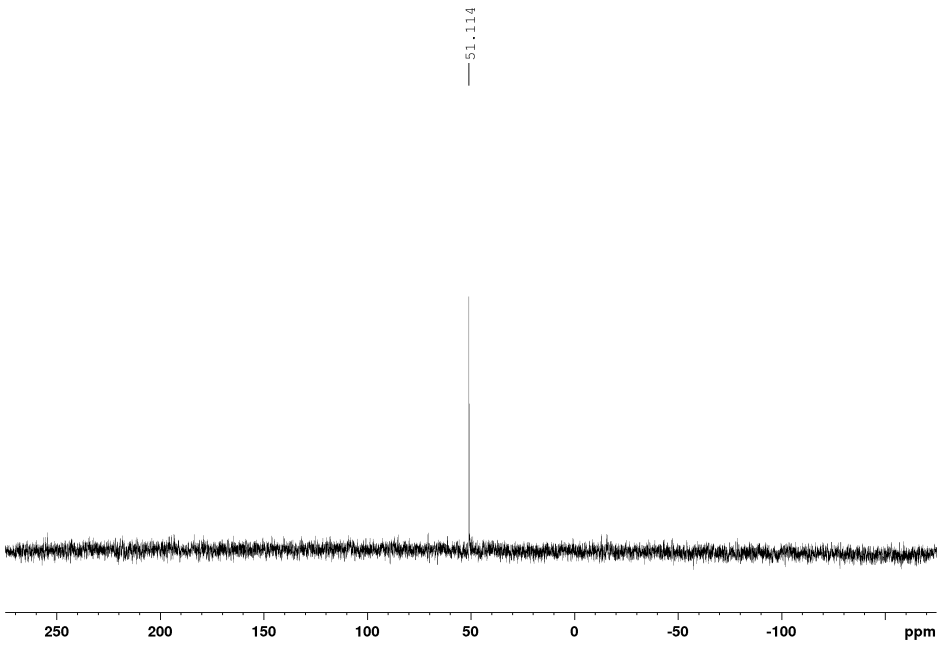

^{1}H NMR Spectrum of Complex **4-C6** ($CDCl_3$, 500.1 MHz)

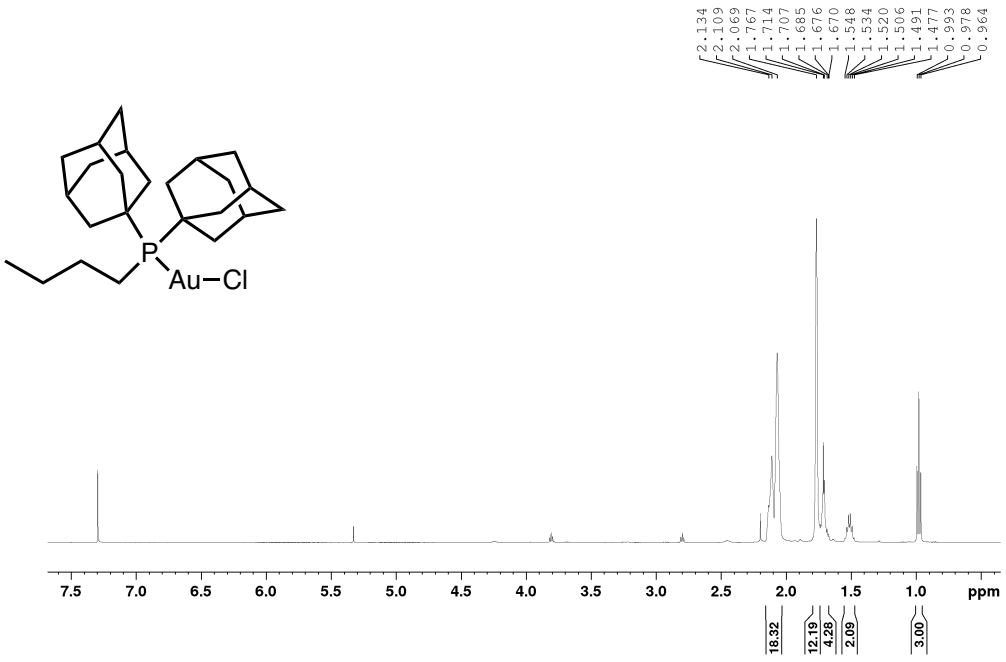

$^{13}C\{^{1}H\}$ NMR Spectrum of Complex **4-C6** ($CDCl_3$, 125.8 MHz)

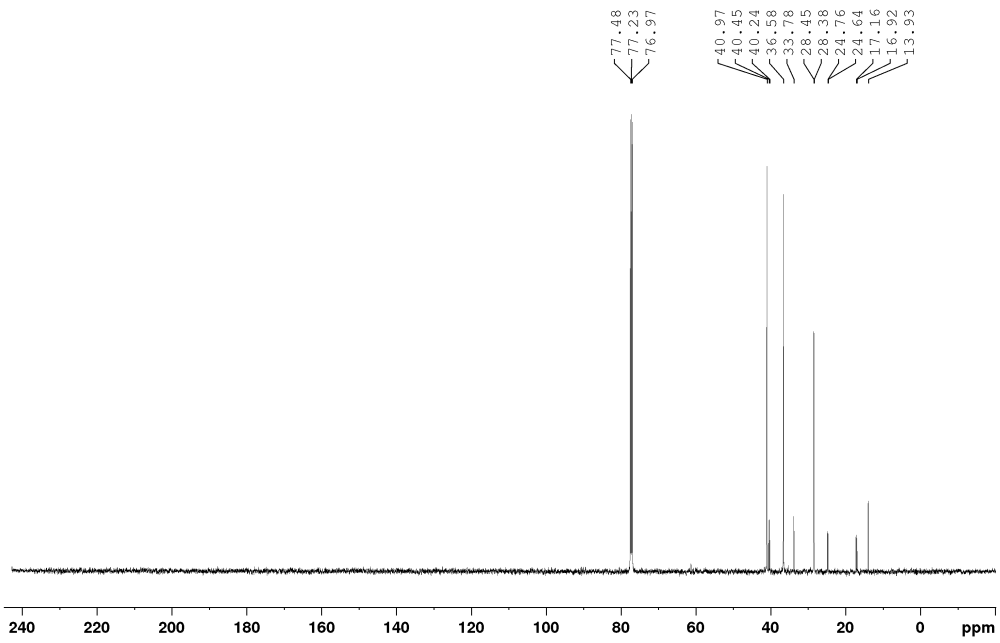

$^{31}P\{^{1}H\}$ NMR Spectrum of Complex **4-C6** ($CDCl_3$, 202 MHz)

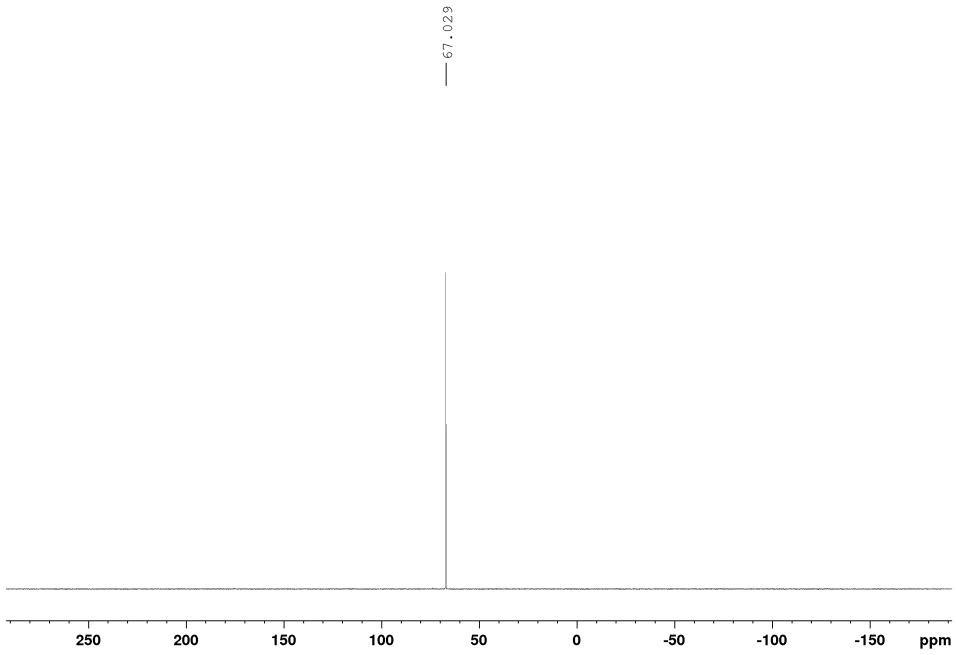

^{1}H NMR Spectrum of Complex **4-C8** ($CDCl_3$, 500.1 MHz)

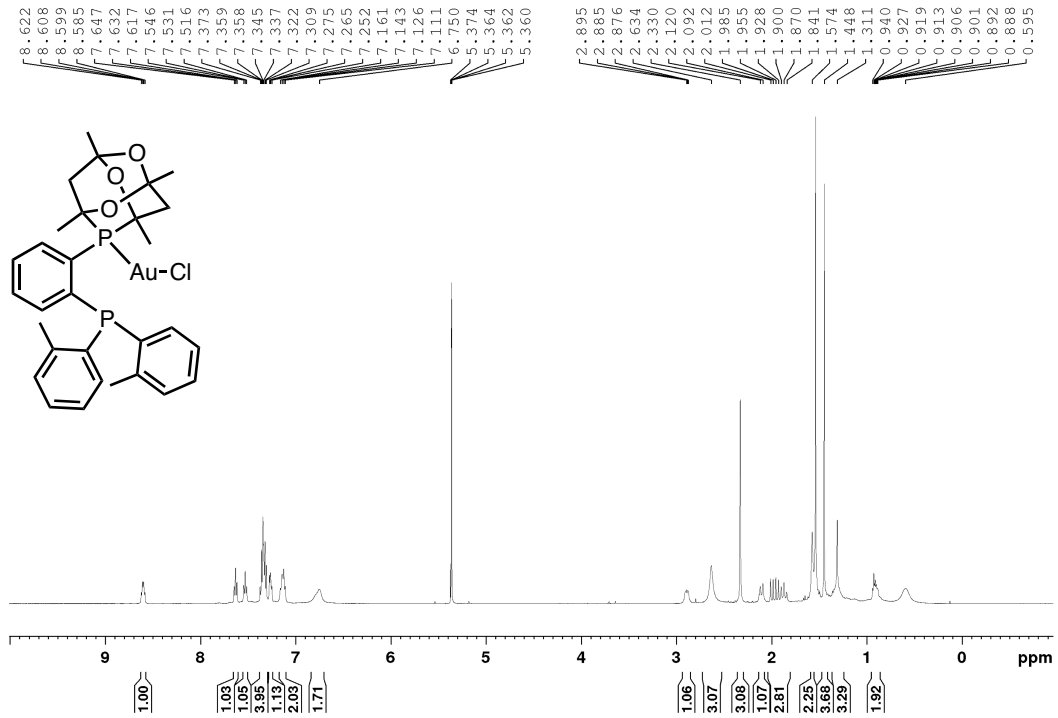

^{13}C{^{1}H} NMR Spectrum of Complex **4-C8** ($CDCl_3$, 125.8 MHz)

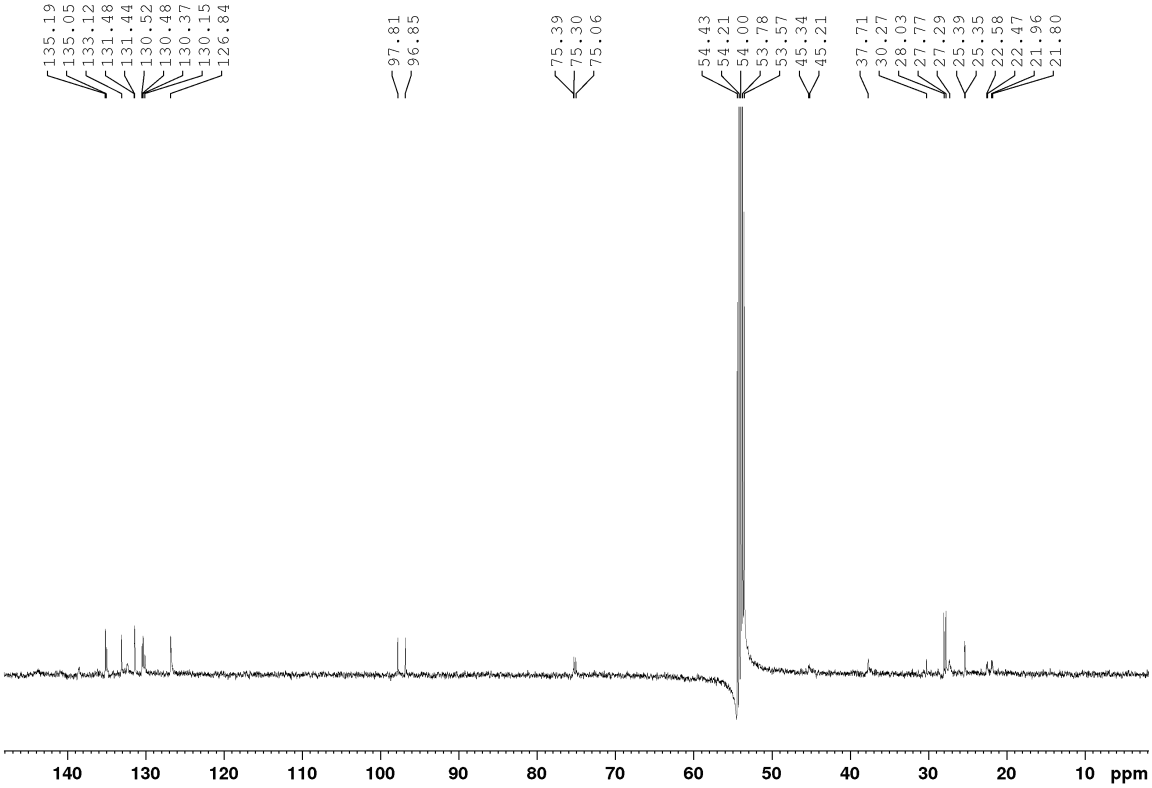

$^{31}P\{^{1}H\}$ NMR Spectrum of Complex **4-C8** ($CDCl_3$, 202 MHz)

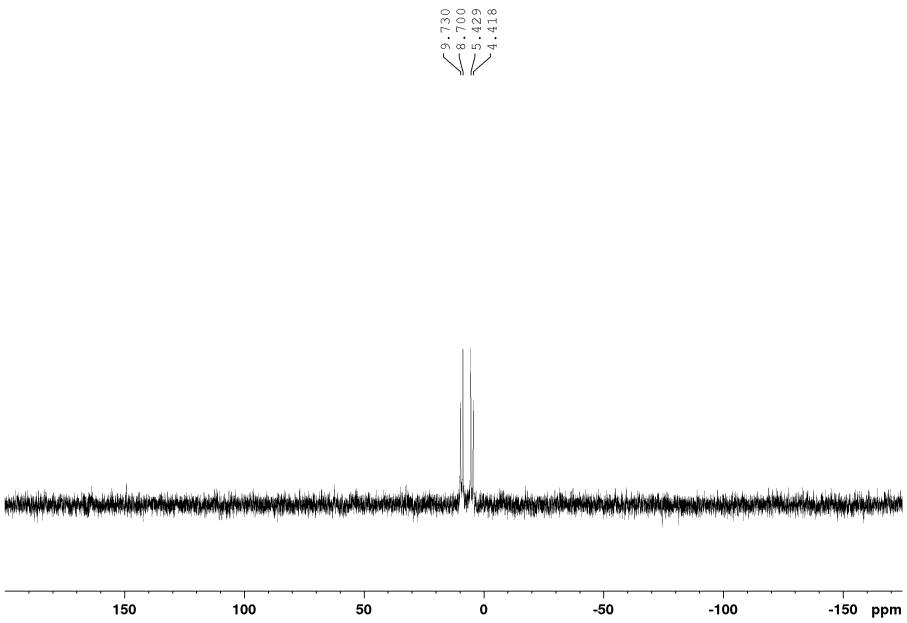

^{1}H NMR Spectrum of Complex **4-C9** ($CDCl_3$, 500.1 MHz)

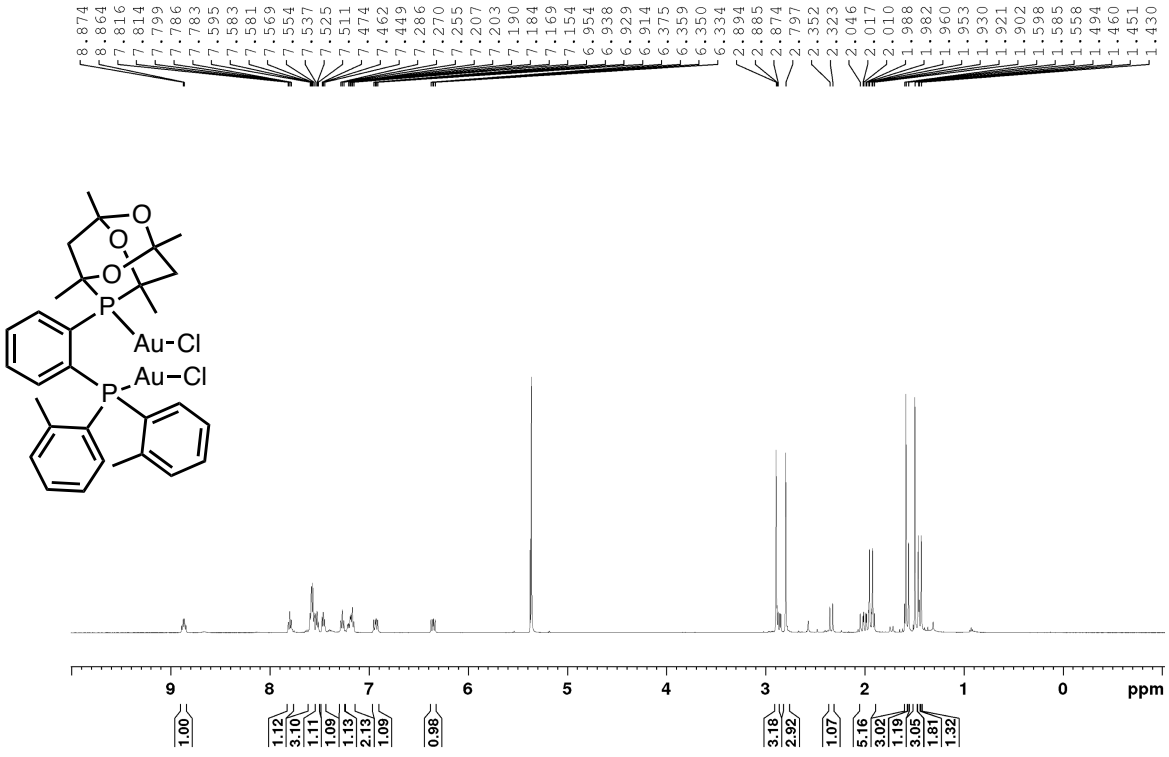

$^{13}C\{^{1}H\}$ NMR Spectrum of Complex **4-C9** ($CDCl_3$, 125.8 MHz)

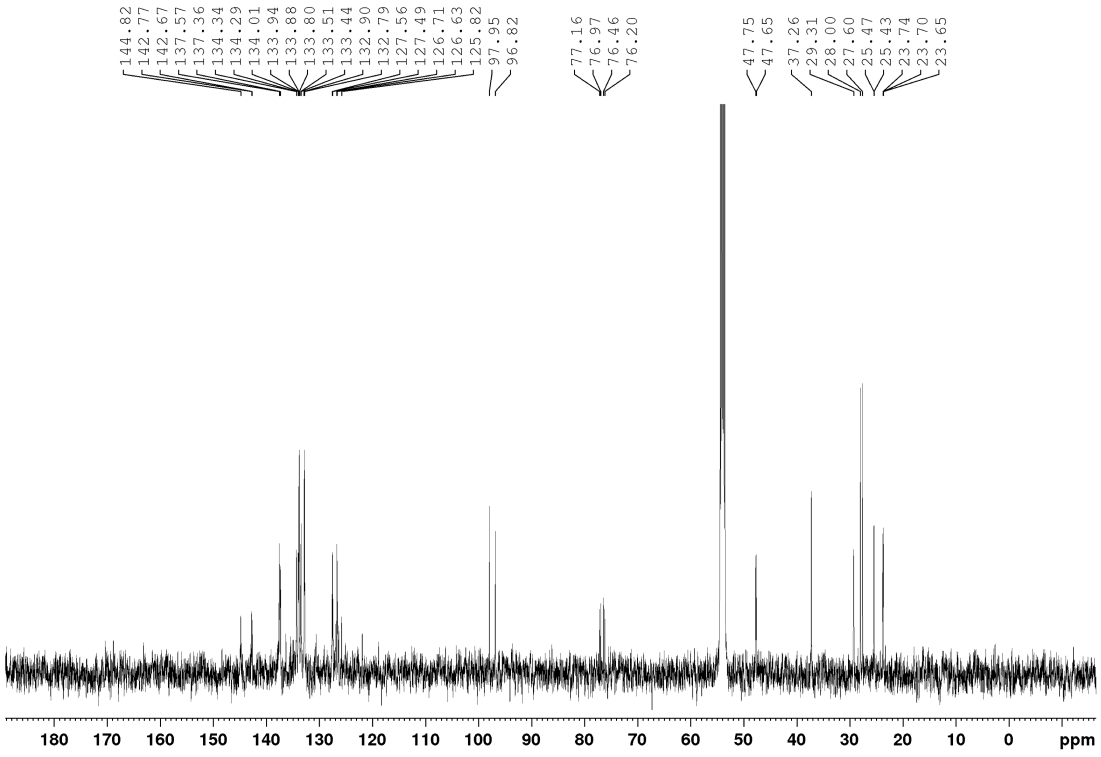

$^{31}P\{^{1}H\}$ NMR Spectrum of Complex **4-C9** ($CDCl_3$, 202 MHz)

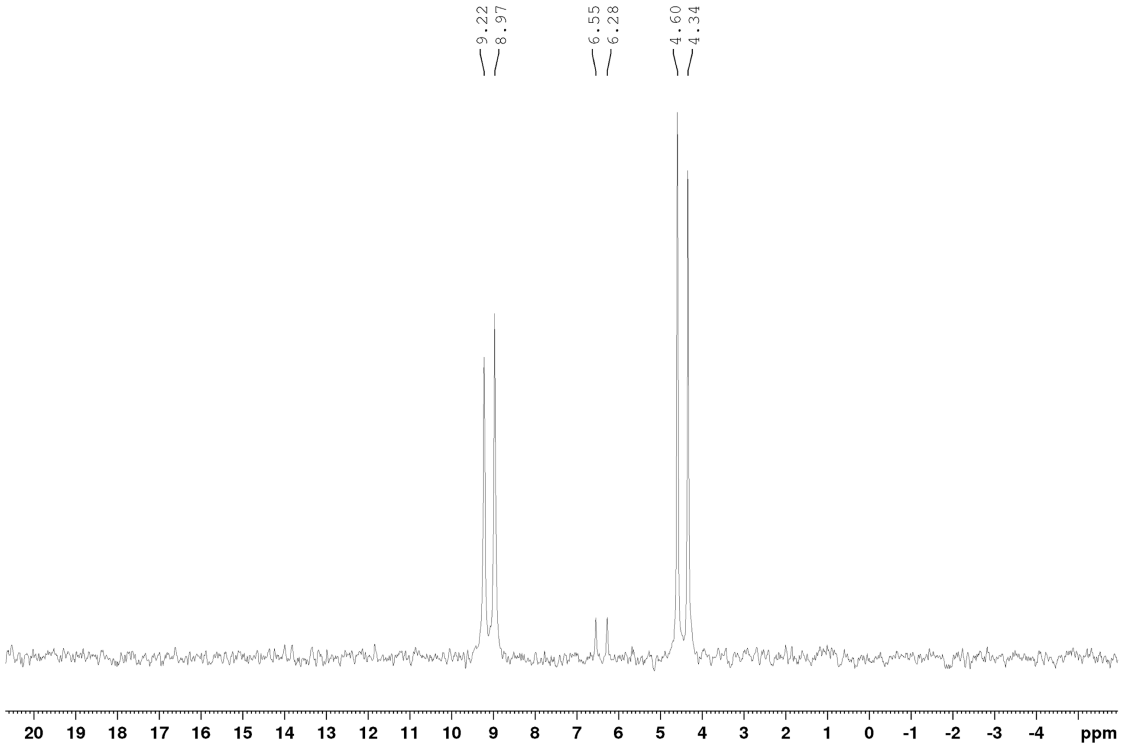

^{1}H NMR Spectrum of (1-(phenyl)ethylidene)hydrazine, **4-1** (C_6D_6, 500.1 MHz)

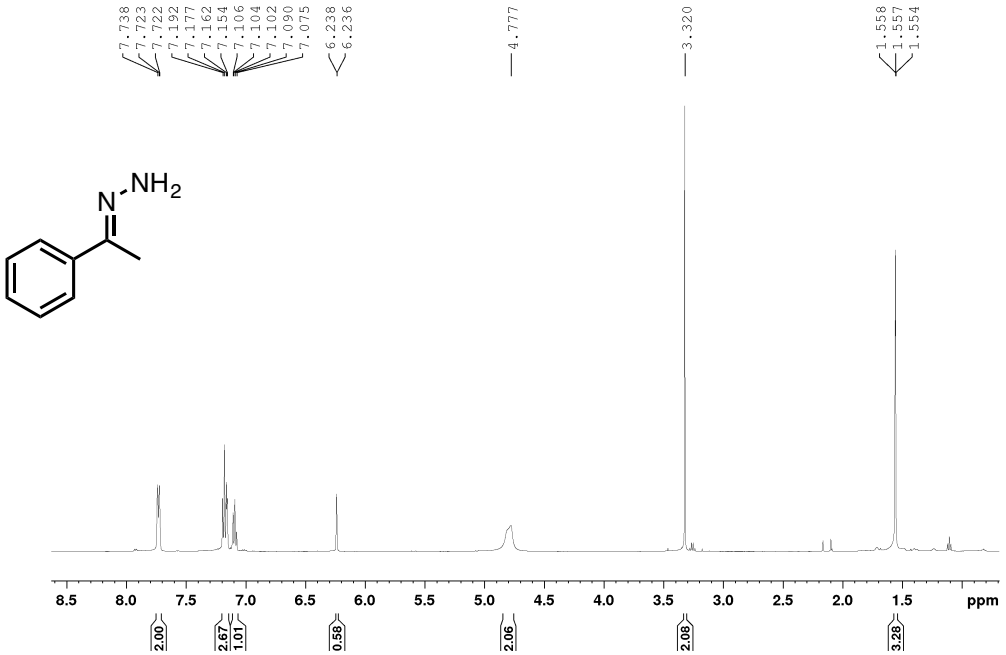

^{1}H NMR Spectrum of (1-(p-tolyl)ethylidene)hydrazine, **4-2** (C_6D_6, 500.1 MHz)

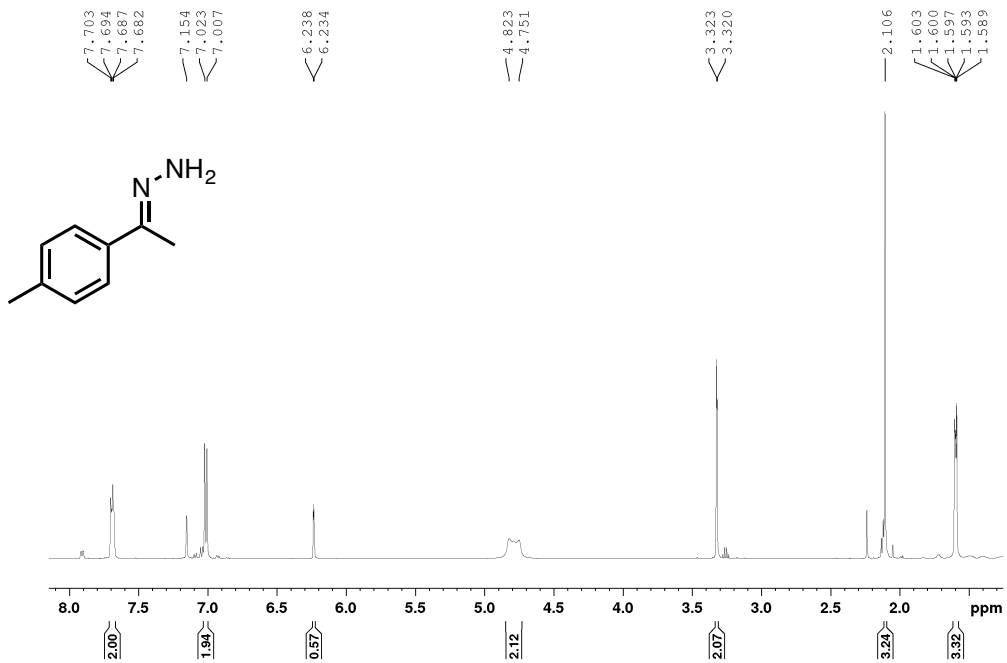

^{1}H NMR Spectrum of (1-(4-pentylphenyl)ethylidene)hydrazine, **4-3** (C_6D_6, 500.1 MHz)

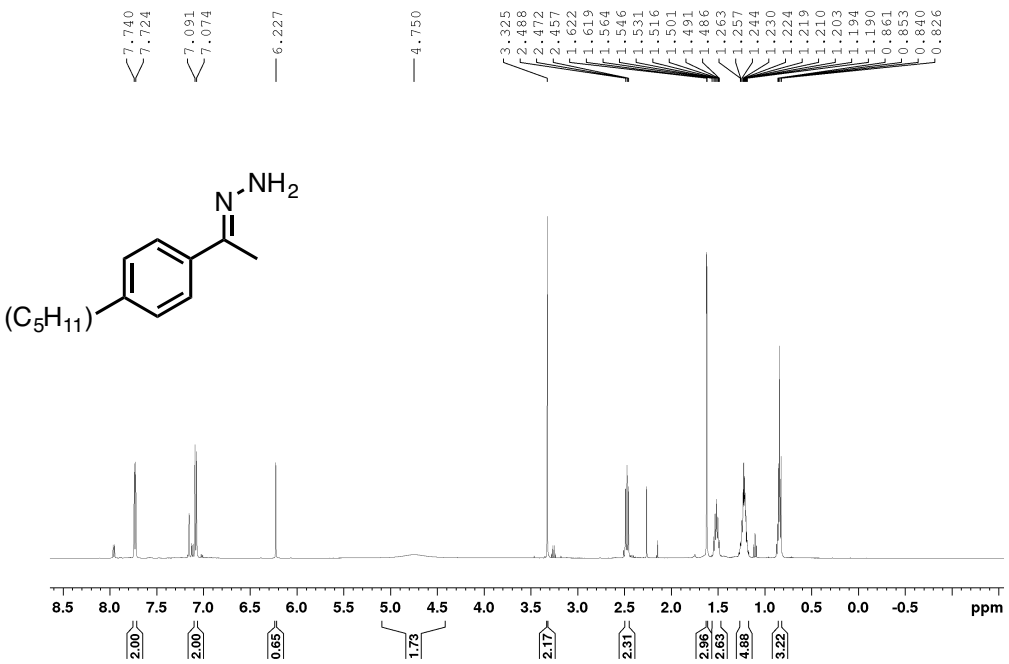

^{1}H NMR Spectrum of (1,2-bis(1-(4-pentylphenyl)ethylidene)hydrazine, **4-3'** ($CDCl_3$, 500.1 MHz)

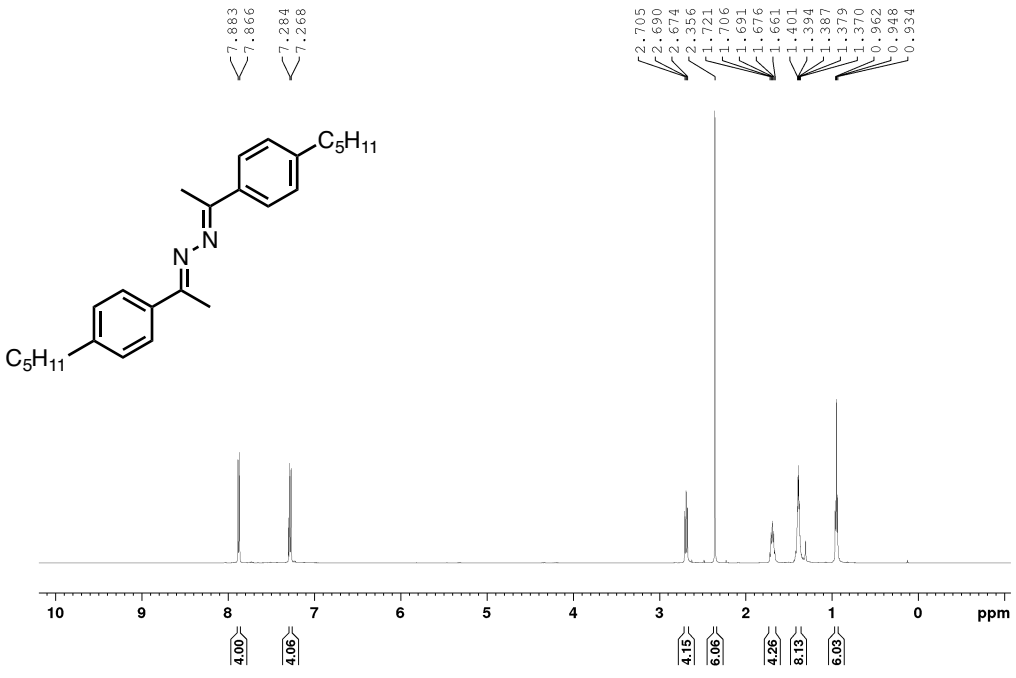

$^{13}C\{^{1}H\}$ NMR Spectrum of (1,2-bis(1-(4-pentylphenyl)ethylidene)hydrazine, **4-3'** ($CDCl_3$, 125.8 MHz)

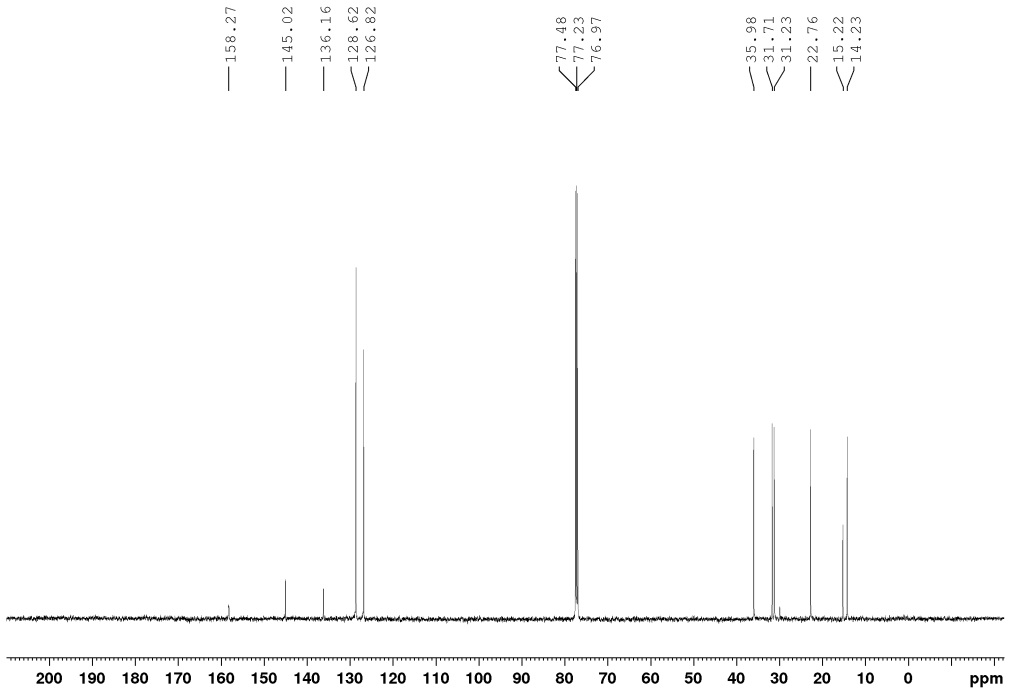

^{1}H NMR Spectrum of (1-(4-methoxyphenyl)ethylidenehydrazine, **4-4** (C_6D_6, 500.1 MHz)

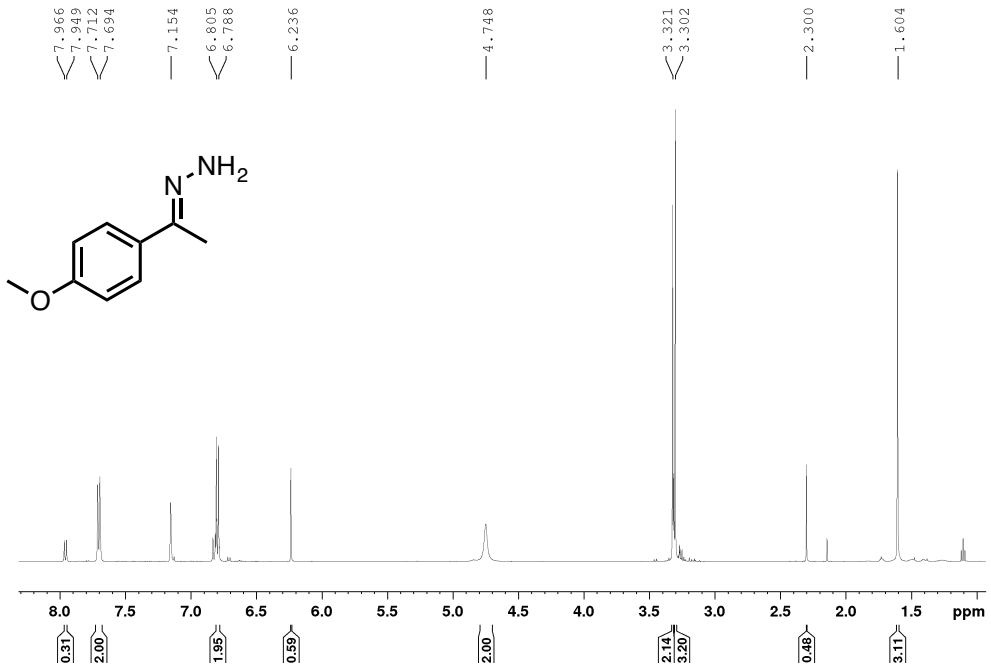

^{1}H NMR Spectrum of (1-(4-fluorophenyl)ethylidene)hydrazine, **4-5** (C_6D_6, 500.1 MHz)

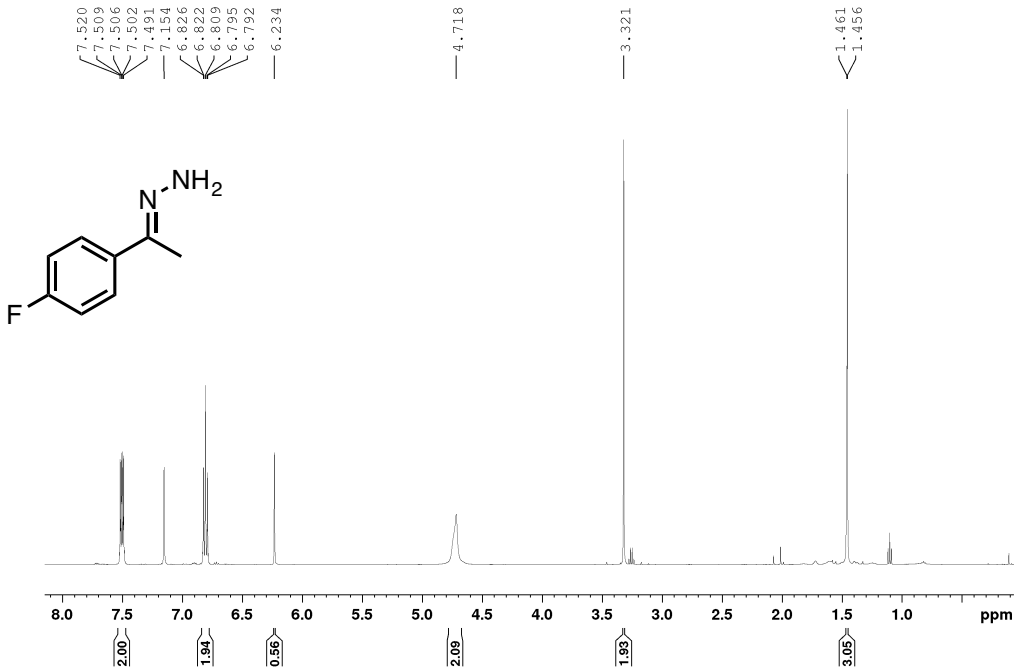

^{1}H NMR Spectrum of (1-(4-bromophenyl)ethylidenehydrazine, **4-6** (C_6D_6, 500.1 MHz)

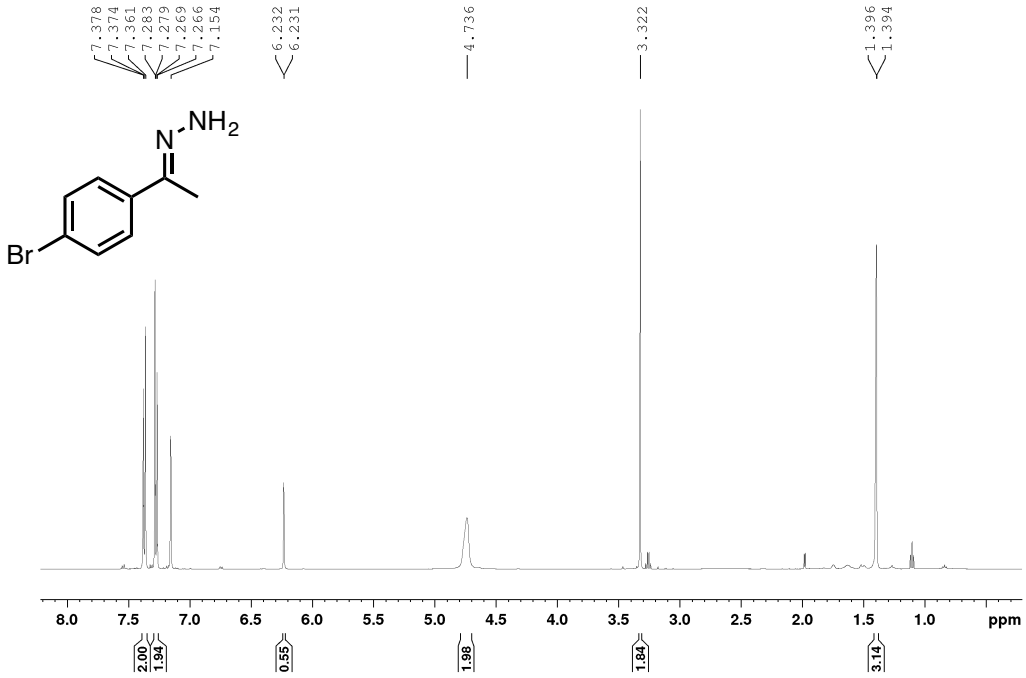

^{1}H NMR Spectrum of (1-(4-trifluoromethyl)phenyl)ethylidene)hydrazine, **4-7** (C_6D_6, 500.1 MHz)

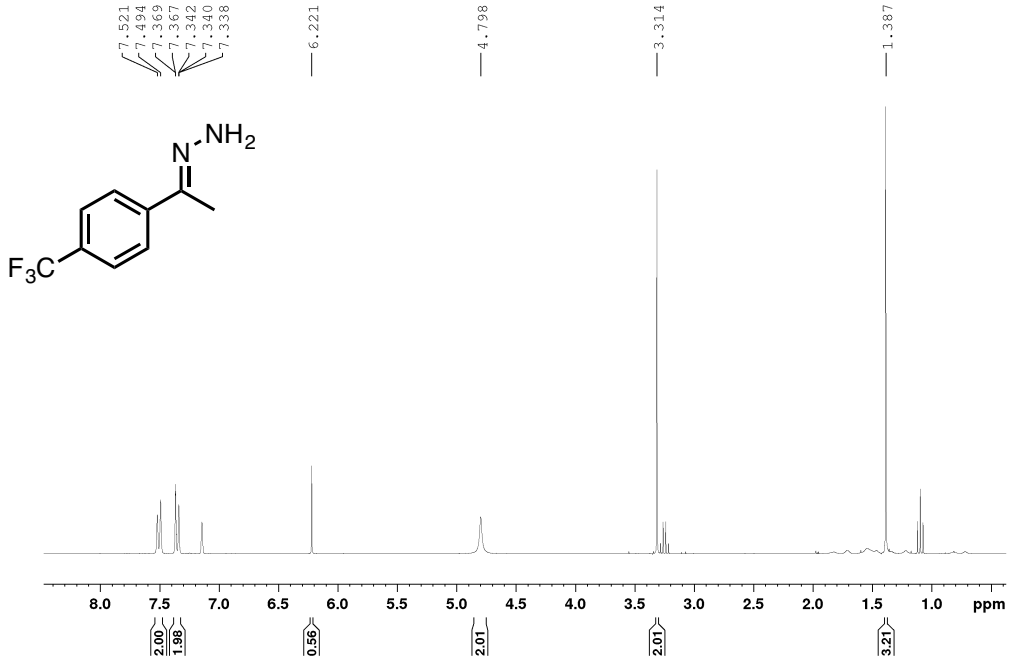

^{1}H NMR Spectrum of 2-(1-hydrazonoethyl)aniline, **4-8** (C_6D_6, 500.1 MHz)

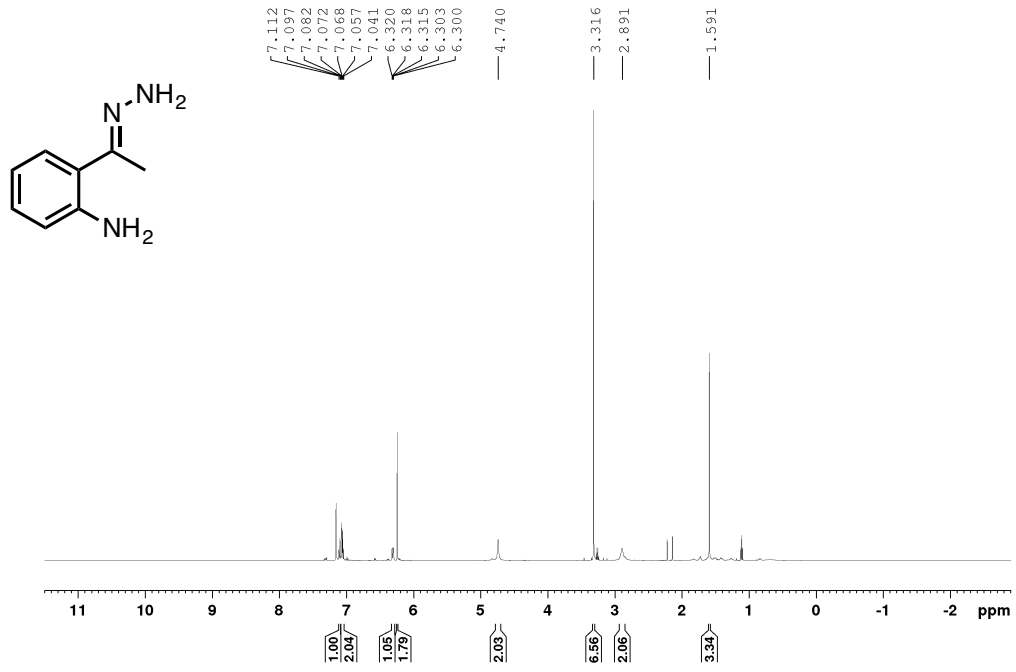

^{1}H NMR Spectrum of (1-phenylpropan-2-ylidene)hydrazine, **4-9** (C_6D_6, 500.1 MHz)

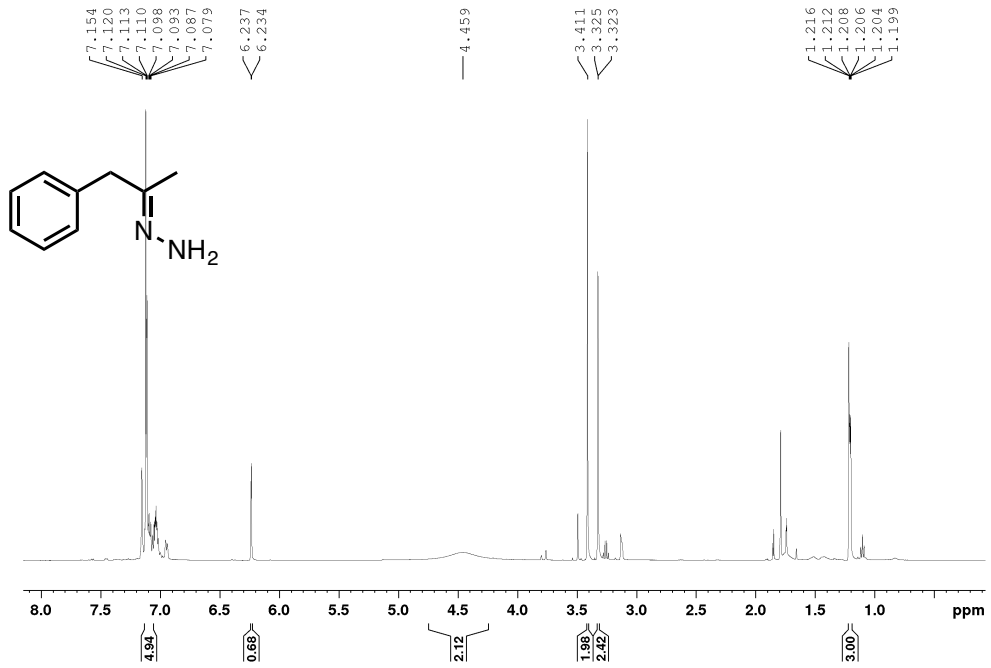

^{1}H NMR Spectrum of 2-(1-hydrazonoethyl)pyridine, **4-10** (C_6D_6, 500.1 MHz)

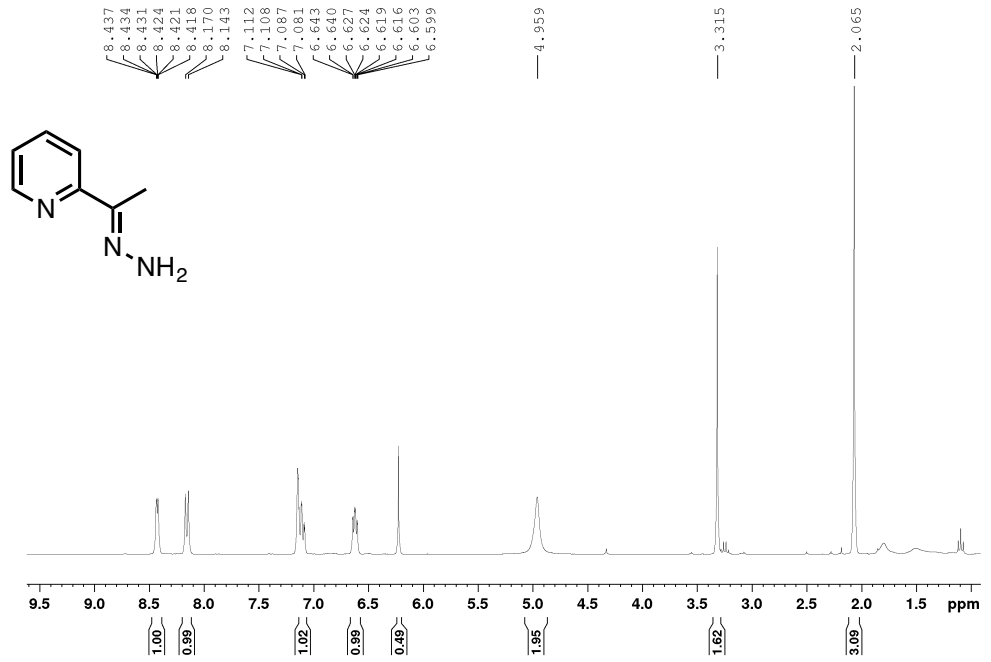

^{1}H NMR Spectrum of (1-(thiophen-3-yl)ethylidene)hydrazine, **4-11** (C_6D_6, 500.1 MHz)

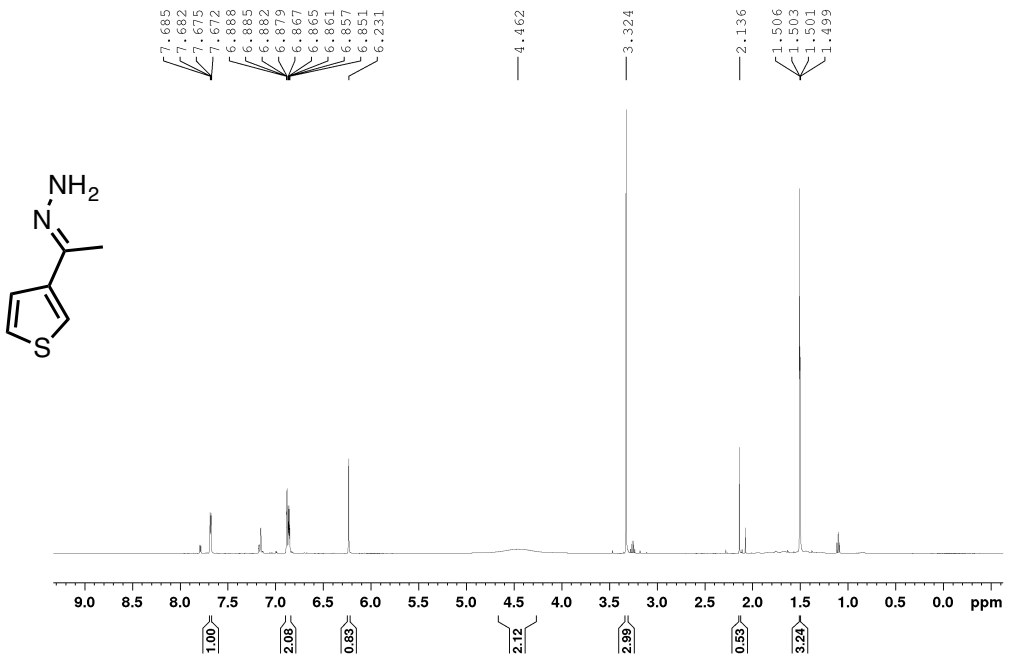

^{1}H NMR Spectrum of (1,2-bis(1-thiophen-3-yl)ethylidene)hydrazine, **4-11'** ($CDCl_3$, 500.1 MHz)

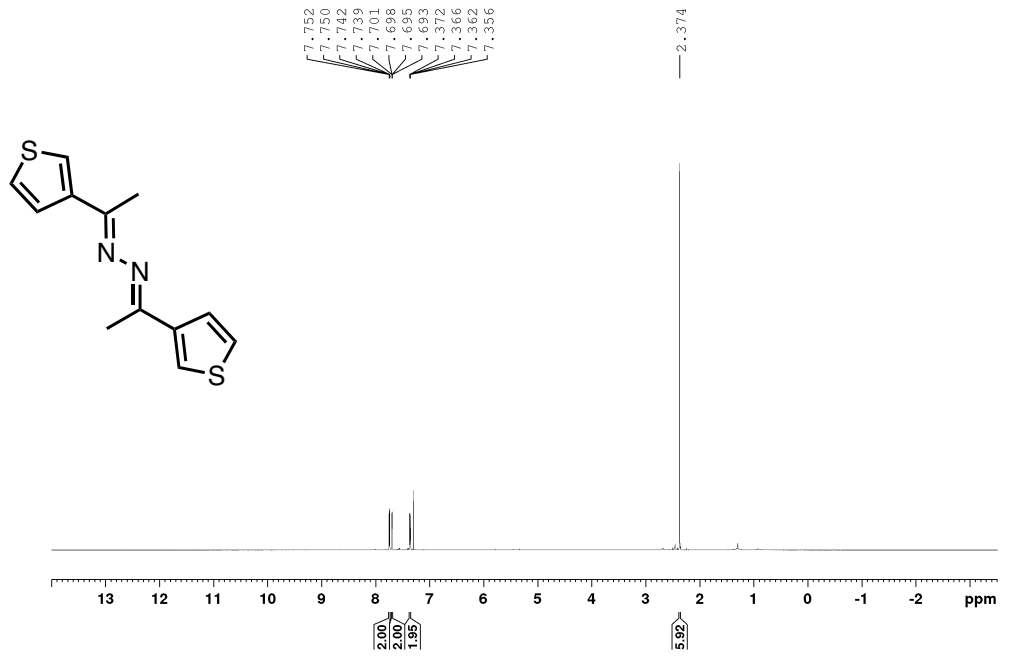

$^{13}C\{^{1}H\}$ NMR Spectrum of (1,2-bis(1-thiophen-3-yl)ethylidene)hydrazine, **4-11'** ($CDCl_3$, 125.8 MHz)

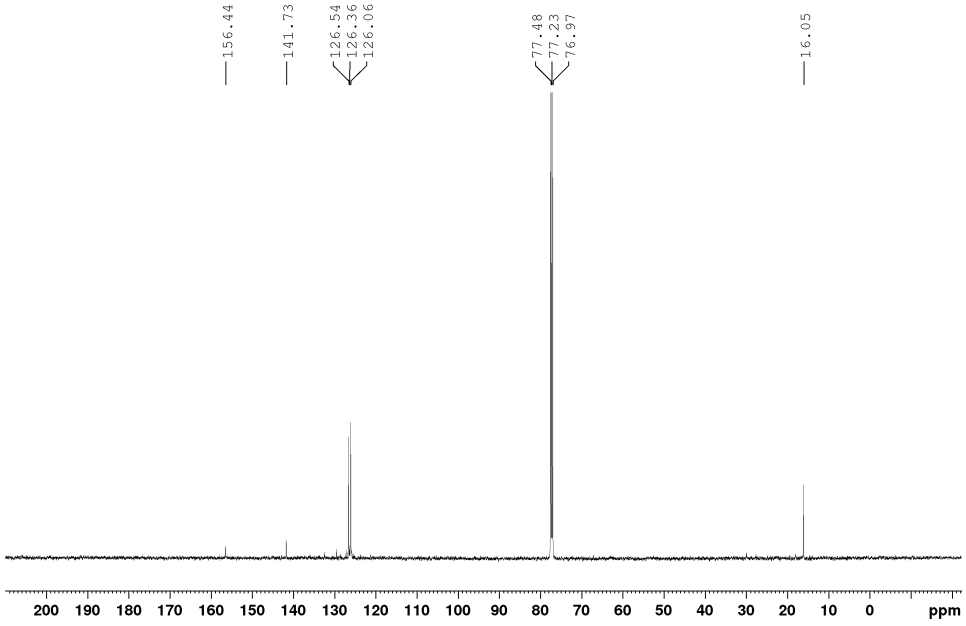

^{1}H NMR Spectrum of (1,2-diphenylethylidene)hydrazine, **4-12** ($CDCl_3$, 500.1 MHz)

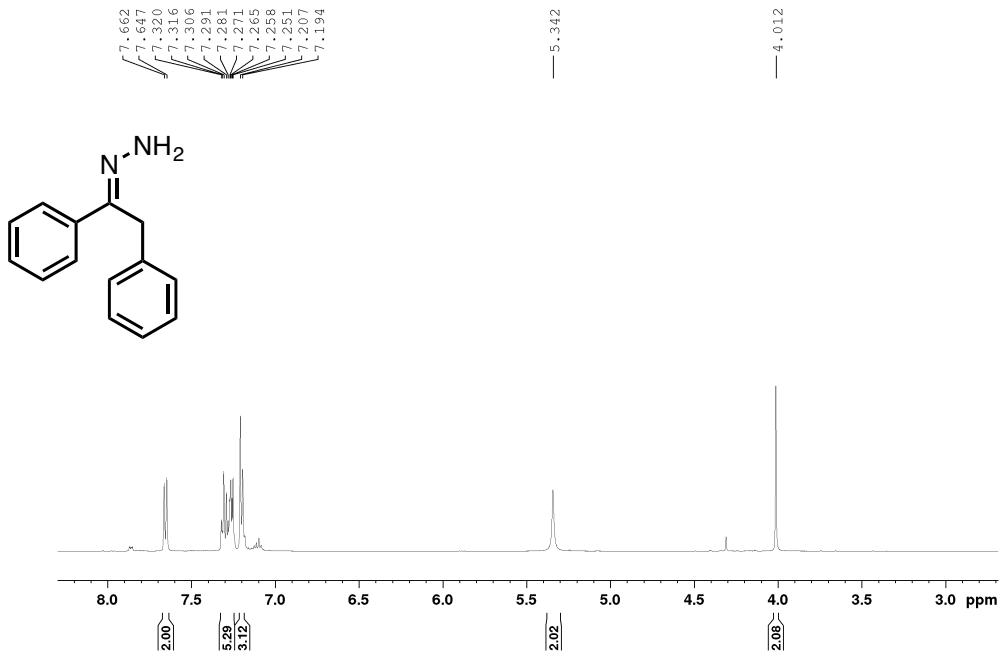

$^{13}C\{^{1}H\}$ NMR Spectrum of (1,2-diphenylethylidene)hydrazine, **4-12** ($CDCl_3$, 125.8 MHz)

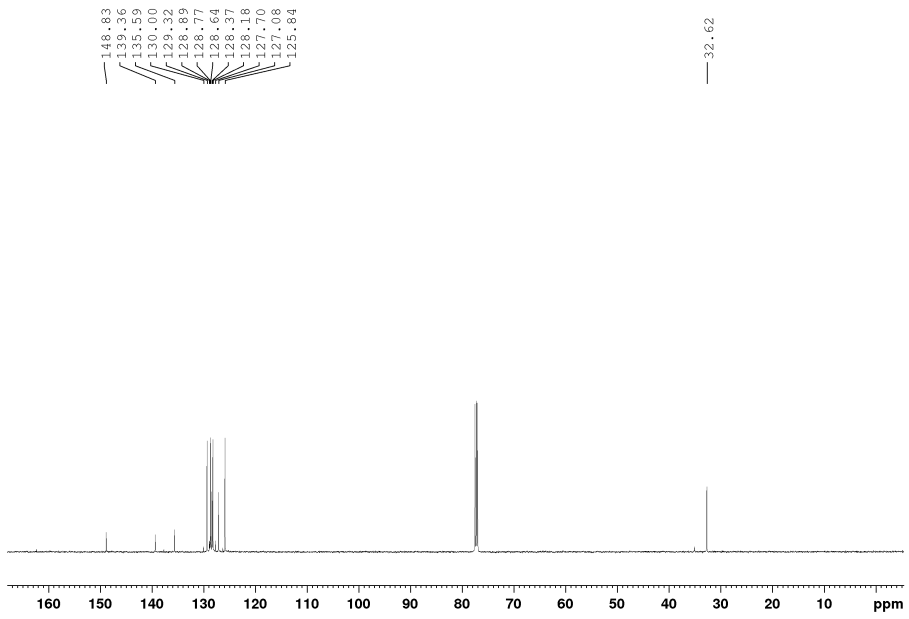

^{1}H NMR Spectrum of Ligand **4-L5** ($CDCl_3$, 500.1 MHz)

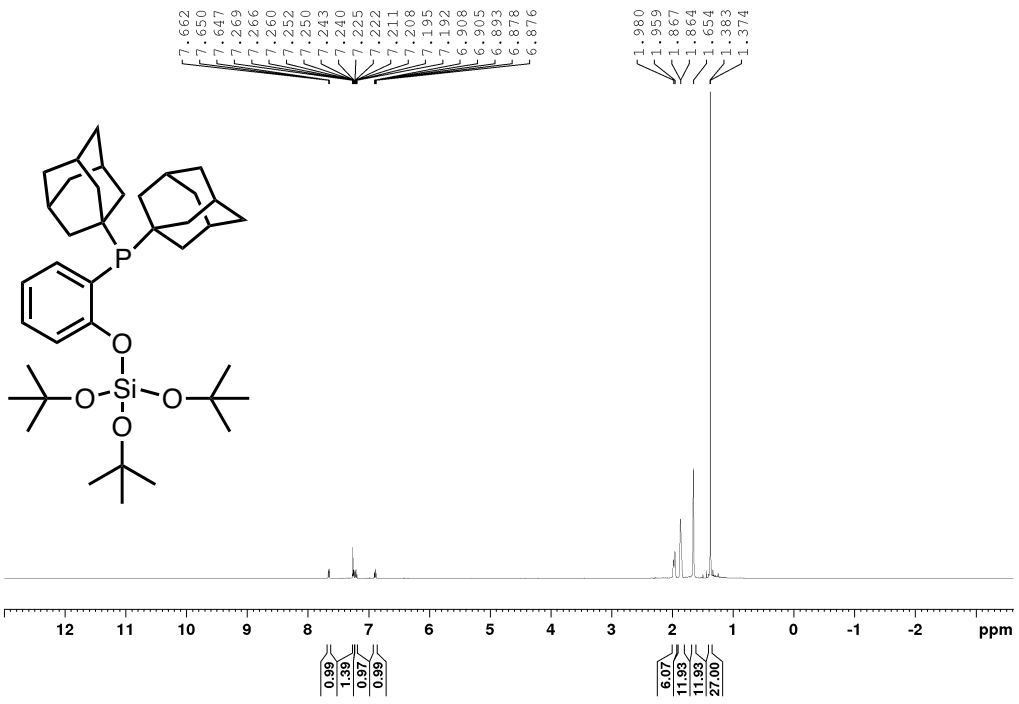

^{13}C NMR Spectrum of Ligand **4-L5** ($CDCl_3$, 500.1 MHz)

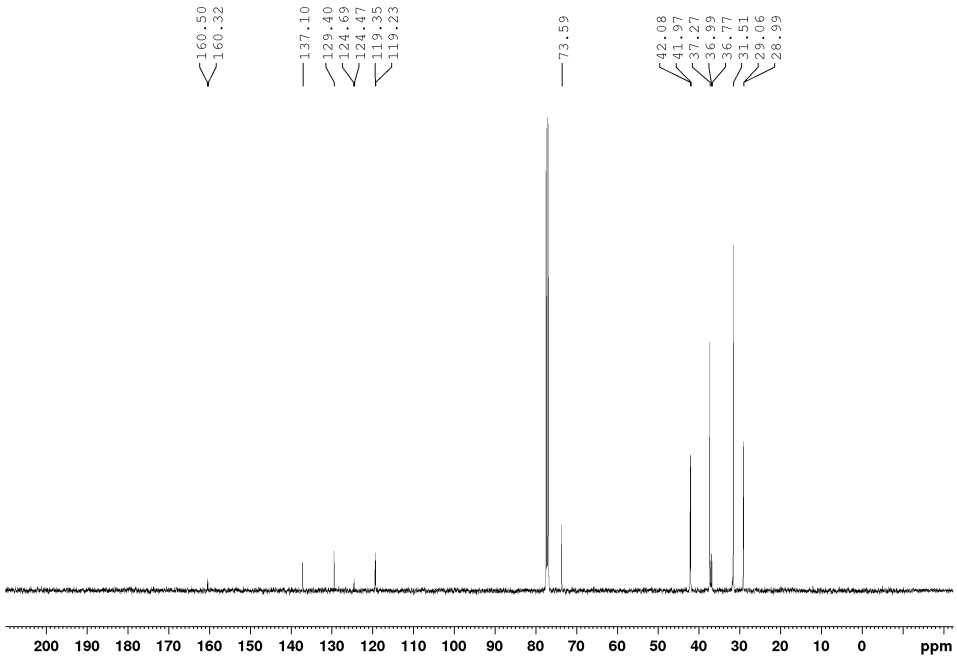

^{31}P NMR Spectrum of Ligand **4-L5** ($CDCl_3$, 500.1 MHz)

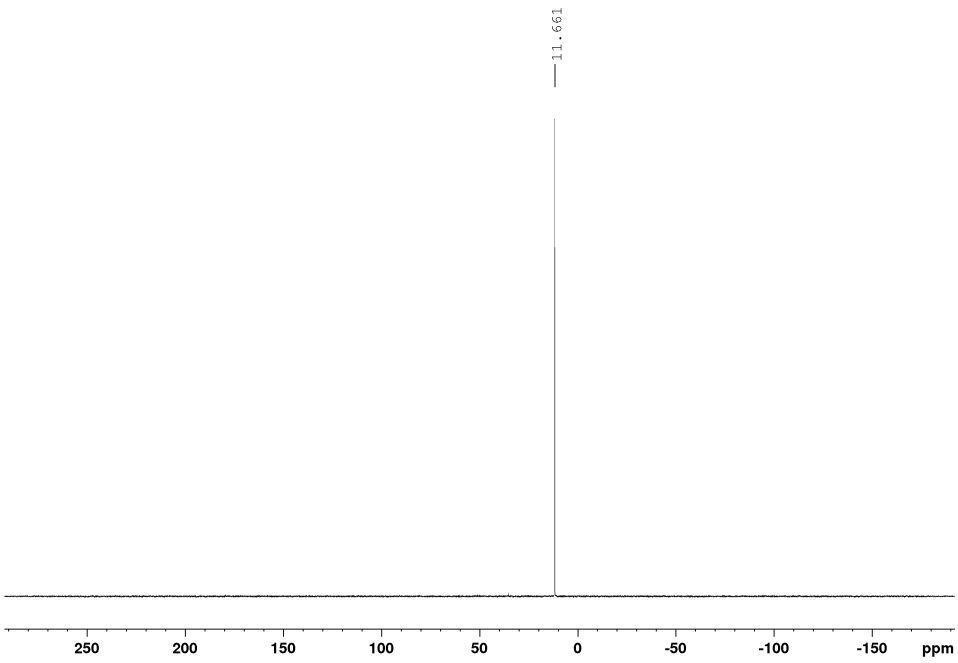

Summary of Selected Bond Lengths (Å) for **4-C1**, **4-C3** to **4-C6**, **4-C8**, **4-C9**.

	4-C1	**4-C3**	**4-C4**	**4-C5**
Au-P	2.243(3)	2.2554(6)	2.2520(5)	2.2637(7)
Au-Cl	2.282(3)	2.3018(6)	2.2999(5)	2.2909(7)
Cl-Au-P	175.37(11)	176.36(2)	172.607(19)	179.34(3)
Au2-P2	-	-	-	-
Au2-Cl2	-	-	-	-
Cl2-Au2-P2	-	-	-	-

	4-C6	**4-C8**	**4-C9**
Au-P	2.2568(8)	2.2285(8)	2.2375(13)
Au-Cl	2.2985(8)	2.2930(9)	2.2863(16)
Cl-Au-P	177.16(3)	171.84(3)	170.04(06)
Au2-P2	-	-	2.2421(13)
Au2-Cl2	-	-	2.2969(14)
Cl2-Au2-P2	-	-	175.62(5)

Appendix 4. Copyright License Agreements

Title: Exploring the Influence of Phosphine Ligation on the Gold-Catalyzed Hydrohydrazination of Terminal Alkynes at Room Temperature

Author: Nicolas L. Rotta-Loria, Alicia J. Chisholm, Preston M. MacQueen, et al

Publication: Organometallics

Publisher: American Chemical Society

Date: Jul 1, 2017

Copyright © 2017, American Chemical Society

Logged in as: Nicolas Rotta

LOGOUT

PERMISSION/LICENSE IS GRANTED FOR YOUR ORDER AT NO CHARGE

This type of permission/license, instead of the standard Terms & Conditions, is sent to you because no fee is being charged for your order. Please note the following:

- Permission is granted for your request in both print and electronic formats, and translations.
- If figures and/or tables were requested, they may be adapted or used in part.
- Please print this page for your records and send a copy of it to your publisher/graduate school.
- Appropriate credit for the requested material should be given as follows: "Reprinted (adapted) with permission from (COMPLETE REFERENCE CITATION). Copyright (YEAR) American Chemical Society." Insert appropriate information in place of the capitalized words.
- One-time permission is granted only for the use specified in your request. No additional uses are granted (such as derivative works or other editions). For any other uses, please submit a new request.

BACK CLOSE WINDOW

Copyright © 2017 Copyright Clearance Center, Inc. All Rights Reserved. Privacy statement. Terms and Conditions.
Comments? We would like to hear from you. E-mail us at customercare@copyright.com

JOHN WILEY AND SONS LICENSE TERMS AND CONDITIONS

Aug 14, 2017

This Agreement between Mr. Nicolas Rotta ("You") and John Wiley and Sons ("John Wiley and Sons") consists of your license details and the terms and conditions provided by John Wiley and Sons and Copyright Clearance Center.

License Number	4164310718995
License date	Aug 08, 2017
Licensed Content Publisher	John Wiley and Sons
Licensed Content Publication	Angewandte Chemie International Edition
Licensed Content Title	Nickel-Catalyzed Monoarylation of Ammonia
Licensed Content Author	Andrey Borzenko,Nicolas L. Rotta-Loria,Preston M. MacQueen,Christopher M. Lavoie,Robert McDonald,Mark Stradiotto
Licensed Content Date	Jan 8, 2015
Licensed Content Pages	5
Type of use	Dissertation/Thesis
Requestor type	Author of this Wiley article
Format	Print and electronic
Portion	Text extract
Number of Pages	2
Will you be translating?	No
Title of your thesis / dissertation	Advances in Late-Metal Carbon-Nitrogen Bond Formation for the Synthesis of Substituted Heterocycles
Expected completion date	Aug 2017
Expected size (number of pages)	210
Requestor Location	Mr. Nicolas Rotta-Loria 20 Longridge Way Markham, ON L6C0J9 Canada Attn: Mr. Nicolas Rotta-Loria
Publisher Tax ID	EU826007151
Billing Type	Invoice
Billing Address	Mr. Nicolas Rotta-Loria 20 Longridge Way Markham, ON L6C0J9 Canada Attn: Mr. Nicolas Rotta-Loria
Total	0.00 USD
Terms and Conditions	

TERMS AND CONDITIONS

This copyrighted material is owned by or exclusively licensed to John Wiley & Sons, Inc. or one of its group companies (each a"Wiley Company") or handled on behalf of a society with

JOHN WILEY AND SONS LICENSE TERMS AND CONDITIONS

Aug 08, 2017

This Agreement between Mr. Nicolas Rotta ("You") and John Wiley and Sons ("John Wiley and Sons") consists of your license details and the terms and conditions provided by John Wiley and Sons and Copyright Clearance Center.

License Number	4164310807295
License date	Aug 08, 2017
Licensed Content Publisher	John Wiley and Sons
Licensed Content Publication	Advanced Synthesis & Catalysis
Licensed Content Title	Utilizing Mor-DalPhos/Palladium-Catalyzed Monoarylation in the Multicomponent One-Pot Synthesis of Indoles
Licensed Content Author	Nicolas L. Rotta-Loria,Andrey Borzenko,Pamela G. Alsabeh,Christopher B. Lavery,Mark Stradiotto
Licensed Content Date	Dec 5, 2014
Licensed Content Pages	7
Type of use	Dissertation/Thesis
Requestor type	Author of this Wiley article
Format	Print and electronic
Portion	Full article
Will you be translating?	No
Title of your thesis / dissertation	Advances in Late-Metal Carbon-Nitrogen Bond Formation for the Synthesis of Substituted Heterocycles
Expected completion date	Aug 2017
Expected size (number of pages)	210
Requestor Location	Mr. Nicolas Rotta-Loria 20 Longridge Way Markham, ON L6C0J9 Canada Attn: Mr. Nicolas Rotta-Loria
Publisher Tax ID	EU826007151
Billing Type	Invoice
Billing Address	Mr. Nicolas Rotta-Loria 20 Longridge Way Markham, ON L6C0J9 Canada Attn: Mr. Nicolas Rotta-Loria
Total	0.00 USD
Terms and Conditions	

TERMS AND CONDITIONS

This copyrighted material is owned by or exclusively licensed to John Wiley & Sons, Inc. or one of its group companies (each a"Wiley Company") or handled on behalf of a society with which a Wiley Company has exclusive publishing rights in relation to a particular work